GEOLOGICAL SURVEY CIRCULAR 861

Geological Studies of the COST Nos. G–1 and G–2 Wells, United States North Atlantic Outer Continental Shelf

Geological Studies of the COST Nos. G–1 and G–2 Wells, United States North Atlantic Outer Continental Shelf

By Peter A. Scholle and Chiye R. Wenkam, *Editors*

GEOLOGICAL SURVEY CIRCULAR 861

1982

United States Department of the Interior

JAMES G. WATT, *Secretary*

Geological Survey

Dallas L. Peck, *Director*

Free on application to the Branch of Distribution, U.S. Geological Survey, 604 South Pickett Street, Alexandria, VA 22304

CONTENTS

ILLUSTRATIONS

TABLES

Geological Studies of the COST Nos. G–1 and G–2 Wells, United States North Atlantic Outer Continental Shelf

By Peter A. Scholle and Chiye R. Wenkam, Editors

ABSTRACT

The COST Nos. G–1 and G–2 wells (fig. 1) are the second and third deep stratigraphic test wells drilled in the North Atlantic Outer Continental Shelf of the United States. COST No. G–1 was drilled in the Georges Bank basin to a total depth of 16,071 ft (4,898 m). G–1 bottomed in phyllite, slate, and metaquartzite overlain by weakly metamorphosed dolomite, all of Cambrian age. From approximately 15,600 to 12,400 ft (4,755 to 3,780 m) the strata are Upper Triassic(?), Lower Jurassic(?), and Middle Jurassic, predominantly red shales, sandstones, and conglomerates. Thin, gray Middle Jurassic beds of shale, sandstone, limestone, and dolomite occur from 12,400 to 9,900 ft (3,780 to 3,018 m). From 9,900 to 1,030 ft (3,018 to 314 m) are coarse-grained unconsolidated sands and loosely cemented sandstones, with beds of gray shale, lignite, and coal. The microfossils indicate the rocks are Upper Jurassic from 10,100 ft (3,078 m) up to 5,400 ft (1,646 m) and Cretaceous from that depth to 1,030 ft (314 m). No younger or shallower rocks were recovered in the drilling at the COST No. G–1 site, but an Eocene limestone is inferred to be disconformable over Santonian strata. The Jurassic strata of the COST No. G-1 well were deposited in shallow marine, marginal marine, and nonmarine environments, which changed to a dominantly shallow marine but still nearshore environment in the Cretaceous.

The COST No. G–2 well was drilled 42 statute miles (68 km) east of the G–1 site, still within the Georges Bank basin, to a depth of 21,874 ft (6,667 m). The bottom 40 ft (12 m) of salt and anhydrite is overlain by approximately 7,000 ft (2,134 m) of Upper Triassic(?), Lower Jurassic(?) and Middle Jurassic dolomite, limestone, and interbedded anhydrite from 21,830 to 13,615 ft (6,654 to 4,153 m). From 13,500 to 9,700 ft (4,115 to 2,957 m) are Middle Jurassic limestones with interbedded sandstone. From 9,700 to 4,000 ft (2,957 to 1,219 m) are Upper Jurassic and Cretaceous interbedded sandstones and limestones overlain by Upper Cretaceous unconsolidated sands, sandstones, and calcareous shales. Pliocene, Miocene, Eocene, and Paleocene strata are disconformable over Santonian rocks; uppermost Cretaceous rocks are missing at this site, as at G–1. The sedimentary rocks in the COST No. G–2 well were deposited in somewhat deeper water, farther away from sources of terrigenous material than those at G–1, but still in marginal marine to shallow marine environments.

Data from geophysical logs and examination of conventional cores, well-cuttings, and sidewall cores show that below 10,000 ft (3,048 m), the strata in both wells have moderate porosities (< 20 percent) and low to moderate permeabilities (< 100 mD) and are thus considered adequate to poor reservoir rocks. Above 10,000 ft (3,000 m) the porosities range from 16 to 39 percent, and the permeabilities are highly variable, ranging from 0.01 to 7,100 mD.

Measurements of vitrinite reflectance, color alteration of visible organic matter, and various organic geochemical properties suggest that the Tertiary and Cretaceous strata of the COST Nos. G–1 and G–2 are not prospective for oil and gas. These sediments have not been buried deeply enough for hydrocarbon generation, and the kerogen and extractable organic matter in them are thermally immature. However, the Jurassic rocks at the G–1 site do contain small amounts of thermally mature gas-prone kerogens. The Jurassic rocks at COST No. G–2 are also gas-prone and are slightly richer in organic carbon and total extractable hydrocarbons than the G–1 rocks, but both sites have only poor to fair oil and gas source-rock potential.

INTRODUCTION

Until the COST Nos. G–1 and G–2 wells were drilled, the only subsurface information on the geology of Georges Bank came from multichannel seismic lines and extrapolation of the stratigraphy from wells on the Scotian shelf, eastern Canada. Although rocks recovered from the COST Nos. G–1 and G–2 wells are easily correlated with named formations on the Scotian shelf, there are differences in the development of the sedimentary section on Georges Bank that affect petroleum source and reservoir potentials.

The COST No. G–1 well was drilled between April 6 and July 26, 1976, by Ocean Production Company acting as operator for 31 participating companies. The well was drilled by the semisubmersible rig SEDCO-J in 157 ft (48 m) of water in the southwestern part of the Georges Bank basin at lat 40°55′52.108″ N., long 68°18′18.917″ W. A total section of 16,071 ft (4,898 m) was drilled.

The COST No. G–2 well was drilled 42 statute miles (68 km) east of COST No. G–1 between January 6 and August 30, 1977, by Ocean Production Company acting as operator for 19 participating companies. G–2 was drilled in 272 ft

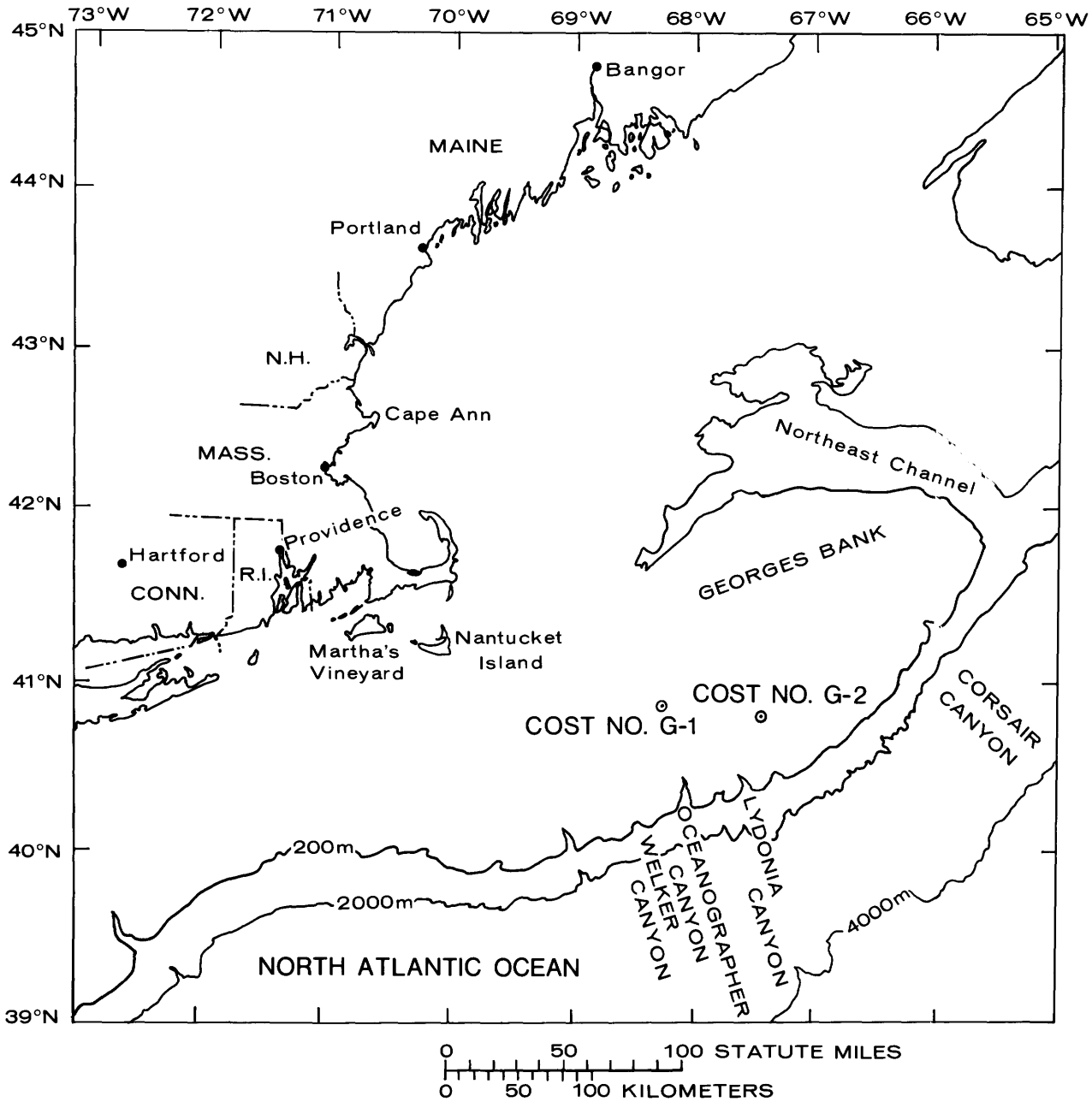

FIGURE 1.—Locations of the COST No. G-1 and G-2 wells in the Georges Bank area. Bathymetric contours in meters.

(83 m) of water by the semisubmersible rig Ocean Victory at lat 40°50′11.410′ N., long 67°30′29.784′ W. A total section of 21,874 ft (6,667 m) was drilled.

This circular summarizes data from previously released reports (Amato and Bebout, 1980, for the COST No. G-1 well and Amato and Simonis, 1980 for the COST No. G-2 well) and contains new data on the lithology, stratigraphy, geochemistry, geology, and geophysics of these two wells from studies by the USGS.

The data presented in the nine different papers were obtained from well cuttings, sidewall cores, conventional cores, electric logs, core descriptions, and multichannel seismic profiles. All well depths are relative to the Kelly Bushing (KB),

which was 98 ft (30 m) above mean sea level and 255 ft (78 m) above the sea floor for the COST No. G-1 well; KB was 79 ft (24 m) above mean sea level and 351 ft (107 m) above the sea floor for the COST No. G-2 well. Units are reported in the primary system of measurement with English or metric equivalents in parentheses. Thus, for depths in the wells, primary units are in feet (with meters as a secondary conversion); for seismic lines, primary measurements are in kilometers or meters (with miles or feet as a secondary conversion). Only the primary units are reported to a valid number of significant figures.

The COST Nos. G-1 and G-2 wells were drilled intentionally off structure in blocks 79 and 141 respectively of North Atlantic Outer Continental Shelf tracts that were part of Lease Sale No. 42, held December 18, 1979. The public disclosure provision of Federal leasing regulations stipulates that the U.S. Geological Survey release all geologic data from deep stratigraphic test wells 60 days after a lease is granted within 50 nautical miles of such a test site. Blocks adjacent to 79 and 141 were leased on February 1, 1980.

ACKNOWLEDGMENTS

Piero Ascoli kindly provided samples from the Scotian basin. Raymond Hall and Doris Low prepared the foraminifera samples. Invaluable technical assistance was provided by Patty Forrestal, Thomas McClurg, Jane Murphy, Jo Ann Taylor, and Jeffery Zwinakis. The authors benefitted from discussions with F. G. Adinolfi, William Dillon, Jurgen Fritsch, John Grow, Leigh Price, D. R. Shaw, and E. K. Simonis. Elazar Uchupi and J. M. Hunt of Woods Hole Oceanographic Institution and C. Wylie Poag, Kim Klitgord, John Schlee, and Elizabeth Winget read various chapters and provided valuable suggestions. O. W. Girard, Jr., and W. H. Butler reviewed the entire manuscript; their comments and suggestions are much appreciated.

Geologic Setting of the Georges Bank Basin

John S. Schlee and Kim D. Klitgord

The COST No. G-1 and G-2 wells were drilled on Georges Bank (fig 2), a broad, shallow platform that extends east of New England. The Georges Bank (25,862 mi²; 67,000 km²) is part of the U.S. Continental Shelf and is flanked on the north by the Gulf of Maine (Uchupi, 1966). The northern one-third of Georges Bank is covered by shallow, north-trending sand shoals, and the remainder is a flat-floored shelf covered with rippled sand. The southern side is indented by several submarine canyons and numerous smaller gullies and ravines. Two shallow channels separate the bank from the other parts of the shelf. To the west, the Great South Channel separates Georges Bank from Nantucket Shoals, and to the east, the Northeast Channel (722 ft; 220 m deep) provides a deep-water entrance to the Gulf of Maine.

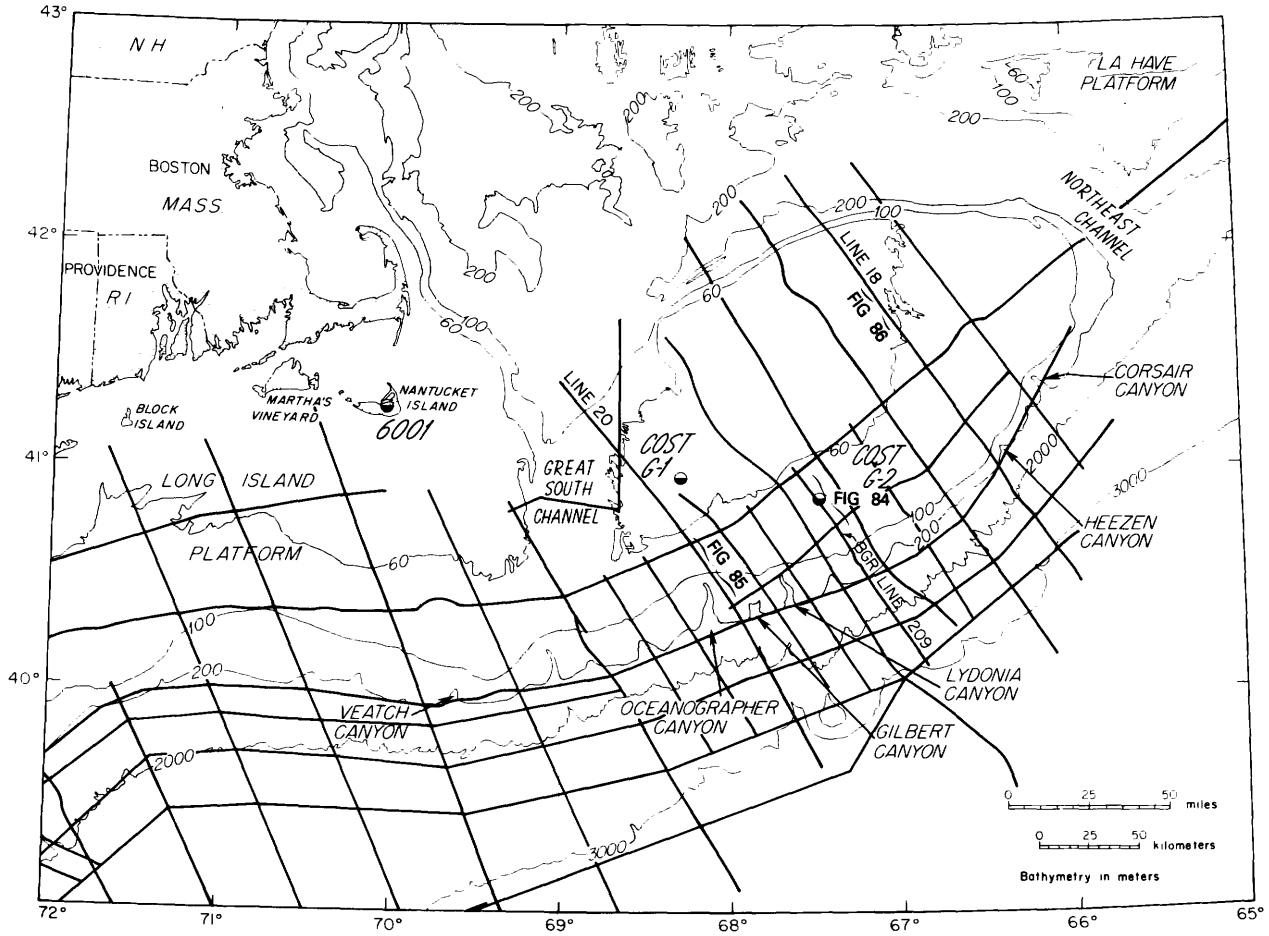

FIGURE 2.—Locations of COST wells Nos. G-1 and G-2, USGS core hole 6001, and the grid of multichannel seismic reflection profiles. Bathymetry is in meters. Bracketed sections of seismic profiles are shown in Klitgord and others (this volume).

STRUCTURE

Georges Bank is underlain by a wedge of Triassic and younger sedimentary rock that overlies rifted basement (fig. 3). Tectonically, Georges Bank is a collection of smaller subbasins, some of which are linear grabens that trend northeast (Ballard, 1975; Austin and others, 1980; Mattick and others, 1981; Schlee and Jansa, 1981). Collectively they are termed the Georges Bank basin, and structurally they are situated between the LaHave platform to the northwest, the Gulf of Maine platform to the north, and the Long Island platform to the west.

The basement deepens seaward from the platforms in a series of steps (half-grabens) (fig. 4). A western set of steps seaward of the Long Island platform can be clearly distinguished as small grabens or subbasins, while an eastern set of steps southeast of the Gulf of Maine platform, can be defined as grabens or subbasins on only some of the seismic lines (figs. 3 and 4). Steps #1 and #3 (fig. 4), landward of the Yarmouth arch, appear to be grabens or half-grabens. Seismic reflection and magnetic data show that these structures trend N. 30° E. There is a high magnetic anomaly along the edge of each graben and a low magnetic anomaly over the graben. The most landward of these grabens (step #1, fig. 4) is a shallow structure that lies along the northern edge of Georges Bank (Ballard and Uchupi, 1972; Oldale and others, 1974). An unconformity over the top of these grabens corresponds approximately to the breakup unconformity of Falvey (1974), and it increases in depth from less than 0.5 km (0.3 mi) below sea level adjacent to the Gulf of Maine to more than 10 km (6.2 mi) beneath the center of the bank. Beneath the southeastern part of the bank is a broad subbasin that lies between the Yarmouth arch and the East Coast magnetic anomaly (ECMA) (fig. 4); this subbasin extends to the northeast where it

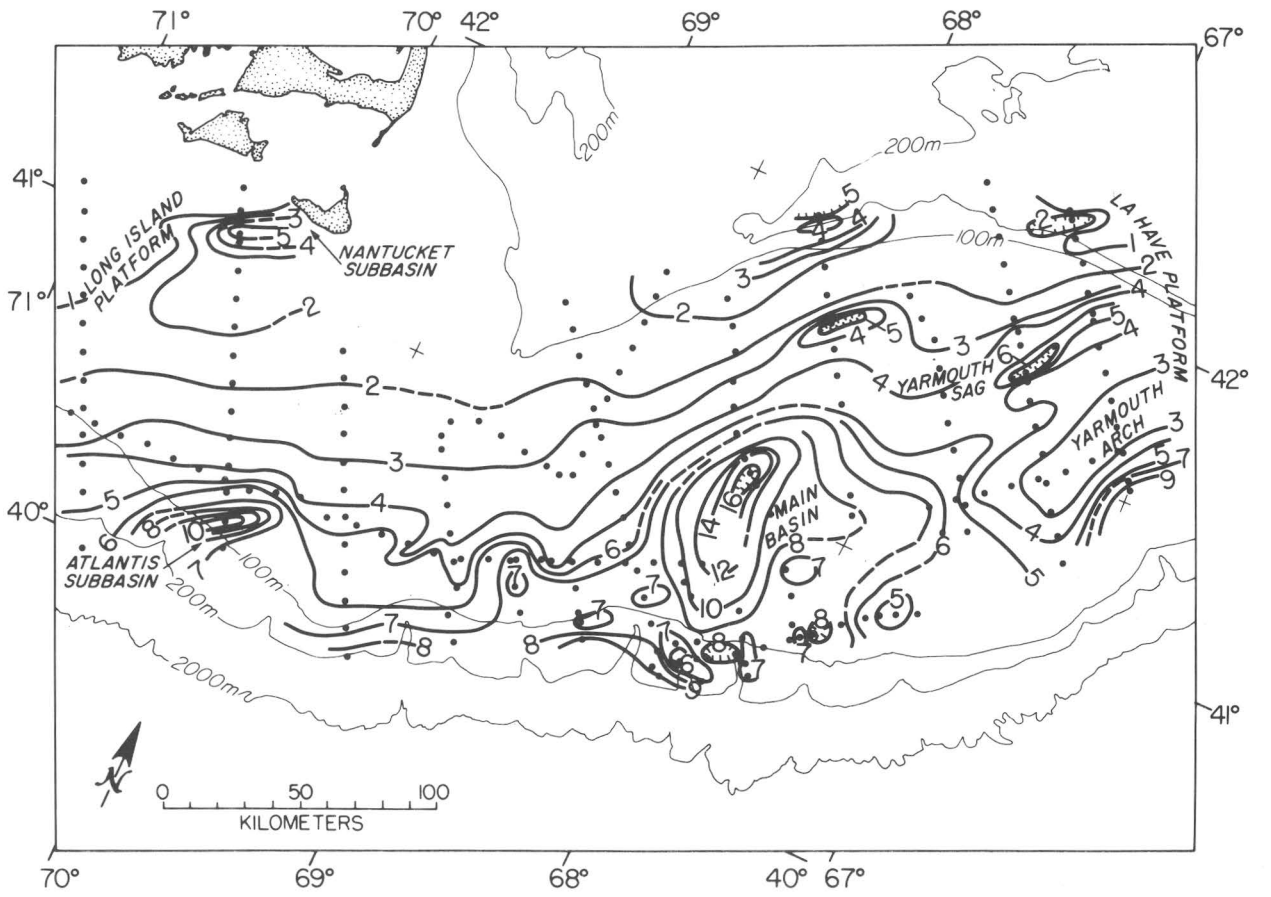

FIGURE 3.—Isopach map of Upper Triassic and younger sedimentary rocks in the Georges Bank basin. Thicknesses in kilometers. Dots show where thickness was measured along the profiles and indicate the control.

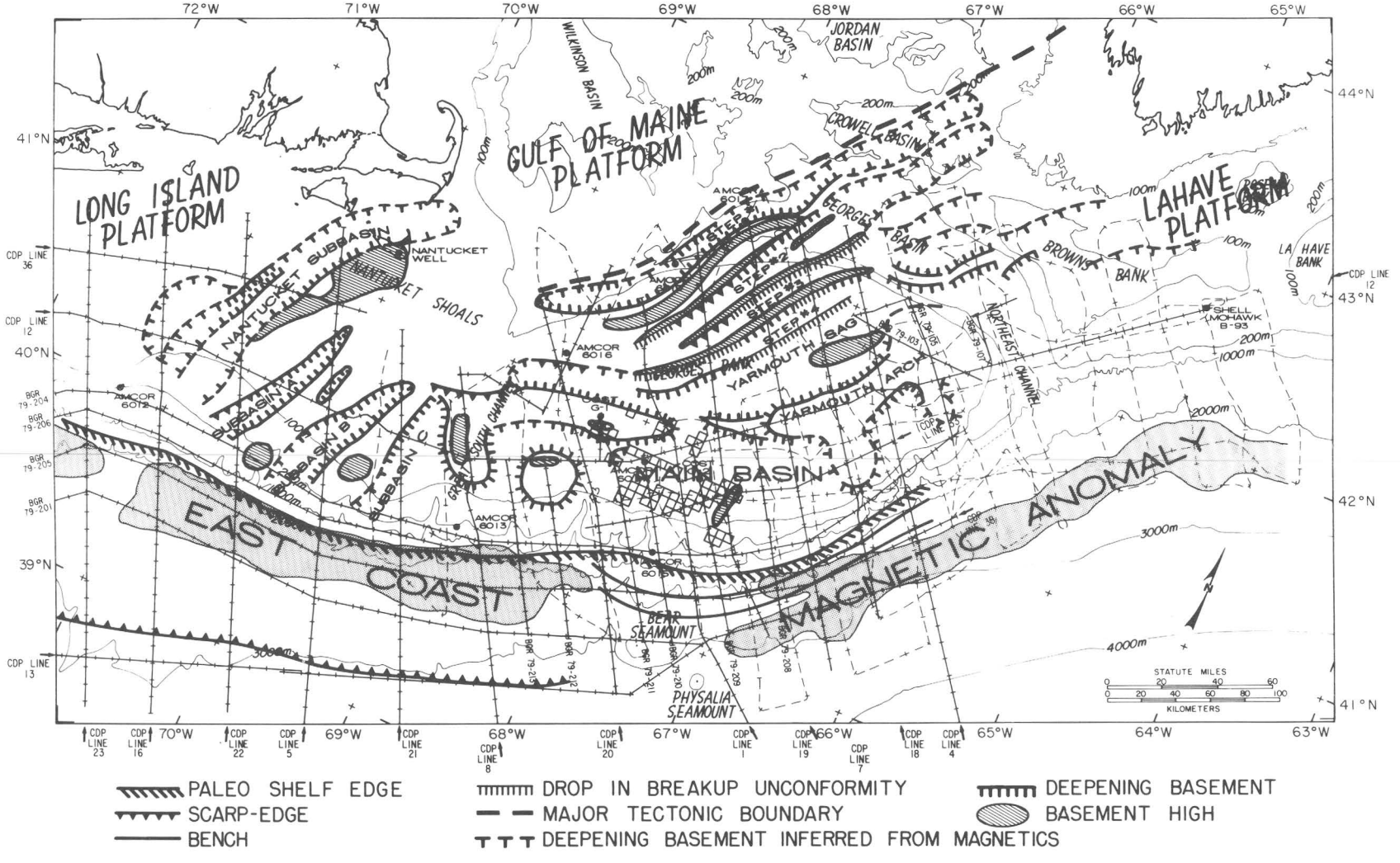

FIGURE 4.—Tectonic-structural map of the Georges Bank region showing the stable, shallow platforms of Paleozoic continental crust, areas of block- faulted crust (subbasins or grabens), steps (half-grabens) and intervening basement highs, and Jurassic oceanic crust. The East Coast magnetic anomaly and the ancient Jurassic shelf edge are indicated at the boundary between the block-faulted zone and the oceanic crust. The New England Seamounts and possible intrusive volcanic bodies are also shown. The lines indicate locations of multichannel seismic profiles.

merges with the Scotian Basin beneath the Canadian shelf. This subbasin may be situated on volcanic crust of Early Jurassic age formed in the area of continental separation; the other subbasins or steps are probably underlain by continental crust of Triassic age or older. The COST No. G-1 well was drilled into a small structural high that may be the southwestward extension of the Yarmouth arch and the COST No. G-2 well was drilled into the southeasternmost subbasin, mentioned above.

The New England Seamount chain intersects the Georges Bank region near lat 40° N., long 68° W., where there is a major gap in the ECMA. Bear Seamount is located at this intersection and its low magnetic dipole signature may mask the continuity of the ECMA across this gap. Within the Georges Bank basin, three buried seamounts or intrusive bodies are inferred to be present from distinctive magnetic anomaly patterns. All three are just landward of the ECMA and have high oval-shaped magnetic anomalies associated with them. Two of these bodies are located near the shelf edge just west of the Great South Channel (about lat 40° N., long 70° W.) within the zone of subbasins formed by grabens. The third and largest body is within the southernmost subbasin about 12.4 mi (20 km) southeast of the COST No. G-2 well (lat 40°8′ N., long 67°20′ W.).

Acoustic basement has a variable character across the margin and only in certain places does it correspond with the base of the sediment fill. The rugged acoustic basement along the northern edge of Georges Bank probably reflects the Paleozoic metamorphic and igneous rocks along the edges of the grabens. Seismic penetration is variable in this area and also farther south where the grabens are at greater depths. The basement surface on some seismic profiles coincides with inferred Paleozoic rocks, and on other profiles the surface of the dipping rift sediments (post-rift unconformity) forms acoustic basement. Acoustic basement between the Yarmouth arch and the ECMA has a shingled aspect that probably represents the top of a carbonate bank complex near the Jurassic shelf edge. Oceanic crust can be traced landward almost to the ECMA on most of the seismic profiles off Georges Bank (Schlee and others, 1976; Grow and others, 1979; Klitgord and Grow, 1980). In this region acoustic basement is a series of small hyperbolic echoes that are typical of oceanic crust.

STRATIGRAPHY

Rocks recovered from COST No. G-1 and G-2 wells provide information on the deep stratigraphy of Georges Bank (fig. 5). The G-1 well (Lachance, 1980; Scholle, Krivoy, and Hennessy, 1980) encountered a sequence mostly of sandstone, shale, and siltstone of Late Jurassic to early Tertiary age, that overlies sandstone, anhydrite, and dolomite of Early Jurassic(?) to Middle Jurassic age. The well penetrated Paleozoic metamorphosed dolomite, quartzite, and phyllite at 15,600 ft (4,755 m) and reached a total depth of 16,071 ft (4,898 m). At the COST No. G-2 site, 42 mi (67 km) to the east, the total section is thicker and contains more carbonate rocks and evaporites. The Upper Jurassic through Tertiary section contains abundant sandstone and mudstone and also has thick beds of limestone toward the base of the Cretaceous. These limestones are probably equivalent to strata sampled in Heezen Canyon by Ryan and others (1978) in 4,100 to 4,265 ft (1,250 to 1,300 m) of water, are Neocomian in age, and were deposited in a reefal environment. Oxfordian and older rocks are dominantly limestone, dolomite, and anhydrite in the COST No. G-2 hole; the well bottomed in salt at 21,874 ft (7,612 m) total depth (Simonis, 1980; Scholle, Schwab, and Krivoy, 1980). The other deep (1,686 ft; 514 m) hole, AMCOR #6001, was drilled on Nantucket Island (Folger and others, 1978). This well encountered poorly consolidated nonmarine and marine shelf silts and clay of Late Cretaceous and Tertiary age and bottomed in weathered basalt approximately 183±8 m.y. old (Early Jurassic).

Several trends are shown by these three holes. The Cretaceous strata apparently thicken and become finer grained and more calcareous toward the COST No. G-2 well. The Jurassic rocks are present only at the Georges Bank sites, where they thicken and become more carbonate-rich to the southeast over the main part of the basin. Multichannel seismic reflection profiles not only here, but off the mid-Atlantic states as well, support inferences that the rocks become more carbonate- and evaporite-rich with age and toward the southeast (Schlee and others, 1976, 1979; Mattick and others, 1981). The carbonate rocks are inferred to extend beneath the continental slope where they form a platform front and interfinger with deep-sea deposits of equivalent age

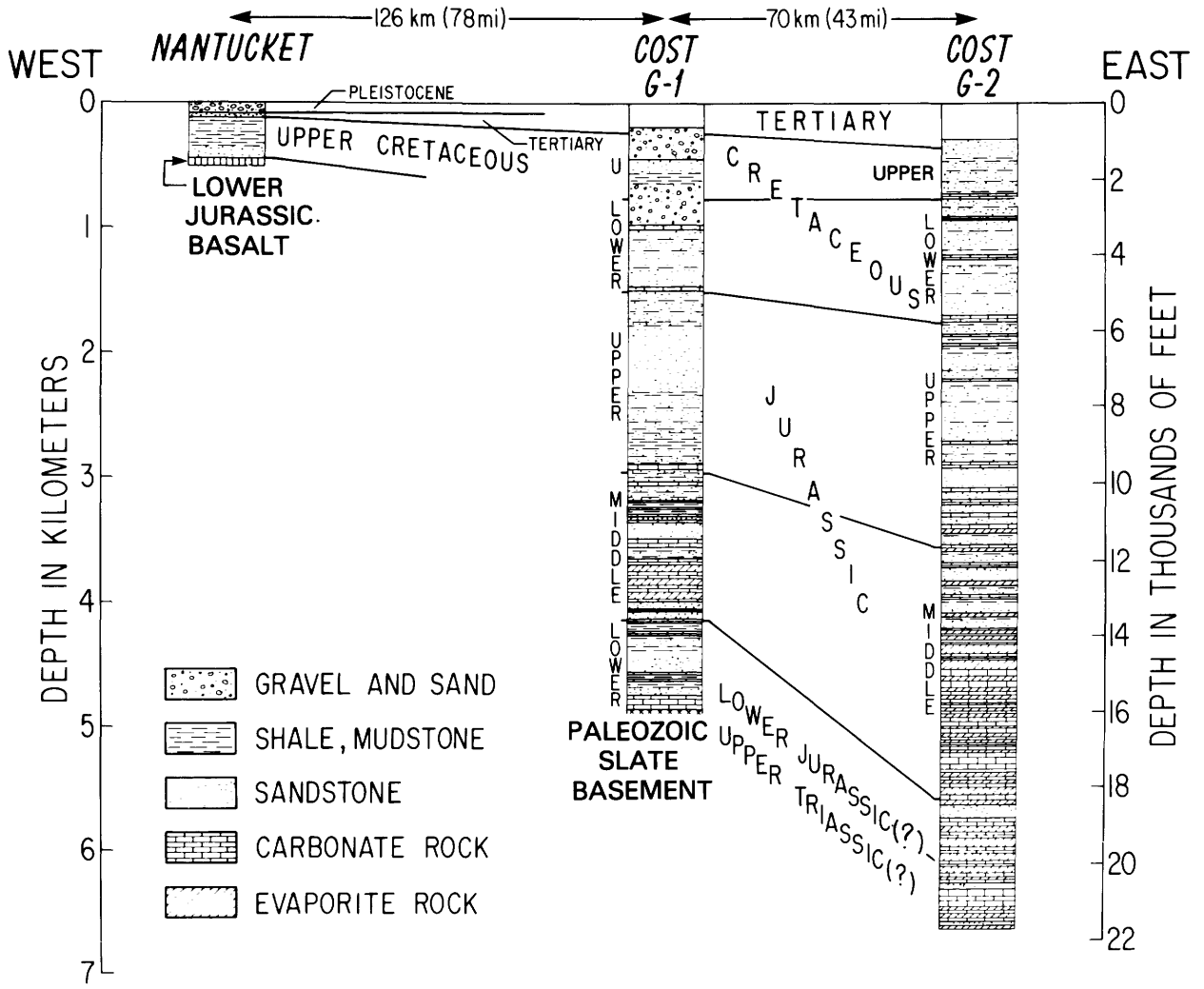

FIGURE 5.—Lithologic logs of the COST Nos. G-1 and G-2 wells and the Nantucket Island well (6001). Modified from Scholle, Krivoy, and Hennessy (1980); Scholle, Schwab, and Krivoy (1980); Judkins and others (1980); and Folger and others (1978).

in the North Atlantic oceanic basin (Schlee and others, 1979). Our multichannel seismic profiles reveal that the seaward edge of the carbonate platform may be expressed as a distinct break in slope (Schlee and others, 1979, fig. 6) or as a shingled offlap of reflectors that are presumably part of a seaward prograding platform (Schlee and others, 1979, fig. 7). Most of the profiles show a sharp break in slope, but line 20 (figs. 2 and 4) in the western part of the basin reveals a distinctly prograded arrangement of reflectors that appears to indicate that the shelf was built seaward 12.4 mi (20 km) over older slope and rise deposits.

These two types of shelf edge are paleoenvironmentally significant because they are related to the amount of deltaic outbuilding that occurs on the shelf. Eliuk (1978, fig. 8) has described these two types of seismic signatures for profiles collected across the Scotian shelf northeast of Georges Bank. He has tied the geophysical data to the lithologic logs from several holes drilled there and found that the prograded arrangement of reflectors resulted from the formation of a large delta complex nearby that caused the carbonate platform to build seaward of earlier ones. Away from the influence of the delta, a well-defined "platform type" shelf break bounds the seaward side of the Scotian carbonate buildup (Abenaki Formation). Eliuk drew analogies to the present-day Great Bahama Bank for the platform type of shelf edge and to the Pleistocene deposits of the Florida Bay for the prograding deltaic

type. The Great Bahama Bank is a sharply defined carbonate platform of bioclastic detritus far from an area of terrigenous input. The Florida Keys deposits show the input of deltaic sand on the ancestral platform near Miami.

The Georges Bank seismic stratigraphy has been tied to Canadian offshore stratigraphy by Wade (1977) and Austin and others (1980) using multichannel seismic reflection profiles. Judkins and others (1980) and Poag (this volume) have tentatively correlated formations and key markers from the stratigraphic section set up for the Scotian margin by McIver (1972), Jansa and Wade (1975a), Gradstein and others (1975), Ascoli (1976), and Given (1977). This correlation was facilitated by presence on Georges Bank of the same major vertical and lateral stratigraphic trends that are seen on the Scotian margin. These trends are an increase in carbonates and evaporites with age in outer shelf holes and an increase in clastic sedimentary rocks, particularly for the Jurassic, at inshore sites.

The oldest rock sequences encountered in the COST Nos. G-1 and G-2 wells are probably equivalent to the Iroquois Formation (dolomite and anhydrite), the Argo Formation (salt at very bottom of the COST No. G-2 well), and the Mohican Formation (sequence of sandstones and shale of early Middle Jurassic to Early Jurassic age present in the COST No. G-1 well). The limestones of Middle Jurassic to earliest Cretaceous age beneath Georges Bank probably correlate with the Abenaki Formation platform limestone and shale sequence on the Scotian shelf: both there and under Georges Bank, the Abenaki Formation or its equivalent changes inshore to the Mic Mac and Mohawk Formations and consists of shelf sandstone, shale and thin-bedded limestone.

Utilizing Canadian outer shelf holes, Judkins and others (1980, pl. 3) have also correlated formations of Cretaceous age with the lithologic units of the COST Nos. G-1 and G-2 wells. Their correlations show a major change in the total thickness of the Jurassic and Cretaceous rocks from the central Scotian basin to the area of COST G-wells. The Cretaceous rocks are thinner on Georges Bank (4,100–4,600 ft; 1,250–1,400 m) than in the northern Scotian basin (9,000–10,000 ft; 2,750–3,050 m), but equivalent age units in the Jurassic System (from the top of the Jurassic to the top of the Argo Formation) are thicker beneath the Georges Bank basin: 15,995 ft vs. 5,496 ft (4,875 m vs. 1,675 m).

This difference in thickness, which is seen in both G-1 and G-2 holes, is a result of rapid sediment accumulation during the Jurassic and lower rates after that time. At least 15,995 ft (4,875 m) of rock accumulated during the first 54 m.y. of basin development at the COST No. G-2 well, whereas only 5,742 ft (1,750 m) of sediment accumulated in the last 141 m.y., and 79 percent of that accumulated during the Cretaceous (141–65 m.y. B.P.). The overall trend is similar to that shown by Poag (1980b, fig. 28) for the COST No. B-2 and No. B-3 wells in the Baltimore Canyon trough on the outer continental shelf.

SUMMARY

The Georges Bank basin is similar in tectonic setting and sedimentary fill to other basins along eastern North America (Schlee and Jansa, 1981; Grow and Sheridan, 1981). Like the Scotian margin, it was built over a complexly faulted basement whose continued movement during the early stages of basin development probably influenced sedimentary facies and thickness (Klitgord and others, this volume; Eliuk, 1978). The deepest, most restricted part of the basin may contain as much as 26,250 ft (8.6 km) of Lower Jurassic and older nonmarine clastic rocks and evaporite deposits. Both COST wells appear to have penetrated a part of this sequence. Middle and Upper Jurassic nonmarine clastic rocks and marine carbonate and evaporitic rocks 0 to 13,100 ft (0 to 4 km) thick were the initial deposits in the subsidence phase of basin development and signify a transition to an open-shelf environment. Buildup of the carbonate rocks probably started on elevated basement blocks and eventually formed a massive platform that covered much of the southern half of the basin. In the western part of the basin, the platform appears to have prograded seaward 12.4 mi (20 km), perhaps in response to deltaic sedimentation. During the Cretaceous, transgressive and regressive marine and nonmarine clastic sedimentary rocks and thin limestone buried the earlier platform as the broad pattern of basin subsidence continued at a diminished rate. The Cenozoic Era was marked by periodic cutback of the continental slope and an even slower rate of sediment accumulation on the bank. As in other eastern

North American basins, the interval of basin development spans the Late Triassic(?) to the present. The Georges Bank basin like others has accumulated more than 32,800 ft (10 km) of sediment in several subbasins, and it shows the change from early rift deposits to a complex carbonate buildup during the early subsidence phase, and later burial by sand, silt, and clay as sea level reached its maximum in the Late Cretaceous and early Tertiary.

Lithology and Petrography of the COST Nos. G-1 and G-2 Wells

By Michael A. Arthur

The following generalized lithologic descriptions for the sedimentary rocks recovered in the COST Nos. G-1 and G-2 wells in the Georges Bank basin are based on initial descriptions of core materials prepared by the Ocean Production Company and on subsequent studies by Lachance (1980) for the G-1 well and Simonis (1980) for the G-2 well. In addition, selected cuttings and thin sections of cuttings from 142 intervals in the G-1 well and 81 intervals in the G-2 well (an average of 10 cuttings per section) have been examined for this study. These observations have been supplemented by descriptions of thin sections of conventional and sidewall cores provided by Core Laboratories, Inc., because the cuttings are inadequate for a complete description of the lithofacies in a well. A total of 190 sections of sidewall cores were described for the G-1 well and 131 sections of sidewall cores were studies for the G-2 well. The boundaries of lithologic units are based on all available lithologic descriptions and data from geophysical logs.

The descriptions of lithology and petrography are given from the bottom of each well to the top in order to facilitate interpretation of the succession of sedimentary environments. All depths are given in feet (meters) below the Kelly Bushing. Ages of lithologic units are based on determinations given in Valentine (this volume) and Poag (this volume).

DESCRIPTION OF COST NO. G-1 SEQUENCE

The COST No. G-1 (fig. 6) sequence is informally divided in this paper into four major lithologic units (fig. 7), which are further divided on the basis of minor lithologic changes. These lithologies are discussed stratigraphically from bottom to top in the well.

UNIT 4 (16,071-15,650 FT; 4,898-4,770 M) PALEOZOIC(?) BASEMENT

The COST No. G-1 well bottomed in black, fissile, graphitic slate, schist, and phyllite (550-450 m.y. old, on the basis of K/Ar dating techniques; Steinkraus, 1980). The material is highly fractured and the fractures are filled with sparry dolomite or calcite and a fibrous sericitic mica. The rock is carbonaceous and consists of foliated quartz and dolomite (including isolated rhombs), euhedral pyrite, and sericite. Secondary overgrowths were detected on many quartz grains. About 20 ft (6 m) of this low-grade metamorphic basement rock was recovered in a conventional core (Core 6) from the bottom of the hole. The average dip of these strata appears to be about 25°, and the cutting samples indicate there is another 50 ft (15 m) of schist and slate above this core. An additional 400 ft (122 m) of dolomite and sandy, argillaceous dolomite that overlies the schistose rocks has also apparently been metamorphosed because much of the dolomitic rock is highly recrystallized and sericitic. The dolomitic rocks are dense, light to dark gray, unfossiliferous, and range from clean to argillaceous, silty, and sandy. Much of the dolomite is micritic and has no discernible original sedimentary structures, but sparry patches and veins are common; some samples exhibit intense recrystallization. Angular quartz and pyrite are common, and some anhydrite-filled voids occur.

DEPTH
FEET METERS
KELLY BUSHING 0
(K. B.)
0
SEA LEVEL
1000
500
2000
3000
1000
4000
5000
1500
6000
2000
7000
8000
SPONTANEOUS POTENTIAL (millivolts)
20 mv
CONDUC-TIVITY (millimhos/m)
6000 4000 2000 0
COMPENSATED FORMATION DENSITY (g/cm³)
1.25 1.50 1.75 2.00 2.25 2.50 2.75 3.00
SYSTEMS, SERIES, AND (OR) STAGE
CORING INTERVALS
LITHOLOGY
DESCRIPTION
TERTIARY AND QUATERNARY
PALEOCENE
UPPER CRETACEOUS
SANTONIAN
CONIACIAN
TURONIAN
CENOMANIAN TO APTIAN
LOWER CRETACEOUS
APTIAN
BARREMIAN TO BERRIASIAN
UPPER JURASSIC
KELLY BUSHING (K. B.)
SEA LEVEL (98 ft; 30 m below K. B.)
SEA FLOOR (255 ft; 78 m below K. B.)
Poorly consolidated gray-white sands and gravels with shell fragments and lignitic stringers or beds
Interbedded sand and shale
Gray shale
Unconsolidated, white, coarse-grained, calcareous sand and gravel with subordinate interbedded, varicolored shales
Argillaceous dolomite
Tan, coarse-grained sandstone, thick, reddish shale interbeds
Unconsolidated, coarse-grained sands
Unconsolidated, coarse-grained pebbly sands and thick, soft claystone
Medium-grained, calcareous sandstone; calcareous shales; thin dolomite beds
Tan-gray shale; fine- to coarse-grained sandstone
Calcareous, fine- to medium-grained, poorly consolidated to moderately cemented sandstone and red-brown shale

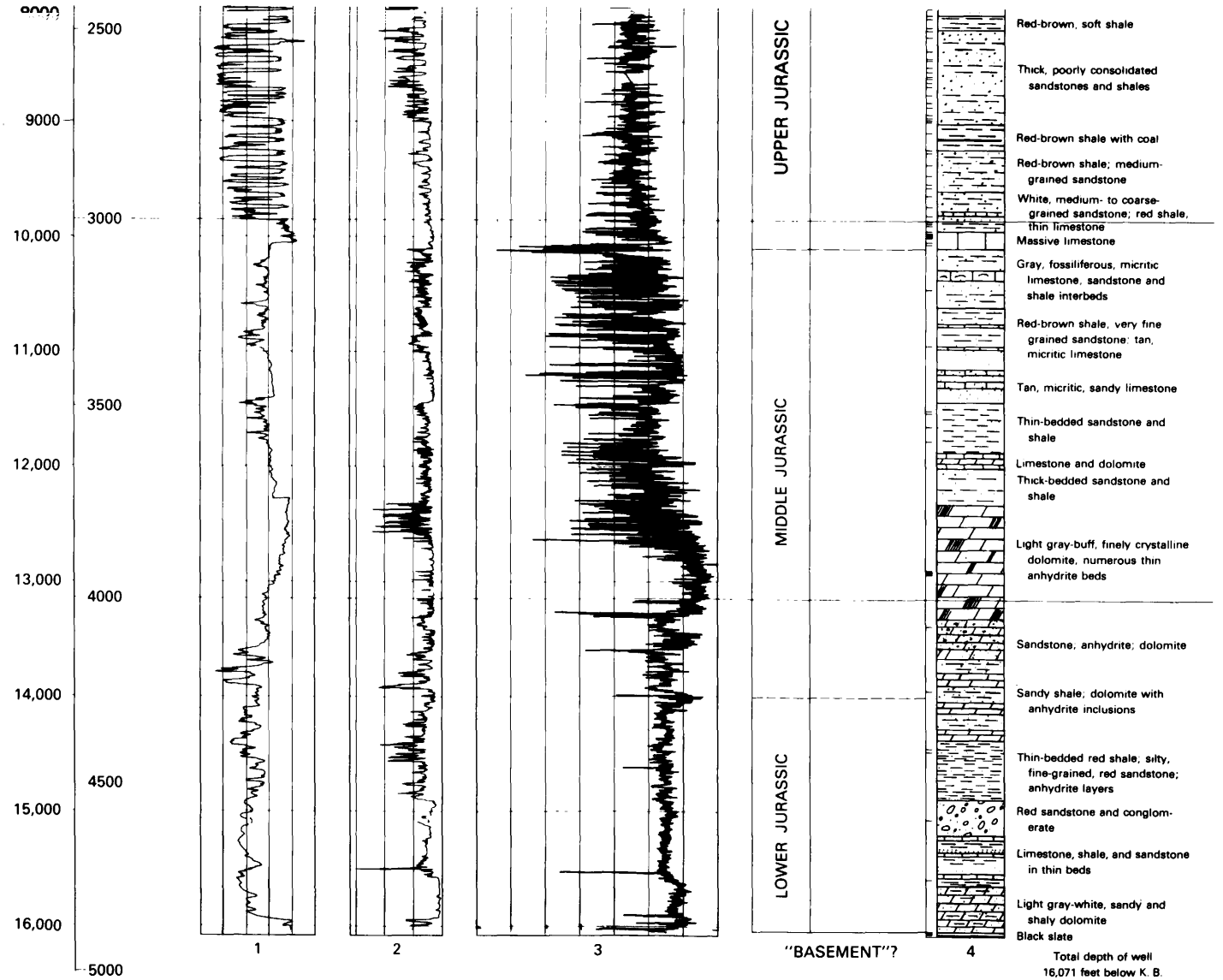

FIGURE 3.—Geophysical logs, lithology, and ages for the COST No. G-1 well. Modified from Scholle, Krivoy, and Hennessy (1980). Stratigraphic boundaries were based on preliminary data and do not match those shown elsewhere in this volume.

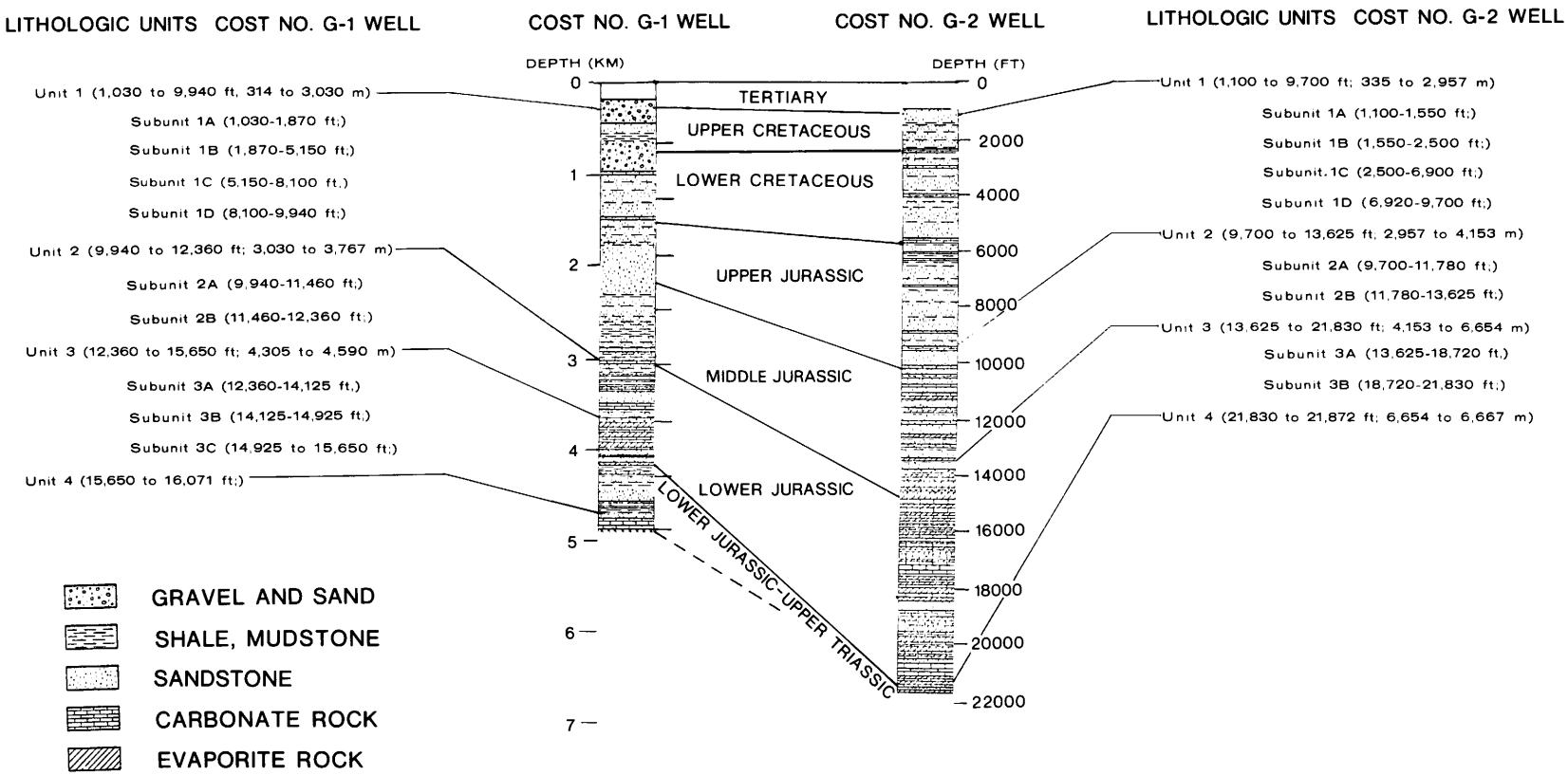

FIGURE 7.—Lithologic correlation between rocks from the COST Nos. G-1 and G-2 wells.

UNIT 3 (15,650–12,360 FT; 4,770–3,767 M) UPPER TRIASSIC TO LOWER JURASSIC

Unit 3 consists of varying proportions of sandstone, conglomerate, shale, dolomite, and anhydrite with minor amounts of limestone. It has arbitrarily been divided into 3 parts: subunit 3C consists of sandstone, conglomerate, conglomeratic sandstone, shale, and minor limestone; subunit 3B is composed of shale, sandy shale, sandstone, and thin interbedded dolomite and anhydrite layers; and in subunit 3A dolomite and anhydrite prevail and have variable amounts of interbedded sandstone and shale.

SUBUNIT 3C (15,650–14,925 FT; 4,770–4,549 M)

The dolomite of unit 4 is overlain by 150 ft (46 m) of pink to red, coarse- to very coarse-grained sandstones and interbedded red-brown shales with traces of lignite. Above this interval is about 350 ft (107 m) of similar rocks containing beds of light- to medium-gray limestone and dolomite. The proportion of conglomerate and conglomeratic sandstone increases upsection, and the uppermost 225 ft (69 m) consists of red to red-pink conglomerate, conglomeratic sandstone, sandstone, and subordinate amounts of shale.

The sandstones range in composition from lithic arenites to quartz wackes and arenites, which range from poorly to well sorted. Subangular to angular quartz predominates in most samples with minor amounts of metamorphic rock fragments (< 15%), potassium feldspar (< 5%), and plagioclase (< 1%). Many of the feldspars are highly altered to clay minerals (sericite and kaolinite). The low porosity of these sandstones is probably due to compaction and formation of carbonate-clay-iron mineral cements. Dolomite is the most common cement and occurs as irregular patches, replacements of framework grains, and as isolated rhombs. Ferruginous clay matrix cements are also common.

Most of these sediments appear to have been deposited in a nonmarine to marginal marine environment. The limestones in the middle of subunit 3C are medium to light gray and slightly argillaceous, and commonly contain pellets, mollusk fragments, and dolomite as isolated rhombs or patches and as zones of replacement of limestone. The limestones appear to have no primary or secondary porosity. Anhydrite occurs locally as blebs and nodules in shale and in a few beds of chickenwire structure.

SUBUNIT 3B (14,925–14,125 FT; 4,549–4,305 M)

This subunit consists largely of interbedded red-brown to dark-gray shale and fine- to medium-grained sandstone. Some sandstone beds are conglomeratic, and dolomite beds and anhydrite nodules and beds occur locally. The sandstones have little or no porosity and are similar in composition and texture, but are generally not as coarse grained as those of subunit 3C. Subunit 3B appears to have been deposited in a nonmarine to highly restricted marginal marine (sabkah-type) environment.

SUBUNIT 3A (14,125–12,360 FT; 4,305–3,767 M)

Subunit 3A is composed largely of dolomite and anhydrite and has lesser amounts of sandstone and shale. The lower 800 ft (244 m) of subunit 3A, which is transitional to 3B, consists largely of pink to red fine- to medium-grained sandstone and dark-gray to red-brown shale interbedded with buff to dark-gray dolomite and anhydrite. The shale and dolomite contain varying amounts of anhydrite as blebs, pore fillings and nodules. Dolomite beds become more abundant towards the top of 3A. The upper 965 ft (294 m) of subunit 3A consists almost entirely of buff to light- to dark-gray dolomite and interbedded thin, white to gray anhydrite layers.

The sandstones in the lower part of the unit range from feldspathic lithic wacke to lithic arenite and from feldspathic quartzarenite to wacke. Most sandstones are fine to medium grained (grains are angular to subangular), but some coarse-grained sandstone and conglomeratic (mainly granitic, based on descriptions of cores) sandstone is present. Quartz is the dominant mineral, ranging from 5 to 20 percent in the samples examined. Plagioclase and microcline equal about one-half the total feldspar in some samples, but potassium feldspars are the most common. Rock fragments vary in abundance, and many are difficult to identify because of their similarity to the framework grains. Granitic rock fragments are the most common and usually compose 5 to 10 percent of the framework grains. Fine-grained schistose and slaty fragments and

reworked carbonate and mudstone rock fragments are also present. Some of the sandstones contain up to 20 percent of clay-hematite matrix. Dolomite, siderite, and anhydrite cements and pore fillings commonly occur in the same sample. Quartz overgrowths are also quite common and result in sandstones with a tight, interlocking, or sutured fabric. Cementation and compaction have reduced porosity to less than 5 percent. Framework feldspars and those in granitic rock fragments are commonly altered to sericitic clay and kaolinite, but dolomite and anhydrite replacements of feldspar have eliminated most of the secondary porosity that may have resulted from the alteration.

The sedimentary sequence in subunit 3A records a change in depositional environment from fluctuating restricted marine and nonmarine at the base to largely restricted marine and shallow marine in the upper part. The dolomites in the upper part of the subunit are primarily micritic, but may exhibit patchy recrystallization. Veins or fractures are also filled with sparry dolomite, and anhydrite vein and pore fillings and nodules are also common. In a few samples, micritic dolomite exhibits a relict pelletal texture, and there are ghosts of replaced ostracod and mollusk fragments in other samples. Algal laminations are also present in some dolomite-anhydrite intervals. The dolomites are probably mostly primary, but dolomite replacement of original intertidal to subtidal carbonate mud probably also occurred.

UNIT 2 (12,360–9,940 FT; 3,767–3,030 M) LOWER JURASSIC (LOWER PLIENSBACHIAN) TO MIDDLE JURASSIC (BAJOCIAN)

The lower boundary of unit 2 represents a sharp lithologic change (also seen in the geophysical logs) from the dolomite-anhydrite interval of subunit 3A to predominantly sandstone and shale with some interbedded dolomite and limestone. Two subunits are defined: subunit 2B (12,360–11,460 ft; 3,767–3,493 m) comprises interbedded fine- to medium-grained sandstone and shale with some interbedded dolomite and limestone; subunit 2A (11,460–9,940 ft; 3,493–3,030 m) consists of interbedded limestone and dolomitic limestone, shale, and some siltstone to fine-grained sandstone. Predominantly carbonate and predominantly clastic intervals seem to alternate or intertongue on the order of thousands of feet (several hundreds of meters) in both subunits.

SUBUNIT 2B (12,360–11,460 FT; 3,767–3,493 M)

Subunit 2B contains interbedded thin- to thick-bedded, tan to pink or red, very fine- to medium-grained sandstone and gray to red-brown, somewhat silty or sandy shale. Thin beds of dense, buff to light-gray micritic dolomite and limestone also occur locally, and a relatively thick interval of dolomite and limestone occurs between 11,900 and 11,975 ft (3,627 and 3,650 m). A few thin lignitic or coaly beds are also present.

The carbonate intervals are micritic; limestone and dolomite occur together as interbedded or interlaminated strata and dolomite as a limestone replacement. These carbonate units are argillaceous, silty, or sandy, and are usually closely associated with clastic rocks. All gradations from silty and sandy carbonate rocks to dolomite- and calcite-cemented siltstone and sandstone are present. Anhydrite as rare laminae or blebs was noted in association with the carbonate rocks in subunit 2B. A few slightly fossiliferous (mollusk debris), pelletal carbonate mudstones were noted, but most beds are dense, micritic, and unfossiliferous. Little or no primary or secondary porosity appears to exist at these depths in the well.

Sandstones and siltstones are similar in composition and texture to those in unit 3, and are predominantly very fine-grained to medium-grained feldspathic quartz wackes or feldspathic lithic wackes. Clay-hematite cements are very common, and in some samples secondary quartz overgrowths are visible. Most sandstones and siltstones, including the more poorly sorted ones, are cemented with dolomite, siderite, or calcite. Porosity is usually less than 5 percent.

SUBUNIT 2A (11,460–9,940 FT; 3,493–3,030 M)

This subunit consists largely of interbedded buff to gray limestone and dolomite; tan to pink siltstone; fine-grained sandstone; and red-brown, green, and gray shale. It is distinguished from subunit 2B by the predominance of carbonate rocks, particularly in the lower 300 ft (91 m) and

the uppermost 150 ft (46 m). Limestone is more abundant than dolomite, and shale and sandy shale are the most common clastic rocks. Beds of lignite or coal occur locally.

The limestones are argillaceous and usually contain less than 10 percent fine sand- or silt-sized quartz. Most carbonate intervals are pyritic. Micritic textures are common, particularly in the lower part of this subunit, but pelletal calcareous mudstones also occur. Dolomite is common in the middle part of the unit in association with minor anhydrite pore fillings in the dominantly micritic dolomite. The uppermost limestone strata are much more fossiliferous: they contain fragments of mollusks, ostracods, benthic foraminifers, and echinoderms (crinoids). In addition, pellets and oolites are common constituents. Textures and compositions vary from pelletal calcareous mudstone to pellet-oolite packstone and fossiliferous calcareous packstone. The limestones have little primary or secondary porosity; sparry calcite or dolomite spar fills most void spaces, and micrite has apparently undergone patchy recrystallization to sparry calcite. There is little compaction or breakage evident in the constituents of packstones and grainstones, which suggests that cementation occurred early in the history of the carbonates of this subunit.

The siltstones and sandstones are similar in composition (feldspathic wacke to feldspathic quartz wacke and subordinate arenites) and texture to those of 2B, and have relatively poor reservoir characteristics.

The lithology of unit 2 records the transition from the prolonged restricted marine sabkah and tidal-flat conditions of subunit 3A to more open shallow marine (subtidal-intertidal) conditions in the lowest part, to alternating nonmarine and shallow marine, and back to shallow marine conditions at the top in lignitic, oolitic, pelletal, and fossiliferous limestone.

UNIT 1 (9,940–1,030 FT; 3,030–314 M) MIDDLE JURASSIC (BAJOCIAN(?)) TO UPPER CRETACEOUS (SANTONIAN)

The base of unit 1 is marked by the sudden disappearance of the fossiliferous limestone of subunit 2A. Lithologic unit 1 contains mostly pebbly sandstone and shale, but has some lignite or coal beds and minor amounts of limestone and dolomite. The abundance, coarseness, and composition of the sands change through the section, and four lithologic subunits are defined on the basis of these changes. Subunit 1D consists of interbedded, thick-bedded, tan to red-brown sandstone and shale and minor thin limestone beds. Subunit 1C contains more tan to red-brown and gray thin-bedded and pebbly sandstone, sandstone with fewer shale interbeds than subunit 1D, and some interbedded coal. Subunit 1B is composed of coarse- to very coarse-grained, commonly pebbly sand and lesser amounts of bedded gray shale, lignite, marlstone, limestone, and dolomite. Subunit 1A consists almost entirely of pebbly, fossiliferous, glauconitic, poorly consolidated quartz sand.

SUBUNIT 1D (9,940–8,100 FT; 3,030–2,469 M)

This subunit is made up of light-gray to tan, pink, and light red, fine- to coarse-grained, mostly poorly to moderately sorted sandstone interbedded with red to red-brown and tan to gray micaceous silty shale and shale. Coal is fairly abundant in the sequence, and there are a few thin, light-gray to buff, micritic, argillaceous limestone beds.

The sandstone beds range from lightly cemented to poorly consolidated. The porosity is as high as 25 percent, but permeabilities (figs. 8 and 9) are low, in part because most of the sandstones are feldspathic quartz wackes, consisting of 60 to 80 percent quartz, 10 to 15 percent feldspar (about equal amounts of K-feldspar and plagioclase), and small percentages of rock fragments. Plant fragments, muscovite, and pyrite and other heavy minerals are trace constituents. Feldspars are commonly altered to clay minerals or replaced by carbonate minerals. The sandstones are cemented by silica-clay mixtures, much of which was probably original matrix material, or by calcite and dolomite. The degree of consolidation generally decreases upward.

The shale and limestone beds are apparently unfossiliferous and typically silty or sandy. Limestones are buff-tan to light gray, argillaceous, and micritic in texture. Because of the absence of fossils and the association of coal, oxidized sands, and shales, the sedimentary rocks of subunit 1D are interpreted as having been deposited in a nonmarine, possibly deltaic, environment.

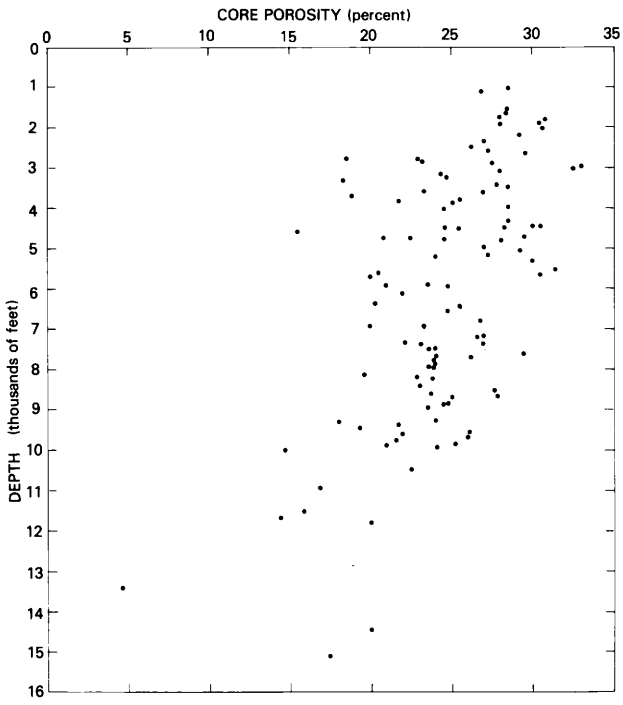

FIGURE 8.—Porosity versus depth for the COST No. G-1 well, from measurements on sidewall cores. After Lachance and Amato (1980); data from Core Laboratories, Inc.

SUBUNIT 1C (8,100–5,150 FT; 2,469–1,570 M)

The sediments of this lithologic subunit differ little from those of subunit 1D, except that the sandstone and shale are apparently more thinly bedded and more frequently interbedded in subunit 1C, and that the sandstone beds are medium to very coarse grained and commonly pebbly as well. Coal is present in subunit 1C, but not as abundant as in subunit 1D. Limestone beds are relatively uncommon, but much of the sandstone is calcareous. The interbedded shales are red-brown to about 6,500 ft (1,983 m), but above that level they are tan to gray and green.

These feldspathic quartz wacke sandstones are similar in composition to those in subunit 1D. The porosity and permeability vary depending on the degree of sorting, but some sandstones with good reservoir potential are present in the interval between 8,000 and 7,000 ft (2,430 and 2,134 m). Carbonate cements are common in some intervals.

The sedimentary rocks of subunit 1C record deposition under nonmarine conditions at the base of the unit and shallow marine conditions near the top, possibly in a deltaic environment.

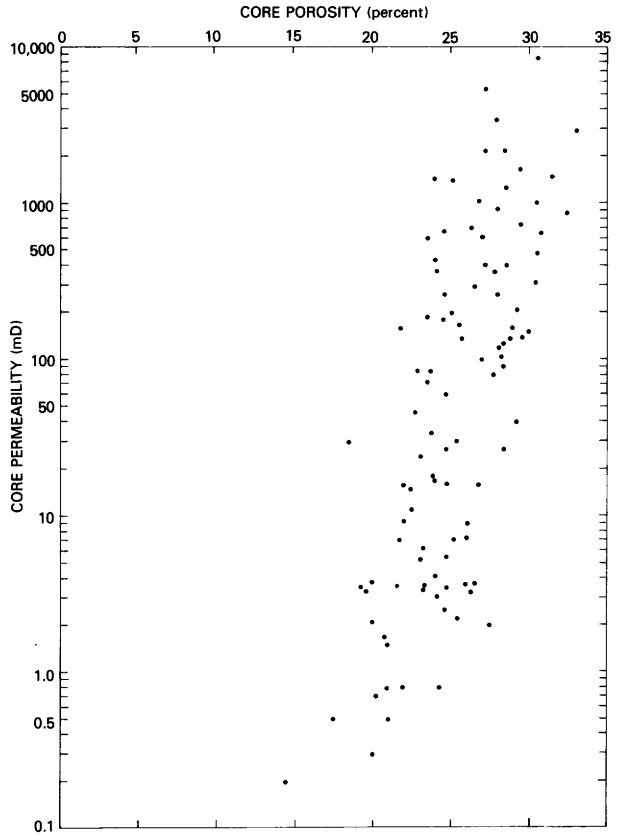

FIGURE 9.—Porosity versus permeability for the COST No. G-1 well, from measurements on sidewall cores. After Lachance and Amato (1980); data from Core Laboratories, Inc.

SUBUNIT 1B (5,150–1,870 FT; 1,570–570 M)

Thin to thick, tan to buff, medium- to coarse-grained sands with interbedded gray to reddish shales and marls and some beds of light-gray-buff argillaceous dolomite characterize lithologic subunit 1B. The sands are poorly consolidated and have porosities up to 35 percent and variable but often high permeabilities (figs. 8 and 9). Sand or sandstone is prevalent from 4,800 to 4,100 ft (1,463 to 1,250 m) and from 3,600 to 2,400 ft (1,097 to 731 m), whereas shale dominates the remainder of the subunit.

Lignite or coal is common in many parts of the sequence, and there is pyrite in both shales and sands. Above 3,650 ft (1,112 m) the sands contain calcareous worm tubes, mollusk fragments, gastropods, foraminifers, bryozoa, and abundant organic (terrestrial plant?) matter. A thick, fossiliferous, sandy dolomite bed occurs between 3,540 and 3,570 ft (1,079 and 1,088 m).

Sands and sandstones are commonly coarse to very coarse grained and poorly sorted, but some very well-sorted beds are present. Grains are angular to subrounded. Quartz pebbles occur in many intervals. The degree of cementation is variable, and calcite, siderite, and dolomite cements are present. The sands and sandstones range from feldspathic quartz wacke to quartz-arenite. The feldspar content seems to generally decline upsection as the degree of sorting increases.

The sediments of subunit 1B were deposited primarily under shallow marine conditions, but intervals of nonmarine deposition are possible.

SUBUNIT 1A (1,870–1,030 FT; 570–314 M)

This subunit consists almost entirely of pebbly, poorly to well sorted, poorly consolidated quartz sand. Pebbles are usually quartzose and the sand is micaceous, glauconitic, pyritic, and fossiliferous, containing numerous fragments and whole skeletons of bryozoans, planktic and benthic foraminifers, and Inoceramids and other mollusks. Clay and calcite or siderite compose the matrix (or cement, when present). Porosities are commonly greater than 25 to 30 percent and permeability is moderate to high (fig. 8). Some glauconitic and sideritic shale is also present in the section. Lignite beds and pyritic, carbonaceous shale occur between 1,500 and 1,575 ft (457 and 480 m). The sequence represents predominantly marine shelf deposition. No cuttings were obtained from above 1,300 ft (396 m).

DESCRIPTION OF THE COST NO. G-2 WELL SEQUENCE

The 21,872 ft (6,667 m) of sedimentary section penetrated in the COST No. G-2 well (fig. 10) in the Georges Bank basin is here divided into four major lithologic units (fig. 7). These are described from the bottom to the top of the well.

UNIT 4 (21,872–21,830 FT; 6,667–6,654 M) UPPER TRIASSIC (RHAETIAN?) OR LOWER JURASSIC

Unit 4 consists of halite with anhydrite inclusions. No cuttings of salt were recovered, probably because it dissolved during drilling and washing. However, the presence of salt is inferred from a sudden increase in penetration rate during drilling, a large increase in the salinity of drilling mud, and the very clear anhydrite crystals. The salt unit is tentatively correlated to the Argo Formation of Early Jurassic age on the Scotian shelf (Bielak and Simonis, 1980).

UNIT 3 (21,830–13,625 FT; 6,654–4,153 M) LOWER TO MIDDLE JURASSIC (HETTANGIAN(?) TO BATHONIAN(?))

This unit is composed of dolomite and limestone, interbedded with anhydrite, and rare fine- to very fine-grained sandstone and shale beds. The sedimentary rocks of unit 3 were deposited in restricted marine and marginal marine environments. Two subunits have been defined: subunit 3B of dolomite and anhydrite with some interbedded limestone, siltstone, sandstone, and shale; and subunit 3A of limestone and dolomite with interbedded anyhydrite.

The organic carbon contents of rocks in unit 3 (Miller and others, this volume) are low, averaging about 0.2 to 0.3 weight percent, and the hydrocarbon source potential of the entire unit appears low. Porosity and permeability (figs. 11 and 12) are also low, suggesting very poor reservoir quality.

SUBUNIT 3B (21,830–18,720 FT; 6,654–5,706 M (LOWER JURASSIC(?))

The lower part of this subunit consists of interbedded anhydrite and dolomite with all intergradations of the two lithologies. The dolomite is light to medium gray and brown and is micritic to sparry. Although some vugs and intercrystalline pores up to 0.5 mm in diameter were noted, these probably resulted from preparation of the sections; remnants of anhydrite or halite(?) were found in many of the pores. Much of the dolomite is massive and micritic or exhibits patchy recrystallization to sparry dolomite (or dolomite pore fillings). In a few zones in the lower part of subunit 3B, dolomite has replaced original oolitic and pelletal limestone. The open and uncompacted structure of the original oolites and pellets suggests early dolomitization.

Limestone is rare in the lower part of subunit 3B, but becomes more abundant upward. There

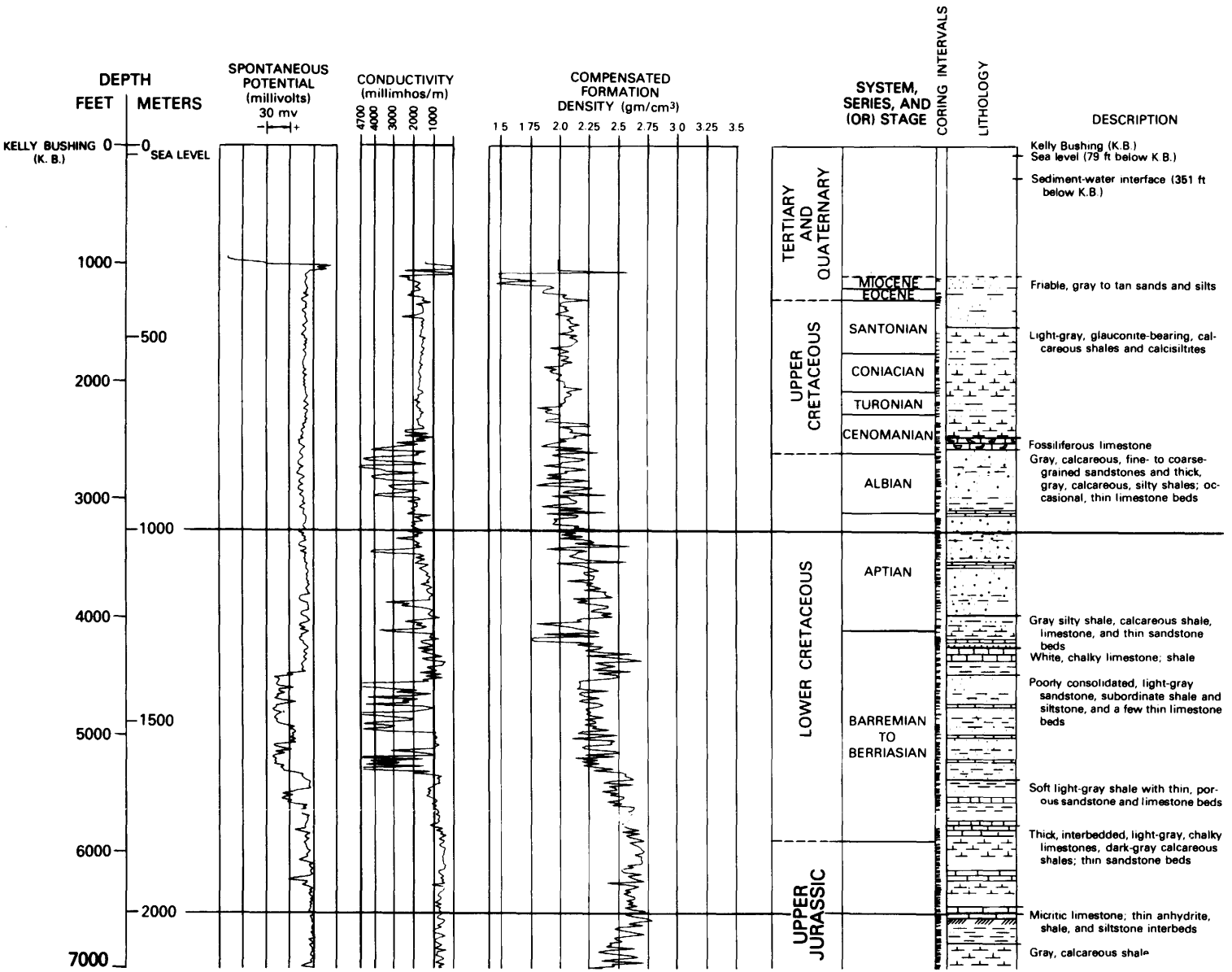
DEPTH
FEET
METERS
KELLY BUSHING (K. B.)
0
SEA LEVEL
1000
500
2000
3000
1000
4000
1500
5000
6000
2000
7000
SPONTANEOUS POTENTIAL (millivolts)
30 mv
CONDUCTIVITY (millimhos/m)
4700
4000
3000
2000
1000
COMPENSATED FORMATION DENSITY (gm/cm³)
1.5
1.75
2.0
2.25
2.5
2.75
3.0
3.25
3.5
SYSTEM, SERIES, AND (OR) STAGE
CORING INTERVALS
LITHOLOGY
DESCRIPTION
TERTIARY AND QUATERNARY
MIOCENE
EOCENE
UPPER CRETACEOUS
SANTONIAN
CONIACIAN
TURONIAN
CENOMANIAN
ALBIAN
LOWER CRETACEOUS
APTIAN
BARREMIAN TO BERRIASIAN
UPPER JURASSIC
Kelly Bushing (K.B.)
Sea level (79 ft below K.B.)
Sediment-water interface (351 ft below K.B.)
Friable, gray to tan sands and silts
Light-gray, glauconite-bearing, calcareous shales and calcisiltites
Fossiliferous limestone
Gray, calcareous, fine- to coarse-grained sandstones and thick, gray, calcareous, silty shales; occasional, thin limestone beds
Gray silty shale, calcareous shale, limestone, and thin sandstone beds
White, chalky limestone; shale
Poorly consolidated, light-gray sandstone, subordinate shale and siltstone, and a few thin limestone beds
Soft light-gray shale with thin, porous sandstone and limestone beds
Thick, interbedded, light-gray, chalky limestones, dark-gray calcareous shales; thin sandstone beds
Micritic limestone; thin anhydrite, shale, and siltstone interbeds
Gray, calcareous shale

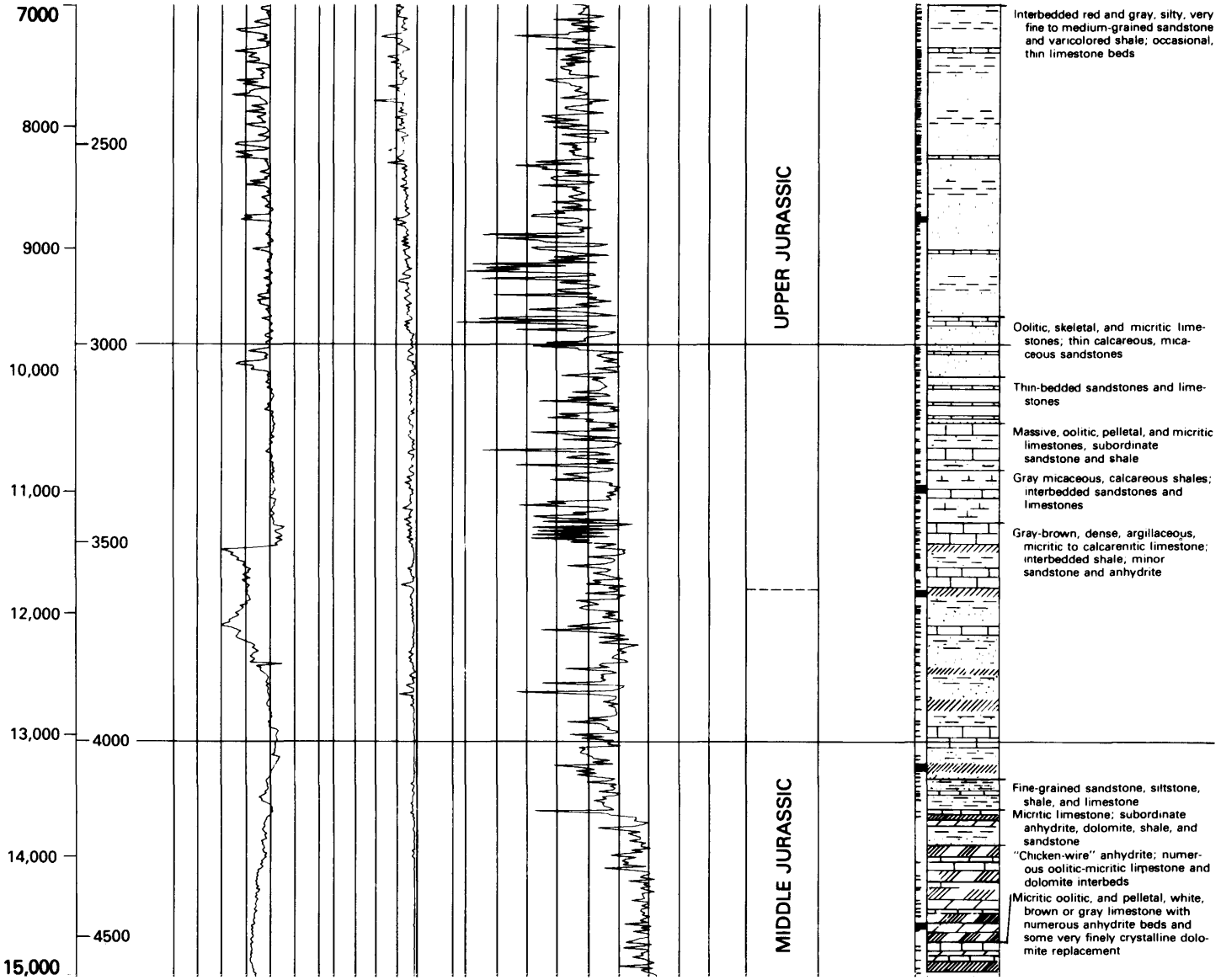

FIGURE 10.—Geophysical logs, lithology, and age for the COST No. G-2 well. Modified from Scholle, Schwab, and Krivoy (1980). Stratigraphic boundaries were based on preliminary data and do not match those shown elsewhere in this volume.

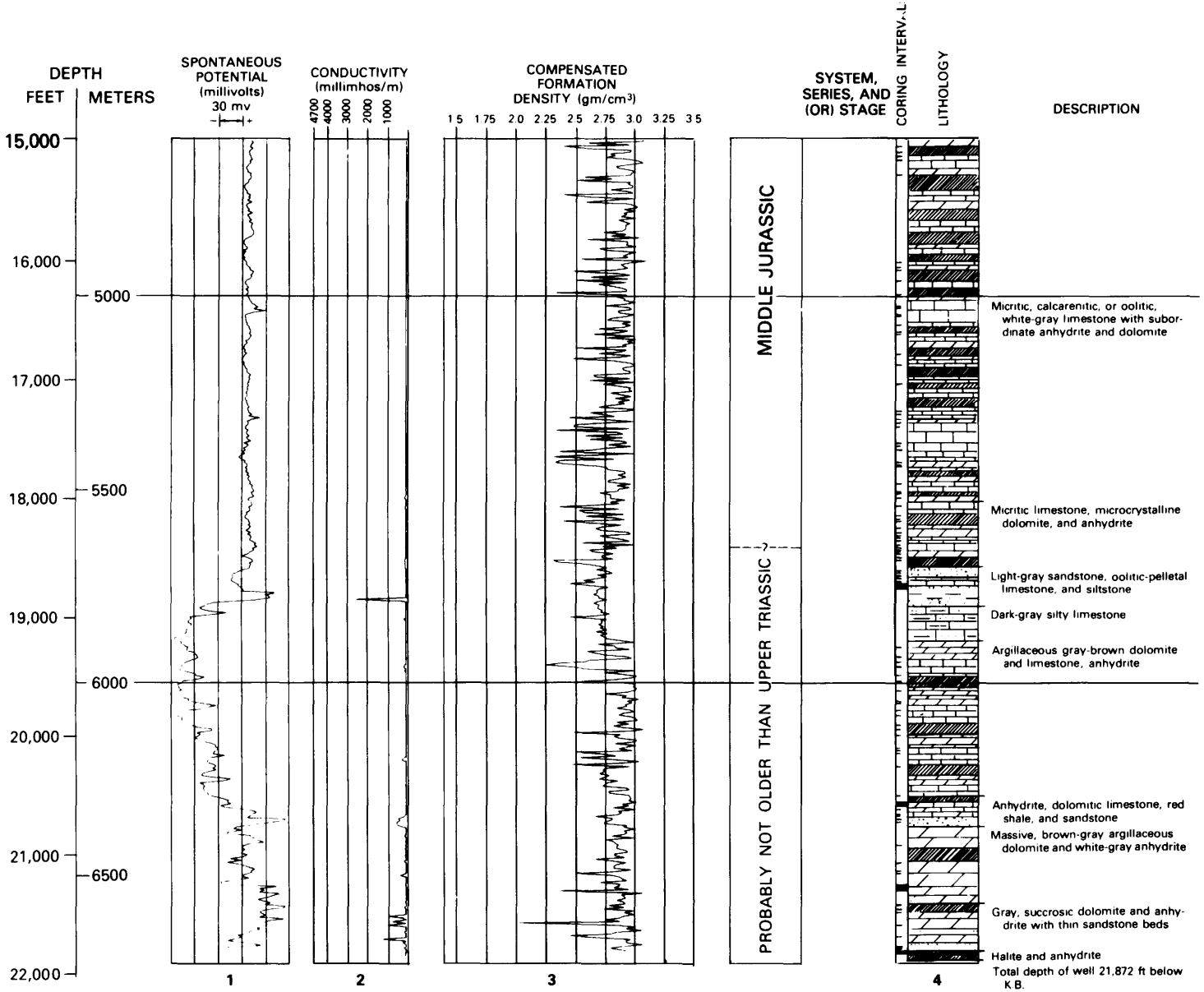

FIGURE 10.—Geophysical logs, lithology, and age for the COST No. G–2 well—Continued

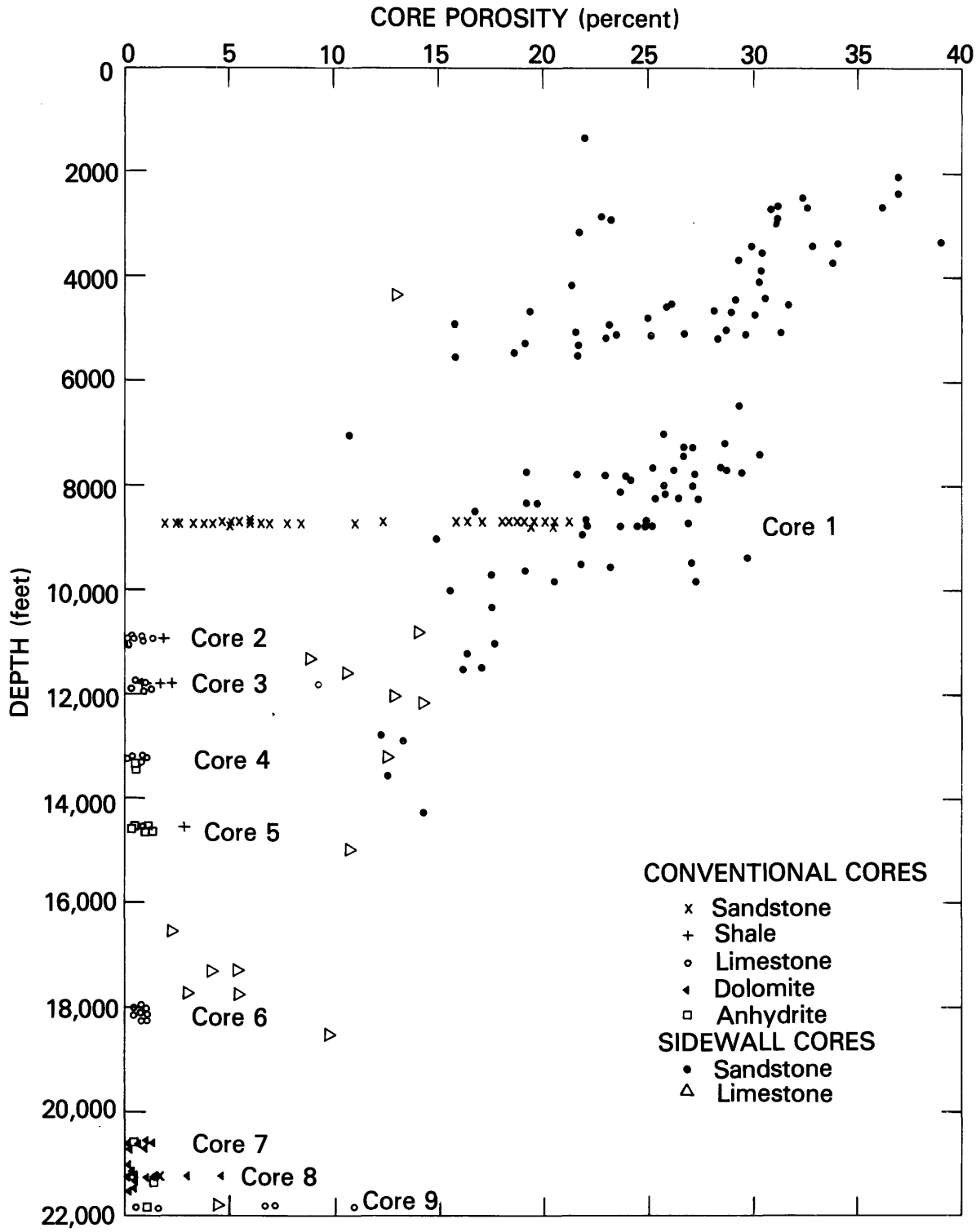

FIGURE 11.—Porosity versus depth for the COST No. G-2 well, from measurements on sidewall cores. After Malinowski (1980); data from Core Laboratories, Inc.

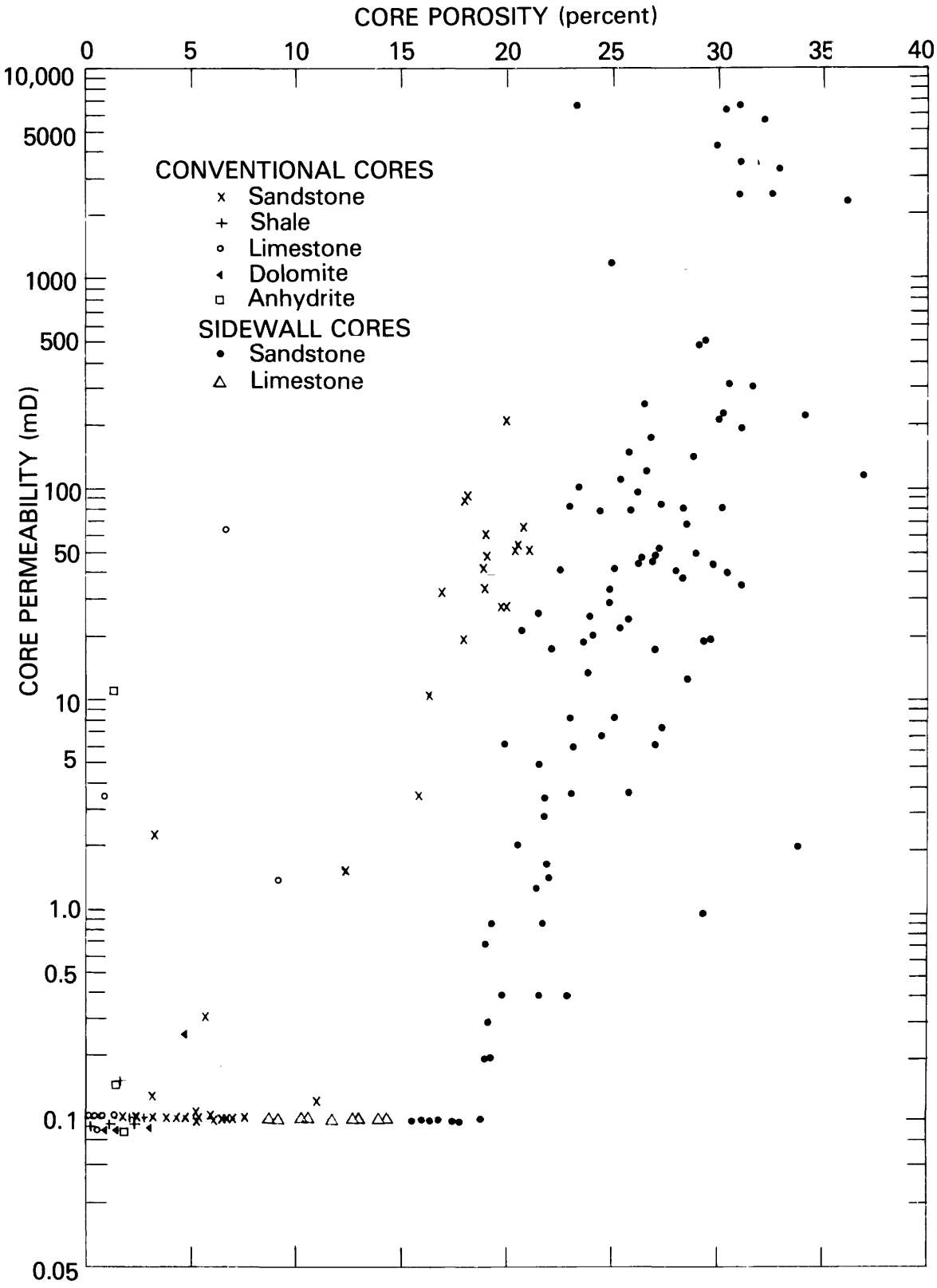

FIGURE 12.—Porosity versus permeability for the COST No. G-2 well, from measurements on sidewall cores. After Malinowski (1980); data from Core Laboratories, Inc.

are several layers of oolite or pellet packstones and grainstones, but calcareous mudstones or dolomitized calcareous mudstones are most common. Some samples suggest the presence of interbedded boundstone layers as well. These algal laminates contain silt-sized subangular quartz and appear to be rich in organic matter. Many of the calcareous mudstones contain fractures or vugs filled with anhydrite. A few fossiliferous calcareous wackestones are also present in subunit 3B, containing fragments of ostracods, large benthic foraminifers, echinoderms, and mollusks. Oolites and calcareous fossils are commonly micritic.

The few sandstones in this subunit are highly compacted, well cemented, fine- to very fine-grained arkosic wackestones and feldspathic quartz wackestones. Feldspars are commonly chloritized and the framework quartz grains have sutured contacts with one another. Clay, micas, and dolomite usually make up the intergranular matrix. A few thin, brown to gray, calcareous and silty shales also occur interbedded with the sandstones and dolomitic sandstones. The upper 60 ft (18 m) of subunit 3B consists of dolomitic sandstones and silty to sandy dolomite. Clastic grains are mostly quartz and reworked carbonate particles such as pellets and fossil fragments. Simonis (1980) noted a green tuffaceous shale layer at 18,960 ft (5,779 m).

SUBUNIT 3A (18,720–13,625 FT; 5,700–4,153 M (LOWER TO MIDDLE JURASSIC)

Subunit 3A comprises tan to medium-gray limestone interbedded and intergradational with dolomite and anhydritic dolomite, and light-gray, white, and translucent, nodular to laminated anhydrite. Sandstone and siltstone beds are rare in the lowermost 50 ft (15 m) of the subunit, where it is transitional to the sandy dolomites and dolomitic sandstones of upper subunit 3B.

The limestone and dolomite are variable in texture. Calcareous mudstones, argillaceous calcareous mudstones, and massive dolomicrites are the most common. There is patchy recrystallization to anhedral sparry calcite or dolomite in some samples. Vugs and other original intercrystalline pore spaces are commonly filled with anhydrite, particularly in the dolomite beds. Small amounts of disseminated silt-sized quartz are common. A second kind of texture is pelletal or oolitic calcareous packstone and wackestone or dolomitized versions of these textures. Some grainstones are also present. Some of these intervals are fossiliferous and contain fragments of ostracods and other mollusks. Many of the calcareous fossil constituents are recrystallized or have micritic envelopes. There is little or no porosity remaining in most intervals. The generally uncompacted textures suggest early cementation, dolomitization, and filling of vugs by anhydrite or carbonate spar. Little secondary porosity has been formed.

UNIT 2 (13,625–9,700 FT; 4,153–2,957 M) MIDDLE AND UPPER(?) JURASSIC (BATHONIAN(?)-OXFORDIAN(?))

Unit 2 differs from the underlying unit in that it is composed almost entirely of limestone with minor interbedded sandstones and very rare intervals of dolomite and anhydrite. Unit 2 represents a change from carbonate-evaporite deposition in restricted marginal-marine and high-energy, open-marine shelf conditions to deposition in a more open carbonate shelf setting of variable energy.

SUBUNIT 2B (13,625–11,780 FT; 4,153–3,590 M) BATHONIAN(?)-CALLOVIAN(?)

The lower 265 ft (81 m) of subunit 2B are brown-red sandstone and silty hematitic-limonitic mudstone and shale. The sandstones are poorly to moderately sorted, very fine- to medium-grained feldspathic quartz wackes. The sandstones are highly compacted and have sutured grain contacts, some dolomitic cement, and dolomite rhombs replacing feldspar. The mudstone and shale are slightly calcareous and contain disseminated silt-sized quartz. This part of the unit probably represents a tongue of nonmarine clastic sediments deposited after restricted marine deposition of carbonates and evaporites and before the limestones formed in more open marine environments.

Brown to medium-gray micritic limestones predominate in the remainder of subunit 2B, but a few beds of pellet and oolite calcareous packstone and grainstone also occur, as do thin layers of gray, calcareous, silty mudstone. Many of the calcareous mudstones are burrow-mottled and contain pellets, articulated ostracod fragments, and fine-grained disseminated quartz silt. Some

beds may be classified as boundstones on the basis of laminated algal texture. Pyrite and disseminated wisps of organic matter are also common. Original or secondary pores are filled by sparry calcite, and some calcareous mudstones exhibit a dismicritic texture. Stylolitic seams are common, as are spar-filled fractures. Rare dolomite rhombs and anhydrite were noted in some samples.

The pelletal and oolitic packstone beds are also tightly cemented, and original voids are filled with sparry calcite. Ostracod fragments, quartz silt, echinoderm plates, and benthic foraminifers are common to abundant in some of the reworked carbonates, which were deposited in an apparently high-energy environment.

Fragments of altered, green, tuffaceous(?) claystone were also found between 11,720 and 12,100 ft (3,572 and 3,688 m). The fragments are vesicular and have a felted, devitrified groundmass surrounding elongate altered feldspar(?) phenocrysts.

SUBUNIT 2A (11,780–9,700 FT; 3,590–2,957 M) CALLOVIAN-OXFORDIAN(?)

The rocks of this subunit, including the limestones, exhibit a more clastic character, indicated by the prevalent angular to subrounded quartz sand and silt grains in mudstone and limestone, and by the abundance of intraclast and oolitic-pelletal limestones. Moderately sorted, fine- to medium-grained sandstone beds of quartz wacke occur in the lower part of the subunit and are somewhat thicker and more common in the upper part. These sandstones are commonly interbedded with argillaceous calcareous mudstones near the base of the subunit and algal intraclast boundstones, intraclast packstones, and pellet or oolite lime mudstones to packstones in the upper part. Some fossiliferous packstones also occur. Most of the limestones are tightly cemented with calcite spar or silty clay filling the original void space, but some samples have porosities as high as 15 percent. Fragments of ostracods are common throughout 2A, and echinoderm plates and spines, mollusk and brachiopod fragments, benthic foraminifers, rare coral and bryozoan fragments, and calcareous algae are also present. Individual grains are usually micritized.

Sandstone beds range from poorly sorted argillaceous types to moderately sorted calcite-cemented varieties in which the cement encloses framework grains, resulting in poikilotopic texture. There is an apparent increase in porosity of the sandstone beds at the top of subunit 2A.

Shale and silty mudstone occur in some parts of the section. The shale and mudstone range from calcareous, gray to black intervals to hematitic, red, silty, nonfossiliferous zones. The organic-carbon and pyrite content of shales in the upper part of subunit 2A is high, commonly greater than 0.6 weight percent.

The depositional environment of subunit 2A sediments apparently varied from high-energy shallow marine to nonmarine, and the proportion of terrigenous clastic sediments increases upward in the section.

UNIT 1: (9,700–1,100 FT; 2,957–335 M) MIDDLE AND UPPER JURASSIC(?) (CALLOVIAN AND OXFORDIAN) TO TERTIARY (MIOCENE AND PLIOCENE)

The sediments of unit 1 are dominantly marine clastics but have intervals of interbedded limestone and a few nonmarine sandstone-coal-shale sequences. The sedimentation rates decrease upward, and shallow-marine conditions prevailed from the Late Cretaceous through the Cenozoic. The sands of this unit possess good reservoir characteristics.

SUBUNIT 1D (9,700–6,920 FT; 2,957–2,109 M) CALLOVIAN AND OXFORDIAN TO UPPER KIMMERIDGIAN

Interbedded white to red sandstone, gray to tan oolitic and algal intraclast limestone, and gray to red and maroon shale with thin coal stringers make up most of subunit 1D. The sediments are predominantly red to 7,840 ft (2,390 m). The sandstones are primarily fine to medium grained and moderately to well sorted, and they vary in degree of cementation. Some intervals are more silt- and clay-rich. Porosity ranges from less than 10 percent in fairly tightly calcite-cemented zones to as much as 30 percent in more friable intervals. The sandstones are feldspathic quartz wackes to arenites. Framework grains are angular to subangular and consist of 60 to 90 percent quartz, less than 15

percent feldspar (K-feldspar and plagioclase), and muscovite, chlorite, some carbonate rock fragments, and a variety of heavy minerals. The feldspars are commonly altered to clay minerals. Dispersed organic material is relatively abundant.

The shales or mudstones are calcareous and silty and have high organic carbon contents (0.5 to 1.2 weight percent), especially in the gray shales within the upper part of the subunit. The more organic-rich intervals, which include thin coal or lignite interbeds, are also pyritic. Dark-gray shales are commonly interbedded with the limestone intervals, whereas red shales are interbedded with tan to red sandstones in the lower part of subunit 1D.

Limestone beds are present throughout the section, but their total thickness is less than that of the sandstone. The limestones are oolitic and pellet packstones and grainstones, algal intraclast packstones and boundstones, and some pellet calcareous mudstones to algal lime mudstones. Relatively little primary or secondary porosity was noted in thin sections of the limestones. Nearly all packstones and grainstones have sparry calcite fillings of void spaces. Ostracod and mollusk fragments, echinoderm plates, and benthic foraminifers are the most common faunal constituents. Apparent laminae of blue-green algae bind some intraclast limestones. Many of the limestone beds are silty and contain variable amounts of organic matter and pyrite.

The depositional environment of subunit 1D apparently varied from a nonmarine delta to a shallow marine, high-energy, mixed carbonate-clastic shelf.

SUBUNIT 1C (6,900–2,500 FT; 2,103–762 M)
UPPER KIMMERIDGIAN TO APTIAN AND ALBIAN

Subunit 1C consists of a mixture of lithologies deposited mainly in marginal marine to shallow marine environments. Limestone intervals are sandwiched between sandstone-shale-coal sequences. Porosity reaches as much as 35 percent, but is quite variable from one interval to another.

The lower 1,200 ft (366 m) of subunit 1C consists of fossiliferous calcareous mudstone and chalky mudstone with minor quartz sand and silt and some interbedded gray calcareous shale. Articulated and fragmented ostracods, gastropods, bivalves, echionoderm plates and spines, and benthic foraminifers are common faunal constituents.

Thick-bedded, coarse- to very coarse-grained, poorly consolidated quartzarenites predominate from about 5,740 to 4,500 ft (1,750 to 1,372 m). These are interbedded with dark-gray to brown-gray, somewhat organic-rich shale or mudstone, coal, and lignite. Fine- to medium-grained, well-sorted sandstone beds also occur, but these are usually tightly cemented by calcite or silica. Calcite cements predominate near the bottom of this interval in transition to the limestone sequence. The proportion of calcareous mudstone beds also increases in the lower part of this interval.

Limestone beds characterize the interval from about 4,500 to 3,950 ft (1,372 to 1,204 m). These are primarily argillaceous, glauconitic, chalky mudstone, but include some fossiliferous oolitic wackestone, packstone, and grainstone beds. Primary or secondary porosity in these beds is fairly high. Glauconitic sandstone and gray calcareous shale is interbedded in the upper part of this interval, and silty calcareous mudstone predominates up to about 300 ft (91 m) in the section.

Sandstone, interbedded with gray, glauconitic silty mudstone, composes the upper 500 ft (153 m) of subunit 1C. The sands range from those that are tightly cemented with calcite to friable, fine- to coarse-grained, granular, moderately to well sorted, subangular to subrounded quartz wackes to arenites. Glauconite is common, as are mollusk fragments, lignite, and foraminifers.

SUBUNIT 1B: (2,500–1,550 FT; 762–472 M)
APTIAN AND ALBIAN TO LOWER SANTONIAN

Argillaceous to silty calcareous mudstone and chalk compose the bulk of subunit 1B. These sediments were deposited in an open marine, possibly outer shelf environment. Glauconite, ostracods, planktic and benthic foraminifers, Inoceramid fragments, molluscan shell fragments, quartz silt and sand, organic matter, and pyrite are common constituents. The degree of induration and cementation by calcite varies, but most coarser grained intervals are fairly tightly cemented.

SUBUNIT 1A: (1,550–1,100 FT; 472–335 M)
LOWER SANTONIAN TO MIOCENE

This subunit is characterized by unconsolidated marine clastic sediment, predominantly tan to white, fine- to coarse-grained, moderately to well sorted, granular to pebbly quartzarenite interbedded with gray, silty, glauconitic calcareous mudstone and glauconitic siltstone.

SUMMARY

The COST No. G–1 well was drilled on a basement high to a depth of 16,071 ft (4,898 m) and is located in shallower water, farther inshore than the COST No. G–2 well, which was drilled to a depth of 21,874 ft (6,667 m). The G–1 well reached Paleozoic basement, consisting of black slate, phyllite, and metadolomite unconformably overlain by Early Jurassic and younger carbonate and clastic rocks. The G–2 well bottomed in a dolomite-evaporite sequence of possible Late Triassic or Early Jurassic age. The sedimentary rocks in both wells reflect deposition primarily in a shallow marine setting. It appears that the strata at G–1 were deposited in shallower water nearer a source of clastic detritus than the strata at G–2, which contain more carbonate rocks deposited in an inner- to outer-shelf setting. Overall subsidence and sediment accumulation rates during the Jurassic and Early Cretaceous at G–1 were lower than those of the shelf in the vicinity of the G–2 well.

Nearly 3,900 ft (1,189 m) of Upper Triassic and Lower Jurassic strata were penetrated in the G–2 well. These consisted mainly of interbedded dolomite and anhydrite and subordinate amounts of limestone, shale, and siltstone or sandstone. The lithologies suggest deposition in a restricted marginal marine setting characterized by net evaporation. Environments ranged from supratidal (indicated by nodular anhydrite, dolomite, and sand), to shallow subtidal (indicated by pelletal calcareous mud and oolitic wackestone to packstone). Triassic rocks probably do not exist in the vicinity of the G–1 well, but about 2,100 ft (640 m) of Lower Jurassic interbedded red shale, sandy-silty shale, red sandstone and conglomerate, sandy dolomite, dolomite, and minor anhydrite were penetrated. These lithologies reflect deposition in nonmarine to restricted marginal-marine environments.

Middle Jurassic strata are present in both the G–2 (6,500 ft; 1,981 m thick) and G–1 (3,900 ft; 1,189 m thick) wells. Interbedded dolomite, anhydrite, and micritic, calcarenitic, and oolitic limestone compose most of the sequence at the G–2 well (plate 1), except for some more sandy, silty and argillaceous beds in the upper part of the Middle Jurassic sequence, again suggesting shallow-shelf to restricted marginal-marine depositional environments. The Middle Jurassic at G–1 is characterized by fine-grained dolomite and subordinate anhydrite beds at the base, which give way upward to mainly thin-bedded sandstone, shale, and sandy limestone.

The Upper Jurassic sequence at the G–1 well is about 4,400 ft (1,341 m) thick and consists largely of medium- to coarse-grained sandstone beds and thick intervals of red to tan shale and silty to sandy shale. Sandstones in the upper part are cemented with calcite or dolomite but are poorly consolidated and more argillaceous in the lower part. The Upper Jurassic at the G–2 well is about 5,800 ft (1,768 m) thick and much more calcareous than that at the G–1 well. Limestones, including oolitic, calcarenitic, and micritic types, predominate in the lower and upper portions of this interval, but sandy limestone, calcareous shale, and fine- to medium-grained calcareous sandstones also occur, particularly in middle and upper intervals. The contrast between lithologies at the G–1 and G–2 wells suggests a predominantly nonmarine or marginal marine-deltaic environment in the vicinity of G–1 and shallow-marine deposition at G–2.

About 3,400 ft (1,036 m) of Lower Cretaceous strata were penetrated at the G–2 well. These units consist largely of micritic limestone, chalk, silty and calcareous shale, and sandstone. Glauconite is common in all strata. The G–2 well encountered about 2,500 ft (762 m) of Lower Cretaceous coarse-grained pebbly sands, coarse-grained calcareous sands, and thin, interbedded claystone, as well as some argillaceous dolomite. Upper Cretaceous strata are 1,400 to 1,600 ft (427 to 488 m) thick at both wells. Coarse-grained sands, gravels and shales predominate at the G–1 well, whereas mainly glauconitic chalks, argillaceous chalks, and fine-grained sands and silts occur in the G–2 well. The lithologic trends of Cretaceous sediments reflect a more nearshore, clastic-dominated depositional environment for the vicinity of the G–1 well and open shelf, even

pelagic, conditions near the G-2 well. The little sediment of Tertiary age recovered from both wells consists mainly of sand.

Reservoir quality is apparently poor in both wells below about 10,000 ft (3,048 m). This can be seen both in a sharp decline in porosity and permeability measured on sidewall core samples (figs. 8, 9, 11, and 12) and from petrographic study of sidewall core and cutting samples. Limestone and dolomite beds in both wells are extremely tight (plate 2); no significant secondary porosity was observed in any samples, and much recrystallization is evident. In the G-2 well, many of the sandstones and siltstones interbedded with calcareous sequences below 10,000 ft (3,048 m) are either highly compacted, exhibiting sutured grain contacts, or tightly cemented with dolomite or calcite. Above 10,000 ft (3,048 m) most samples were calcite cemented; cementation appears to have been relatively early, before significant compaction. Poikilotopic textures are common. Sandstones above 10,000 ft (3,048 m) in the G-1 well are commonly argillaceous and typically cemented by hematite, ankerite or siderite, or, less commonly, calcite. However, some primary porosity is preserved in many of the better sorted sands.

PLATE 1

Thin-section photomicrographs of characteristic carbonate rocks recovered in the COST No. G-2 well (all with crossed nicols; field of view approximately 0.5 mm, except in D, which is 2 mm).

Figure A. Pellet packstone containing pyrite, ostracod fragments, echinoderm plates and fragments, angular quartz grains, and sparry calcite void filling. From 12,140 ft (3,700 m).

B. Dolomitized oolitic grainstone showing relatively loose packing and remanent concentric structure of original oolites; void space filled by dolospar. From 12,770 ft (3,892 m).

C. Tight anhedral to euhedral mosaic of dolomite crystals containing no recognizable fossil constituents. Abundant wisps of organic matter. From 21,500 ft (6,553 m).

D. Dark, organic-rich, dolomitic lime mud with void space that had been filled by anhydrite (now dissolved during making of thin section).

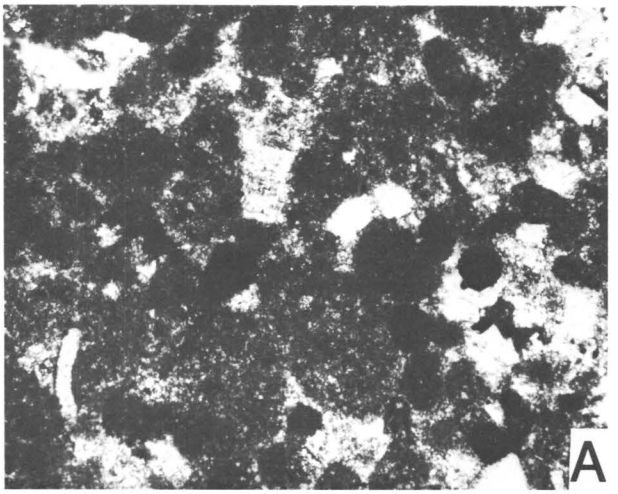
A

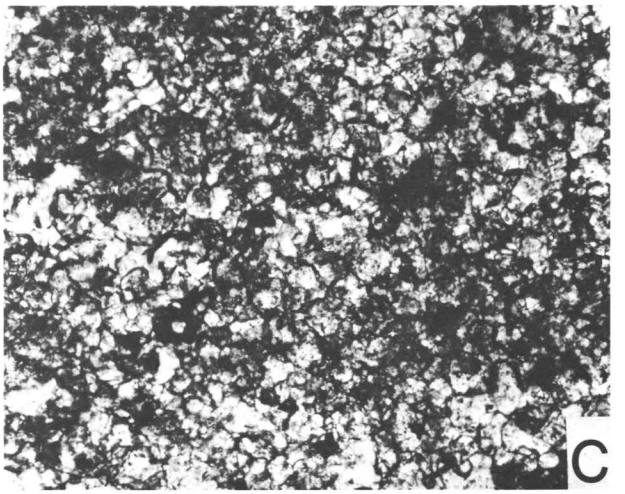
C

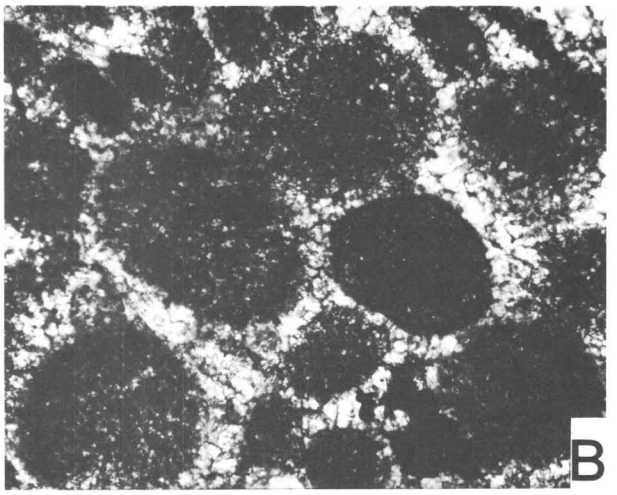
B

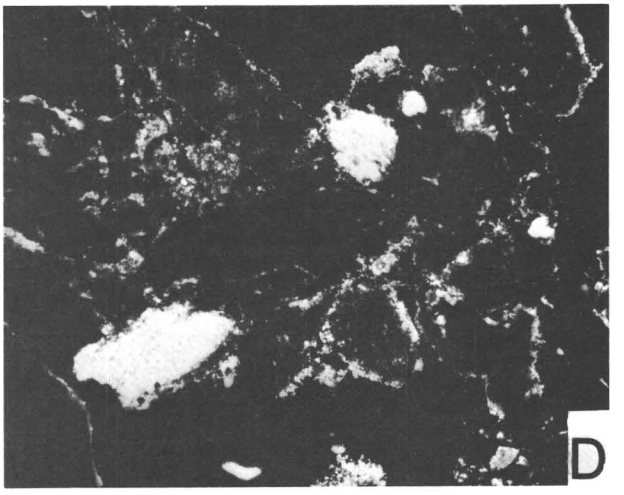
D

PLATE 2

Thin-section photomicrographs of representative clastic sedimentary rocks from the COST Nos. G-1 and G-2 wells (all with crossed nicols; field of view in A and D approximately 2mm; all others approximately 0.5 mm).

Figure A. Sandy or silty lime mudstone containing angular sand- and silt-sized quartz grains, glauconite, benthic foraminifers, Inoceramid prisms, and echinoderm fragments set in lithified chalk matrix. From 1,320 ft (402 m) in well G-2.

B. Fine-grained quartz sandstone with poikilotopic calcite cement. From 7,570 ft (2,307 m) in well G-2.

C. Hematite-cemented (dark areas), medium- to fine-grained quartz sandstone. From 9,910 ft (3,020 m) in well G-1.

D. Slightly argillaceous, fine-grained quartz sandstone; sutured grain contacts, no pore-filling cement (porosity is 5-10 percent), and chloritized feldspars. From 9,190 ft (2,801 m) in well G-1.

E. Iron-stained quartz siltstone to fine-grained sandstone. Some hematite cement is present, but grains are tightly packed and have sutured contacts; feldspar grains are chloritized. From 13,490 ft (4,112 m) in well G-2.

F. Fine-grained arkosic sandstone with dolomite and calcite cement in some parts, sutured grain contacts in others; no primary or secondary porosity; feldspar chloritized.

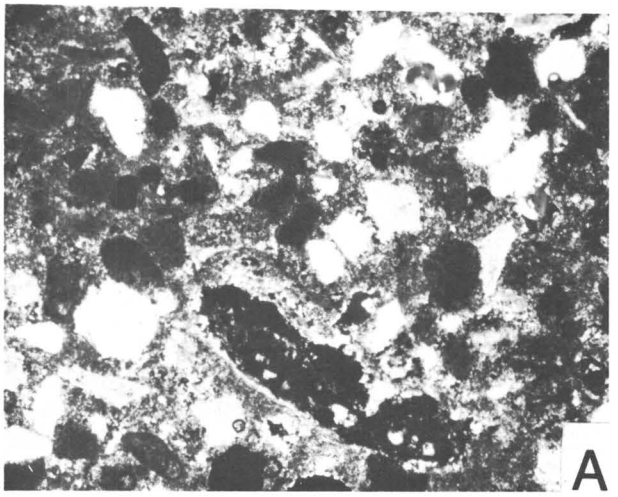
A

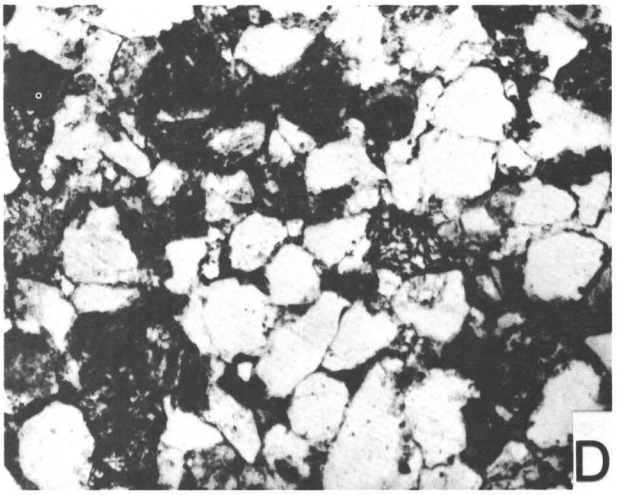
D

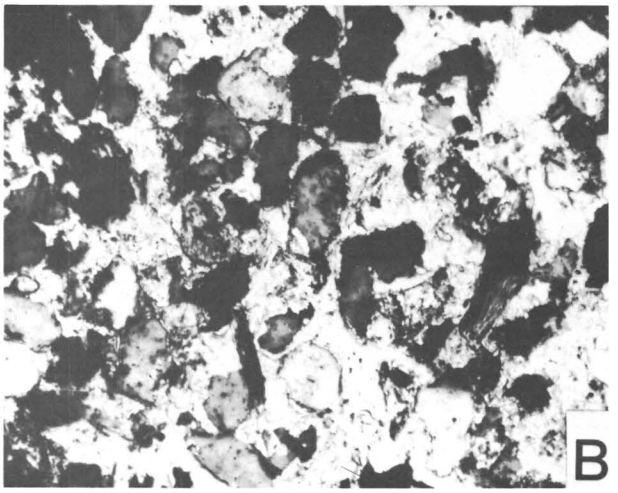
B

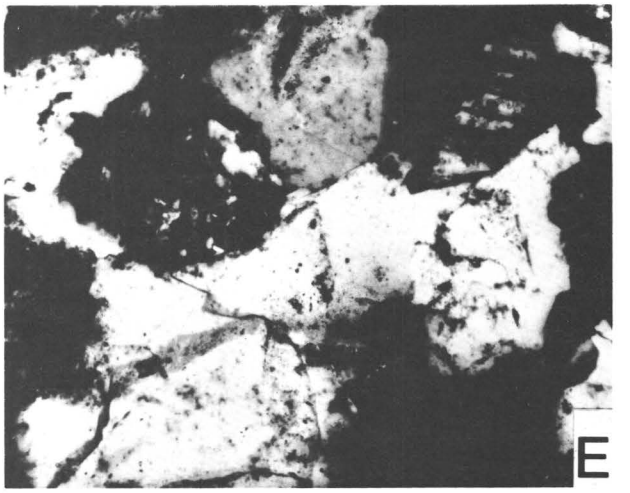
E

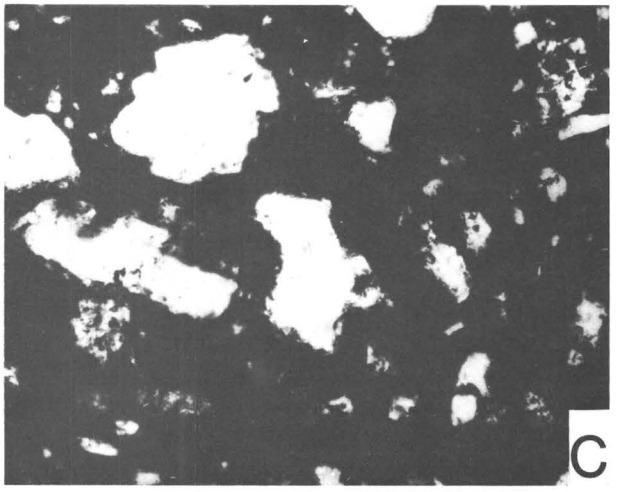
C

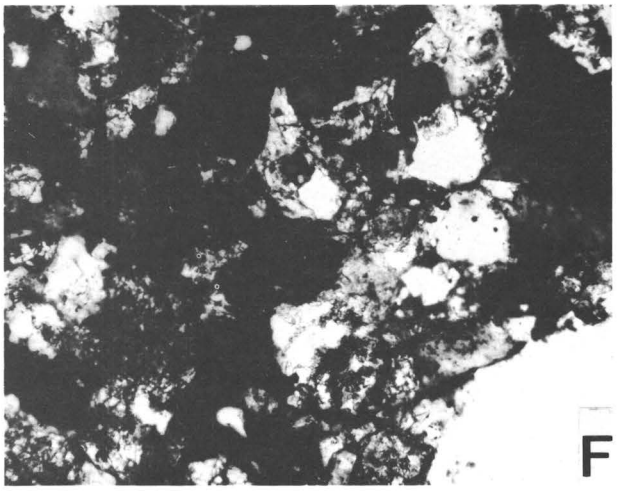
F

Calcareous Nannofossil Biostratigraphy and Paleoenvironment of the COST Nos. G-1 and G-2 Wells in the Georges Bank Basin

Page C. Valentine

The oldest sedimentary rocks sampled in the COST Nos. G-1 and G-2 wells are not fossiliferous and are of questionable Early Jurassic to Late Triassic age. During Jurassic and Early Cretaceous time, most of the sediments in the Georges Bank basin were deposited in a fluctuating nonmarine to shallow marine environment. Within this sequence, however, there is evidence that deeper marine shelf conditions occurred during the Berriasian at both well sites and also during Valanginian and Hauterivian time at the G-2 site. Marine shelf environments existed during most of the Late Cretaceous, except during the Cenomanian, when there was shallower water over the COST No. G-1 site. There is a hiatus at the Cretaceous-Tertiary boundary, and Campanian and Maestrichtian strata are missing from both sections. There may be other major hiatuses, but the lack of microfossils in some parts of the section makes it difficult to accurately define them. Study of samples of Tertiary strata shows that a marine carbonate shelf province existed in the Georges Bank basin during the Eocene.

BIOSTRATIGRAPHY AND PALEOENVIRONMENT OF THE COST NO. G-1 WELL

The COST No. G-1 well was drilled to a depth of 16,071 ft (4,898 m). Calcareous nannofossil biostratigraphy is primarily based on the study of rotary drill cuttings collected over 10- to 30-ft (3- to 9-m) intervals. The cutting samples from 1,030 to 2,710 ft (314 to 836 m) were studied at intervals of 90 ft (27 m) or less; from 2,710 to 2,443 ft (826 to 745 m), samples were studied at 60- to 120-ft (18- to 37-m) intervals, and from 8,010 to 15,310 ft (2,441 to 4,666 m) at 290-ft (88-m) intervals or less. Smear slides were made from individual rock fragments representing each of the lithologic units present in a single cutting sample. The oldest assemblage identified in a sample was used to determine the age of the strata at that level. In all, 296 samples from 97 levels in the well were analyzed. Sample depths are relative to the Kelly Bushing, which was 98 ft (30 m) above sea level and 255 ft (79 m) above the sea floor. Selected information from the reports on the COST No. G-1 well by International Biostratigraphers, Inc. (1976) and Amato and Bebout (1980) has been incorporated into the present study. The highest and lowest occurrences of stratigraphically important calcareous nannofossil species were determined from this study and from the study by International Biostratigraphers, Inc. (1976) (fig. 13).

EOCENE (972 FT; 296 M)

Casing was set at 972 ft (296 m), apparently in Eocene strata that form a prominent seismic horizon that is widespread beneath Georges Bank (Oldale and others, 1974, figs. 4, 8). This horizon was cored in the Franklin Basin on the northwest flank of Georges Bank and dated as Eocene (Hathaway and others, 1979). In the COST No. G-1 well, sidewall cores and cuttings were collected starting below the casing, and calcareous nannofossils are common and moderately preserved in limestone cuttings from samples from 1,060 and 1,090 ft (323 and 332 m) that are probably cavings. The nannofloras are middle to late Eocene in age and contain, among other species, *Chiasmolithus grandis, Cyclococcolithina formosa, Dictyococcites scrippsae, Neococcolithes dubius, and Reticulofenestra umbilica.* The limestone was deposited on a marine carbonate shelf.

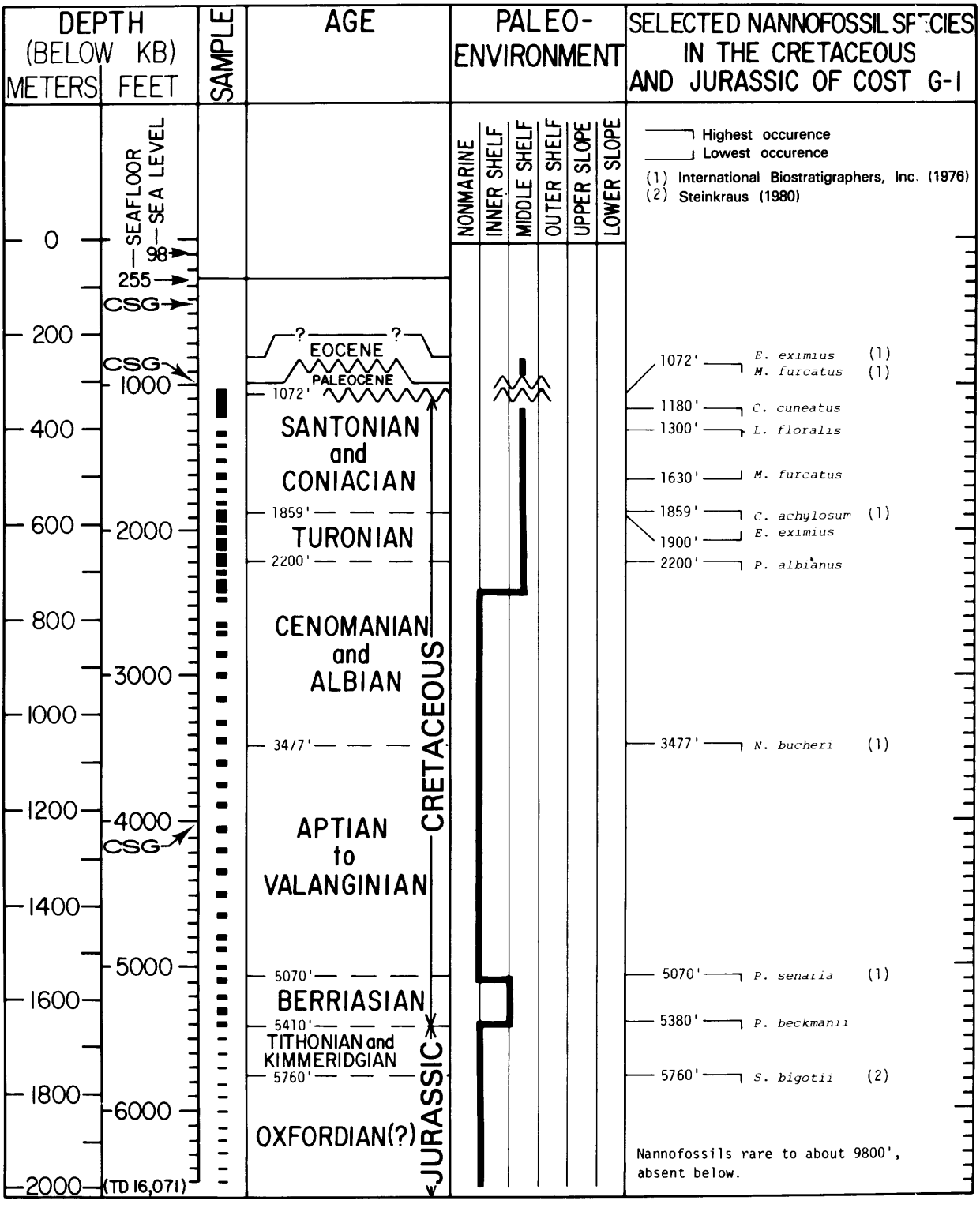

FIGURE 13.—Calcareous nannofossil biostratigraphy and paleoenvironments of the upper 6,500 ft (1,981 m) of the COST No. G-1 well. Paleoenvironment curves are qualitative and depict only trends. Depths are relative to the Kelly Bushing (KB), 98 ft (30 m) above sea level. Water depth is 157 ft (48 m). CSG indicates a casing point. In sample column, black areas indicate a complete sequence of samples studied. Ages are based on findings of this study but incorporate some biostratigraphic information from International Biostratigraphers, Inc. (1976).

SANTONIAN AND CONIACIAN (1,072–1,859 FT; 327–567 M).

The 100-ft (30-m) interval between the casing at 972 ft (296 m) and the top of Santonian and Coniacian strata at 1,072 ft (327 m) contains few fossils. Paleocene dinoflagellates and a Cretaceous pollen specimen are present in a sidewall core from 1,013 ft (309 m), but calcareous nannofossils and foraminifers are absent (International Biostratigraphers, Inc., 1976). A cutting sample from 1,030 to 1,060 ft (314 to 323 m) contains quartz sand and mollusk shell fragments, as well as cement chips that are contaminated with both Tertiary and Cretaceous nannofossils. The next sample down (1,060–1,090 ft; 323–332 m) is also predominantly quartz sand and cement, but calcareous glauconitic siltstone clasts are also present; some of these clasts contain nannofossils of middle to late Eocene age, and others contain a sparse Late Cretaceous flora. Maestrichtian and Campanian strata were not recovered and are apparently missing at the site. Disconformities probably exist below the Eocene limestone and also between the thin Paleocene strata and the underlying Santonian and Coniacian calcareous siltstone.

Undifferentiated Santonian and Coniacian strata 787 ft (240 m) thick are present from 1,072 to 1,859 ft (327 to 567 m). Fossiliferous calcareous siltstone is interbedded with quartz sand and mollusk shell fragments that were deposited in a marine shelf environment. *Marthasterites furcatus,* a species that is not known to range above the Santonian, and *Eiffellithus eximius* are present in sidewall cores at 1,072 ft (327 m) (International Biostratigraphers, Inc., 1976). Two species that also are not known to range above the Santonian, *Chiastozygus cuneatus and Lithastrinus floralis,* are found at 1,180 ft (360 m) and 1,300 ft (396 m), respectively.

TURONIAN (1,859–2,200 FT; 567–671 M)

The top of the Turonian is placed at the highest occurrence of *Corollithion achylosum,* in a sidewall core from 1,859 ft (567 m) (International Biostratigraphers, Inc., 1976). *Eiffellithus eximus,* a Turonian (and younger) species, is not present below 1,900 ft (579 m). *Podorhabdus albianus,* a species that ranges from the Albian into the lower Turonian, does not occur above 2,200 ft (671 m) in the COST No. G–1 well, and its highest occurrence marks the provisional lower boundary of this interval. The Turonian is 341 ft (104 m) thick and consists of calcareous siltstone, coarse quartz sand, and mollusk shells that are indicative of a marine-shelf environment.

CENOMANIAN AND ALBIAN (2,200–3,477 FT; 671–1,060 M)

The 1,277-ft (389-m) section from 2,200 to 3,477 ft (671 to 1,060 m) is chiefly quartz sand, except for about 200 ft (61 m) of calcareous siltstone at the top of the interval. At about 2,400 ft (732 m), quartz sand and gravel become dominant and are associated with mica, lignite, and mollusk shell fragments, and the few sedimentary clasts that are present do not contain calcareous nannofossils. These strata represent a nonmarine to shallow marine environment. Spores and pollen are present, and Albian species are reported from the lower part of the interval; foraminifers are absent and dinoflagellates are rare (International Biostratigraphers, Inc., 1976).

APTIAN TO VALANGINIAN (3,477–5,070 FT; 1,060–1,545 M)

The top of the Aptian to Valanginian section is provisionally placed at 3,477 ft (1,060 m) based on the highest occurrence of *Nannoconus bucheri* from a sidewall core (International Biostratigraphers, Inc., 1976). This interval is 1,593 ft (486 m) thick and is characterized by coarse quartz sand and gravel, lignite, mica, and sandstone. Calcareous nannofossils and foraminifers are rare in the sandstone, although several sidewall cores near 3,500 ft (1,067 m) contain sparse assemblages. Dinoflagellates are present in the upper part of this section; spores and pollen occur throughout (International Biostratigraphers, Inc., 1976). Casing was set at 4,023 ft (1,226 m) and the underlying 700 ft (213 m) of cuttings are quartz sand devoid of sedimentary rock fragments. Lower Cretaceous stages cannot be differentiated in the Aptian to Valanginian interval, and hiatuses may be present. These beds were deposited in a nonmarine to shallow marine environment.

BERRIASIAN (5,070–5,410 FT; 1,545–1,649 M)

Berriasian calcareous siltstone 340 ft (104 m) thick is present from 5,070 to 5,410 ft (1,545 to 1,649 m). The top of this interval is placed at the

highest occurrence of the Berriasian nannofossil species *Polycostella senaria* in a sidewall core from 5,070 ft (1,545 m) (International Biostratigraphers, Inc., 1976). A small assemblage composed of *Cyclagelosphaera margerelii, Micrantholithus obtusus, Polycostella beckmannii, P. senaria, Watznaueria barnesae,* and *W. communis* that is indicative of Berriasian Age was observed in the sample from 5,380 to 5,410 ft (1,640 to 1,649 m). The Jurassic-Cretaceous boundary is drawn here at the lowest occurrence of *Polycostella senaria. Polycostella beckmannii* is present also somewhat lower in the section, and it has been reported from conventional cores and sidewall cores from 5,478.3 ft (1,670 m), 5,531 ft (1,686 m), and 5,699 ft (1,737 m) (International Biostratigraphers, Inc., 1976). Dinoflagellates are rare or absent in overlying strata, but they are more abundant in the Berriasian beds (International Biostratigraphers, Inc., 1976), which were probably deposited in a marine shelf environment.

JURASSIC (5,410–15,310 FT; 1,649–4,666 M)

The Jurassic-Cretaceous boundary is drawn at the lowest occurrence of *Polycostella senaria* at 5,410 ft (1,649 m). International Biostratigraphers, Inc. (1976), reported nannofossil assemblages of Jurassic aspect that included *Polycostella beckmannii, Ethmorhabdus gallicus, Cyclagelosphaera margerelii,* and *Polypodorhabdus escaigii* from cores in the interval 5,475.8–5,767 ft (1,669 to 1,758 m), but sidewall cores and conventional cores from 5,839 to 15,851 ft (1,780 to 4,831 m) contain no nannofossils. The cutting samples from 5,410 to 6,300 ft (1,649 to 1,920 m) are barren or contain few nannofossils, and only the species *Cyclagelosphaera margerelii* is present. However, one sample from 6,400 to 6,410 ft (1,951 to 1,954 m) contains rare, moderately preserved specimens of *Stephanolithion bigotii, Polypodorhabdus escaigii, Cyclagelosphaera margerelii,* and *Vagalapilla stradneri* and is probably Oxfordian in age. Steinkraus (1980) reported the Callovian-Oxfordian species *Stephanolithion bigotii* in cuttings from 5,760 to 5,770 ft (1,756 to 1,759 m) and 6,400 to 6,410 ft (1,951 to 1,954 m). Oxfordian strata also may exist lower in the section. Four species, *Cyclagelosphaera margerelii, Ethmorhabdus gallicus, Polypodorhabdus escaigii,* and *Watznaueria barnesae,* are present sporadically from 6,710 to 7,710 ft (2,045 to 2,350 m), and an assemblage containing *Cyclagelosphaera margerelii, Ethmorhabdus gallicus, Watznaueria barnesae,* and *W. crucicentralis* is present at 9,800–9,810 ft (2,987–2,990 m). All cutting samples below this level contain no calcareous nannofossils. The Jurassic section down to about 10,000 ft (3,048 m) is interbedded sandstone and shale that were deposited in a nonmarine environment interrupted by occasional marine incursions. Below about 10,000 ft (3,048 m), interbedded limestone, dolomite, sandstone, and shale contain predominantly terrestrial palynomorphs (International Biostratigraphers, Inc., 1976) and are indicative of deposition in nonmarine and shallow marine carbonate bank environments.

BIOSTRATIGRAPHY AND PALEOENVIRONMENT OF THE COST NO. G–2

The COST No. G–2 well was drilled to a depth of 21,874 ft (6.667 m). Rotary cutting samples from the COST No. G–2 well were collected and processed for the study of calcareous nannofossils as described for the COST No. G–1 well. From 1,100 to 8,800 ft (335 to 2,682 m), the samples studied were generally at intervals of 30 ft (9 m) or less, but several samples were as much as 60 ft (18 m) apart. Deeper in the well, down through 21,850 ft (6,660 m), most samples were studied at 260-ft (79-m) intervals or less, although a few were as much as 360 ft (110 m) apart. A total of 777 samples from 238 levels in the well were analyzed (fig. 14). Sample depths are relative to the Kelly Bushing, which was 79 ft (24 m) above sea level and 351 ft (107 m) above the sea floor. Selected information from the reports on the COST No. G–2 well by International Biostratigraphers, Inc. (1977) and Amato and Simonis (1980) has been incorporated into the present study. The highest and lowest occurrences of stratigraphically important calcareous nannofossil species were determined from this study and from the study by International Biostratigraphers, Inc. (1977) (fig. 14).

EOCENE (~ 1,000–1,310 ft; ~305–399 M)

Casing was set at 505 ft (154 m) and also at 1,061 ft (323 m), probably in the Eocene seismic reflector, and samples were collected starting at 1,100 ft (335 m). Cuttings from 1,100 to 1,460 ft (335 to 445 m) are characterized by glauconite,

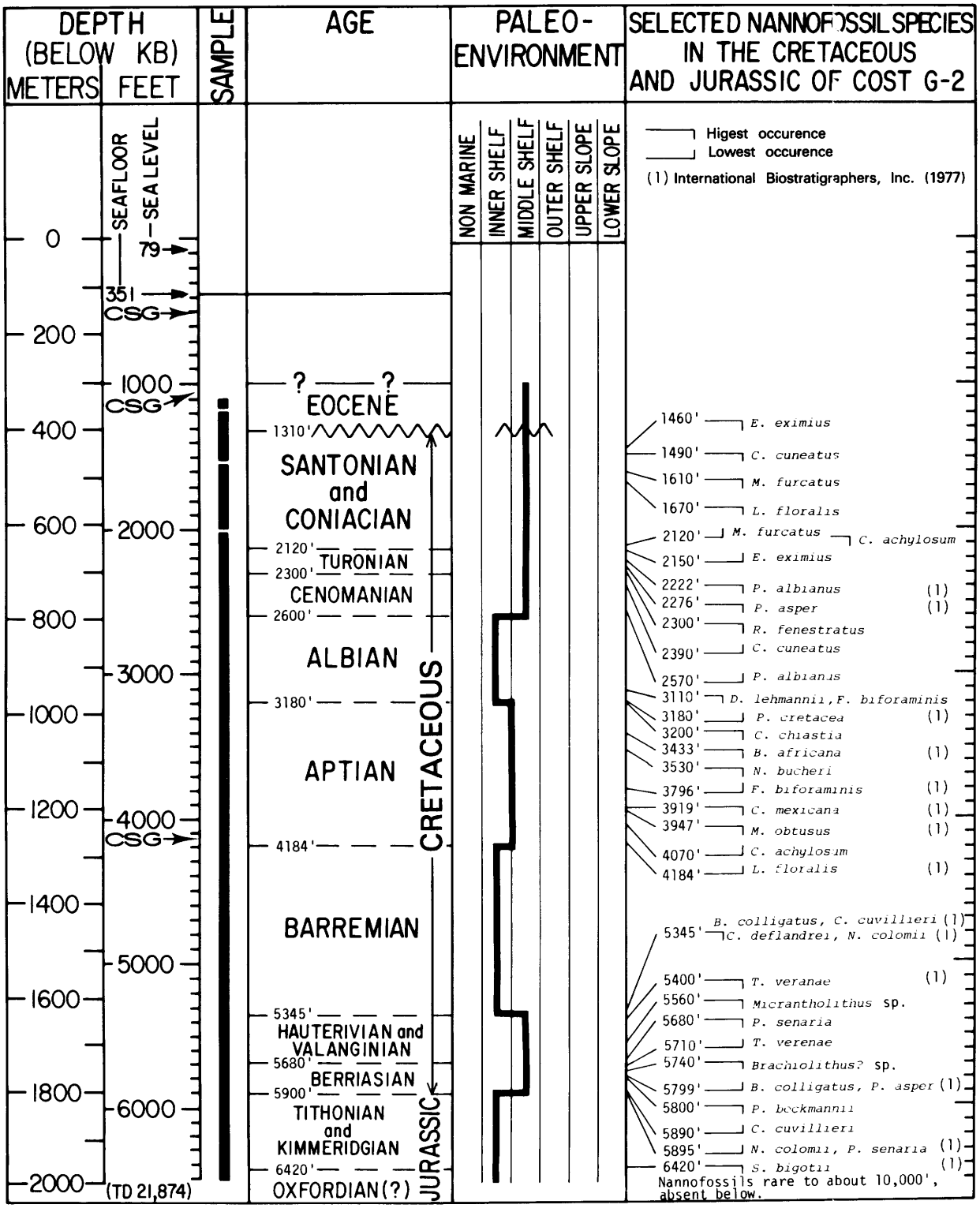

FIGURE 14.—Calcareous nannofossil biostratigraphy and paleoenvironments of the upper 6,500 ft (1,981 m) of the COST No. G-2 well. Paleoenvironment curves are qualitative and depict only trends. Depths are relative to the Kelly Bushing (KB), 79 ft (24 m) above sea level. Water depth is 272 ft (83 m). CSG is a casing point. In sample column, black areas indicate a complete sequence of samples studied. Ages are based on findings of this study, but incorporate some biostratigraphic information from International Biostratigraphers, Inc. (1977), and Steinkraus (1980).

quartz sand, fragments of bivalves and bryozoans, and abundant cement. Sedimentary clasts are not common, and most are barren, although glauconitic limestone fragments containing a rich, diverse, well-preserved, calcareous nannofossil assemblage were sampled at 1,310 ft (399 m). The following species are present, among others, and they are indicative of the upper Eocene *Discoaster barbadiensis* zone of Bukry (1973, 1975): *Chiasmolithus oamaruensis, Cyclococcolithina formosa, Dictyococcites bisectus, Discoaster saipanensis, Reticulofenestra reticulata,* and *R. umbilica.* International Biostratigraphers, Inc. (1977), reported a foraminiferal fauna of late middle Eocene age from a sidewall core at 1,289 ft (393 m). The Eocene cuttings are indicative of a marine shelf environment. The cuttings may be mostly cavings, but together with the sidewall core they confirm the presence at the COST No. G-2 site of a widespread Eocene limestone unit that has been sampled elsewhere beneath Georges Bank and in submarine canyons on the slope (Weed and others, 1974; Ryan and others, 1978; Hathaway and others, 1979; Valentine, 1981). Upper Eocene limestone cavings are present in samples down to 4,120 ft (1,256 m).

SANTONIAN AND CONIACIAN (1,310–2,120 FT; 399–646 M)

Paleocene, Maestrichtian, and Campanian strata were not observed in the COST No. G-2 well, suggesting that there is a major disconformity at the Cretaceous-Tertiary boundary at about 1,300 ft (396 m). International Biostratigraphers, Inc. (1977), reported *Inoceramus* shell prisms and Upper Cretaceous foraminifers in cuttings at 1,310 ft (399 m) and a Santonian foraminiferal assemblage in a sidewall core from 1,324 ft (404 m). In the present study, a mixed assemblage of rare, poorly preserved Eocene and Upper Cretaceous nannofossils was observed at 1,340 ft (408 m); and a poorly preserved flora of probable Santonian Age containing *Eiffellithus eximius, Tetralithus obscurus,* and *T. ovalis* was found at 1,460 ft (445 m).

Santonian and Coniacian nannofloras are present in a 796-ft (243-m) -thick section of glauconitic, silty limestone and gray calcareous siltstone from 1,460 to 2,120 ft (445 to 646 m). The nannofossils are abundant and well-preserved. The highest occurrence of *Chiastozygus cuneatus,* a species that is not known to range above the Santonian, is at 1,490 ft (454 m). *Marthasterites furcatus* (1,610 ft; 491 m) and *Lithastrinus floralis* (1,670 ft; 509 m) are also present lower in this interval. The abundant glauconite and mollusk-shell fragments, particularly *Inoceramus* prisms, are indicative of deposition in a marine shelf environment.

TURONIAN (2,120–2,270 FT; 646–692 M)

A relatively thin (150-ft; 46-m) section of richly fossiliferous, gray, argillaceous limestone of Turonian Age is present from 2,120 to 2,270 ft (646 to 692 m). These beds are lithologically similar to the overlying Santonian and Coniacian strata, and the top of the Turonian is drawn at the highest occurrence of *Corollithion achylosum. Podorhabdus albianus,* a species that is restricted to Turonian and older rocks, appears in a sidewall core from 2,222 ft (667 m) in the COST No. G-2 well (International Biostratigraphers, Inc., 1977). Two species, *Marthasterites furcatus and Eiffellithus eximius,* which are restricted to Turonian and younger strata, are absent below 2,120 ft (646 m) and 2,150 ft (655 m), respectively. Cuttings from the Turonian interval contain mollusk-shell fragments that indicate deposition in a marine-shelf environment.

CENOMANIAN (2,270–2,600 FT; 692–792 M)

Cenomanian gray calcareous siltstone is approximately 330 ft (101 m) thick and is somewhat more siliceous than the overlying strata. Nannofossils are common and well preserved. The top of the Cenomanian is placed at the highest occurrence of the planktic foraminifer *Rotalipora cushmani* in a cutting sample from 2,270 ft (692 m) and in a sidewall core from 2,276 ft (694 m) (International Biostratigraphers, Inc., 1977). *Porhabdolithus asper* and *Reinhardites fenestratus* are not present in the COST No. G-2 well above 2,276 ft (694 m) and 2,300 ft (701 m), respectively; these nannofossil species become extinct at or near the Cenomanian-Turonian boundary.

The base of the Cenomanian is arbitrarily drawn at 2,600 ft (792 m), where the lithology of the section changes from a shelly siltstone to a calcareous quartz sandstone containing lignite, mica, and mollusk-shell fragments. Sidewall cores from about 2,600 to 3,100 ft (792 to 945 m) contain almost no calcareous nannofossils and foraminifers, but cuttings contain benthic foraminifers

no younger than Albian age at about 2,650 ft (808 m) (International Biostratigraphers, Inc., 1977). Cenomanian strata were deposited in a marine-shelf environment, probably shallower than that of Turonian, Coniacian, and Santonian time.

ALBIAN (2,600–3,180 FT; 792–969 M)

Albian, Aptian, and Barremian strata approximately 2,745 ft (837 m) thick are present from 2,600 to 5,345 ft (792 to 1,629 m). Most of this section contains few fossils and is difficult to date; therefore, the stratigraphic boundaries are provisional. The upper 580 ft (177 m), from 2,600 to 3,180 ft (792 to 969 m), is gray calcareous sandstone and shale with associated mollusk shells, glauconite, and lignite, and indicates deposition in a marine inner-shelf environment. Sidewall cores contain almost no calcareous nannofossils and foraminifers, and dinoflagellates are less common than in overlying strata (International Biostratigraphers, Inc., 1977). These beds are assigned to the Albian based on the lowest occurrence of *Prediscosphaera cretacea* in a sidewall core from 3,180 ft (969 m).

APTIAN (3,180–4,184 FT; 969–1,275 M)

The strata from 3,180 to 4,184 ft (969 to 1,275 m) are more fossiliferous than the overlying Albian beds. This 1,004-ft (306-m) interval is provisionally assigned to the Aptian based on the highest occurrences of *Nannoconus bucheri, Conusphaera* mexicana, and *Micrantholithus obtusus,* and the lowest occurrences of *Flabellites biforaminis, Corollithion achylosum,* and *Lithraphidites floralis.* Nannofossils are not abundant, and preservation is only moderate. The Aptian beds are chiefly sandstone and shale containing mollusk shell fragments. They are more calcareous and contain less lignite than the overlying Albian strata, and they were laid down in a marine shelf environment.

BARREMIAN (4,184–5,345 FT; 1,275–1,629 M)

Casing was set at 4,120 ft (1,256 m), apparently at a lithologic boundary. The 1,161-ft (354-m) section from 4,184 to 5,345 ft (1,275 to 1,629 m) is calcareous sandstone containing lignite and mica and a few fossils. It was deposited in an inner-shelf environment similar to that of the Albian. Sidewall cores from this interval contain almost no calcareous nannofossils and foraminifers, but palynomorphs are present, and the top of the Barremian is based on the highest occurrences of several dinoflagellate species (International Biostratigraphers, Inc., 1977).

HAUTERIVIAN AND VALANGINIAN (5,345–5,680 FT; 1,629–1,731 M)

Hauterivian and Valanginian argillaceous limestone 335 ft (102 m) thick extends from 5,345 to 5,680 ft (1,629 to 1,731 m). Moderately preserved calcareous nannofossils are common. Species indicative of Hauterivian and older strata are present at 5,345 ft (1,629 m). The highest occurrences in sidewall cores of *Bipodorhabdus colligatus, Cruciellipsis cuvillieri,* and *Cyclagelosphaera deflandrei* are at 5,345 ft (1,629 m), and *Tubodiscus verenae* is present at 5,400 ft (1,646 m). *Micrantholithus* sp. (Valentine, 1980, pl. 2, fig. 13) is present in two cutting samples from the interval 5,560 to 5,650 ft (1,695 to 1,722 m) in the Hauterivian and Valanginian and in one sample from the underlying Berriasian strata. A single occurrence of this species was reported from the Hauterivian and Valanginian of the COST No. B-3 well on the continental slope off New Jersey (Valentine, 1980). The Hauterivian-Valanginian argillaceous limestone at the COST No. G-2 site was probably deposited in a marine shelf environment.

BERRIASIAN (5,680–5,900 FT; 1,731–1,798 M)

The Berriasian is represented by a short interval (210 ft; 64 m) of light-gray limestone that extends from 5,680 to 5,900 ft (1,731 to 1,798 m). The Berriasian-Valanginian boundary is placed at the highest occurrence of the Berriasian nannofossil *Polycostella senaria.* The highest occurrence of *Polycostella beckmannii,* a species that ranges from the Tithonian into the Berriasian, is at 5,800 ft (1,768 m). Several stratigraphically important species that are restricted to Berriasian and younger rocks and have their lowest occurrences in this interval of the well are *Bipodorhabdus colligatus* and *Parhabdolithus asper* at 5,799 ft (1,768 m), *Cruciellipsis cuvillieri* at

5,890 ft (1,795 m), and *Nannoconus colomii* and *Polycostella senaria* at 5,895 ft (1,797 m). *Brachiolithus*? sp. (Valentine, 1980, pl. 2, figs. 1, 2) is present at 5,800 ft (1,768 m) and in several lower samples in the COST No. G-2 well. This species is restricted to the Berriasian of the COST No. B-3 well (Valentine, 1980) and may prove to be a valuable marker for that stage. In addition, the Cretaceous dinoflagellate *Pseudoceratium pelliferum* is not present in sidewall cores below 5,856 ft (1,785 m) (International Biostratigraphers, Inc., 1977). The Berriasian limestone probably was deposited in a marine shelf environment similar to that of the overlying Hauterivian and Valanginian beds.

JURASSIC (5,900–21,874? FT; 1,798–6,667? M)

The Jurassic-Cretaceous boundary is provisionally placed at 5,900 ft (1,798 m), near the lowest occurrences of the nannofossil species *Cruciellipsis cuvillieri*, *Nannoconus colomii*, and *Polycostella senaria*. Below this depth nannofossil diversity is low and the limestone is partly recrystallized. International Biostratigraphers, Inc. (1977), studied sidewall cores from the boundary interval and observed a Late Jurassic dinoflagellate assemblage at 5,962 ft (1,817 m); the Jurassic dinoflagellate *Meiourogonyaulax staffensis* is present from 6,155 to about 7,500 ft (1,876 to about 2,286 m), and the Tithonian-Berriasian nannofossil species *Polycostella beckmannii*, is present down to 6,270 ft (1,911 m). In this study, cuttings that are almost barren of calcareous nannofossils appear at about 5,900 ft (1,798 m). Except for Lower Cretaceous cavings, most samples down to about 10,000 ft (3,048 m) are barren or contain poorly preserved specimens of two long-ranging Jurassic-Cretaceous species, *Cyclagelosphaera margerelii* and *Watznaueria barnesae*.

Samples of the present study from below 10,000 ft (3,048 m) are barren of nannofossils. However, International Biostratigraphers, Inc. (1977), reported the presence of the nannofossil *Stephanolithion bigotii*, of Callovian-Oxfordian Age, in five sidewall cores from 6,420 to 6,818 ft (1,957 to 2,078 m) and in two sidewall cores from 10,135 and 10,247 ft (3,089 and 3,123 m); the upper five samples are from a part of the section dated as Kimmeridgian and Tithonian using foraminifers and palynomorphs. At the COST No. G-1 well, *Stephanolithion bigotii* was observed in a cutting sample of the present study from 6,400 to 6,410 ft (1,951 to 1,954 m); and Steinkraus (1980) reported the species in cuttings from the same level and also from 5,760 to 5,770 ft (1,756 to 1,759 m). Thus, in both wells, *Stephanolithion bigotii*, a species that does not normally range above the Oxfordian, is present in strata that have been provisionally dated as Kimmeridgian and Tithonian on the basis of palynomorphs and foraminifers. Below about 9,500 ft (2,896 m) in the COST No. G-2 well, palynomorphs and foraminifers indicate that strata are Oxfordian, Callovian, and possibly Late Triassic to Early Jurassic in age (International Biostratigraphers, Inc., 1977). The Jurassic section in the COST No. G-2 well is about 16,000 ft (4,877 m) thick. It is predominantly shallow marine limestone, but it also includes dolomite and beds of anhydrite; halite is present at the bottom of the well.

SUMMARY

The Jurassic stratigraphy of the COST Nos. G-1 and G-2 sites is not well defined. Strata dated as Middle and Late Jurassic age using terrestrial and marine palynomorphs are present in both wells, but the stages are difficult to delineate. The deeper, less fossiliferous beds may be as old as Early Jurassic or late Triassic. The section in the COST No. G-1 well from the Jurassic-Cretaceous boundary at 5,410 ft (1,649 m) down to about 10,000 ft (3,048 m) is composed of calcareous and noncalcareous shale, siltstone, and sandstone, all of which contain dinoflagellates, terrestrial palynomorphs, and sparse calcareous nannofossils. From 10,000 ft (3,048 m) down to the metasedimentary basement rocks at about 15,600 ft (4,755 m), shale and sandstone are interbedded with limestone, dolomite, and anhydrite; terrestrial palynomorphs are present, but dinoflagellates and calcareous nannofossils are extremely rare. Jurassic strata at the G-1 site were deposited in alternating nonmarine and shallow marine environments. The COST No. G-1 well was drilled on a basement high (Klitgord and Behrendt, 1979, fig. 7c; Waetjen, 1980, pl. 4), whereas the COST No. G-2 well is in a deeper part of the Georges Bank basin where the Jurassic section contains more calcareous sediment

and is representative of a shallow marine environment. At the G-2 site, calcareous shale and sandstone are interbedded with limestone from 5,900 to about 10,000 ft (1,798 to about 3,048 m), below which ooltic limestone is the principal rock type down to about 13,500 ft (4,115 m); below 7,500 ft (2,286 m), marine and terrestrial palynomorphs are present, but calcareous nannofossils and foraminifers are rare or absent. Limestone, dolomite, and anhydrite dominate the section from about 13,500 ft (4,115 m) down to the salt encountered near the bottom of the hole; palynomorphs are rare, and calcareous nannofossils and foraminifers are absent in this part of the section.

Lower Cretaceous and Cenomanian rocks at the COST No. G-1 site are present from 2,400 to 5,410 ft (732 to 1,649 m). They are chiefly coarse-grained quartz sand and lignitic, micaceous sandstone interbedded with calcareous siltstone representing deposition in nonmarine and shallow marine environments. These strata contain few fossils, and neither the Lower Cretaceous stages nor the Albian-Cenomanian boundary can be delineated accurately. Terrestrial palynomorphs are present throughout the section, whereas dinoflagellates, calcareous nannofossils, and foraminifers are absent except in shallow marine beds near 3,500 ft (1,067 m) and in the Berriasian strata at the base of the interval.

At the COST No. G-2 site, the upper part of the Lower Cretaceous, from 2,600 to 5,345 ft (792 to 1,629 m), is mainly calcareous siltstone and shale containing mollusk shells, glauconite, and lignite. Albian and Barremian strata of this interval are notably less fossiliferous than the intervening Aptian beds; all were deposited in a marine inner-shelf environment. At both sites, the Aptian strata show more marine influence than Albian or Barremian strata. The Hauterivian, Valanginian, and Berriasian strata from 5,345 to 5,900 ft (1,629 to 1,798 m) are fossiliferous limestone also of marine shelf origin. The Lower Cretaceous at the G-2 site is slightly thicker and generally more fossiliferous than at the G-1 site. The Hauterivian and Valanginian strata in the G-2 well were deposited in a marine shelf environment; strata of the same age in the G-1 well represent nonmarine to shallow marine conditions. The Berriasian is marine in both wells.

The Upper Cretaceous sections are comparable in thickness at both sites. Cenomanian beds at the COST No. G-2 site are calcareous siltstone of marine shelf origin. At the COST No. G-1 site, the Cenomanian and Albian quartz sand was deposited in a nonmarine to shallow marine environment. Santonian, Coniacian, and Turonian strata at the two well sites represent different sedimentary facies, but they indicate a marine shelf environment at both sites; at G-1, calcareous siltstone is interbedded with shelly quartz sand, whereas coeval strata at G-2 are glauconitic, argillaceous limestones that represent a facies deposited farther offshore.

Maestrichtian and Campanian beds were not observed in either well; there is a hiatus in the 100- to 200-ft (30- to 61-m) interval of poorly fossiliferous, reworked beds between Santonian and Eocene strata. The Eocene in both wells is a glauconitic limestone rich in calcareous nannofossils that was deposited on a marine carbonate shelf.

Foraminiferal and Seismic Stratigraphy, Paleoenvironments and Depositional Cycles in the Georges Bank Basin

C. Wylie Poag

In this paper geologic information from the COST Nos. G-1 and G-2 wells and auxiliary shallow coreholes is combined with interpretations of multichannel seismic reflection profiles to provide a stratigraphy and depositional history of the Georges Bank basin (fig. 15). The biostratigraphic summary is based on the foraminiferal assemblages sampled from rotary cuttings taken at 10- to 90-ft (3- to 29-m) intervals, except for wider spacing in the Oxfordian(?) to Hettangian(?) section of the COST No. G-1 well. Sidewall cores provided by International Biostratigraphiers, Inc., were also examined for foraminifers. (See Amato and Bebout, 1980, and Amato and Simonis, 1980, for locations of sidewall cores.) Age sequences are described from the youngest to the oldest. The zonation of the COST Nos. G-1 and G-2 wells is based on the final appearances of diagnostic planktic and benthic foraminifers. Established planktic foraminiferal

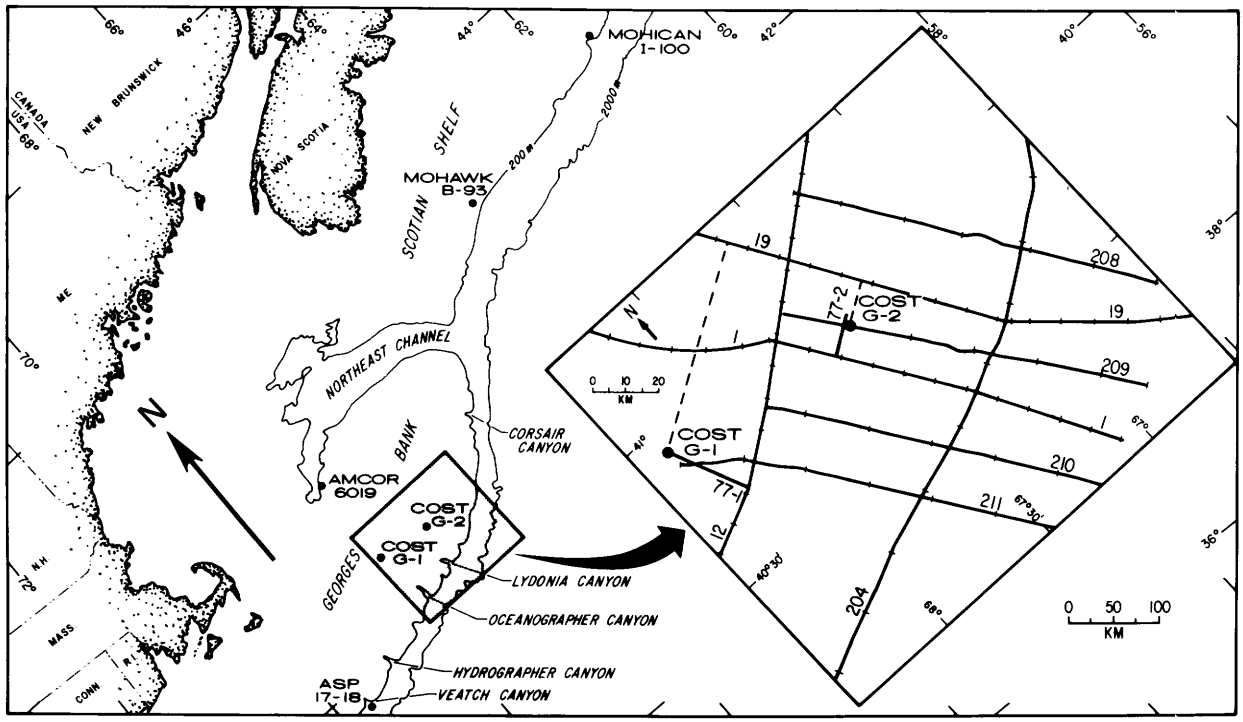

FIGURE 15.—Locations of well and core sites and seismic reflection profiles on North Atlantic Outer Continental Shelf and slope.

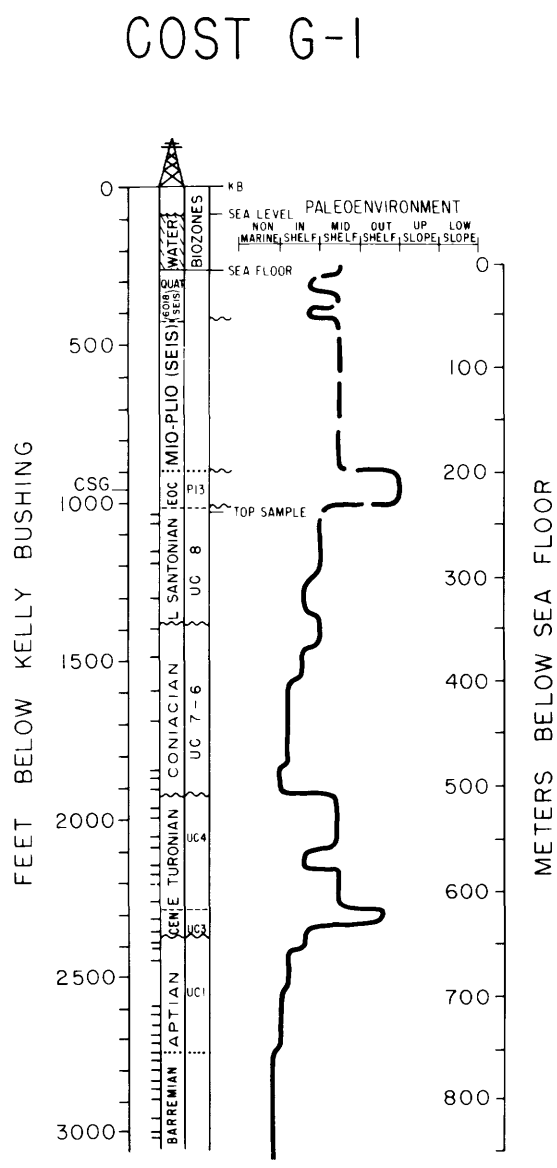

FIGURE 16.—Stratigraphic column of COST No. G-1 well showing chronostratigraphy, biozones, and paleoenvironments. The age terms abbreviated in the left side column are spelled out on figure 17.

zonations are used where possible (Blow, 1969: Berggren and Van Couvering, 1974; Hardenbol and Berggren, 1978; Pessagno, 1967; Stainforth and others, 1975; van Hinte, 1976a, b). The benthic foraminiferal zonation of Ascoli (1976) was used to date Mesozoic assemblages. The biostratigraphic interpretations presented here are preliminary and later studies may modify and refine them.

The biostratigraphic analyses are used with interpretations of the seismic sequences to deter-

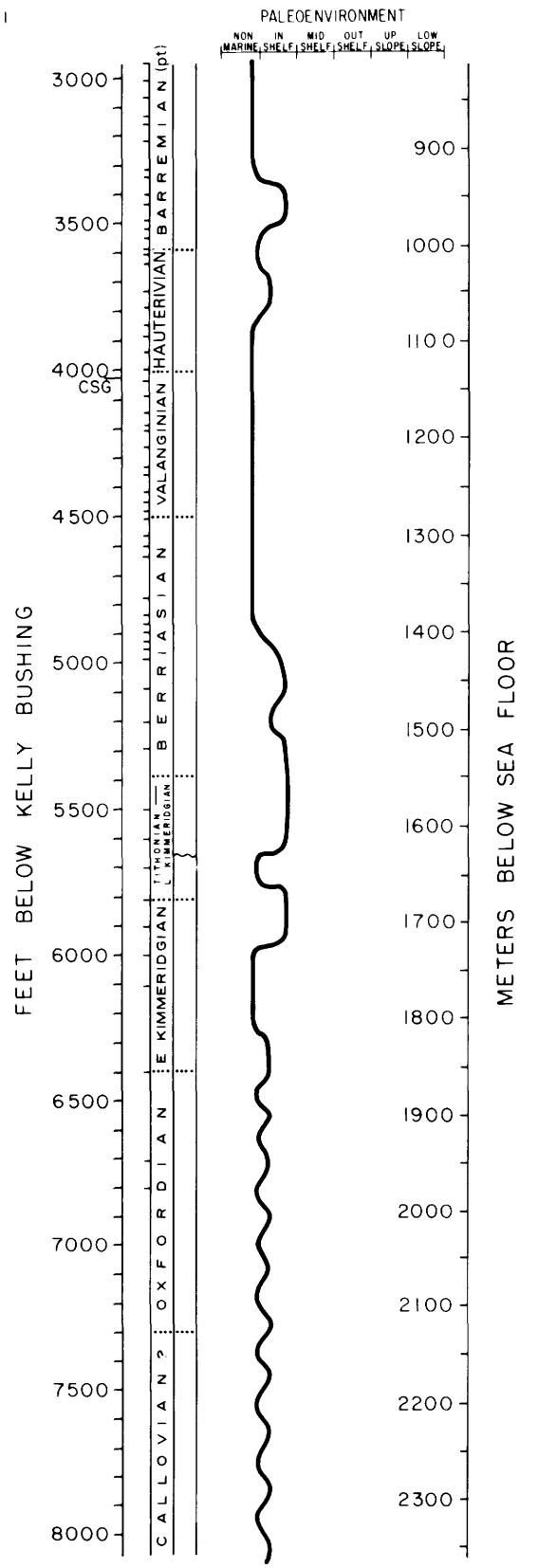

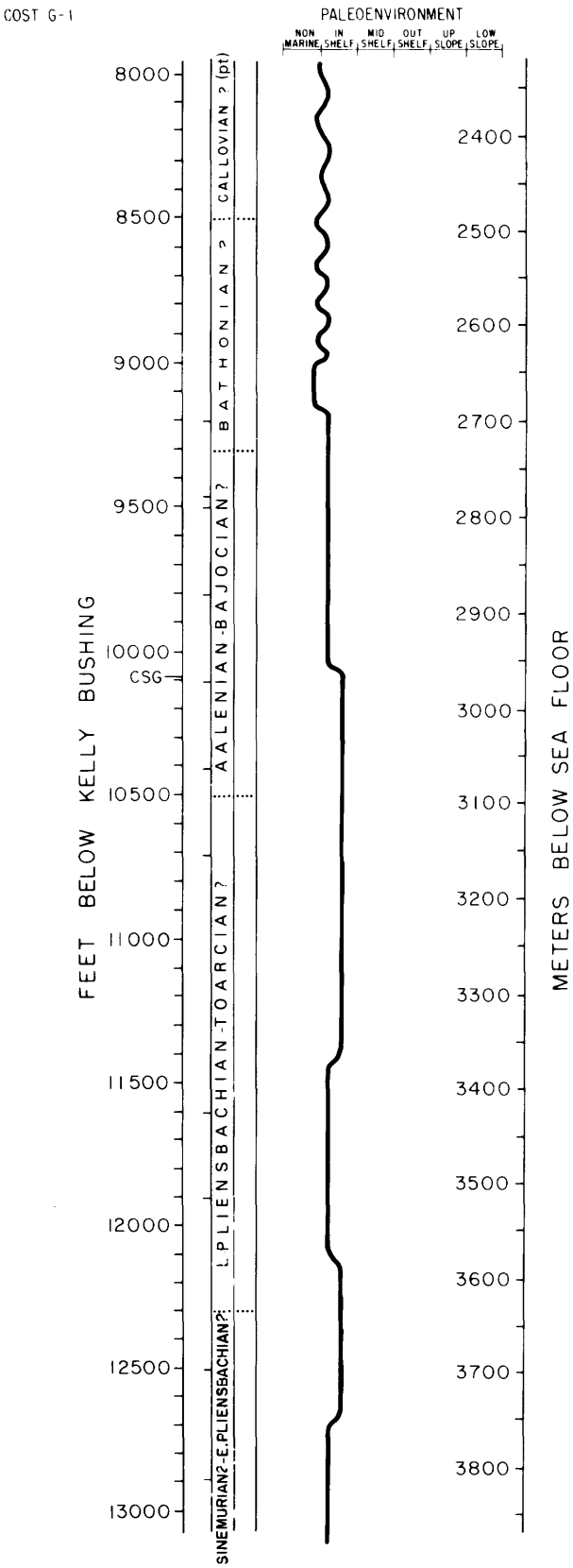

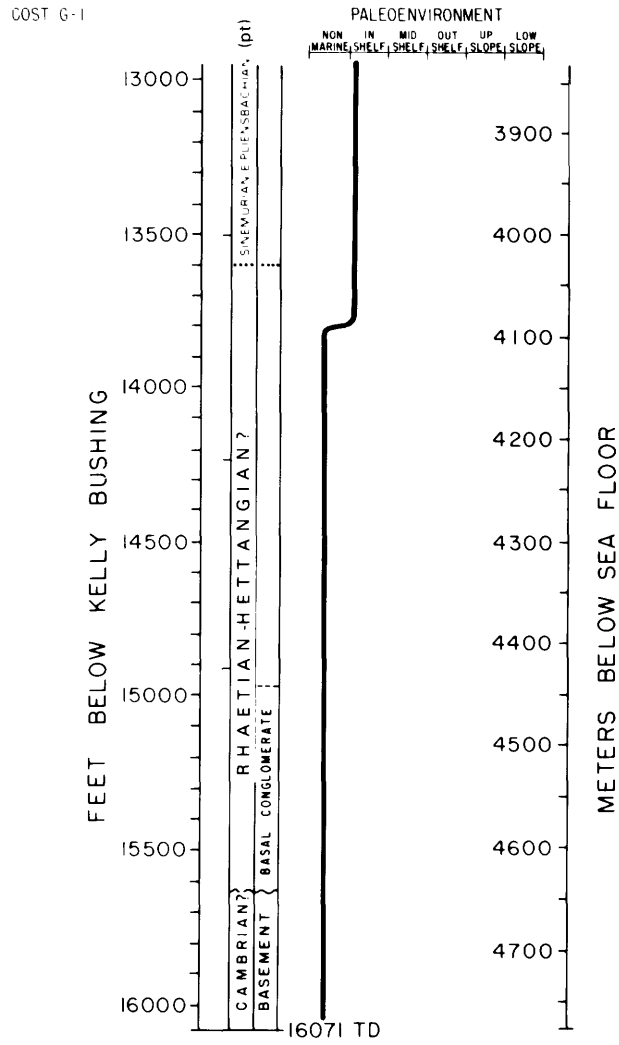

mine the presence of unconformities and to establish a chronostratigraphic framework for each well. The chronostratigraphic sequences are then used to calculate sediment accumulation rates. The chronostratigraphic and lithostratigraphic units are compared with those of the Scotian basin of Canada, and correlations are established between the COST No. G-2 and Shell Mohican I-100 wells. The stratigraphic nomenclature used in this basin is extrapolated from that used in wells on the Scotian shelf of Canada.

The paleoenvironmental analysis is based on the microfossil record of the COST Nos. G-1 and G-2 wells and an interpretation of seismic facies along USGS multichannel line 19. The biostratigraphic, paleoenvironmental, and seismic sequence data are combined to determine depositional cycles. The lack of microfossils through

AGE
FORMATION
SPONTANEOUS POTENTIAL (millivolts)
LITHOLOGY
RESISTIVITY (ohms)
LITHOLOGY
DEPTH
feet
meters
Datum-Kelly Bushing (KB)
SEA LEVEL 98ft BELOW KB
SEA FLOOR 255ft BELOW KB
CENOZOIC
PLEISTOCENE
PLIOCENE-MIOCENE
PALEOGENE
LAURENTIAN
BANQUEREAU
LATE CRETACEOUS
SANTONIAN
CONIACIAN
E. TURONIAN
L. CENOMANIAN
LOGAN CANYON-DAWSON CANYON
EARLY CRETACEOUS
APTIAN
BARREMIAN
HAUTERIVIAN
VALANGINIAN
BERRIASIAN
MISSISAUGA
"O" MARKER
BACCARO LS
LATE JURASSIC
TITHONIAN-LATE KIMMERIDGIAN
EARLY KIMMERIDGIAN
OXFORDIAN?
MIDDLE JURASSIC
CALLOVIAN?
MIC MAC-MOHAWK
1
2
SANDSTONE and GRAVEL: unconsolidated coarse, abundant shell fragments; glauconite, lignite.
SHALE: gumbo-like, interbeds of coarse sand, gravel; glauconite
SANDSTONE: unconsolidated coarse to very coarse, in part calcareous, interbeds of red and gray gumbo-like SHALE; lignite, pyrite; argillaceous DOLOMITE near base
SHALE: gray (gumbo), few beds of unconsolidated SANDSTONE; coal near top
SAND: very coarse, scattered pebbles, thin beds of gray SHALE (gumbo); COAL or LIGNITE at base
SHALE and CLAY: light gray; interbeds of coarse SAND; thin beds of DOLOMITE and SHALE near base.
SAND and loosely cemented SANDSTONE, medium to coarse; few COAL and lignite beds; in part shaly, pyritic, micaceous.
SHALE: orange-brown, dolomitic; abundant lignite, pyrite, few thin interbeds of fine to coarse SANDSTONE.
SANDSTONE and SHALE: about 60-40 SANDSTONE: coarse to very coarse, loose; traces of pyrite, lignite. SHALE: red, yellow, gray, brown, in part silty, micaceous.
SANDSTONE: unconsolidated, coarse to very coarse, slightly arkosic, some pea-gravel; thin interbeds of brown-red and variegated SHALE
0
1000
500
2000
3000
1000
4000
5000
1500
6000
2000
7000
8000

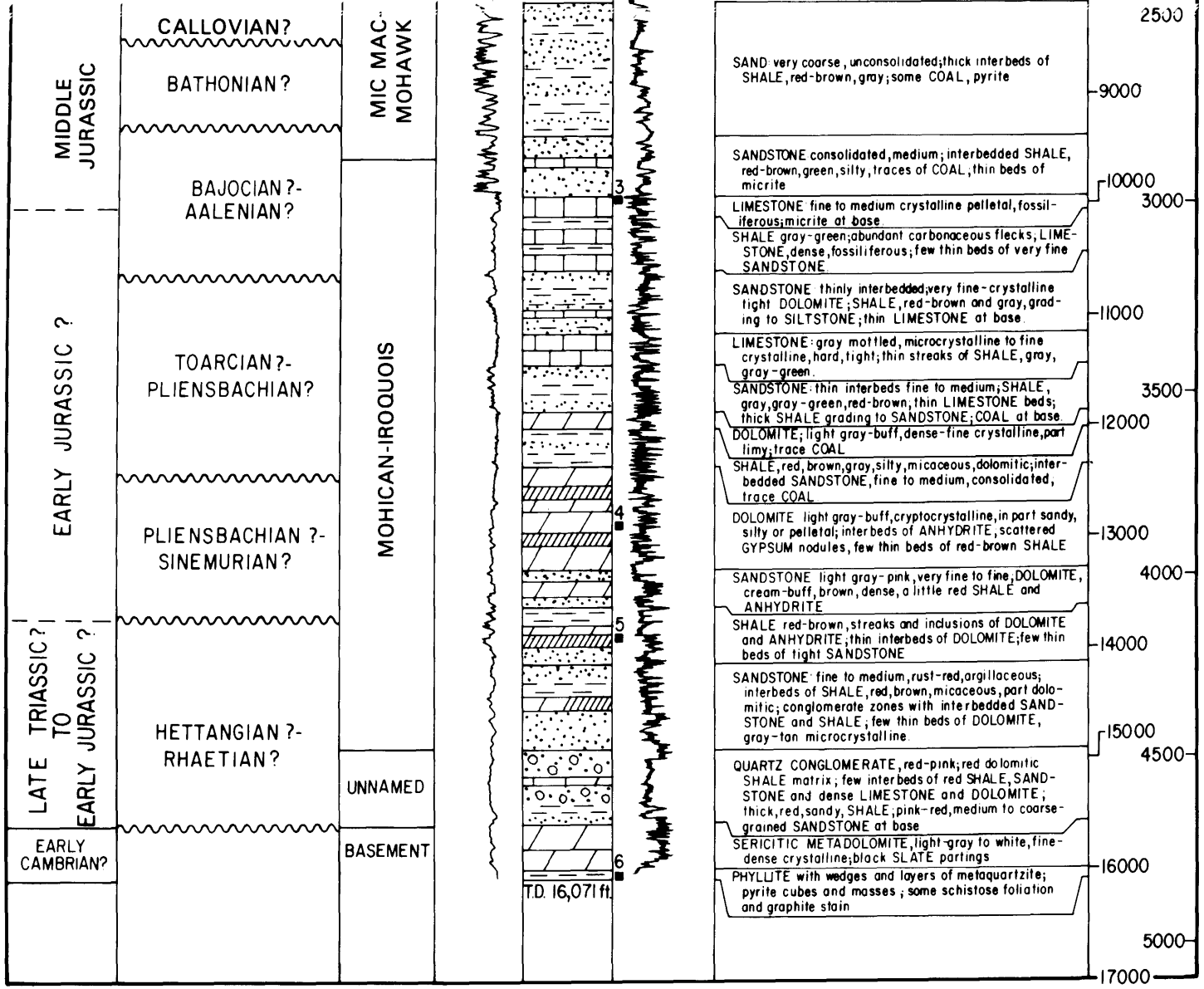

FIGURE 17.—Geologic column of COST No. G-1 well. The formation names in this paper are those of similar rocks on the Scotian shelf of Canada.

most of the thick Jurassic carbonate sections makes identification of older depositional cycles difficult, but first-order cycles can be easily recognized in the Cretaceous and Cenozoic.

Finally, comparisons of stratigraphic and depositional sequences between the Georges Bank wells, the Scotian basin, and deep-sea sites reveal some marked regional similarities in geologic history.

BIOSTRATIGRAPHY AND CHRONOSTRATIGRAPHY OF THE COST No. G-1 WELL

CENOZOIC ROCKS (157-1,030 FT; 48-314 M)

The youngest cutting sample from the COST No. G-1 well in this study is from 1,030 ft (314 m) and is considered to be Santonian in age (figs. 16 and 17). However, it does contain a few middle Eocene foraminifers (*Acarinina bulbrooki*) and some Paleocene foraminifers (*Pseudohastigerina wilcoxensis*) which indicate the presence, higher in the well, of unsampled Cenozoic strata.

Seismic correlation with the COST No. G-2 well indicates that the Santonian strata are unconformably overlain by 120 ft (37 m) of Paleogene rocks (probably mainly middle Eocene), 475 ft (145 m) of Neogene rocks (probably chiefly Miocene), and 170 ft (57 m) of Pleistocene rocks. At the G-1 well site, 161 ft (49 m) of Pleistocene rocks was recovered from USGS AMCOR site No. 6018 (Hathaway and others, 1979).

A prominent seismic reflector 650 ft (198 m) below the sea floor at the G-1 site (Hathaway and others, 1976) apparently marks a middle Eocene limestone unit (fig. 18). This middle Eocene limestone was penetrated and sampled at AMCOR site No. 6019, 60 mi (100 km) to the northwest (fig. 15), and at the G-2 well site (figs. 19, 20, 21), and its upper surface can be correlated seismically between the three sites. At AMCOR No. 6019 the middle Eocene limestone is white,

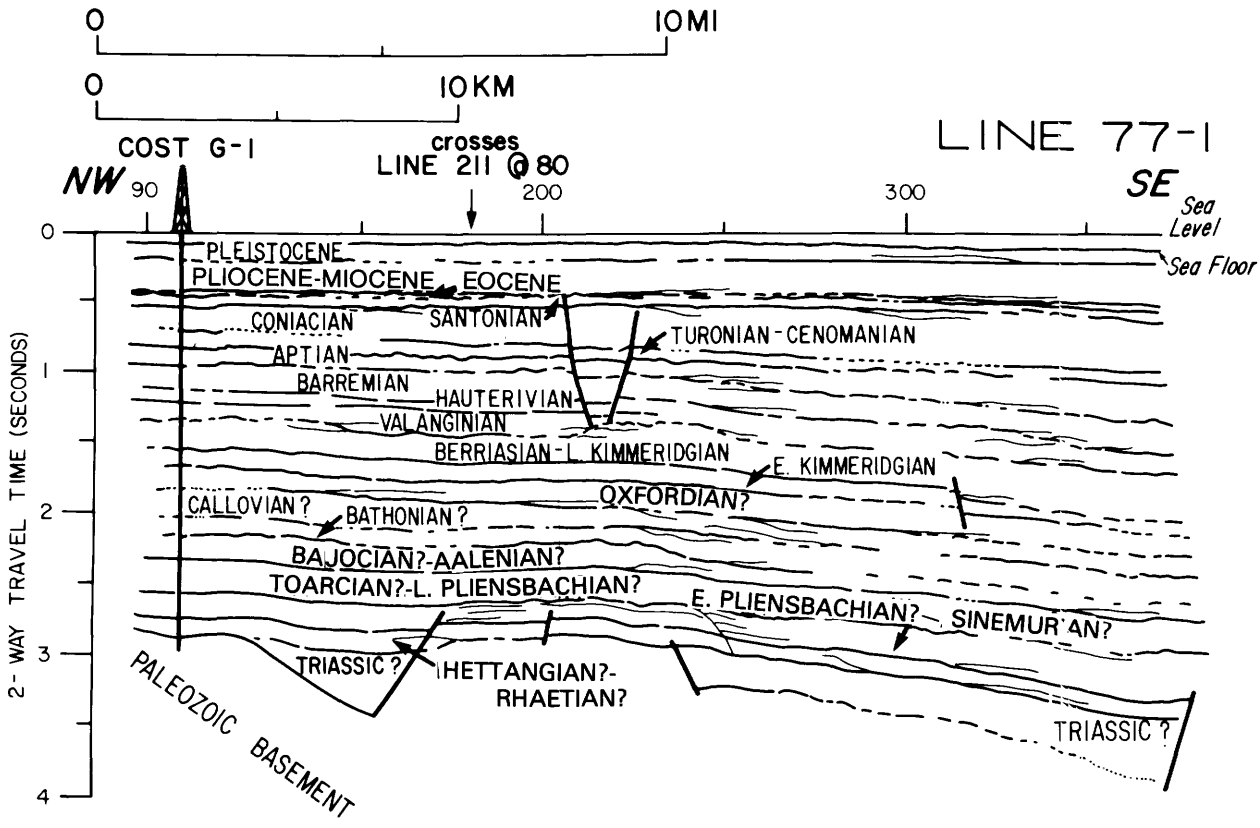

FIGURE 18.—Structural and chronostratigraphic interpretation of seismic reflection profile line 77-1, which crosses the G-1 well site along dip.

glauconitic, and bioclastic and contains abundant foraminifers and bryozoan remains. Small to medium fragments of this limestone were present in the uppermost G-1 sample. Some fragments have been altered and have a dense, light-gray, weathered appearance.

CRETACEOUS ROCKS

SANTONIAN (1,030–1,390 FT; 314–424 M)

The top cutting sample, collected at 1,030 ft (314 m), contains a predominantly Cretaceous assemblage of *Archaeoglobigerina cretacea, Hedbergella delrioensis, Heterohelix* sp., *Arenobulimina americana, Kyphopyxa christneri, Epistomina supracretacea, Gavelinella* sp., *Vaginulina wadei, Marginulina silicula,* and *Bolivinita eleyi.* This assemblage could be as young as early Campanian, but seismic correlation with the G-2 well (fig. 21) suggests that the strata are probably Santonian (fig. 16; see below). This is in agreement with palynomorph and nannofossil evidence (Steinkraus, 1980; Valentine, this volume). The lower Santonian indicator foraminifer *Marginotruncana sinusoa,* appears at 1,150 ft (351 m) along with *Archaeoglobigerina blowi* and *Globotruncana lapparenti.*

CONIACIAN (1,390–1,940 FT; 424–951 M)

At 1,390 ft (424 m) there is a slight increase in the number of specimens and an increase in species diversity that coincide with a major unconformable seismic reflector and the appearance of gypsum and siderite nodules (figs. 16, 18, 21). *Whiteinella* sp. cf. *W. aprica* makes its first appearance[1] here along with the first specimens of *Epistomina spinulifera colomi,* and a few redeposited specimens of *Rotalipora cushmani* and *Guembelitria harrisi.*

LOWER TURONIAN (1,940–2,320 FT; 591–707 M)

At 1,941 ft (593 m) the early Turonian species *Marginotruncana helvetica* and *Praeglobotruncana stephani* first appear in a sidewall core (fig. 16). This occurrence coincides with a major unconformable seismic reflector (figs. 18, 21). The first occurrence of these species in cuttings is slightly lower at 1,960 ft (597 m), where they are accompanied by *Hedbergella amabilis, Whiteinella archaeocretacea,* and abundant *Epistomina spinulifera colomi.*

UPPER CENOMANIAN (2,320–2,380 FT; 707–725 M)

The first non-redeposited *Rotalipora cushmani* occur in abundance at 2,320 ft (707 m), which coincides with a major seismic unconformity (figs. 16, 18, 21). This species is accompanied by abundant *Guembelitria harrisi;* however, *G. harrisi* is abundant without *R. cushmani* slightly higher in the well at 2,260 ft (689 m).

APTIAN (2,380–2,750 FT; 725–838 M)

At 2,380 ft (725 m) a change in the foraminiferal assemblage accompanied by lignite and red shale corresponds to an unconformable seismic reflector that can be correlated with the top of the Aptian interval in the G-2 well (figs. 16, 21); Albian rocks appear to be missing. The Aptian species *Lenticulina nodosa* and *Vaginulina aptiensis* are present in G-1, as is a large number of *Epistomina chapmani.* The rest of the Aptian rocks at G-1 contain only a sparse, poorly preserved assemblage of foraminifera and occasional siderite nodules. Steinkraus (1980) reported Aptian dinoflagellates as deep as 3,671 ft (1,119 m) in a sidewall core.

BARREMIAN (2,750–3,600 FT; 838–1,097 M).

The unconformable boundaries of the Barremian Stage at the G-1 site are determined from an analysis of seismic sequences (Vail and others, 1977) on reflection profiles 77-1 and 19, and by seismic correlation with the G-2 site. The foraminiferal assemblage in this interval is sparse and appears to be chiefly derived from cavings. Steinkraus (1980) reported Aptian dinoflagellates in the lower part of this section.

HAUTERIVIAN (3,600–4,000 FT; 1,097–1,219 M)

The unconformable boundaries of the Hauterivian Stage at the G-1 site are inferred from the analysis of seismic sequences on lines 77-1 and

[1]In this paper, "first appearance" refers to the point at which a species is first encountered in examining the well core from top to bottom. Biostratigraphically, this is the last appearance of the species.

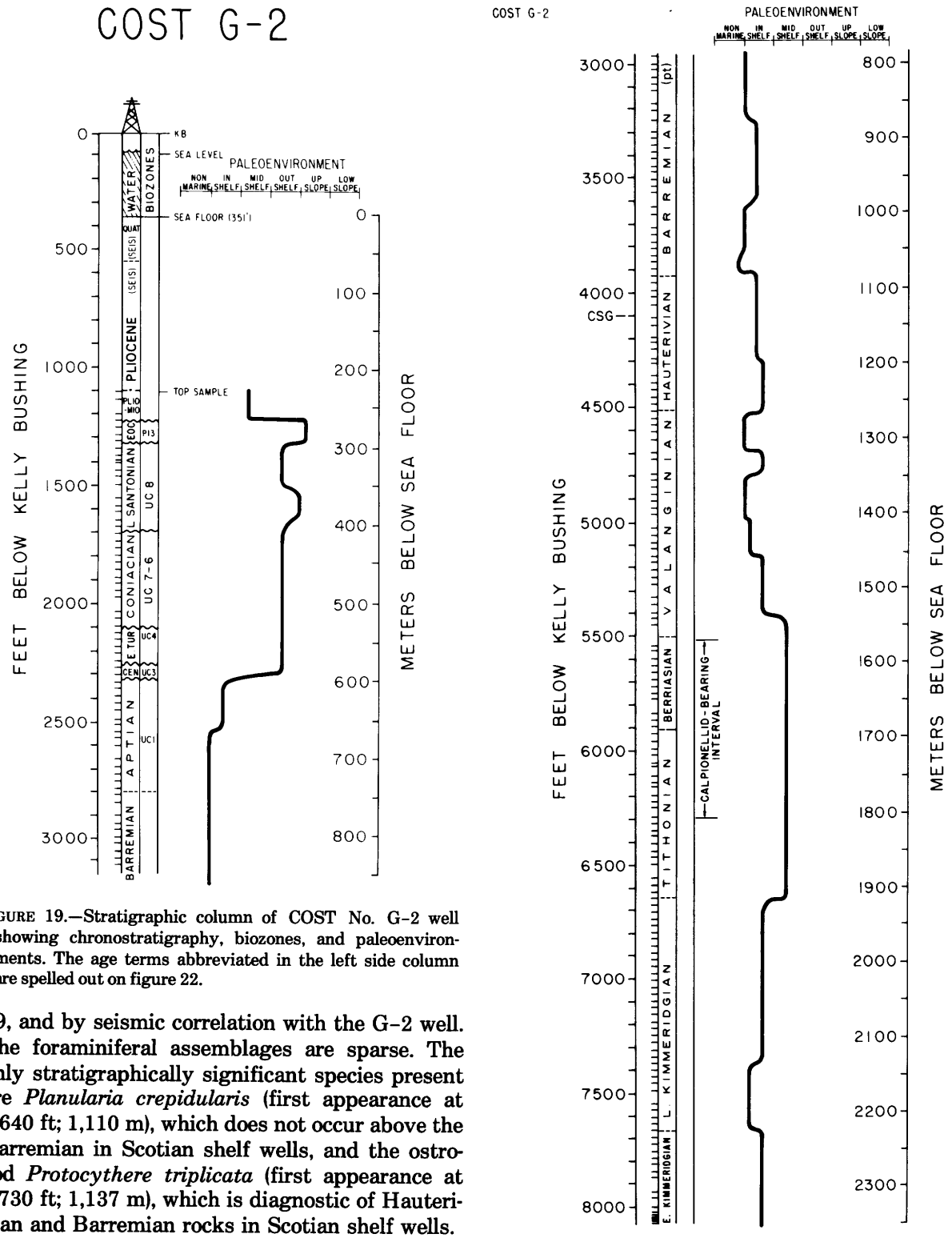

FIGURE 19.—Stratigraphic column of COST No. G-2 well showing chronostratigraphy, biozones, and paleoenvironments. The age terms abbreviated in the left side column are spelled out on figure 22.

19, and by seismic correlation with the G-2 well. The foraminiferal assemblages are sparse. The only stratigraphically significant species present are *Planularia crepidularis* (first appearance at 3,640 ft; 1,110 m), which does not occur above the Barremian in Scotian shelf wells, and the ostrocod *Protocythere triplicata* (first appearance at 3,730 ft; 1,137 m), which is diagnostic of Hauterivian and Barremian rocks in Scotian shelf wells.

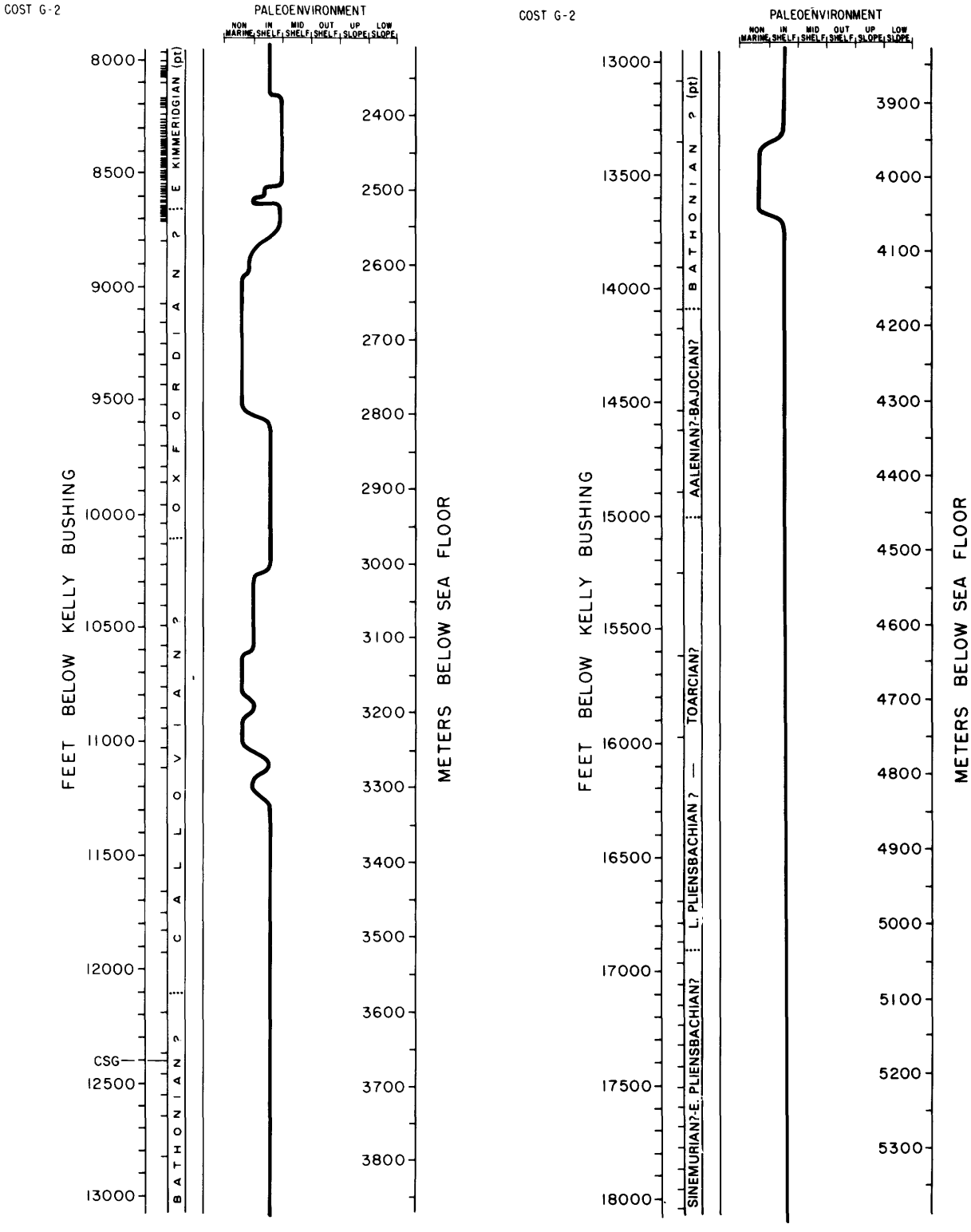
COST G-2
PALEOENVIRONMENT
NON MARINE
IN SHELF
MID SHELF
OUT SHELF
UP SLOPE
LOW SLOPE
FEET BELOW KELLY BUSHING
METERS BELOW SEA FLOOR
8000
8500
9000
9500
10000
10500
11000
11500
12000
CSG
12500
13000
2400
2500
2600
2700
2800
2900
3000
3100
3200
3300
3400
3500
3600
3700
3800
BATHONIAN ? CALLOVIAN ? OXFORDIAN ? E. KIMMERIDGIAN (pt)
COST G-2
PALEOENVIRONMENT
FEET BELOW KELLY BUSHING
METERS BELOW SEA FLOOR
13000
13500
14000
14500
15000
15500
16000
16500
17000
17500
18000
3900
4000
4100
4200
4300
4400
4500
4600
4700
4800
4900
5000
5100
5200
5300
SINEMURIAN?-E. PLIENSBACHIAN?
L. PLIENSBACHIAN ? — TOARCIAN?
AALENIAN?-BAJOCIAN?
BATHONIAN ? (pt)

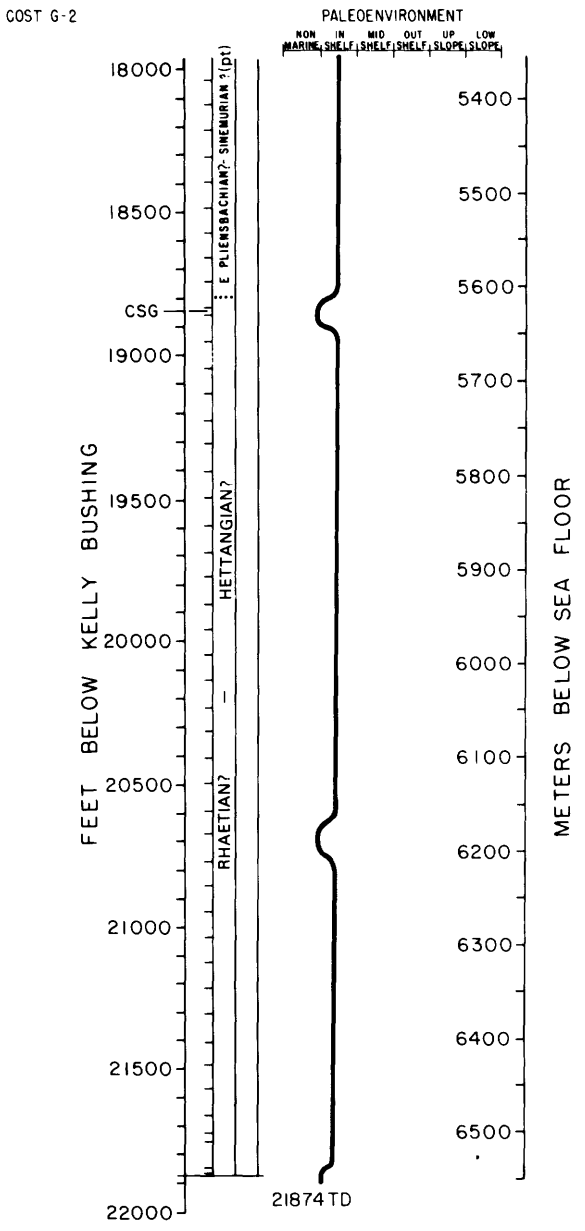

FIGURE 19.—Stratigraphic column of the COST No. G-2 well—Continued.

VALANGINIAN (4,000–4,500 FT; 1,219–1,372 m)

The unconformable boundaries of the Valanginian Stage at the G-1 site are estimated from an analysis of seismic sequences on lines 77-1 and 19, and by seismic correlation with the G-2 site. Microfossils are rare and not diagnostic.

BERRIASIAN (4,500–5,380 FT; 1,372–1,640 M)

The unconformable upper boundary of the Berriasian Stage at the G-1 site is estimated from an analysis of seismic sequences on lines 77-1 and 19, and by seismic correlation with the G-2 site. At 5,080 ft (1,548 m) a major faunal and lithologic change takes place. At the top of a thick sandstone unit, the first specimens of coarse-grained *Everticyclammina virguliana* appear and are accompanied by a small, fragile *Haplophragmoides* sp., coal fragments, and red shale. Steinkraus (1980) reported Berriasian nannofossils in a sidewall core at 5,070 ft (1,545 m).

JURASSIC ROCKS

TITHONIAN AND UPPER KIMMERIDGIAN
(5,380–5,800 FT; 1,640–1,768 M)

At 5,380 ft (1,640 m) (fig. 16) *Epistomina uhligi* first appears in low numbers, *Eoguttulina* aff. *E. liassica* appears in moderate numbers, a few specimens of *Cytherella index* appear, and *Everticyclammina virguliana* specimens have finer grained tests than younger specimens of that species. These changes are typical of the top of the Tithonian in other U.S. and Canadian shelf wells, and the Tithonian Age is in agreement with the interpretation of palynomorph and nannofossil assemblages (Steinkraus, 1980).

LOWER KIMMERIDGIAN (5,800–6,400 FT; 1,768–1,951 M)

The unconformable upper and lower boundaries of the lower part of the Kimmeridgian Stage at the G-1 site are estimated from analysis of seismic sequences on lines 77-1 and 19 and seismic correlation with the G-2 well. The upper boundary lies within an oxidized zone of foraminifera and siderite nodules (5,700 to 6,000 ft; 1,737 to 1,829 m). Steinkraus reported lower Kimmeridgian dinoflagellates in a sidewall core at 6,543 ft (1,994 m).

OXFORDIAN(?) TO AALENIAN(?)
(6,400–10,500 FT; 1,951–3,201 M)

From 6,400 to 10,000 ft (1,951 m to 3,048 m) is a thick sequence of coarse, ligritic sandstones interbedded with brown to red shales, which con-

tains few calcareous microfossils (fig. 16). Below 10,000 ft (3,048 m), the carbonate content is much greater (fig. 17). Interbedded pelletal limestones, gray-green shale, finely crystalline dolomite, and fine-grained sandstones and siltstones are found down to 10,500 ft (3,201 m), but free tests of foraminifera are absent. The unconformable boundaries of stages and groups of stages within this interval are estimated from analysis of seismic sequences on USGS multichannel lines 77-1 and 19 (figs. 18, 21) as follows:

Oxfordian(?), 6,400-7,400 ft (1,951-2,256 m;
Callovian(?), 7,400-8,500 ft (2,256-2,591 m);
Bathonian(?), 8,500-9,300 ft (2,591-2,835 m);
Bajocian(?) to Aalenian(?), 9,300-10,500 ft (2,835-3,201 m).

TOARCIAN(?) TO SINEMURIAN(?) (10,500-13,600 FT; 3,201-4,145 M)

The rocks from 10,500 to 13,600 ft (3,201 to 4,145 m) are chiefly carbonates (gray, microcrystalline to finely crystalline limestones, gray to buff, finely crystalline to cryptocrystalline dolomite, and anhydrite) with thin interbeds of sandstone and shale, occasional coal beds, and scattered gypsum nodules (fig. 17). No foraminifera were recovered in this interval, but it can be divided into two parts through analysis of seismic sequences on lines 77-1 and 19, (figs. 16, 18, 21) as follows: Toarcian(?) to upper Pliensbachian(?), 10,500-12,300 ft (3,201-3,749 m), and Lower Pliensbachian(?) to Sinemurian(?), 12,300-13,600 ft (3,749-4,145 m).

HETTANGIAN(?) TO RHAETIAN(?) (13,600-15,630 FT; 4,145-4,764 M)

The age of these sedimentary rocks is estimated from analysis of seismic sequences as interpreted from USGS lines 77-1 and 19. The upper rocks are chiefly sandstones and shales with thin intervals of dolomite and anhydrite (13,600-14,970 ft; 4,145-4,563 m). Late Triassic dinoflagellates have been recovered from the lower part of this unit (anonymous oral commun., 1980). From 14,970 to 15,630 ft (4,563 to 4,764 m) is a quartz conglomerate with a matrix of red dolomitic shale and interbeds of red shale, sandstone, and dense limestone and dolomite (fig. 17). The conglomerate lies unconformably upon a metamorphic basement composed of sericitic metadolomite and black slate (15,630-16,000 ft; 4,764-4,877 m), which overlies graphitic phyllite, metaquartzite and gneiss (16,000-16,071 ft; 4,877-4,899 m). Radiometric dates of 450 to 550 m.y. (K/Ar) indicate that the metamorphism took place in the Cambrian or Ordovician (Steinkraus, 1980).

BIOSTRATIGRAPHY AND CHRONOSTRATIGRAPHY OF THE COST NO. G-2 WELL

CENOZOIC ROCKS (351-1,324 FT; 107-404 M)

The first cutting sample in the COST No. G-2 well was collected at 1,100 ft (335 m) (fig. 19). From there to 1,250 ft (381 m) a sparse benthic fauna consisting chiefly of *Brizalina bradyi*, *Globobulimina auriculata*, *Bulimina elongata*, *Lentliculina spinosa*, *L. americana*, *Cassidulina "carinata"*, *Florilus pizzarensis*, and *Cibicidoides* aff. *C. floridanus* indicates rocks of Pliocene to Miocene age. A few radiolarians and reworked Cretaceous planktic foraminifers also are present in this interval. Seismic sequence analysis and results from AMCOR drilling (Hathaway and others, 1979) indicate that Pliocene to Miocene rocks are present up to 550 ft (168 m) in the section, and are overlain unconformably by 260 ft (61 m) of Quaternary rocks (figs. 19, 21, 22).

Below 1,250 ft (381 m) the number of foraminiferal specimens and the diversity of species increases dramatically, and there is an abundance of large fragments of cheilostome bryozoans. Among the many planktic species present, *Truncorotaloides rohri* and *Acarinina bullbrooki* indicate that this rich assemblage is of middle Eocene age. These same planktic species are present in a sidewall core from 1,289 ft (393 m), along with *Morozovella spinulosa*, *Truncorotaloides topilensis*, *Eoglobigerina senni*, and *Globigerinatheka subconglobata*. This middle Eocene assemblage continues to 1,324 ft (404 m); and additional middle Eocene species, such as *Acarinina pentacamerata*, appear within this interval. The presence of a few specimens of *Globigerina opima opima* at 1,289 ft (393 m) suggest that a thin interval of late Oligocene strata may lie unconformably above the middle Eocene rocks.

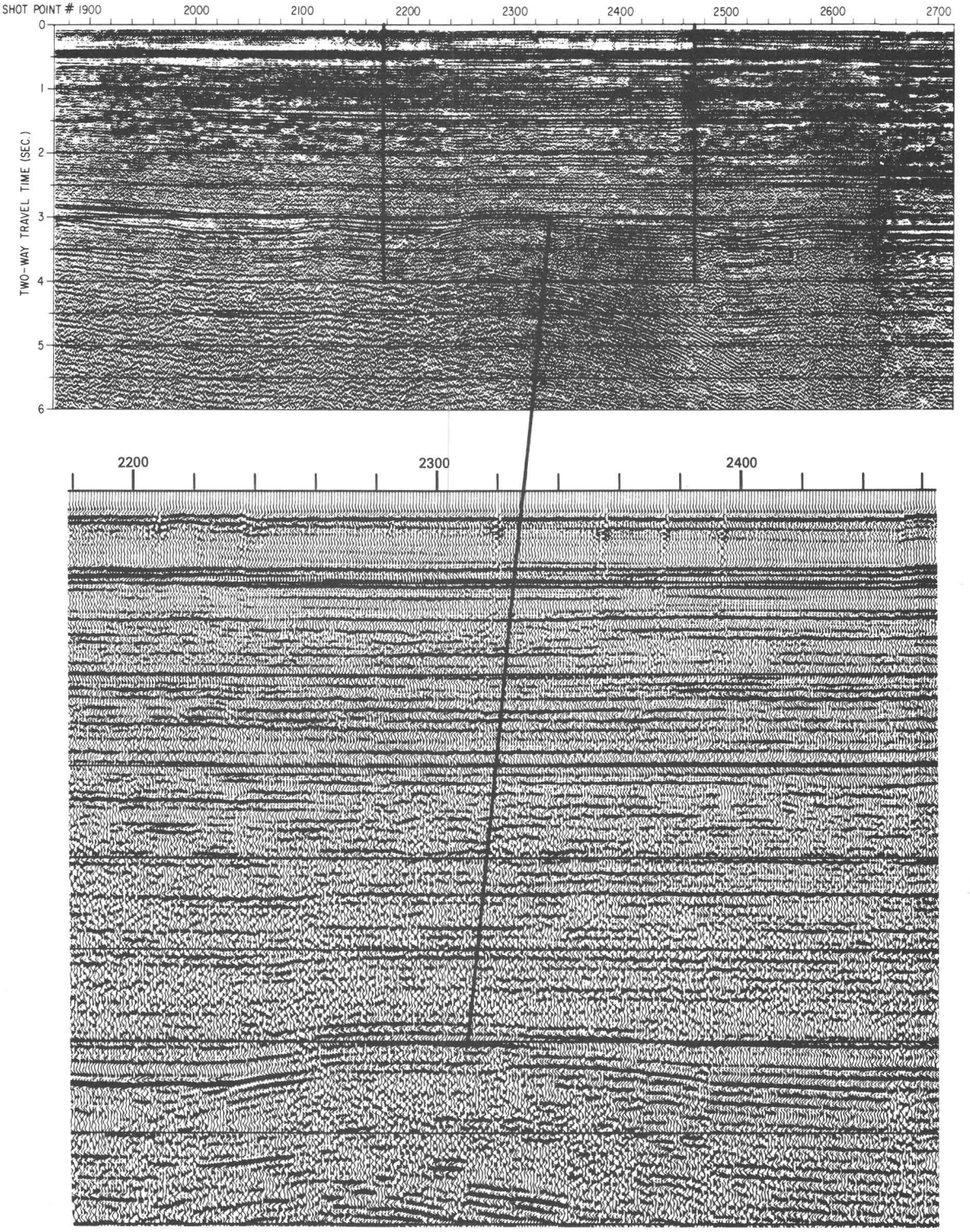

FIGURE 20.—Uninterpreted portion of seismic reflection profile line 19, which traverses the Georges Bank basin along dip approximately 15 km (9.3 mi) northeast of the COST No. G-2 well.

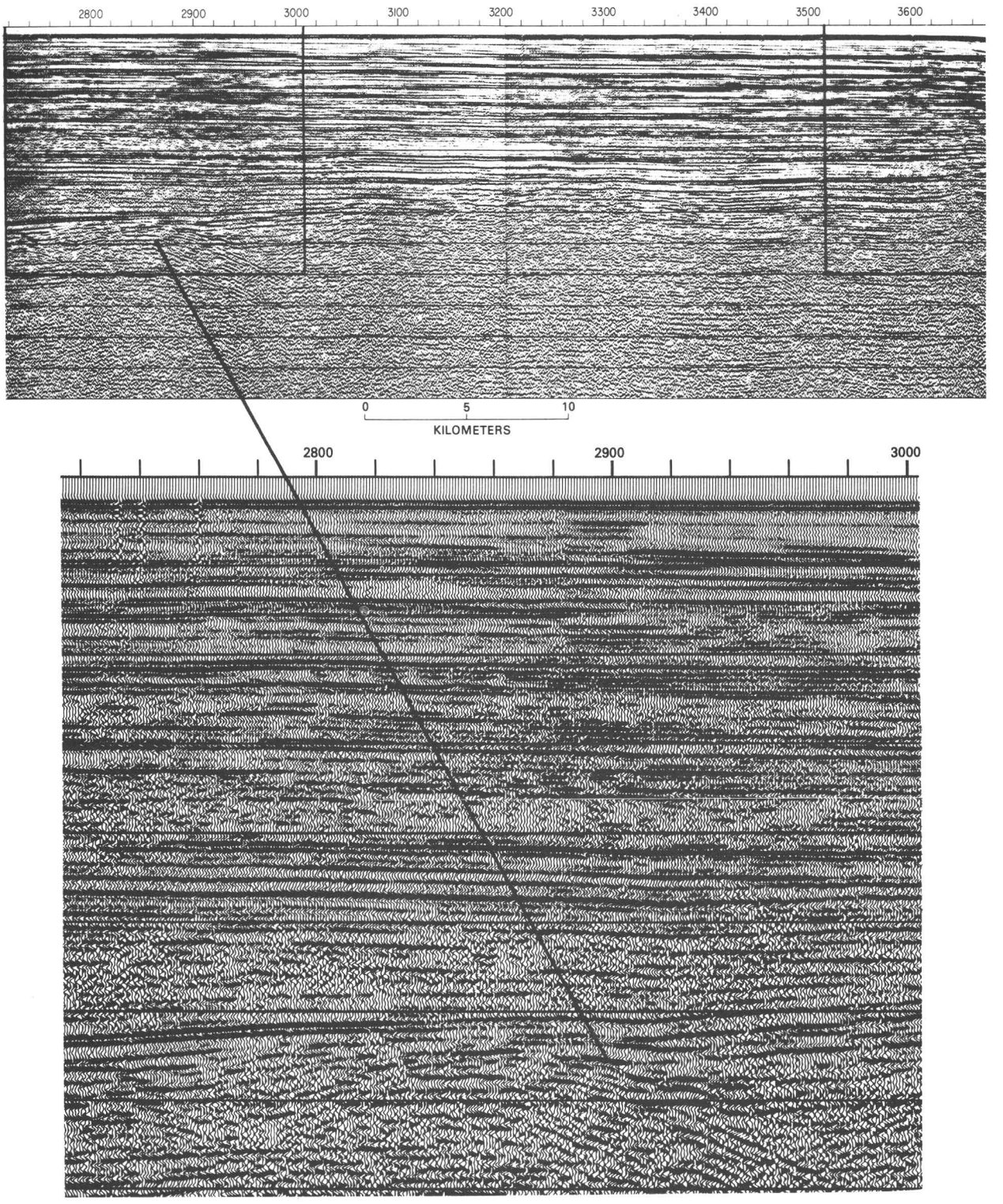

FIGURE 20.—Uninterpreted portion of seismic reflection profile line 19—Continued.

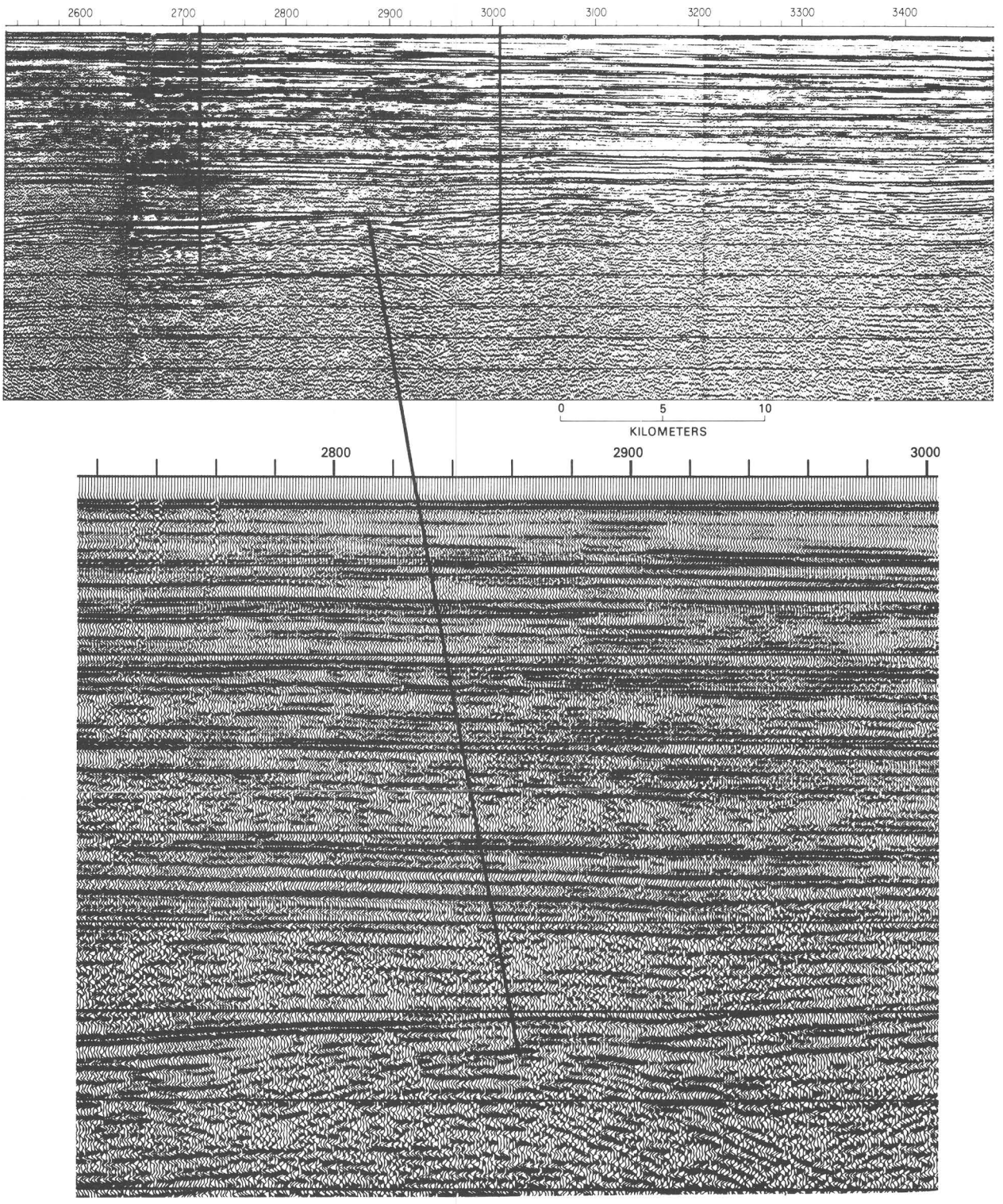

FIGURE 20.—Uninterpreted portion of seismic reflection profile line 19—Continued.

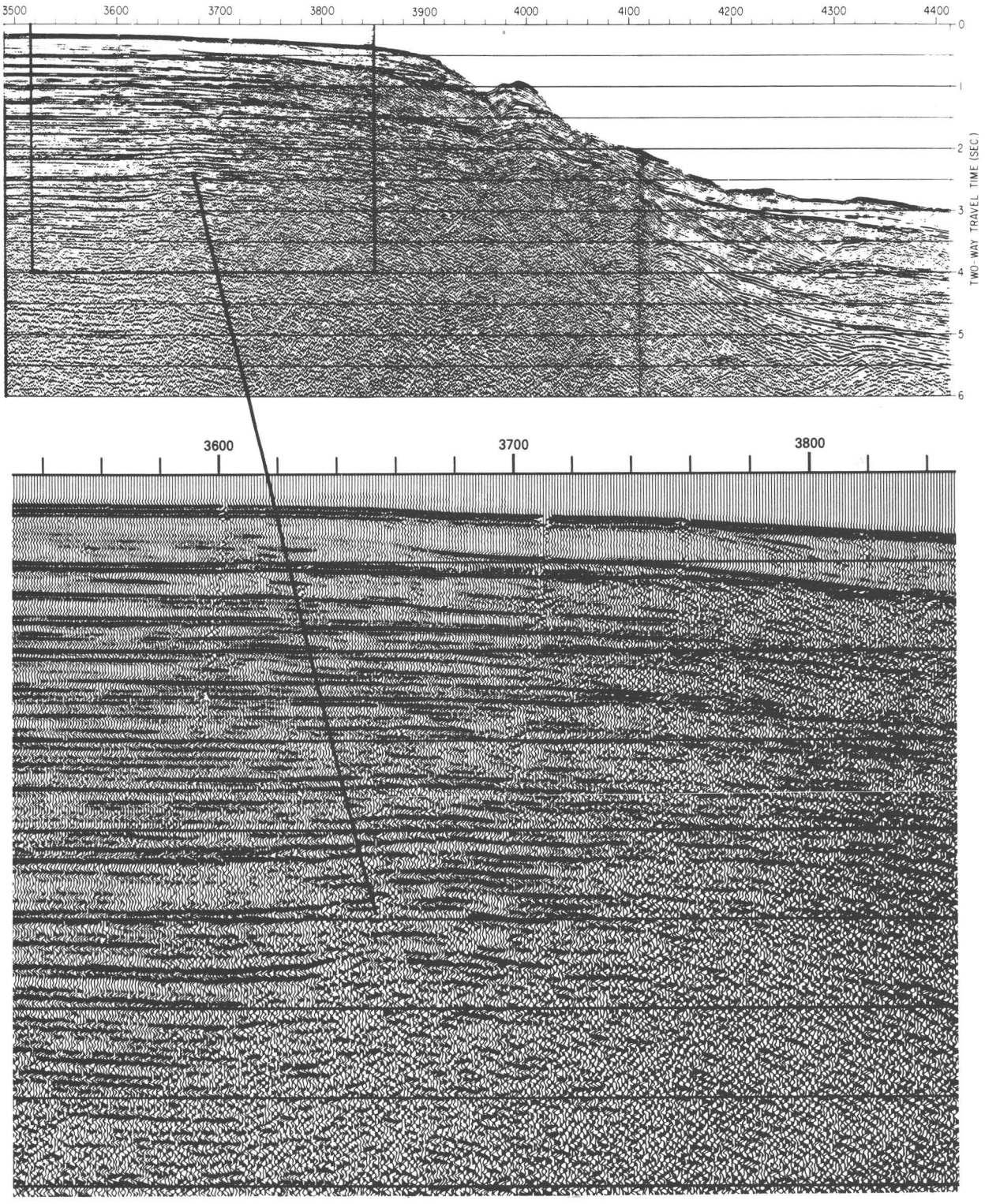

FIGURE 20.—Uninterpreted portion of seismic reflection profile line 19—Continued.

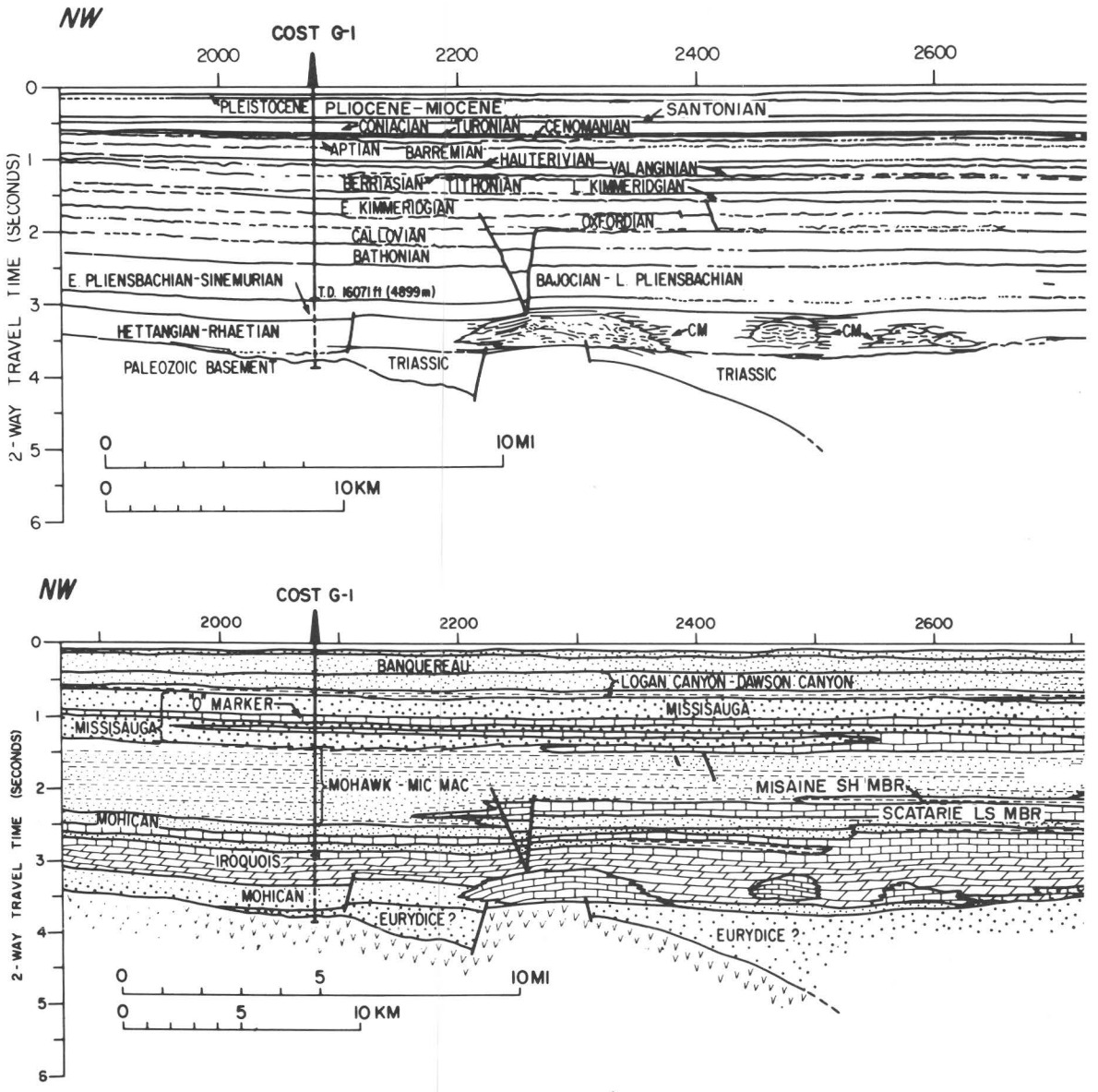

FIGURE 21.—Interpretations of structure, chronostratigraphy, and lithostratigraphy of the portion of seismic line 19 shown in figure 20. COST well locations are projected northeastward along strike to line 19. Section at G-1 projection is thicker than at the actual well site; chronostratigraphic boundaries are adjusted to accomodate this difference. CM, carbonate mound. Many of the age terms shown are uncertain. The formation names in this paper are those of similar rocks on the Scotian shelf of Canada.

CRETACEOUS ROCKS

LOWER SANTONIAN (1,324–1,700 FT; 404–518 M)

The first non-redeposited Cretaceous assemblage occurs in cuttings at 1,400 ft (427 m) and is characterized by *Marginotruncana sinuosa, Globotruncana lapparenti, Heterohelix striata* and *Archaeoglobigerina cretacea*, an early Santonian association. A sidewall core at 1,324 ft (404 m) contains a similar association. The presence of well preserved *Globorotalites pseudomenardii* in the 1,400-ft (427-m) sample indicates that a thin interval of Paleocene rock is present above the Santonian. No evidence of Maestrichtian or Campanian strata was observed. Santonian rocks are present down to 1,700 ft (518 m) and *Sigalia ornatissima, Globigerinelloides prairiehillensis, Hedbergella planispira, Archaeoglobigerina blowi*, and *Mar-*

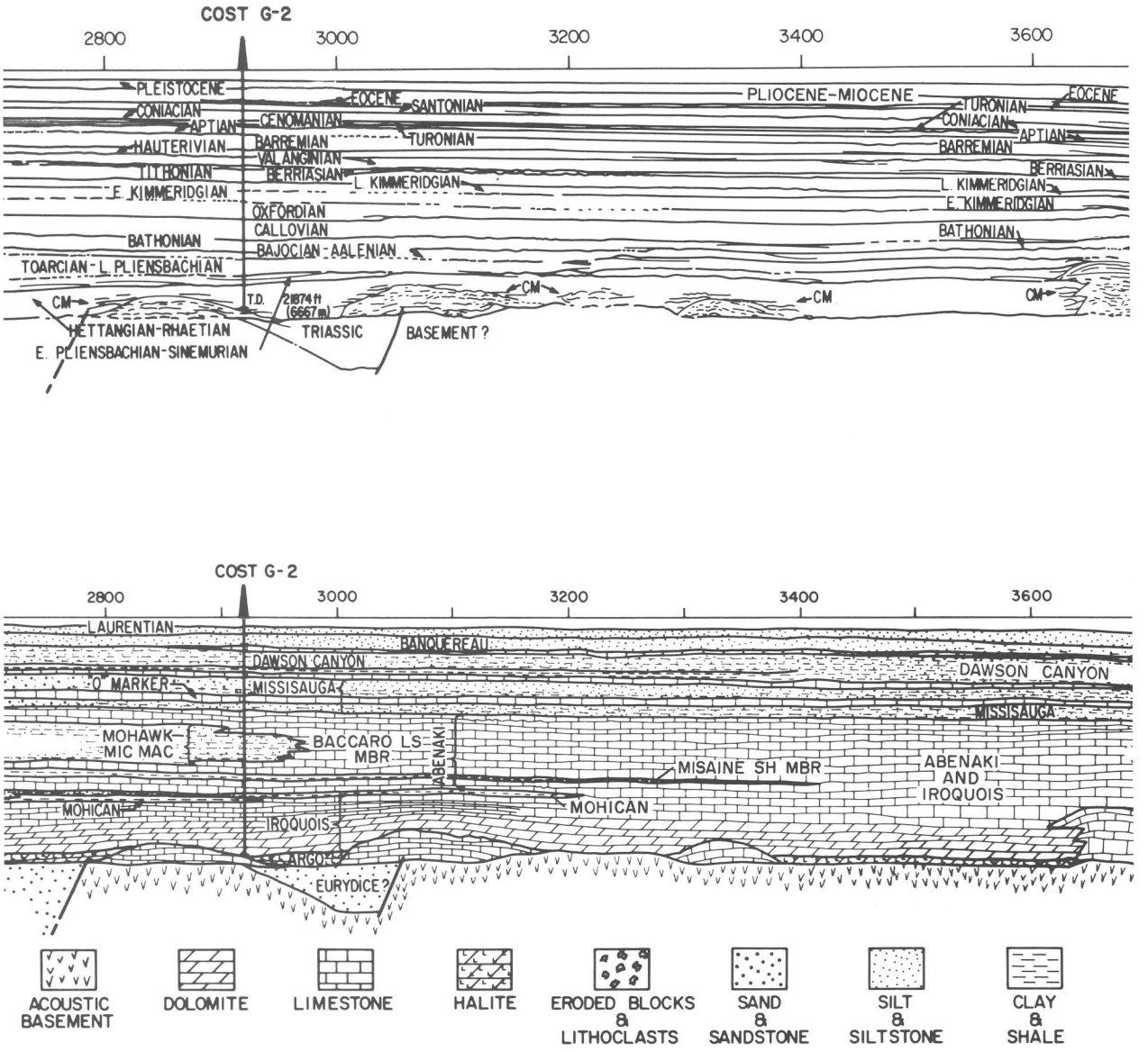

FIGURE 21.—Interpretations of a portion of seismic line 19—Continued.

ginotruncana renzi are part of the assemblage in this interval. Dinoflagellate and nannofossil assemblages also indicate that this interval is of Santonian Age (Bebout, 1980; Valentine, this volume).

CONIACIAN (1,700–2,120 FT; 518–646 M)

At 1,700 ft (518 m) the presence of *Whiteinella archaeocretacea* and *Marginotruncana schneegansi* marks the top of the Coniacian interval. *Globotruncana sigali* appears at 1,760 ft (536 m), and *Clavihedbergella simplex* and *Hedbergella amabilis* appear in abundance at 1,850 ft (564 m). *Marginotruncana concavata* also was observed at 1,970 ft (600 m), but this occurrence is clearly much older than its known range.

LOWER TURONIAN (2,120–2,270 FT; 646–692 M)

At 2,120 ft (646 m) *Praeglobotruncana stephani* and *Marginotruncana* cf. *M. helvetica* appear and mark the top of the early Turonian zone UC4. In a sidewall core *P. stephani* occurs at 2,186 ft (666 m). *Lingulogavelinella turonica* appears at 2,180 ft (664 m).

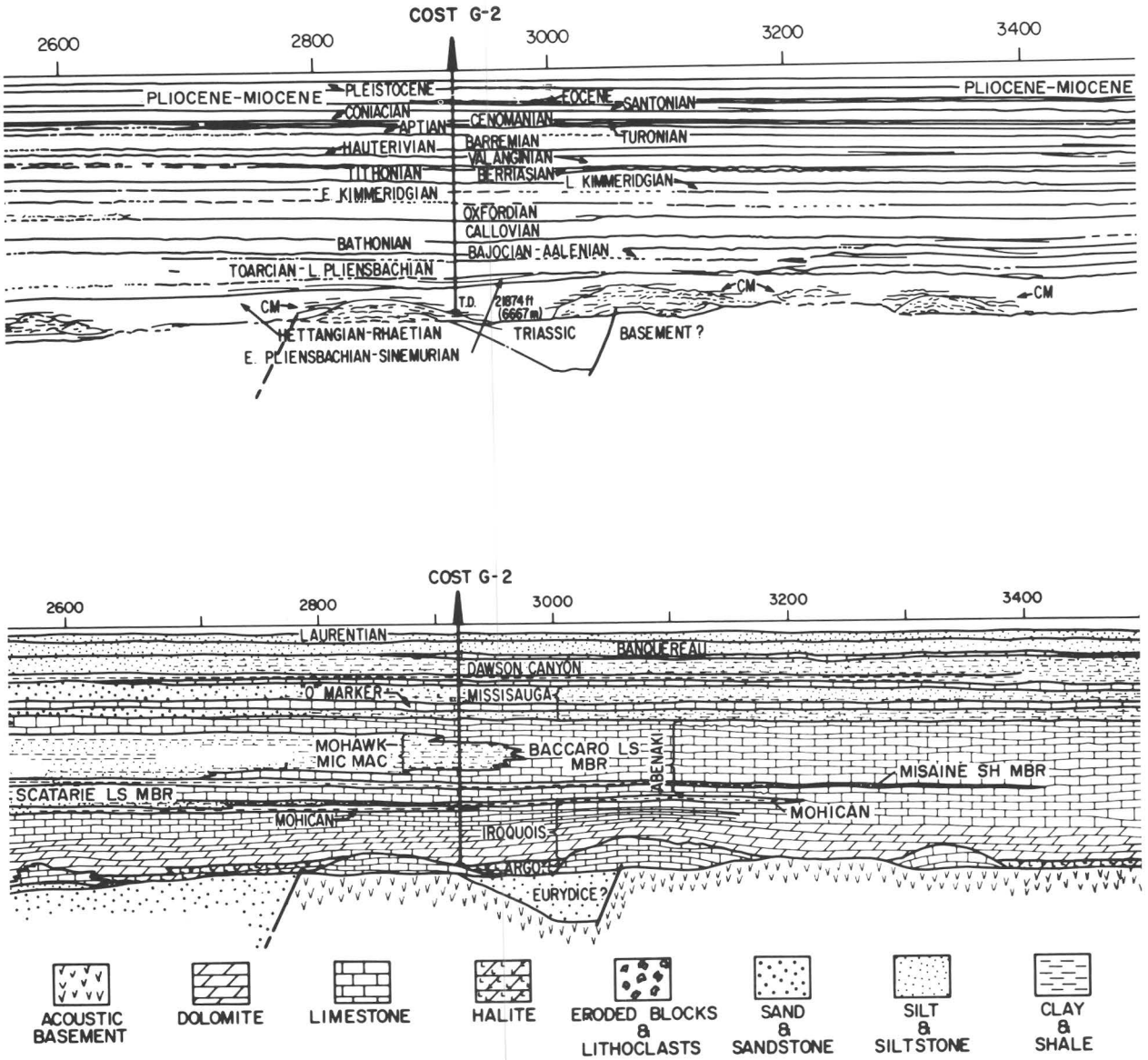

FIGURE 21.—Interpretations of a portion of seismic line 19—Continued.

UPPER TO MIDDLE CENOMANIAN
(2,270–2,330 FT; 692–710 M)

At 2,270 ft (692 m), the appearance of *Rotalipora cushmani* marks the Cenomanian. (*Guembelitria harrisi* appears 30 ft (9 m) above this in the Turonian interval.) *Rotalipora cushmani* is accompanied at 2,270 ft (692 m) by *R. greenhornesis,* which indicates that the top part of zone UC3 is missing or very thin. This rotaliporid association is also found in a sidewall core at 2,276 ft (694 m). *Whiteinella aprica, Epistomina chapmani,* and *Gavelinopsis cenomanica* also first appear at 2,270 ft (692 m), as do numerous specimens (presumably redeposited) of *Lenticulina nodosa,* an Aptian marker (Ascoli, 1976).

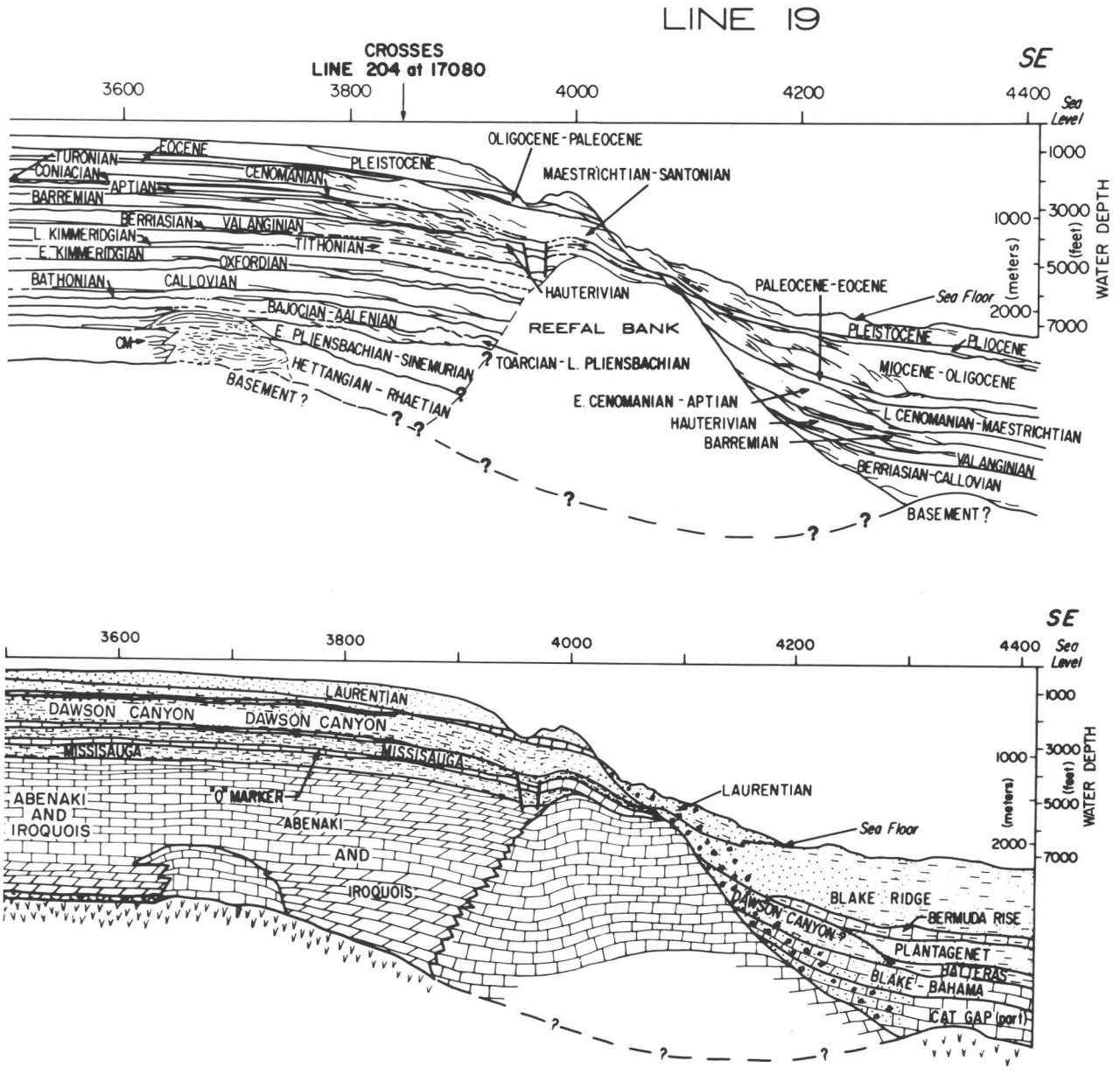

FIGURE 21.—Interpretations of a portion of seismic line 19—Continued.

APTIAN (2,330–2,810 FT; 710–857 M)

At 2,330 ft (710 m) seismic, faunal, and sedimentological data indicate that a major unconformity separates the very thin middle to upper Cenomanian strata from the Aptian. Here, the lithofacies changes, the fauna is somewhat diminished and more poorly preserved, and the number of rotaliporids decreases, but the number of *Lenticulina nodosa* remains high. At 2,360 ft (719 m) the foraminifer *Lenticulina* aff. *L. gaultina* and the ostracod *Hechticythere derooi* appear. *Lenticulina nodosa* is an amphiatlantic marker for Aptian rocks (Bartenstein, 1974), and *Lenticulina* aff. *L. gaultina* ranges no higher than the Aptian on the Scotian shelf (Ascoli, 1976). At 2,360 ft (719 m) the sample contains abundant oxidized, calcareous sandstone and lignite. Below this depth the species diversity is further reduced. Similar lithologic and faunal changes mark the unconformable Cenomanian-Aptian contact in the Shell Mohawk B-93 well, the

AGE
FORMATION
SPONTANEOUS POTENTIAL (millivolts)
LITHOLOGY
RESISTIVITY (ohms)
LITHOLOGY
DEPTH
feet
meters
Datum: Kelly Bushing (KB)
SEA LEVEL 79 FEET BELOW KB
SEA FLOOR 351 FEET BELOW KB
CENOZOIC
LATE CRETACEOUS
EARLY CRETACEOUS
LATE JURASSIC
MIDDLE JURASSIC?
PLEISTOCENE
PLIOCENE-MIOCENE
PALEOGENE
E. SANTONIAN
CONIACIAN
E. TURONIAN
L. & M. CENOMANIAN
APTIAN
BARREMIAN
HAUTERIVIAN
VALANGINIAN?
BERRIASIAN?
TITHONIAN-LATE KIMMERIDGIAN
EARLY KIMMERIDGIAN
OXFORDIAN?
CALLOVIAN?
LAURENTIAN
BANQUEREAU
DAWSON CANYON
MISSISAUGA
"O" MARKER
MISSISAUGA
ABENAKI
BACCARO LS MBR
MOHAWK - MIC MAC
ABENAKI
BACCARO LS MBR
MISAINE SH MBR
SAND: unconsolidated, coarse, rounded; abundant glauconite and shells; interbedded SILTSTONE: gray, soft, clayey.
CLAYSTONE and SILTSTONE: light gray, very calcareous, ranging to LIMESTONE: argillaceous, chalky; glauconite, fossiliferous; carbonaceous plant fragments, mica, pyrite.
LIMESTONE, coarse shell fragments; interbedded SANDSTONE: fine to medium calcite - cemented.
SAND: very coarse, rounded; SANDSTONE medium to fine, subangular, calcite - cemented; interbeds of gray silty MUDSTONE; streaks of COAL; shells; glauconite.
MUDSTONE: gray, silty, glauconitic, in part calcareous; interbeds of SANDSTONE gray, fine to medium, muddy.
LIMESTONE bioclastic, partly oolitic grainstone, packstone and wackestone ranging to argillaceous micrite and light gray calcareous claystone; SHALE: gray fissile.
SAND: very coarse to medium, subrounded to subangular; SANDSTONE: white to light gray, fine, cemented with calcite and silica, angular-subangular, moderately to well sorted; interbeds of COAL, dark brown LIGNITE, brown-gray SHALE, light gray MUDSTONE; pyrite, glauconite.
MUDSTONE: gray silty, calcareous, few beds of SANDSTONE and LIMESTONE.
LIMESTONE: light gray, micrite, chalky, argillaceous, interbedded with SHALE gray, silty, calcareous, pyrite, glauconitic; few beds of SANDSTONE.
SANDSTONE: light gray, some stained red, fine to medium, subangular-subrounded, poorly to well sorted, cemented with calcite; muscovite, biotite, chlorite;
SHALE: gray, in part very calcareous and silty; red-brown to maroon, silty, micaceous MUDSTONE; muddy SILTSTONE.
LIMESTONE: light gray oolite and algal-clast grainstone to mudstone, sandy; thin streaks of COAL.
LIMESTONE: brown-gray oolitic and oncolitic grainstone and packstone; interbeds of fine, well-sorted SANDSTONE, gray silty SHALE.
LIMESTONE: brown-gray micrite, argillaceous; minor oolite-bioclast grainstone and light gray micrite ranging to calcareous CLAYSTONE and gray SHALE; few SANDSTONE beds.
SHALE: gray, in part very calcareous; red near top; few beds of brown-gray micrite LIMESTONE; very fine to fine SANDSTONE; pyrite.
0
1000
500
2000
3000
1000
4000
5000
1500
6000
2000
7000
8000
2500
9000
10000
3000
11000

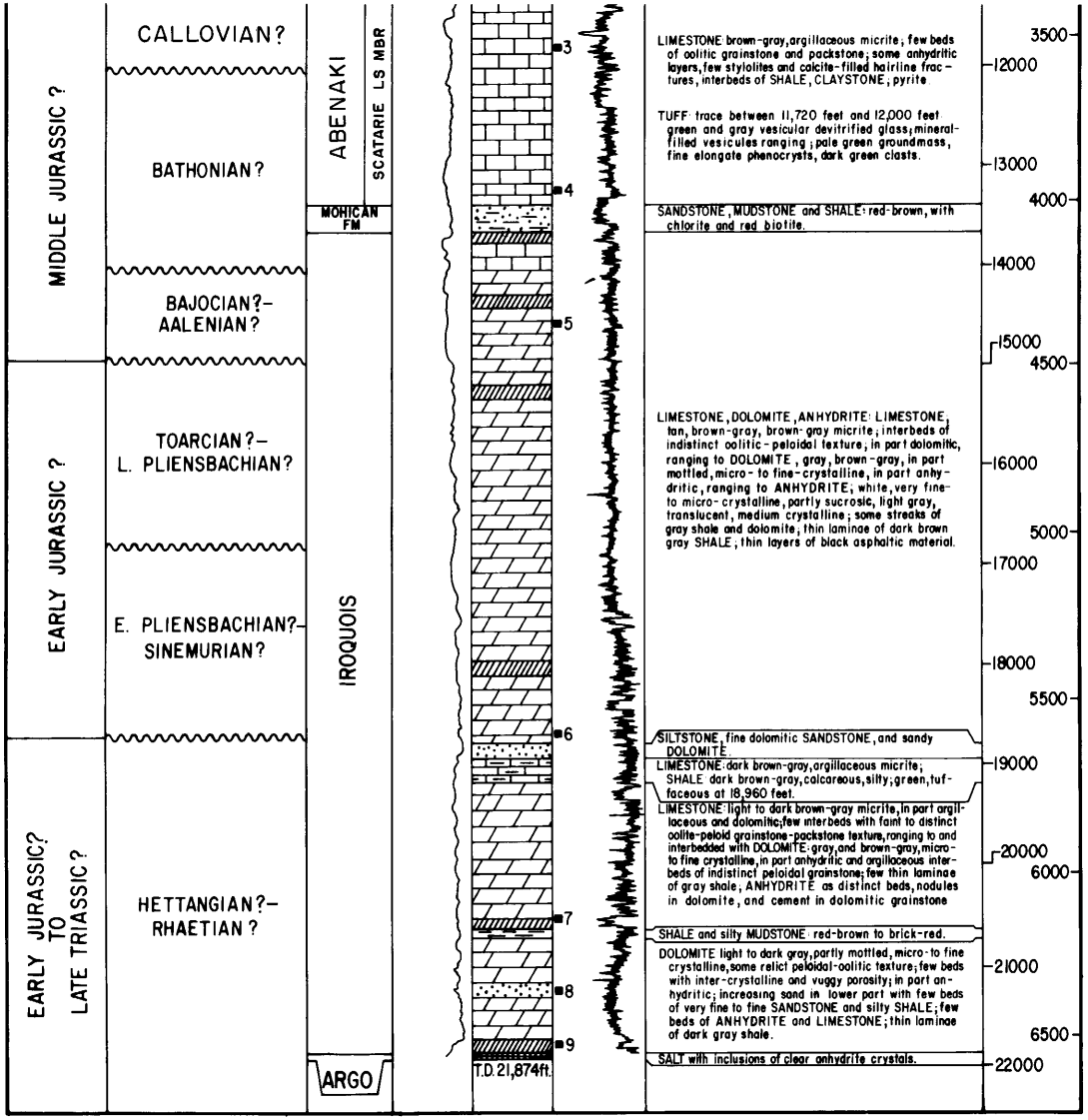

FIGURE 22.—Geologic column of COST No. G-2 well. The formation names in this paper are those of similar rocks on the Scotian shelf of Canada.

closest drill hole on the Scotian shelf. Analysis of seismic sequences shows that this unconformity is a strong reflector (figs. 20, 21) that displays irregular physiographic relief and terminates underlying reflectors, indicating that it is an erosional surface. Single specimens of *Ticinella roberti, T. breggiensis,* and *T. primula* between 2,300 and 2,390 ft (701 and 728 m) suggest that a thin remnant of Albian strata may have been penetrated at this site, but no other firm evidence of Albian rocks in the COST No. G-2 well has been observed. (See also Bebout, 1980.)

BARREMIAN (2,810–3,920 FT; 857–1,195 M)

The next significant faunal change occurs at 2,810 ft (857 m), where *Conorboides bulgaricus* becomes a persistent part of the sparse foraminiferal assemblage. This form is diagnostic of Barremian rocks in the Scotian basin (P. Ascoli, written commun., April 1980) and in Europe (Bartenstein and others, 1971). Other benthic foraminifers and ostracods diagnostic of Barremian strata in the Scotian basin occur just below this: *Conorotalites bartensteini* at 2,960 ft (902 m); *Schuleridea* sp. 9 of Ascoli (1976) at 2,990 ft (911 m); *Epistomina ornata* at 3,260 ft (994 m); *Neocythere* aff. *N. mertensi* at 3,260 ft (994 m) and *Conorboides hofkeri* at 3,290 ft (1,003 m). Bebout (1980) placed this interval in the Aptian Stage on the basis of a single dinoflagellate species believed to be restricted to the Aptian.

HAUTERIVIAN (3,920–4,510 FT; 1,195–1,375 M)

At 3,920 ft (1,195 m), there is a increase in foraminifers and the species *Haplophragmoides concavus, Planularia crepidularis, Lenticulina saxonica* and *Lamarckina lamplughi* appear, which are typical of Hauterivian intervals in the Scotian basin (Ascoli, 1976). The Hauterivian species *Marssonella kummi, Hechticythere hechti,* and *Hutsonia* sp. 3 of Ascoli (1976) are found at 4,010 ft (1,222 m); *Dolocytheridea* sp. 1 and *Macrodentina* sp. 1 of Ascoli (1976) at 4,130 ft (1,259 m); *Eoguttulina* spp. and the ostracod *Rehacythereis senckenbergi* group at 4,300 ft (1,311 m). The highest occurrence of *Choffatella decipiens* is at 3,950 ft (1,204 m), but I interpret this level to be older than its known time of extention. Bebout (1980) used *C. decipiens* and several dinoflagellates to assign most of this interval to the Barremian.

VALANGINIAN(?) (4,510–5,440 FT; 1,375–1,658 M)

A major lithological and faunal change occurs at 4,510 ft (1,375 m), where there is coarse to medium sandstone which contains an assemblage of small, fragile, loosely cemented specimens of *Ammobaculites* and *Haplophragmoides* along with gypsum crystals. Although this fauna is not age-diagnostic, the sedimentological and faunal changes appear to coincide with a strong, unconformable seismic reflector near this depth (figs. 20, 21). The underlying reflectors that terminate against it indicate an erosional surface, which is in accordance with the low sea level postulated for Valanginian time by Vail and others (1977). Bebout (1980) reported one pre-Hauterivian dinoflagellate species from 4,450 ft (1,356 m).

BERRIASIAN(?) (5,440–5,920 FT; 1,658–1,804 M)

At 5,440 ft (1,658 m) there is an increase in the diversity and number of specimens and a change from sandstone to mudstone (figs. 19, 22). This level is marked by a strong unconformable seismic reflector which terminates underlying reflectors, indicating erosion (figs. 20, 21). These events correlate well with the sea-level changes postulated for the Berriasian by Vail and others (1977). The foraminiferal fauna cannot be assigned a Berriasian Age, but Bebout (1980) identified Berriasian spores in his samples of the COST No. G-2 well at 5,020(?) to 5,920 ft (1,530(?) to 1,804 m). *Everticyclammina virguliana,* a distinctive agglutinated benthic forminifer, first appears at 5,530 ft (1,686 m), but this is older than its known Valanginian range. At 5,650 ft (1,722 m) a tuberculate form of *Epistomina* appears, and it is quite abundant in deeper samples. P. Ascoli (written commun., April 1980) has noted this same form in the Scotian basin where it ranges from the late Kimmeridgian to the early Valanginian. It may prove to be useful for approximating the top of the Berriasian.

P. Ascoli has examined thin sections of cutting samples from the COST No. G-2 well for of calpionellids. Calpionellids are planktic microfossils that occupy a narrow biostratigraphic zone of

Valanginian to Tithonian Age in Europe (Alleman and others, 1971) and in Canadian offshore wells (Jansa and others, 1980). Jansa (written commun., 1980) reports that they are absent above 5,530 ft (1,686 m), but appear in low numbers down to 5,710 ft (1,740) and are abundant from 5,710 to 5,950 ft (1,740 to 1,808 m; fig. 19).

JURASSIC ROCKS

TITHONIAN (5,920–6,700 FT; 1,804–2,042 M)

The first rare *Epistomina uhligi* appears in cuttings at 5,920 ft (1,804 m) (fig. 19). It occurs in a sidewall core at 5,962 ft (1,817 m) and becomes more abundant below 6,040 ft (1,841 m). This form is a consistent Tithonian marker in the Baltimore Canyon trough and the Scotian basin (Poag, 1980b; Ascoli, 1976). Rocks in this depth interval also were assigned a Tithonian age on the basis of nannofossils and palynomorphs (Bebout, 1980). *Epistomina stellicostata*, another Tithonian form in the Scotian basin (Ascoli, 1976), appears at 6,610 ft (2,015 m). Calpionellids are absent below 6,300 ft (1,920 m).

UPPER KIMMERIDGIAN (6,700–7,660 FT; 2,042–2,335 M)

At 6,700 ft (2,042 m) the fauna is sparse and *Cytherella index*, a species that last appears in upper Kimmeridgian strata in the Scotian basin (P. Ascoli, oral commun., April 1980) is present. At 6,910 ft (2,106 m) in cuttings and at 7,148 ft (2,179 m) in a sidewall core, *Eoguttulina liassica* occurs in great abundance at a lithologic change from limestone above to dark shale below (fig. 22). In abundance this species is typical of Kimmeridgian strata elsewhere (Lloyd, 1962). Other species present in the G–2 well that range no higher than Kimmeridgian in the Scotian basin are *Lenticulina bruckmanni* at 6,970 ft (2,125 m) and *L. varians* at 7,060 ft (2,152 m). A strong seismic reflector at 6,700 ft (2,040 m) is interpreted as an erosional unconformity because underlying reflectors terminate against it (figs. 20, 21).

LOWER KIMMERIDGIAN (7,660–8,660 FT; 2,335–2,640 M)

Alveosepta jaccardi, which marks the top of the lower Kimmeridgian in the Scotian basin, appears and is abundant at 7,660 ft (2,335 m) (fig. 19). Another Kimmeridgian marker found in the Scotian basin, *Schuleridea triebeli*, occurs at 7,690 ft (2,344 m). The Kimmeridgian species *Cytherelloides weberi* occurs at 8,530 ft (2,600 m), and *Galliaecytheridea* sp. 2 of Ascoli (1976) occurs at 8,610 ft (2,624 m).

OXFORDIAN(?) (8,660–10,100 FT; 2,640–3,079 M)

The large numbers of *Alveosepta jaccardi* that occur at 8,660 ft (2,640 m) are typical of Oxfordian assemblages of the Scotian basin (P. Ascoli, written commun., April, 1980; fig. 19). This faunal increase coincides with a strong unconformable reflector on seismic profiles 19 and 209 (figs. 20, 21). Oxidized sediments are also associated with the upper boundary.

CALLOVIAN(?) TO UPPER PLIENSBACHIAN(?) (10,100–16,900 FT: 3,079–5,151 M)

The boundaries of the stages in this interval are estimated from the presence of prominent, unconformable reflectors on seismic lines 77–2, 19, and 209. The tentative stage determinations and depth intervals are as follows:

Callovian(?), 10,100–12,100 ft (3,079–3,688 m);
Bathonian(?), 12,100–14,100 ft (3,688–4,298 m);
Bajocian(?) and Aalenian(?), 14,100–15,000 ft (4,298–4,572 m);
Toarcian(?) and upper Pliensbachian(?), 15,000–16,900 ft (4,572–5,151 m).

LOWER PLIENSBACHIAN(?) AND SINEMURIAN(?) (16,900–18,800 FT; 5,151–5,730 M)

The boundary between the upper and lower parts of the Pliensbachian(?) Stage and the lower boundary of the Sinemurian(?) Stage are estimated from an analysis of seismic sequences on lines 77–2, 19, and 209, where they appear as prominent unconformable reflectors (figs. 20, 21). A calcareous quartzose sandstone is associated with the lower Sinemurian(?) boundary (fig. 19). Bebout (1980) tentatively assigned this interval to the Middle Jurassic on the basis of a few palynomorphs.

HETTANGIAN(?) AND RHAETIAN(?)
(18,800–21,874 ft; 5,730–6,667 M)

The upper boundary of the Hettangian(?) Stage is estimated from seismic sequence analysis of lines 77–2, 19, and 209 to be the prominent reflector at 18,800 ft (5,730 m) at the G–2 site (figs. 19, 20, 21, 22). The halite-bearing strata at 21,874 ft (6,667 m) appear to be of Rhaetian Age (Late Triassic), on the basis of seismic sequence analysis, correlation with the Rhaetian section in the COST No. G–1 well, and the presence of Triassic dinoflagellates in rocks overlying it (Anonymous, oral commun., 1980). If this interpretation is correct, this evaporitic section is equivalent to the Argo Formation of the Scotian basin (Eliuk, 1978; Barss and others, 1979). Seismic lines 77–2 and 209 indicate that basement lies 1,000 ft (305 m) below the bottom of the COST No. G–2 well. A prominent unconformable reflector just below the bottom of the well on line 209 may mark the Rhaetian-Norian boundary, and if so, the oldest rocks above basement at this site are probably of Norian (Late Triassic) age. However, Bebout (1980) identified no fossils definitely older than Middle Jurassic.

SEDIMENT ACCUMULATION RATES

Knowing the detailed chronostratigraphy of the COST Nos. G–1 and G–2 wells allows the calculation of sediment accumulation rates at these sites. These rates can be extrapolated to other parts of the Georges Bank basin using seismic data.

Figure 23 shows the rates of sediment accumulation the G–1 and G–2 sites and compares them with rates at the three other Atlantic COST wells. During the Jurassic and Early Cretaceous the rates at G–2 exceeded those at G–1, but this pattern was reversed during the Late Cretaceous, and rates were nearly equal during the Cenozoic. The general trend from high to low rates with decreasing age can be seen in all the wells, but there are some exceptions, such as the high middle Miocene rates in the COST No. B–3 well (Poag, 1980b). The accumulation rates calculated for the Callovian and older rocks in the COST Nos. G–1 and G–2 wells are minimum rates, because there is no way to estimate from the seismic stratigraphy how much time each unconformity represents. The stage thicknesses determined from seismic stratigraphy have been divided by the duration of the stage, as given by Vail and Mitchum (1979).

During deposition of the oldest rocks penetrated (Hettangian?-Rhaetian?), the accumulation rates at G–1 and G–2 were 6.8 cm/kyr (2.7 in/kyr) (kyr=1,000 years) and (10.0 cm/kyr) (4 in/kyr) respectively. The rates decreased at each location in the early Pliensbachian(?)-Sinemurian(?) and remained nearly the same or decreased slightly through the Toarcian(?). In the Bajocian(?)-Aalenian(?) the rates dropped to half or less than half of what they were in the Toarcian(?): at G–1 the rate was 3.5 cm/kyr (1.4 in/kyr), and at G–2 the rate was 2.7 cm/kyr (1.1 in/kyr). These lower rates continued at G–1 through the Bathonian(?), but not at G–2. In the Callovian(?) at G–1 and in the Bathonian(?) at G–2, the rates resumed approximately their pre-Bajocian(?)-Aalenian(?) values. Maximum rates in both wells occurred during the Kimmeridgian. At G–1 the rate was 8.9 cm/kyr (3.6 in/kyr) and at G–2 the early Kimmeridgian rate was 15.0 cm/kyr (6 in/kyr). The rate dropped to 7.5 cm/kyr (3 in/kyr) in the late Kimmeridgian to Tithonian at G–2, but fell even more dramatically at G–1 to 2.2 cm/kyr (0.9 in/kyr). From the Berriasian to the Barremian the rates varied from 2.2 to 4.5 cm/kyr (0.9 to 1.8 in/kyr) at G–1 and from 2.0 to 6.0 cm/kyr (0.8 to 2.4 in/kyr) at G–2. A significant drop occurred at each well site in the Aptian: at G–1 the rate was 1.5 cm/kyr (0.6 in/kyr), and at G–2 the rate was 2.1 cm/kyr (0.8 in/kyr). During the Cenomanian to Santonian interval, rates ranged from 2.8 to 6.0 cm/kyr (1.1 to 2.4 in/kyr) at G–1, but only from 2.0 to 3.0 cm/kyr (0.8 to 1.2 in/kyr) at G–2.

Cenozoic rates ranged from 0.6 to 3.3 cm/kyr (0.2 to 1.3 in/kyr) at G–1 and from 0.5 to 3.8 cm/kyr (0.2 to 1.5 in/kyr) at G–2. The highest Cenozoic rates prevailed during the Pleistocene.

CORRELATION WITH SCOTIAN BASIN WELLS

The offshore Canadian well nearest the Georges Bank wells is the Shell Mohawk B–93, drilled 195 statute miles (310 km) northeast of the COST No. G–2 well on a small basement high (Mohawk ridge) on the southwestern margin (western shelf) of the broad Lahave platform (fig. 15). Because of

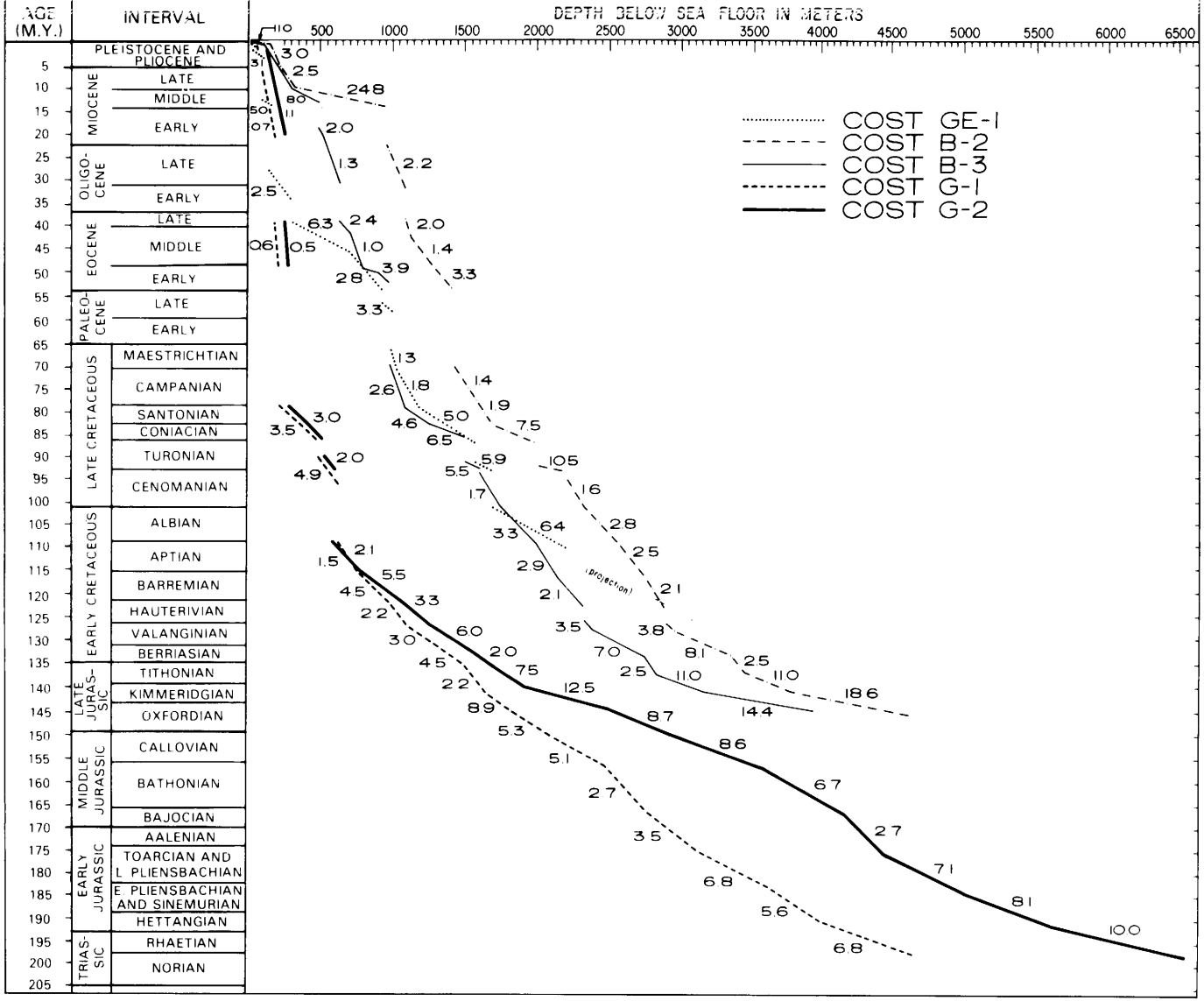

FIGURE 23.—Sediment accumulation rate curves for the COST Nos. G-1 and G-2 wells compared with those for the COST Nos. GE-1, B-2 and B-3 wells. Values are centimeters per thousand years. Gaps in curves are hiatuses, detected by faunal and lithic analyses. Unconformities inferred entirely from the seismic profiles are not shown because the magnitudes of time gaps are not known. As a result, the accumulation rates in the Triassic, Jurassic, and earliest Cretaceous are minimum rates. The formation names in this paper are those of similar rocks on the Scotian shelf of Canada.

its high structural position, the Mohawk B-93 well reached granitic basement at 6,930 ft (2,112 m) and penetrated sedimentary rocks as old as Bathonian (Barss and others, 1979). The nearest well in the Scotian basin (Mohican subbasin) is the Shell Mohican I-100 (313 mi (504 km) NE. of COST No. G-2; fig. 15). This well is more like the COST G wells (especially G-2) in structural setting than the Mohawk B-93, and reached salt at 14,322 ft (4,365 m) after penetrating rocks of Early Jurassic age (early Sinemurian?-late Hettangian?) (fig. 24; Barrs and others, 1979). Both Canadian wells are located 18 mi (29 km) landward of the Upper Jurassic shelf-edge bank, a paleogeographic position similar to that of the COST No. G-2 well (Eliuk, 1978). The sequence of rocks, paleoenvironments, and faunal assemblages in the COST G wells is similar to that of the Canadian wells and allows correlation of the Scotian shelf formations (McIver, 1972; Given, 1977) with the rocks beneath Georges Bank (figs. 17, 21, 22, 24).

In general, the updip Jurassic formations of the Scotian basin and the LaHave platform are chiefly nonmarine sandstones and shales; these grade diachronously downdip into the marine shales, mudstones, limestones, dolomites, and evaporites found in wells nearer the basin. The lateral relationships among these formations are extremely complex (Given, 1977, Eliuk, 1978) and the lithostratigraphic terminology presently employed is not entirely satisfactory, but it simplifies the discussion of the depositional facies involved.

ARGO FORMATION

The name Argo Formation has been given to salt deposits at or near the base of the Jurassic section beneath the Scotian shelf (McIver, 1972). At least 2,500 ft (762 m) of relatively pure, white, coarsely crystalline halite with a few shale and anhydrite interbeds have been penetrated, and seismic evidence indicates that several thousand feet of salt occupies the Orpheus, Abenaki, and Sable basins. At the Mohican I-100 well, 92 ft (28 m) of Argo Formation was penetrated directly under rocks of Sinemurian to Hettangian Age (Barss and others, 1979). In the COST No. G-2 well, the 41 ft (12 m) of halite and anhydrite that lies below rocks of inferred Hettangian to Rhaetian Age (figs. 21, 24) is thought to represent the Argo Formation.

IROQUOIS FORMATION

Overlying the Argo Formation in the Scotian basin is a sequence of dominantly brown, anhydritic dolomite, red to brown shale interbeds, and some limestones in the upper part. Given (1977) reported that two types of dolomite have been recognized in the Iroquois Formation: a microcrystalline dolomitic (commonly anhydritic) mudstone indicating shallow, restricted marine, often supratidal, deposition; and a dolomitized oolitic and pelletal grainstone that represents higher energy marine deposition.

In the Mohican I-100 well, 1,900 ft (579 m) of dolomitic Iroquois Formation was penetrated (fig. 24). It ranges in age from Bajocian to Hettangian (Barss and others, 1979). In the COST No. G-2 well an 8,200-ft (2,499 m) section of dolomite, limestone, and anhydrite equivalent to the Iroquois constitutes the lower Bathonian(?) to Rhaetian(?) interval immediately above inferred Argo Formation (figs. 21, 24). This section is more than four times thicker than that penetrated in the Scotian basin. This sequence in the COST No. G-2 well is also sandy near its base as in the Mohican I-100 well.

MOHICAN FORMATION

The carbonate regime of the Scotian shelf was interrupted in the early Middle Jurassic by deposition of the widespread siliciclastic Mohican Formation. Given (1977) described the Mohican as chiefly sandstones, generally immature texturally, poorly sorted, dolomitic, silty, argillaceous, kaolinitic, and locally interbedded with varicolored shale. Given (1977) further suggested that the Mohican sands may represent the first depositional phase of onlapping sands after the breakup of North America and Euro-Africa, but in the Georges Bank basin available seismic data suggest the continental breakup occurred earlier.

In the Mohican I-100 well 55 ft (17 m) of argillaceous sandstone and shale constitutes the type section of the Mohican Formation. It is chiefly of Bathonian Age, but the base is upper Bajocian (Barss and others, 1979). In the COST No. G-2 well, a 30-ft (9-m) interval of sandstone, mudstone, and shale separates the Iroquois from the Abenaki Formation and is of early Bathonian(?) age; these terrigenous rocks are presumed to

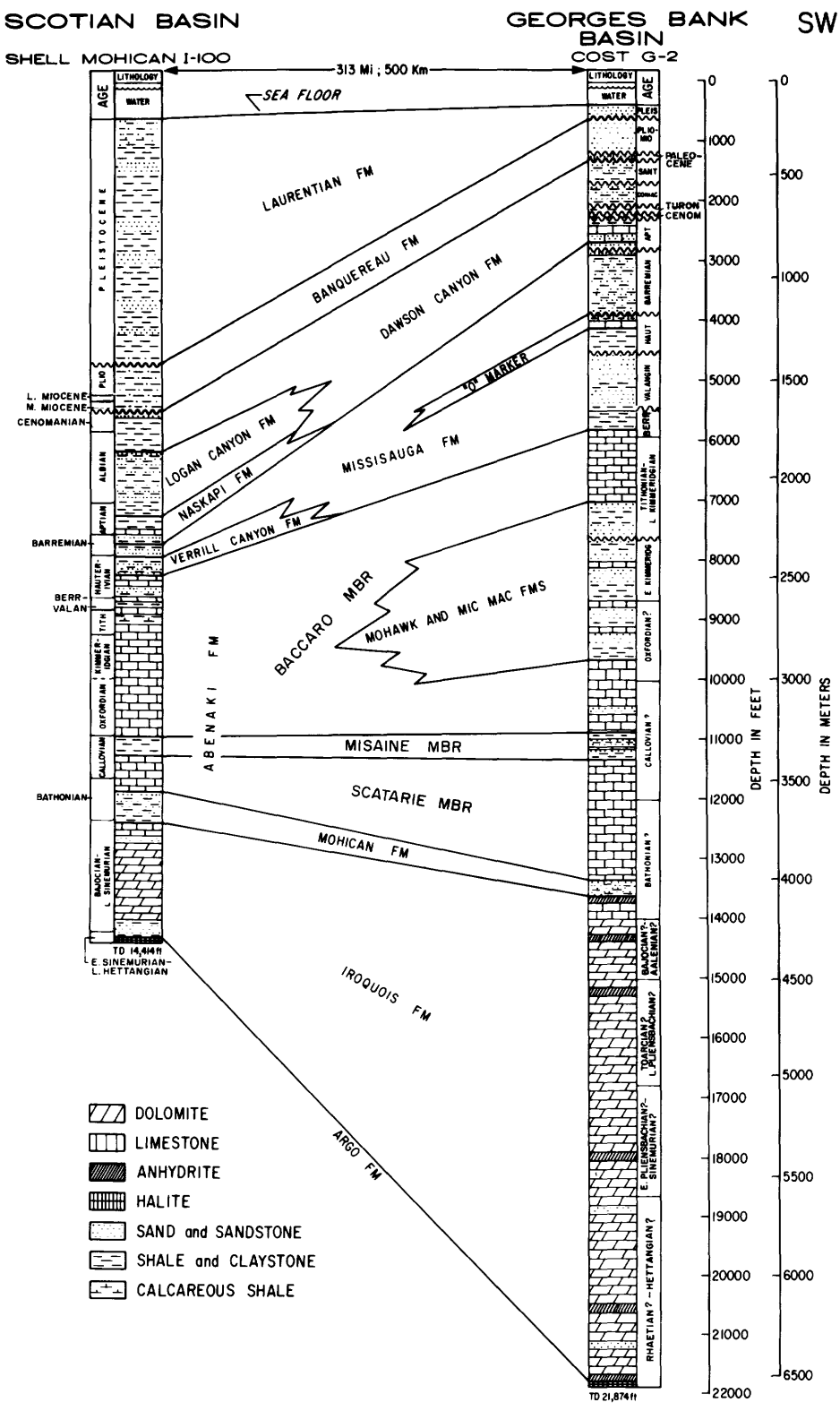

FIGURE 24.—Lithologic correlations between the Shell Mohican I-100 and COST No. G-2 wells. The formation names given are those that have been applied to similar rocks on the Scotian shelf of Canada. The age terms abbreviated in the left and right side columns are spelled out on figure 22.

represent the equivalent of the Mohican Formation (figs. 21, 24).

At the G-1 site, the lower 6,000 ft (1,829 m) of sedimentary rocks appears to be a repetitious interfingering of Iroquois dolomite and limestone with sandstone, shale, and siltstone of the Mohican Formation (figs. 17, 24). The age of the interval is Bajocian(?) to Rhaetian(?). The lower third is quartz conglomerates, fine to medium-grained sandstones, and red-brown shale; the middle third is dolomite and anhydrite; the upper third is limestone and sandstone; a thick Mohican sandstone tongue constitutes the top of the sequence.

ABENAKI FORMATION

On the Scotian shelf the Mohican Formation is overlain by dominantly oolitic, reef-bearing limestones of the Abenaki Formation. The lowest or Scatarie Limestone Member of the Abenaki is oolitic lime packstone to grainstone; it accumulated in warm, agitated, shallow marine waters. The Scatarie reaches a maximum thickness of 600 ft (183 m) in the Mohican I-100 well and is of Bathonian and Callovian Age. In the COST No. G-2 well, a 2,000-ft (610-m) section of argillaceous micrite and oolitic grainstone and packstone of Bathonian(?) and Callovian(?) age constitutes the Scatarie Limestone Member equivalent (figs. 21, 24).

The middle member is the Misaine Shale Member, a dark-olive-gray to gray-brown, somewhat calcareous, sparsely fossiliferous shale, which has a maximum thickness of 560 ft (171 m) on the Scotian shelf. In the Mohican I-100 well, the Misaine Shale Member is 330 ft (101 m) thick and is late Callovian in age. In the COST No. G-2 well, the Misaine Shale Member equivalent is 475 ft (145 m) thick and is of middle Callovian(?) age.

The thickest member of the Abenaki Formation on the Scotian shelf is the Baccaro Limestone Member. The limestone comprises pelletal, oolitic fossiliferous, and "reefal" facies, and the member includes shale, sandstone, and dolomite. All the dolomites analyzed have been diagenetically altered limestones (Eliuk, 1978). The Baccaro is as much as 3,680 ft (1,122 m) thick and was deposited during Middle and Late Jurassic and Early Cretaceous time.

In the Mohican I-100 well the Baccaro Limestone Member is a 2,700-ft (823-m) -thick limestone (micritic to oolitic and oncolitic) with sandstone, claystone, and shale interbeds of late Callovian(?) and early Oxfordian age (figs. 21, 24). The upper part of 1,360 ft (396 m) of micritic limestone of Tithonian or late Kimmeridgian to early Berriasian age.

MOHAWK AND MIC MAC FORMATIONS

Updip equivalents of the Baccaro Limestone Member of the Abenaki Formation are the sandy Mohawk Formation and the shaley Mic Mac Formation. The sandstones of the Mohawk are distinguished from the Mohican sandstones by their more mature texture, better sorting, and locally calcareous nature.

The Mic Mac shales are medium to dark brown to olive gray and have fine-grained sandstone and limestone interbeds. These finer lithologies are not developed at the Mohican I-100 or Mohawk B-93 locations (Eliuk, 1978). At the COST No. G-2 well, a 2,500-ft (762-m) sequence of coaly sandstone, shale, and limestone intertongues with the Baccaro equivalent and appears to represent both Mohawk and Mic Mac lithologies (figs. 21, 24). The age of the sequence is Oxfordian to late Kimmeridgian or Tithonian. Updip in the G-1 well, the Abenaki carbonates are not present, but the equivalent of the Mohawk and Mic Mac Formations is a 3,900-ft (1,189-m) sequence of coarse- to very coarse-grained coaly sandstones, and red, yellow, gray, brown, and variegated shales (figs. 17, 21). The age range of this unit is Bajocian(?) to Tithonian.

MISSISAUGA AND VERRILL CANYON FORMATIONS

Above the Abenaki and its updip equivalents on the Scotian shelf are the sandy Missisauga Formation and its downdip shalely equivalent, the Verrill Canyon Formation. Massive sandstones (maximum thickness 3,800 ft; 1,158 m) grade downdip to thinner sand units. A persistent calcareous seismic marker near the base of the Barremian, named the "0" marker, is present over most of the Scotian shelf about 1,000 ft (305 m) below the top of the Missisauga. It consists of about 150 ft (46 m) of thin limestone beds and calcareous shales that contain a characteristic foraminiferal fauna dominated by *Choffatella decipiens*. Downdip, the Missisauga interfingers

with medium-gray to brown carbonaceous shale of the Verrill Canyon Formation, whose maximum thickness is around 1,200 ft (366 m). The Missisauga and Verrill Canyon Formations range in age from Tithonian to Barremian. The "0" marker persists near the base of the Barremian Stage.

In the Mohican I-100 well, the Missisauga and Verrill Canyon Formations overlap, constituting a 500-ft (152-m) unit of shale, sandy shale, and sandstone of Hauterivan to Barremian Age (fig. 24). The "0" marker is not developed there.

At the COST No. G-2 site, massive, lignitic, coarse-grained sandstones and mudstones assignable to the Missisauga Formation are 1,100 ft (335 m) thick; their age is Berriasian to Hauterivian. These are overlain by a 550-ft (168-m) section of calcareous claystones and gray fissile shales, topped by a 225-ft (69-m) interval of bioclastic limestone and calcareous shale. These upper carbonates are of late Hauterivian age and contain the characteristic *Choffatella descipiens* fauna of the "0" marker.

Updip at G-1, four massive, coaly, medium- to very coarse-grained sandstone units and two thick, gray shale units (total 3,200 ft (975 m) thick) constitute the Missisauga Formation equivalent of late Kimmeridgian or Tithonian to early Aptian age; figs. 17, 21). A thin argillaceous dolomite at the top of the Hauterivian Stage (1,000 ft (305 m) below top of Missisauga) may be the equivalent of the "0" marker, but *Choffatella decipiens* was not observed in the sparse faunas of this well.

Commonly overlying the Missisauga Formation on the Scotian shelf is the Naskapi Formation, 500 to 600 ft (152 to 183 m) thick, which is gray and olive-gray to dusky-red, fissile, carbonaceous shale of early Aptian age. In the Mohican I-100, the Naskapi Formation is 500 ft (152 m) thick and represents late Barremian through early Aptian deposition. The middle part is sandy and calcareous. In the COST Nos. G-1 and G-2 wells, the Naskapi Formation is not recognized.

LOGAN CANYON AND DAWSON CANYON FORMATIONS

On the Scotian shelf these lateral equivalents overlie the Naskapi and Missisauga Formations. The Logan Canyon Formation is the sandier updip unit, consisting of 3,000 ft (914 m) of alternating sandstone, mudstone, and shale, separated into two parts by an olive-green middle unit (Sable shale) 200 to 300 ft (61 to 91 m) thick. The Dawson Canyon Formation is the shalier downdip unit consisting of 900 ft (274 m) or more of calcareous, marly to glauconitic shale, becoming siltier at the base. The Logan Canyon is late Aptian to late Cenomanian in age, whereas the Dawson Canyon Formation can be as young as late Maestrichtian. The thin Petrel Limestone Member is a widespread marker in the Turonian part of the Dawson Canyon. The Logan Canyon Formation underlies the Dawson Canyon Formation in the Mohican I-100 well; the two formations have a total thickness of 1,700 ft (518 m) and represent the late Aptian and Cenomanian (fig. 24).

At the COST No. G-2 well the mudstones and sandstones equivalent to the Logan Canyon Formation also underlie the claystone and siltstone of the Dawson Canyon equivalent, and the two are separated by a 200-ft (61-m) thick shelly limestone of Aptian Age that may represent the Petrel Limestone Member, although it is older here than on the Canadian shelf (figs. 21, 22). The Logan Canyon equivalent is 1,200 ft (366 m) thick, and is of Barremian through early Aptian age; the Dawson Canyon equivalent is 1,000 ft (305 m) thick and represents the late Aptian to Santonian interval. At the COST No. G-1 well, 1,450 ft (442 m) of unconsolidated, massive, coarse-grained, glauconitic, lignitic sandstone and gravel, and gray, glauconitic shale beds represent both the Logan Canyon and Dawson Canyon Formations and are Cenomanian to Santonian in age (figs. 17, 21).

BANQUEREAU FORMATION

The Tertiary strata of the Scotian shelf have not yet been subdivided into formations: the varied siliciclastic sandstones, mudstones, shales, siltstones, and claystones are lumped together into the Banquereau Formation. In the Mohican I-100 well, the Banquereau Formation is 750 ft (229 m) thick and includes middle Miocene, upper Miocene, and Pliocene siltstones.

In contrast to the siliciclastic Tertiary strata of the Scotian shelf, the Tertiary of the Georges Bank basin contains carbonates of Paleocene, Eocene, and possibly Oligocene age, which should eventually be designated as a separate formation or formations from the terrigenous Miocene and

Pliocene strata. Therefore, Banquereau is not a satisfactory term to use for the Paleogene units of Georges Bank. White bioclastic limestone mostly of Eocene age similar to that found further offshore is present throughout the Coastal Plain province of North America and crops out as the Ocala, Cooper, Castle Hayne, and other formations. One of these Coastal Plain names could probably be appropriately applied to the offshore Eocene strata, including those of the Georges Bank basin.

LAURENTIAN FORMATION

The Laurentian Formation of the Scotian shelf consists of Quaternary glacial drift and stratified proglacial sediments ranging in thickness from 100 ft (30 m) to 4,000 ft (1,220 m) (Jansa and Wade, 1975a). The rocks are even thicker near the shelf edge. The Mohican I-100 well penetrated more than 4,200 ft (1,280 m) of Laurentian sands, silts, and clays that represent several glacial cycles (fig. 24; G. L. Williams, written commun., 1974). The thickness of the Laurentian Formation is variable on the upper continental slope as a result of submarine slumping and erosion, but Jansa and Wade (1975a) estimated a maximum thickness of more than 6,000 ft (> 1,800 m) on the lower slope and rise.

The Laurentian Formation equivalent appears to be no more than 200 ft (61 m) thick in the COST Nos. G-1 and G-2 wells and consists of glacially derived sands (figs. 17, 22). It thickens toward the shelf edge, reaching 800 ft (244 m) on line 19 (fig. 21). (See also Lewis and Sylvester, 1977; Hathaway and others, 1979.) It may be somewhat thicker on the lower slope and rise, where it constitutes a chaotic olisthostrome. (See Comparison with Deep-Sea Sedimentary Sequences, this chapter).

LITHOLOGIC FACIES AND PALEOENVIRONMENTS AT THE COST G WELL SITES AND ALONG SEISMIC LINE 19

The analyses of lithologic facies and paleoenvironments of the COST Nos. G-1 and G-2 wells and vicinity are based on foraminiferal and lithologic interpretations of well samples and on seismic facies analysis of nearby seismic lines (Vail and others, 1977). The discussion herein proceeds from oldest to youngest rocks. Line 19 is the closest long profile to which both the G-1 and G-2 wells can be projected along strike (figs. 15, 20, 21). This line is augmented by dip line 77-1 (fig. 18), which nearly crosses the G-1 site, and strike line 204 (collected by the Bundesanstalt für Geowissenschaften und Rohstoffe; BGR), which crosses line 19 near the shelf edge (fig. 25). BGR line 209 crosses the G-2 well site but is not discussed here because the G-1 well cannot be projected to it along strike (fig. 15). However, my analysis of line 209 and that of Klitgord and others (this volume) confirm the features inferred from line 19.

HETTANGIAN(?) AND RHAETIAN(?) ROCKS

Hettangian(?) or Rhaetian(?) rocks lie on a block-faulted basement which is believed to be Paleozoic metasedimentary strata. Thick accumulations of Triassic arkosic sandstones and marine interbeds (indicated by the dinoflagellates in the G wells) fill the basement grabens (figs. 18, 21). At G-1 the basal 1,600 ft (488 m) of sedimentary rocks are sandstones, shales, and conglomerates. Pink, red, and red-brown colors (fig. 17) suggest oxidizing, high-energy environments in an alluvial or fluvial depositional regime. Thin interbeds of anhydrite and dolomite indicate occasional flooding by shallow marine waters.

Seismic lines 77-1 (fig. 18) and 19 (figs. 20, 21) show that the coarse siliciclastic part of the Hettangian(?)-Rhaetian(?) sequence fills a basement low that extends southeastward from the G-1 well site. The discontinuous, subparallel, slightly chaotic reflectors in these updip siliciclastics are characteristic of accumulation under rapidly fluctuating environments in a high-energy regime (Vail and others, 1977). Downdip the beds onlap and interfinger with a sequence of somewhat chaotic reflectors near shotpoint 2300 that are interpreted to come from an elongate carbonate mound, which overlies a basement high. This high may be the southern end of the Yarmouth arch (see Klitgord and others, this volume). Two more small carbonate mounds occur between s.p. 2400 and 2600.

The uppermost 300 ft (91 m) of Hettangian(?)-Rhaetian(?) rocks in the G-1 well comprises red-brown shale with dolomite and anhydrite inclusions, some thin interbeds of dolomite, and a few

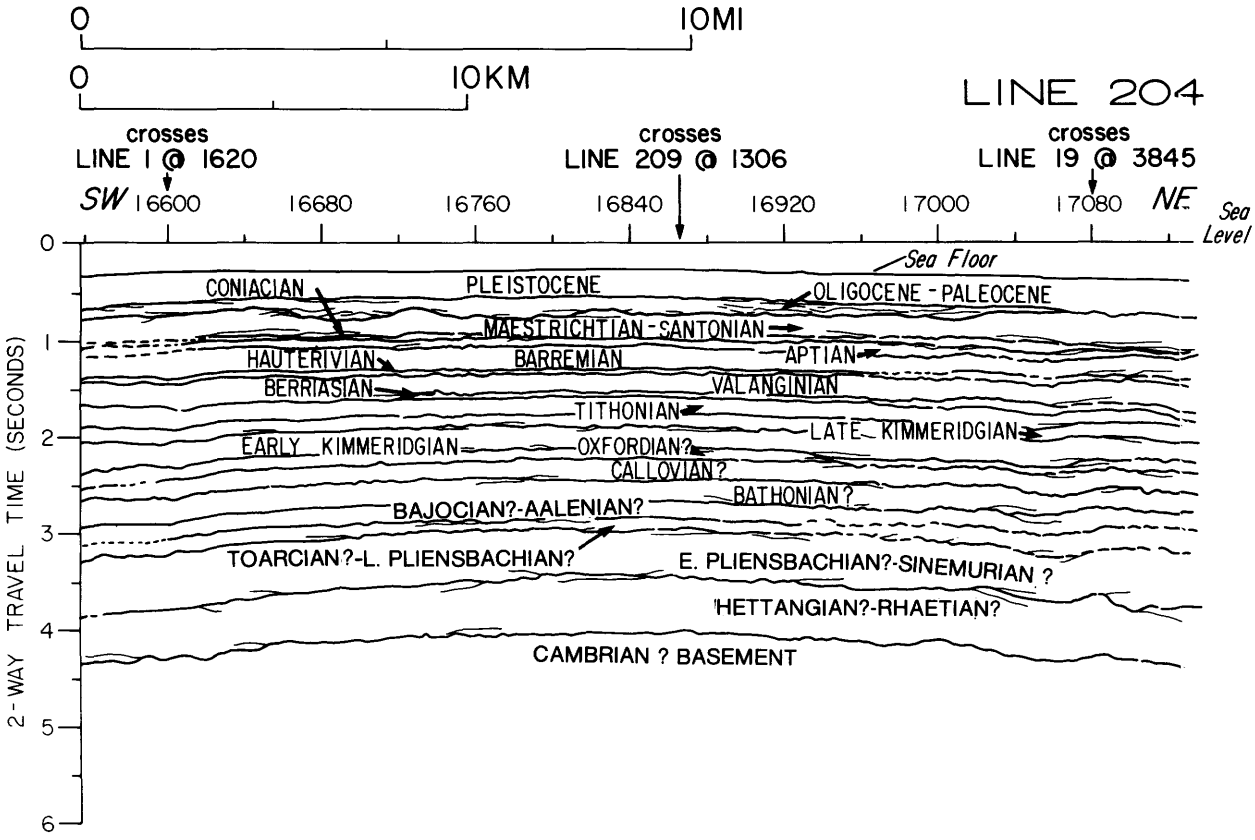

FIGURE 25.—Structural and chronostratigraphic interpretation of seismic reflection profile line 204 (collected by the Bundesanstalt für Geowissenschaften und Rohstoffe, Hanover, West Germany), which traverses the outer part of the Georges Bank basin along strike.

beds of well cemented sandstone (fig. 17). The seismic profiles show few reflectors in this interval, indicating either lithologic homogeneity or bedding too thin to detect with the seismic frequencies used (figs. 18, 20, 21). Nearshore marine to nonmarine paleoenvironments are inferred for this interval. The reflection-free interval extends from the updip end of line 19 to approximately s.p. 2200. At this position a series of high-amplitude reflectors appear and lap onto the carbonate mound.

Downdip from s.p. 2200, a series of continuous, parallel, high-amplitude reflectors extend to about s.p. 2760. These continuous reflectors are typical of uniform, low-energy environments, and their high amplitudes, interpreted along with rocks recovered from the well, suggest discrete strata within carbonate rock sequences (Vail and others, 1977). The continuity of these reflectors is interrupted at s.p. 2480 and 2580 by the more chaotic high-amplitude reflectors of the carbonate mounds. Farther downdip the continuous reflectors become intermittent and onlap both flanks of a large carbonate mound just updip from the projected G-2 well site (figs. 20, 21). This carbonate mound (or perhaps another) is also visible at a similar paleogeographic position on line 209, but is much smaller there. The G-2 well penetrated mostly carbonates in the Hettangian(?)-Rhaetian(?) interval (fig. 22). A 3,000-ft (914-m) sequence of light- and dark-brown-gray, micritic and oolitic, pelloidal limestone, gray and brown-gray, fine to crystalline dolomite, bedded anhydrite, and interbeds of fine- to very fine-grained sandstone and dark-brown-gray, calcareous, silty shale overlies 40 ft (12 m) of halite. (Acoustic basement appears to be about 1,500 ft (457 m) below the top of the halite.) Presumably, the salt accumulated in restricted shallow marine waters in an arid climate. The overlying rocks probably accumulated chiefly in quiet, nearshore marine waters and in supratidal sabkhas, but intervals of higher energy marine conditions are indicated by the oolitic strata.

On line 19, downdip from the G-2 projection, high-amplitude, intermittent, subparallel carbonate reflectors persist to about s.p. 3340, but are interrupted by three zones of more chaotic, arched reflectors interpreted here as carbonate mounds (figs. 20, 21). Between s.p. 3340 and s.p. 3680 the reflectors regain some of their updip continuity and parallelism, suggesting quieter, more uniform deposition than that near the mounds. The somewhat chaotic bedding of another large mound is present, however, between s.p. 3680 and 3750. Downdip from this mound the reflectors become indistinct as the strata intersect the shelf-edge reefal bank.

LOWER PLIENSBACHIAN(?) AND SINEMURIAN(?) ROCKS

At G-1, the early Pliensbachian(?) and Sinemurian(?) are represented by 1,200 ft (366 m) of light-gray to buff, crypotocrystalline to pelletal dolomite with interbeds of anhydrite, thin beds of red-brown shale, fine- to very fine-grained sandstone, and gypsum nodules (fig. 17). The seismic character on line 77-1, which crosses near the G-1 well site, shows nearly reflector-free intervals above and below a single, high-amplitude, continuous reflector that occupies the middle of the sequence (fig. 18). At the G-1 projection on line 19, a zone of faint subparallel reflectors crosses the well site and extends updip to the end of the profile (figs. 20, 21). These characteristics suggest rather uniform shallow marine paleoenvironments much like those of the Hettangian(?)-Rhaetian(?) interval.

On line 19, at about s.p. 2120, the parallel reflectors become more continuous and their amplitude increases as the section thins and drapes over the underlying carbonate mound (figs. 20, 21). These reflector characteristics suggest more strongly defined bedding and less uniform, shallow-water carbonate environments than observed updip. Downdip from the carbonate mound, the lower Pliensbachian(?) and Sinemurian(?) rocks thicken somewhat, reaching a maximum thickness of 0.2 seconds (two-way traveltime) in a small trough near s.p. 2520. In this interval, the low-amplitude, discontinuous reflectors suggest more uniform depositional conditions. From near s.p. 2520 to the G-2 projection the lower Pliensbachian(?)-Sinemurian(?) interval is nearly reflector-free, suggesting lithologic homogeneity or very thin bedding.

At the G-2 well site the lower Pliensbachian(?) and Sinemurian(?) section is tan to brown-gray to dark-brown-gray micritic limestone with oolitic and pelloidal interbeds, gray to light-gray to brown-gray, fine-grained to microcrystalline dolomite and white, very fine-grained to microcrystalline anhydrite (fig. 22). All these characteristics suggest shallow nearshore marine and sabkha-like environments (fig. 19). Alternating zones of low- to high-amplitude, continuous reflectors (shallow-water carbonates) extend downdip from the G-2 projection and onlap the arched reflectors of a low carbonate mound between s.p. 3620 and s.p. 3720 (figs. 20, 21). Downdip from this mound, the lower Pleinsbachian(?)-Sinemurian(?) rocks appear to thicken considerably as the reflectors lose definition in the shelf-edge reefal bank.

BAJOCIAN(?) TO UPPER PLIENSBACHIAN(?) ROCKS

In the G-1 well, the Bajocian(?)-upper Pliensbachian(?) rocks are a 4,000-ft (1,219-m) sequence of generally thin-bedded, alternating units of limestone, sandstone, and shale, with some dolomite near the base (fig. 22). The evaporitic rocks common in the underlying section are not present. The limestones include microcrystalline to medium crystalline, pelletal, and micritic textures; sandstones are medium to very fine grained; shales are red-brown, gray-green, green, and gray. Thin coal beds are scattered throughout the sequence.

On profile 77-1 the Bajocian(?)-upper Pliensbachian(?) interval displays continuous high-amplitude reflectors in the lower two-thirds, but the reflectors are discontinuous and of lower amplitude in the upper one-third (fig. 18). At the G-1 projection on line 19, similar reflector characteristics with lower amplitudes mark the Bajocian(?)-upper Pliensbachian(?) section (figs. 20, 21). These lithologic and seismic characteristics suggest high-energy regimes in fluctuating shallow marine and nonmarine coastal environments (fig. 16). The seismic characteristics and thickness of the interval are constant on line 19 from the updip limit to s.p. 2740. At this point the unit begins to thin markedly and the reflectors became intermittent, more widely separated vertically, and of higher amplitude. These changes persist downdip to the G-2 projection.

In the G-2 well, the 2,800-ft (853 m) section of

Bajocian(?)-upper Pliensbachian(?) rocks is a continuation of the thick sequence of shallow marine limestones, dolomites, and anhydrites that make up the underlying lower Pliensbachian(?) and Sinemurian(?) rocks. This unit continues downdip from the G-2 projection with approximately the same thickness and seismic characteristics to near s.p. 3040, where it lies unconformably above Hettangian(?)-Rhaetian(?) rocks. Where the Bajocian(?)-upper Pliensbachian(?) rocks resume contact with the lower Pleinsbachian(?)-Sinemurian(?) rocks (near s.p. 3180), their seismic character changes to include wide nonreflective intervals between high-amplitude, moderately continuous reflectors, and the unit thins even more. The section becomes even thinner where the Bajocian(?)-upper Pleinsbachian(?) rocks onlap the carbonate mound near s.p. 3600. The unit thickens again downdip from the carbonate mound, becoming indistinguishable in the shelf-edge reefal bank. Rocks as old as Pliensbachian may be present in the basal sedimentary sequences on the oceanic side of the reefal bank. (See Comparison with Deep Sea Sedimentary Sequences, this chapter.)

BATHONIAN(?) ROCKS

At the G-1 well site Bathonian(?) rocks are very coarse-grained, unconsolidated sandstones with thick interbeds of red-brown and gray shale and scattered coal seams and pyrite (fig. 22). The seismic reflectors on lines 77-1 and 19 are discontinuous, subparallel, and of moderate to low amplitude (figs. 20, 21). These characteristics are typical of nonmarine fluvial and shallow-marine environments (fig. 16). These discontinuous reflectors extend downdip to near s.p. 2230 where the lower reflectors become more continuous and increase in amplitude, which is indicative of carbonate facies. Near s.p. 2460 the seismic characteristics of carbonates appear throughout the entire Bathonian(?) section. They persist to the G-2 well, which penetrated brown- gray micritic limestones, a few oolitic beds, and layers of anhydrite. Interbeds consist of shale, claystone, and sandstone; traces of tuff occur between 11,720 and 12,000 ft (3,572 to 3,658 m). Alternating shallow-marine and nonmarine environments are inferred for most of the time interval represented by this section (fig. 19).

Downdip, near s.p. 3280, the thickness of the Bathonian(?) unit is half its thickness updip at s.p. 2230; the amplitude and continuity of reflectors increase, suggesting perhaps the absence of the nonmarine facies at the downdip site. The Bathonian(?) rocks drape over the carbonate mound near s.p. 3680 and can be traced as indistinct reflectors to about s.p. 3940 where they abut the shelf-edge reefal bank. Bathonian rocks may be present on the oceanic side of the reefal bank.

CALLOVIAN(?) ROCKS

At the G-1 well site the Callovian(?) rocks comprise 1,200 ft (366 m) of very coarse-grained, unconsolidated, slightly arkosic sandstones, some pea gravel, and red, yellow, gray, brown, and variegated shales with a few coal and pyritic beds (fig. 17). The seismic reflectors on lines 77-1 and 19 are discontinuous, parallel, and of variable amplitude (figs. 20, 21). These characteristics sugest deposition in fluctuating nonmarine fluvial and shallow-marine coastal environments (fig. 16). Near s.p. 2480 on line 19 the reflectors become more continuous and increase in amplitude, suggesting more uniform marine conditions and carbonate deposition. The high-amplitude, continuous reflectors extend downdip and cross the G-2 projection.

At G-2 the inferred Callovian unit comprises 2,000 ft (610 m) of chiefly brown-gray, oolitic, oncolitic, bioclastic limestones with interbeds of well-sorted, fine-grained sandstones, and gray to red silty and partly calcareous shales (fig. 22). The reflections nearly disappear downdip at s.p. 3400, which suggests very thin bedding or more homogeneous lithology. The continuous, high-amplitude reflectors reappear near s.p. 3680 where they drape over the buried carbonate mound. The reflectors are indistinguishable downdip from s.p. 3940 as they enter the shelf-edge reefal bank. A series of intermittent high-amplitude reflectors above basement on the oceanic side of the shelf-edge reefal bank may include Callovian rocks.

OXFORDIAN(?) ROCKS

At the G-1 well site the Oxfordian(?) rocks comprise 900 ft (274 m) of alternating coarse- to very coarse-grained, loosely consolidated, lignitic and pyritic sandstone and red, yellow, gray,

brown, silty, micaceous shale (fig. 17). The intermittent, variable-amplitude seismic reflectors on lines 77–1 and 19 (figs. 20, 21) are typical of nonmarine fluvial and shallow-marine coastal deposits (fig. 16). The sparse benthic assemblages of this section appear to be entirely cavings and the lack of indigenous fauna could indicate nonmarine deposition or diagenetic destruction of the original assemblages. Steinkraus (1980) reports dinoflagellates in a core at 6,543 ft (1,994 m), indicating that some marine beds are present in the upper part of the Oxfordian section.

Downdip between s.p. 2500 and 2700 are bursts of discontinuous, parallel, very high amplitude reflectors, which indicate high-energy nonmarine deposition. Between s.p. 2700 and the G–2 projection the loss of internal reflectors suggests either uniform lithology or very thin bedding. The G–2 well encountered 1,400 ft (427 m) of alternating sandstone, shale, mudstone, and limestone (fig. 22). The sandstone is white, gray, and red, fine to medium grained, poorly to well sorted, coaly, and micaceous; the shales and mudstones are gray, dark gray, red brown, and maroon; limestones, which are concentrated in the lower part of the section, are tan to light gray, oolitic, and oncolitic. These characteristics indicate fluctuating, mostly nonmarine fluvial environments for the upper parts of the unit and chiefly shallow-marine conditions for the lower part (fig. 19). The foraminiferal assemblages are typical of shallow marine Tethyan faunas of western Europe and the Scotian basin. Agglutinated species predominate, chiefly *Alveosepta jaccardi*, accompanied by *Everticyclammina virguliana*, *Epistomina* spp., and *Trocholina* spp. High-spired microgastropods, ostracods, fish teeth, and charophytes are also present.

Just downdip from the G–2 projection, the greater continuiuty and higher amplitude of the reflectors suggests a change to widespread shallow-water carbonate deposition (figs. 20, 21). The Oxfordian rocks drape over the buried carbonate mound at s.p. 3680 and become indistinguishable downdip in the shelf-edge reefal bank. A series of intermittent high-amplitude reflectors above basement on the oceanic side of the reefal bank may include Oxfordian rocks.

LOWER KIMMERIDGIAN ROCKS

The lower Kimmeridgian rocks at G–1 are chiefly sandstones and shales similar to the underlying Oxfordian rocks, except for some oolitic limestones in the upper part of the interval. Siderite nodules are scattered throughout the section (fig. 17). The faunas consist mainly of sparse, poorly preserved, and often oxidized foraminifers and ostracods. *Everticyclammina virguliana* is the predominant foraminifer, accompanied by a few lenticulinids. Seismic reflectors on lines 77–1 and 19 are discontinuous, parallel, and of variable amplitude (figs. 20, 21). All these characteristics indicate deposition in alternating nonmarine fluvial and shallow marine coastal environments, perhaps including some "middle shelf" deposits (fig. 16).

On line 19, the intermittent seismic reflectors persist downdip to the G–2 projection. The G–2 well penetrated sandstones and shales (comparable to the Oxfordian(?) sandstones and shales) in the lower part of the lower Kimmeridgian section (fig. 22). Gray oolitic limestones are present near the middle and at the top of the section.

The foraminiferal assemblages at G–2 are somewhat more abundant and more diverse than at G–1. Tethyan shallow-marine agglutinated forms still predominate, chiefly *Everticyclammina virguliana* and various species of *Haplophragmoides* and *Ammobaculites*. Among the calcareous forms *Eoguttulina* is prominent. Ostracods and high-spired microgastropods are sparse. Oolites, lignite, and oxidized shale and sandstone fragments are common in the washed rotary cuttings.

These characteristics suggest greater marine influence at G–2 than at G–1 (fig. 19). The continuity and amplitude of seismic reflectors increase downdip from the G–2 projection, with the exception of a nearly reflector-free interval between s.p. 3100 and 3560 (figs. 20, 21). The high-amplitude reflectors are especially prominent downdip from s.p. 3680 but become indistinguishable in the shelf-edge reefal bank. A series of intermittent high-amplitude reflectors on the oceanic side of the reefal bank may include lower Kimmeridgian rocks.

UPPER KIMMERIDGIAN TO BERRIASIAN ROCKS

In the G–1 well, the 1,300-ft (396-m) upper Kimmeridgian-Berriasian interval is divided into two sandstone sections separated by interbedded shale and dolomite (fig. 17). The sandstones are chiefly medium to very coarse grained, lignitic,

micaceous, and pebbly; the shale and dolomite are light gray. In the shales and lower sandstones foraminifers are common and ostracods and high-spired microgastropods are present. Dominant foraminifers are *Everticyclammina virguliana*, small, fragile *Haplophragmoides*, *Eoguttulina* sp., *Trocholina* sp., *Epistomina* spp. and *Lenticulina* spp. The seismic reflectors at the G-1 projection on lines 77-1 and 19 are parallel and of variable continuity and amplitude (figs. 23, 24). A single high-amplitude reflector appears to represent the dolomitic zone.

All these characteristics suggest deposition in fluctuating nonmarine fluvial to shallow marine inner-shelf environments (figs. 16). The intermittent variable-amplitude reflectors and the dolomite reflector can be traced downdip on line 19 to near s.p. 2520, where the strata just above the inferred dolomite begin to display closely spaced, continuous, parallel, high-amplitude reflectors (figs. 20, 21). This pattern suggests a basinward change to more carbonate-rich facies. The inferred carbonate interval thickens toward the basin from s.p. 2520 until it makes up the entire Berriasian to upper Kimmeridgian interval at the G-2 projection. The G-2 well encountered a 1,300-ft (417-m) interval of light-gray to tan, micritic to chalky limestone bounded above by 200 ft (61 m) of mudstone and below by 600 ft (183 m) of sandstone (fig. 22).

Rich, diversified foraminiferal assemblages occur throughout this section. *Everticyclammina virguliana*, *Choffatella decipiens*, *Lenticulina* spp., and *Epistomina* spp. predominate, accompanied by *Trocholina*, *Conorboides*, *Ophthalmidium*, and *Eoguttulina*. Ostracods and high-spired microgastropods also are abundant in some intervals. The presence of common to abundant calpionellids in the upper, more calcareous part of this unit suggests moderately deep, open marine conditions (300 ft; 100 m) (fig. 19). Intervals containing well-developed assemblages alternate with more sparsely populated intervals in which leached specimens, lignite, gypsum, and oxidized clays all suggest shoaling and perhaps subaerial exposure.

Downdip from the G-2 projection (figs. 20, 21) the vertical spacing of reflectors is variable, few reflectors are continuous, and many have high amplitudes and are parallel. These characteristics suggest continued carbonate deposition in a variable shallow-marine environment. Upper Kimmeridgian and Tithonian reflectors can be traced to the shelf-edge reefal bank near s.p. 3950, but the thin Berriasian unit can be traced no farther than s.p. 3930.

Reefal rocks of Berriasian and Neocomian (Hauterivian to Barremian) Age have been collected from Heezen Canyon, northeast of line 19 (fig. 15; Ryan and others, 1978). The Berriasian limestone sample was identified on the basis of pelagic calpionellids, and it also contained remains of the pelagic crinoid *Saccocoma*, abundant corals, hydrozoa, calcareous algae, and large foraminifers. This unit is interpreted to have accumulated in an ocean-facing reef environment. Neocomian samples contained rudistids, echinoids, bivalves, bryozoans, ostracods, benthic foraminifera, and calcareous algae, but lacked the corals and other colonial organisms. These associations probably accumulated in non-reefal parts of the carbonate platform. Equivalent facies on line 19 would be expected between s.p. 4000 and 4100 (figs. 20, 21).

A series of high-amplitude, discontinuous reflectors on the seaward side of the shelf-edge reefal bank may include upper Kimmeridgian to Berriasian carbonate rocks of hemipelagic and pelagic origin.

VALANGINIAN ROCKS

In the G-1 well, Valanginian rocks consist of very coarse-grained pebbly sandstones, interbeds of gray shale, and coal and lignite at the base (fig. 17). These sandstones may be a continuation of the sandstones of the underlying Berriasian section. The Valanginian microfossils are sparse and may be entirely cavings.

On seismic line 77-1 the reflectors in the Valanginian interval are intermittent and of low amplitude. At the G-1 projection on line 19, a single intermittent reflector with variable amplitude occupies the middle of an otherwise reflector-free Valanginian section (figs. 20, 21).

These characteristics indicate dominantly nonmarine fluvial deposits that accumulated under uniform conditions (fig. 16). The same seismic characteristics extend downdip on line 19 to the G-2 projection (figs. 23, 24). The G-2 well also encountered a thick sandstone unit of Valanginian Age. The sandstone is very coarse to fine grained and white to gray and has interbeds of coal, lignite, dark-gray shale, light-gray mudstone, pyrite, and glauconite (fig. 22).

A sparse to moderately well developed microfauna is scattered throughout the Valanginian rocks at G-2. The large shallow-marine Tethyan agglutinated foraminifer *Choffatella decipiens* is prominent, as are large *Ammobaculites* sp., small fragile *Ammobaculites* sp., and *Trochammina* sp. In the lower 350 ft (107 m) of the Valanginian section, calcareous microfossils are more abundant and include *Epistomina* spp., *Lenticuluina* spp., *Planularia* sp., and *Conorboides* sp. These lithologic, seismic, and faunal characteristics are typical of deposits that accumulated in fluctuating nonmarine fluvial and shallow-marine coastal environments (fig. 19).

Downdip from the G-2 projection the Valanginian section nearly doubles in thickness, reaching a maximum near s.p. 3860. As the section thickens, more reflectors are present, but they are intermittent and of variable amplitude (figs. 20, 21). Near s.p. 3860, a delta-like wedge of intermittent, variable-amplitude, sigmoid clinoform reflectors fills a faulted depression landward of the shelf-edge reefal bank. Oceanward of the reefal bank, Valanginian rocks may be present as a thin, rather reflector-free unit lying above the high-amplitude Berriasian(?) to Callovian(?) reflectors.

HAUTERIVIAN ROCKS

At G-1 the upper part of the 400-ft (122-m) Hauterivian section is a thin argillaceous dolomite. A thin, unconsolidated, very coarse-grained sandstone separates the dolomite from a thick, gray shale unit that contains a coal bed near the top. The microfossil assemblages in the Hauterivian rocks are sparse and are probably all cavings from overlying fossiliferous beds. On seismic line 77-1 the Hauterivian interval contains characteristic discontinuous reflectors of variable amplitude. On seismic line 19 at the G-1 projection, a single, central, nearly continuous reflector of variable amplitude characterizes the Hauterivian interval; the reflector can be traced downdip to near s.p. 2580 (figs. 20, 21). These characteristics indicate early deposition in chiefly nonmarine fluvial environments followed by a shallow marine incursion in the late Hauterivian (fig. 16).

On line 19 from s.p. 2580 to near s.p. 2880 the central Hauterivian reflector becomes more intermittent than at updip positions. At s.p. 2880 a second low-amplitude reflector appears and both reflectors cross the G-2 projection site. The G-2 well penetrated 600 ft (183 m) of bioclastic, partly oolitic limestone, argillaceous micrite, light-gray calcareous claystone, and gray, fissile, silty shale in the Hauterivian interval (fig. 22).

A moderately rich foraminiferal assemblage is present in the G-2 Hauterivian rocks. *Choffatella decipiens* is prominent, along with *Lenticulina* spp., *Planularia* sp., *Marssonella* sp., and occasional floods of *Eoguttulina* sp., and *Trocholina* sp. High-spired microgastropods, ostracods, echinoid spines, free ooids, and occasional charophytes also are typical. These elements suggest that here Hauterivian rocks accumulated in shallow marine to coastal nonmarine environments (fig. 19).

Downdip from the G-2 projection the seismic reflectors are widely separated, intermittent, and of variable amplitude, suggesting continued shallow-marine and coastal nonmarine environments. Hauterivian rocks appear to be severely eroded near s.p. 3860, but the section thickens again in the structural low behind the shelf-edge reefal bank. This unit is the first that can be traced with some confidence across the top of the reefal bank. The crossing reflectors are discontinuous, have variable amplitudes, and appear to pinch out or to be truncated near s.p. 4100. Hauterivian rocks are inferred to reappear near s.p. 4140 on the seaward flank of the shelf-edge reefal bank.

BARREMIAN ROCKS

At G-1 the Barremian rocks are 825 ft (251 m) of unconsolidated, coarse- to very coarse-grained partly calcareous sandstones with interbeds of red and gray sticky shale, lignite, and pyrite (fig. 17). The microfauna are sparse and are probably cavings from overlying fossiliferous beds. However, a sidewall core from 3,274 ft (998 m) contained *Trochammina* sp. and *Lenticulina* spp., and a few of the lenticulinids and epistominids in the cuttings may be indigenous. On lines 77-1 and 19 the Barremian interval contains parallel, discontinuous, variable-amplitude reflectors at the G-1 location and its projection (figs. 20, 21). These characteristics suggest deposition in nonmarine fluvial and shallow-marine environments with variable energy regimes (fig. 16).

On seismic line 19, the Barremian reflectors maintain constant characteristics downdip to the

G-2 projection, although the unit thickens. At G-2, the top one-quarter of the 1,100-ft (335-m) section is very coarse, rounded sand and medium- to fine-grained, subangular, calcareous sandstone with interbeds of gray silty mudstone and some coal and glauconite (fig. 22). The lower three-quarters are gray, silty, glauconitic, partly calcareous mudstone with interbeds of medium- to fine-grained sandstone.

Microfossils at G-2 are not abundant in the Barremian interval. The fauna consists of the foraminifers *Epistomina* spp., *Lenticulina* spp., *Gavelinopsis* sp., *Trochammina* sp., and high-spired microgastropods and ostracods. These characteristics indicate greater marine influence than at G-1, but nearshore marine environments may have been replaced occasionally at G-2 by nonmarine fluvial environments (fig. 19).

On line 1 downdip from the G-2 projection, the seismic characteristics of the Barremian section change very little (figs. 23, 24). Between s.p. 3620 and 3940, a series of low- to high-angle, sigmoid clinoform reflectors indicate progradation of fine-grained hemipelagic deposits as low-energy turbidites. This unit thins in front of and across the buried shelf-edge reefal bank and pinches out or is truncated near s.p. 4080. A slope-front fill facies of Barremian Age appears to lie above the inferred Hauterivian and Valanginian units seaward of the shelf-edge reefal bank.

APTIAN ROCKS

In the G-1 well the Aptian rocks are 400 ft (122 m) thick and are similar in lithology to the underlying Barremian sandstones and mudstones (fig. 18). Fossils are rare or absent except in the upper samples where there are abundant *Epistomina chapmani. Lenticulina nodosa* and *Vaginulina aptiensis* are also probably indigenous. There are also abundant specimens from cavings of the overlying, richly fossiliferous Cenomanian and Turonian strata.

On seismic lines 77-1 and 19, the G-1 location and its projection are characterized by intermittent, parallel to subparallel, variable-amplitude reflectors indicative of nonmarine fluvial to shallow marine deposits (figs. 16, 20, 21). The fauna at the top of the section indicates a shallow marine origin. The subparallel reflectors may indicate somewhat higher energy regimes during the Aptian than during deposition of older rocks at this site.

Near s.p. 2380 (line 19) the reflectors are more continuous and parallel, suggesting lower energy regimes and more uniform environmental conditions; these persist to the G-2 projection. At G-2, the upper part of the 475-ft (145-m) Aptian sequence comprises coarse, shelly limestones interbedded with fine- to medium-grained, calcite-cemented quartz sandstones. Sandstone is more abundant in the lower part of the section.

Microfossils are rare in the sandy lower part of the Aptian sequence, but in the calcareous upper part, abundant *Epistomina chapmani* and *Lenticulina nodosa*, plus a few *Lenticulina* sp., *Vaginulina procera*, *Gavelinella* sp. and ostracods appear to be indigenous.

All these characteristics suggest that the lower part of the Aptian section at G-2 is of nonmarine fluvial origin, but the upper part accumulated in shallow marine shelf environments (fig. 19).

Downdip from the G-2 projection, intermittent, parallel, variable-amplitude reflectors extend to near s.p. 3700. The distal portion of the Aptian section is completely truncated by an erosional unconformity and can be traced no farther than s.p. 3850. Aptian rocks appear to be part of a slightly chaotic, slope-front fill sequence that onlaps the seaward side of the shelf-edge reefal bank.

CENOMANIAN ROCKS

Erosion during the mid-Cenomanian low sea-level stand has eliminated most or all of the Albian rocks from both G wells, and the seismic interpretations of lines 19 and 209 suggest that Albian rocks are missing over most of the Georges Bank basin (figs. 20, 21). At G-1, Aptian rocks are overlain by a thin, glauconitic, gray shale and claystone unit of Cenomanian Age (fig. 19). The microfauna at G-1 is moderately rich and diverse and contains an abundance of planktic foraminifers. The predominant benthic genera are *Lingulogavelinella*, *Vaginulina*, *Bolivinita*, *Lenticulina*, *Gavelinopsis*, and *Epistomina*. The Cenomanian interval is so thin (75 ft; 23 m) that it cannot be distinguished on seismic line 77-1, but on line 19, it appears as a narrow reflector-free zone at the G-1 projection. Downdip the Cenomanian interval thins and thickens over the eroded Aptian surface (fig. 24). All these seismic,

lithologic and faunal characteristics suggest that deposition took place in a moderately deep middle to outer shelf marine environment under a low-energy regime (fig. 16).

At the G-2 projection on line 19, the Cenomanian interval is still thin (60 ft; 18 m) and reflector-free. The claystones here contain a very rich and diverse microfauna, including abundant planktic foraminifers. The predominant benthic genera are *Epistomina, Gavelinopsis, Lingulogavelinella, Lenticulina, Vaginulina, Bolivinita, Praebulimina,* and *Frondicularia.* Pyritized microgastropods are also common. The faunal, lithologic, and seismic characteristics suggest that deposition took place in an outer shelf marine environment under a low-energy regime (fig. 19). The seismic character and thickness change little downdip from the G-2 projection. The Cenomanian section may be entirely truncated by erosion near s.p. 3800, or it may be too thin to identify on line 19. A prominent slope-front fill sequence, which onlaps the seaward edge of the shelf-edge reefal bank, appears to include Cenomanian rocks.

LOWER TURONIAN ROCKS

At G-1, the lower Turonian rocks are 350 ft (107 m) of gray, sticky, glauconitic shales bounded by coarse-grained sand and gravel with lignite at the top and base (fig. 17). Pyrite is common throughout the section. On seismic line 77-1, the entire interval contains parallel, intermittent, variable-amplitude reflectors. The lower Turonian interval is very thin on line 19 and shows up as a reflectorless zone bounded by strong unconformable reflectors (figs. 20, 21). The microfauna at the COST No. G-1 well is abundant and diverse and includes abundant planktic foraminifers in most samples. The predominant benthic genera are *Epistomina, Lingulogavelinella, Gavelinella, Lenticulina,* and *Marssonella.* High-spired microgastropods are common.

These faunal, lithologic, and seismic characteristics suggest that most lower Turonian deposition occurred in low energy middle shelf marine environments (fig. 16). Shallower marine conditions and perhaps nonmarine fluvial conditions prevailed during the two sandy intervals.

Seismic characteristics on line 19 do not change downdip to the G-2 projection (figs. 20, 21). At G-2 the lower Turonian rocks are 150 ft (46 m) of calcareous, glauconitic claystone (fig. 22). The abundant, diverse microfauna contains abundant planktic foraminifers. Predominant benthic genera include *Epistomina, Gavelinella, Lingulogavelinella, Lenticulina, Neoflabellina, Gaudryina, Bolivinita,* and *Praebulimina.* These characteristics suggest that deposition took place in a low-energy regime on an open marine outer shelf (fig. 19). On line 19 the lower Turonian rocks are uniform in thickness and seismic character from the G-2 projection downdip to an apparent pinchout or erosional truncation near s.p. 3740. Turonian rocks may be included in a sequence of horizontal basin-fill reflectors that onlap the inferred early Cenomanian to Aptian sequence on the seaward side of the shelf-edge reefal bank.

CONIACIAN ROCKS

At the COST G-1 well the lower part of the 550-ft (168-m) section of Coniacian rocks consists of unconsolidated coarse-grained sandstone and gravel overlain by a thin shale unit (fig. 17). On seismic line 77-1, the Coniacian reflectors at G-1 are intermittent, subparallel, and of variable amplitude. At the G-1 projection on line 19, the reflectors are discontinuous, of low amplitude, and parallel (figs. 20, 21). A single, more continuous, higher amplitude reflector can be seen near the top of the interval. The microfauna in the sandy lower part of the Coniacian interval is sparse. Benthic forms include a few *Epistomina, Ceratobulimina,* and *Neobulimina.* A slightly richer fauna occurs in the shale at the top of the section, including a moderate assemblage of planktic foraminifera. Predominant benthic forms are *Epistomina, Vaginulina,* and *Gavelinella.*

These faunal, lithologic, and seismic characteristics suggest that deposition at G-1 during the early part of the Coniacian occurred in nonmarine fluvial to shallow marine coastal environments in a relatively high-energy regime (fig. 16). Water depth increased and the energy level dropped during deposition of the shale layer.

Downdip from the G-1 projection on line 19 high-amplitude reflectors several miles long appear (fig. 20, 21). At the G-2 projection a single high-amplitude reflector occupies the middle of the Coniacian interval. In the G-2 well the Coniacian rocks are 425 ft (130 m) of chiefly light-gray calcareous claystones and siltstones with one

thin argillaceous limestone in the middle of the interval (fig. 22).

The microfauna in the G–2 well is abundant and includes a varied planktic foraminiferal assemblage. Benthic forms include *Gavelinella* spp., *Stensioina, Allomorphina, Valvulineria, Nodosaria, Lingulina, Eouvigerina, Epistomina,* and *Neoflabellina.* These faunal characteristics suggest that deposition took place in a low-energy, open marine, outer shelf environment (fig. 19).

Downdip from the G–2 projection the central high-amplitude reflector disappears near s.p. 3460 (fig. 23, 24). The Coniacian interval may be truncated near s.p. 3900, beyond which it cannot be indentified. Coniacian rocks may be included in the sequence of horizontal basin-fill reflectors that onlap the early Cenomanian(?)-Aptian(?) sequence seaward of the shelf-edge reefal bank.

SANTONIAN ROCKS

At the COST No. G–1 site Santonian rocks consist of 380 ft (116 m) of unconsolidated coarse-grained sandstone and gravel containing some glauconite and lignite (fig. 17). The microfaunas are moderately rich and planktic foraminifers are common. The predominant benthic forms are *Epistomina, Gavelinella, Lenticulina, Frondicularia,* and *Vaginulinopsis.* On seismic line 77–1 the Santonian interval at the G–1 projection is reflector-free, but at the G–1 projection on seismic line 19, a very high amplitude, continuous reflector occurs in the middle of the Santonian interval; this appears to be a "follow" cycle beneath the principal unconformable reflector that separates the Santonian rocks from overlying Tertiary strata (figs. 23, 24). These lithologic, faunal, and seismic characteristics indicate that Santonian rocks accumulated under uniform high-energy conditions in near-shore, inner to middle shelf marine environments (fig. 16).

The seismic character of the Santonian interval does not change appreciably on line 19 between the G–1 and G–2 projections. At G–2 the rocks are 420 ft (128 m) of unconsolidated, coarse-grained sand and gray, soft, clayey siltstone (fig. 22). The Santonian microfossil assemblage in the G–2 well is diverse and contains an abundance of planktic foraminifers. The predominant benthic forms are *Eouvigerina, Epistomina, Planulina, Gavelinella, Nodosaria, Marginulina, Stensioina,* and *Gaudryina.* Caved Eocene specimens are abundant in these samples. These faunal, lithologic, and seismic characteristics suggest that Santonian deposits at G–2 accumulated in open marine, middle to outer shelf depths in a moderate- to low-energy regime (fig. 19).

The high-amplitude central reflector in the Santonian interval continues downdip from the G–2 projection, and as the section thickens, the reflector moves closer to the top of the section (figs. 20, 21). Occasional downlapping high-amplitude reflectors appear at the base of the otherwise reflector-free Santonian sequence. The section becomes thicker near s.p. 3640, and prograding, chaotic reflectors are present from s.p. 3740 to 3960, where the sequence is nearly four times as thick as it was at the G–2 well. This thickened sequence may also include Campanian and Maestrichtian rocks. Maestrichtian rocks have been collected from Veatch, Oceanographer, and Heezen Canyons, which border Georges Bank (fig. 15); Campanian rocks have been cored in Veatch Canyon (Ryan and others, 1979; Valentine and others, 1980). Santonian rocks crop out in Veatch and Oceanographer Canyons and have been cored at Atlantic Slope Project (ASP) site 18 in Veatch Canyon (figs. 15, 26). At these locations the rocks are chiefly indurated mudstones and siltstones at least 400 ft (128 m) thick. Moderately well developed planktic and benthic foraminiferal assemblages include *Bolivinoides, Epistomina, Stensionina, Lenticulina, Gavelinella, Globorotalites, Gaudryina, Brizalina, Nodosaria, Gyroidina,* and miliolids. All these faunal, lithologic, and seismic characteristics suggest that deposition took place in outer shelf to upper slope environments.

Santonian rocks may be part of a sequence of horizontal basin-fill reflectors that onlap the early Cenomanian to Aptian sequences seaward of the shelf-edge reefal bank.

CAMPANIAN ROCKS

Though Campanian rocks have not been identified in either of the COST G wells, they are known from one corehole drilled for the Atlantic Slope Project (ASP 18) in the lower part of Veatch Canyon (figs. 15, 26). Dark-olive-gray to brownish-gray laminated and massive siltstone with minor amounts of dark-olive-gray sand and medium-gray clay was penetrated between

3,975 ft and 4,095 ft (1,212 to 1,248 m) below sea level. The abundance of *Bolivinoides, Gavelinella, Lenticulina, Gaudryina, Marssonella, Praebulimina,* and *Arenobulimina* and the presence of fewer *Nodosaria, Pleurostomella,* and *Valvulineria* suggest outer shelf to upper slope deposition.

Campanian rocks also may be part of the basin-fill sequence indicated by horizontal, variable-amplitude, intermittent reflectors that onlap the inferred early Cenomanian to Aptian reflectors seaward of the shelf-edge reefal bank.

MAESTRICHTIAN ROCKS

Maestrichtian rocks have also not been identified in the two G wells, but they have been sampled in ASP corehole 18 (figs. 15, 26). There, 190 ft (58 m) of early Maestrichtian, dark-olive-gray to brownish-gray, laminated and massive siltstone with minor amounts of dark-olive-gray sand and medium-gray clay are present between 3,785 and 3,975 ft (1,154 to 1,212 m) below sea level. The abundance of *Osangularia, Eouvigerina, Bolivinoides, Brizalina, Nodosaria, Praebulimina, Gyroidina, Robertina,* and *Pseudouvigerina* suggests an upper slope paleoenvironment. In addition, lower Maestrichtian hemipelagic deposits have been collected from outcrops at depths of 4,659 to 5,134 ft (1,452 to 1,565 m) in Oceanographer and Corsair Canyons (fig. 15; Ryan and others, 1978; Gibson and others, 1968; Valentine and others, 1980).

Maestrichtian rocks may be included in the basin-fill facies represented by the horizontal, variable-amplitude, intermittent reflectors that onlap the inferred early Cenomanian to Aptian reflectors seaward of the shelf-edge reefal bank.

PALEOCENE ROCKS

A few specimens of Paleocene planktic foraminifers were found in the uppermost samples of both the G-1 and G-2 wells, indicating the presence of some Paleocene strata above the Santonian section. Steinkraus (1980) also reported Paleocene dinoflagellates in the G-1 well. These samples, along with planktic Paleocene assemblages recovered from silty claystones in Oceanographer Canyon and Veatch Canyon (fig. 15, ASP 17; Poag, 1978) indicate open marine conditions as far updip as G-1 during the Paleocene and bathyal conditions at the canyon localities. The Paleocene interval is either missing or too thin to be observed on most of the seismic profiles over the shelf. However, a thickened wedge of inferred Paleogene age between s.p. 3860 and 4020 on line 19 may include Paleocene strata (figs. 20, 21). Paleocene strata also may be present in a thin zone of very high-amplitude, nearly continuous reflectors that form a basin-fill facies overlying the inferred Maestrichtian to late Cenomanian basin fill between s.p. 4200 and the seaward end of line 19. The high-amplitude reflectors and lithologic extrapolation from DSDP coreholes (such as site 108) suggest these rocks may be cherty carbonates.

EOCENE ROCKS

The bulk of Paleogene strata in both the G-1 and G-2 wells appears to be of middle Eocene age. Even so, the middle Eocene interval is thin and cannot be recognized with confidence on seismic line 19 between the G-1 and G-2 well projections (figs. 23, 24). At G-1 the few planktic specimens of middle Eocene age indicate open marine conditions (fig. 16). Farther updip, at AMCOR 6019, 49 ft (15 m) of light- to dark-green, glauconitic clay and hard, gray to white bioclastic limestone contains outer shelf to upper slope middle Eocene foraminiferal faunas (fig. 15; Poag, 1978; Hathaway and others, 1979). Chunks of this white bioclastic limestone are present in the upper cutting samples at G-1.

At G-2, where a strong reflector is inferred to mark the top of the middle Eocene (figs. 20, 21), the dominant benthic forms are *Gyroidina, Nodosaria, Dentalina, Bulimina, Cibicidoides, Globocassidulina, Anomalinoides, Brizalina, Turrilina, Uvigerina,* and *Siphonina.* Large fragments of cheilostome bryozoans and echinoid spines are common. The lithology is dark-green, coarse-grained, glauconitic sand and leached, white, glauconitic, quartzose, bioclastic limestone. These fauna and lithologies indicate outer shelf to upper slope environments in a low-energy regime. On the shelf, downdip from s.p. 3000 on line 19, the Eocene is very thin and may be missing in places. Eocene strata from outcrops in Oceanographer and Corsair Canyons (fig. 15; Gibson and others, 1968; Ryan and others, 1978) are brown, silty mudstones, glauconitic calcarenites,

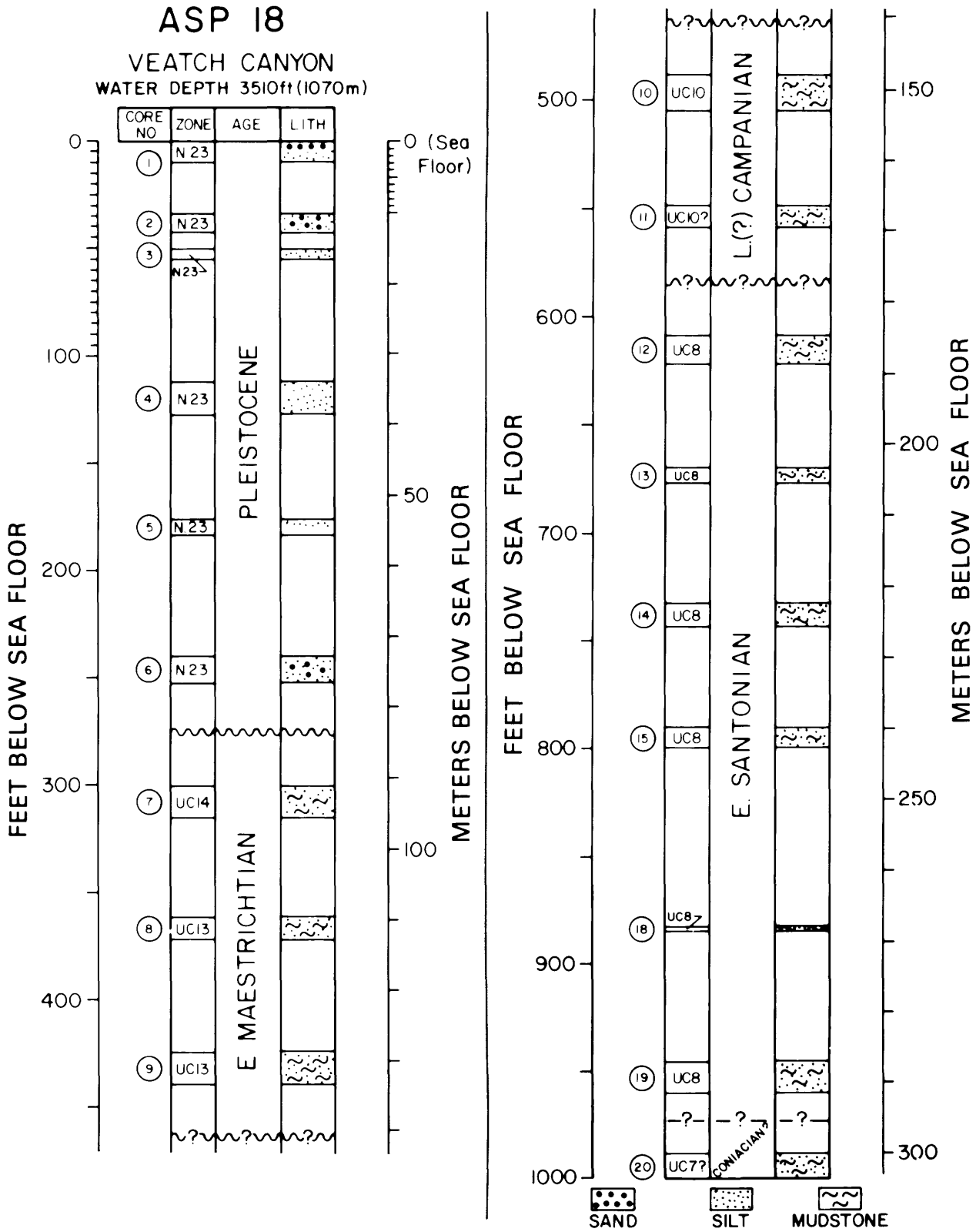

FIGURE 26.—Geologic column of Atlantic Slope Project (ASP) core 18 (taken in 1967 by Exxon, Chevron, Gulf, and Mobil oil companies as part of their Atlantic Slope Project), near the mouth of Veatch Canyon. See figure 15 for location.

and white pelagic chalks, representing hemipelagic channel deposition to pelagic basin deposition. A few early Eocene planktic specimens are also present in ASP 17 in Veatch Canyon (Poag, 1978).

Similar Eocene strata may be present beneath the upper slope as seen on line 19 (figs. 20, 21). A discrete wedge of high-amplitude, nearly continuous reflectors between s.p. 3860 and 4020 is interpreted to be chiefly Eocene limestones and mudstones of presumably bathyal origin. Between s.p. 4200 and the seaward end of line 19, a series of high-amplitude, intermittent, basin-fill reflectors is interpreted to include calcareous, cherty strata of Eocene age.

OLIGOCENE ROCKS

Oligocene strata have not been identified in the G wells, but a few Oligocene planktic specimens in G–2 suggest that a thin Oligocene unit may lie above the highest sampled interval. The only other Oligocene strata known from the Georges Bank basin were dredged from Oceanographer Canyon (Gibson and others, 1968). The rocks are buff, calcareous clay and brown, glauconitic, sandy clay, both containing abundant planktic foraminifers indicating open marine depositional environments in low-energy regimes. The wedge of high-amplitude reflectors between s.p. 3860 and 4020 on line 19 may also include bathyal Oligocene strata (figs. 20, 21).

Beneath the lower continental slope and rise, between s.p. 4100 and the seaward end of line 19, is a thick sequence of chaotic, steeply dipping to subhorizontal, discontinuous reflectors of variable amplitude representing slope-front and basin-fill facies presumably deposited by high-energy debris flows and turbidity currents (Vail and others, 1977). Oligocene strata may be included in this sequence.

PLIOCENE-MIOCENE ROCKS

The only Neogene strata recovered on Georges Bank occur at the G–2 well site. Here, tan to yellow-brown, micaceous, clayey siltstone contains a sparse Miocene to Pliocene benthic fauna. The dominant benthic forms are *Bulimina elongata, Lenticulina spinosa, Florilus pizzarensis,* and *Cassidulina* sp. A series of continuous, parallel, variable-amplitude reflectors are present at the G–2 projection on seismic line 77–2. On line 19 the reflectors are less continuous across the G–2 projection, but become more continuous downdip. The thick sequence of chaotic reflectors overlying presumed Paleocene and Eocene strata between s.p. 4140 and the seaward end of line 19 probably contains Pliocene and Miocene sediments.

Updip from the B–2 projection the parallel reflectors can be traced to about s.p. 2480, but most of them are faint between there and the G–1 projection. Discontinuous, parallel reflectors with highly variable amplitudes develop in the upper part of the Pliocene-Miocene section at the G–1 projection and extend updip from it to the end of line 19.

These characteristics suggest that at G–2 and downdip from the site, shallow inner to middle shelf marine environments were present during the Pliocene-Miocene deposition (fig. 19). Updip, shallow marine to nonmarine fluvial environments prevailed (fig. 16).

PLIESTOCENE ROCKS

Pleistocene strata were sampled at the G–1 well site by AMCOR corehole 6018. A 161-ft (49-m) section of coarse, shelly sand that was recovered contained a few organic-rich layers and scattered specimens of benthic foraminifers, such as *Elphidium* spp. and *Buccella* sp. (Poag, 1978; Hathaway and others, 1979). At least one interval contains *Epistominella* and *Buliminella* with pyritized diatoms and radiolarians. These characteristics indicate that shallow-water, inner shelf to coastal lagoon and perhaps nonmarine fluvial environments prevailed during the Pleistocene at this site when it was not covered with ice (fig. 16).

The Pleistocene unit can be traced downdip as it thickens to 200 ft (61 m) at the G–2 projection (figs. 20, 21). The unit is nearly reflector-free between the two G-well projections except for a strong "follow cycle" beneath the sediment-water interface. Downdip from the G–2 projection, the Pleistocene unit becomes thicker, until it is approximately 0.27 seconds (two-way traveltime) thick at s.p. 3760, where it develops into two separate prograding wedges and continues to thicken downdip. An erosional channel cuts

through the Pleistocene strata into presumed Paleocene to Oligocene strata between s.p. 3940 and 3965, but from s.p. 3965 to 4015 the Pleistocene cover forms a topographic mound. On the middle and lower continental slope, a thick unit of divergent, discontinuous, variable-amplitude reflectors make up a slope-front fill deposit that is probably a Pleistocene submarine fan. This unit also undoubtedly includes talus from eroded Tertiary and Cretaceous strata that crop out along the bank margin and in submarine canyons. (See Ryan and others, 1978.) On the continental rise (s.p. 4200 to the end of line 19), the Pleistocene sequence contains a few scattered high-amplitude reflectors. This sequence presumably represents homogeneous, silty, hemipelagic, distal turbidite deposits.

COMPARATIVE GEOLOGIC HISTORY OF THE GEORGES BANK AND SCOTIAN BASINS

During the block faulting phase of early rifting, coarse continental and evaporitic rocks accumulated in the Scotian shelf area in narrow basement grabens under arid climatic conditions (McIver, 1972; Given, 1977). After these rift valleys were filled by the terrigenous and evaporitic Eurydice, Argo, Iroquois, and Mohican Formations, the resulting broad basin floor became the site of restricted marine deposition during late Iroquois time. A similar history has been inferred for the Georges Bank basin (Schlee and others, 1976) and is confirmed by the record in the COST Nos. G-1 and G-2 wells, although the Eurydice Formation equivalent was not recovered. There are differences in detail between the two regions, however. The Georges Bank basin grabens in the area of the COST Nos. G-1 and G-2 wells seem to have been filled by the end of Hettangian(?)-Rhaetian(?) time (figs. 20, 21), and the presence of Triassic dinoflagellates at G-1 and G-2 is a sign of occasional marine incursions. These characteristics, the persistent influx of micritic and oolitic normal marine limestones throughout the 8,200-ft (2,499-m) Iroquois sequence at G-2 (fig. 22), and the widespread development of carbonate mounds (figs. 20, 21), are evidence of more frequent and earlier connection to open marine Tethyan waters at Georges Bank than on the Scotian shelf.

Given (1977) has postulated that continental drift began near the end of Iroquois deposition (end of Aalenian Stage) and that the upper Mohican (Bajocian) detrital rocks represent the first deposits above a breakup unconformity. On the Scotian shelf, widespread marine deposition began with the Scatarie Limestone Member of the Abenaki Formation, and the maximum Jurassic marine transgression took place during depositon of the Misaine Shale Member (Callovian; Given, 1977). But in the part of the Georges Bank basin considered here, the Misaine equivalent is not traceable seismically very far updip or downdip from the G-2 well (figs. 20, 21). Major Late Jurassic transgressions may have occurred here during deposition of the lower and upper parts of the Baccaro Limestone Member (Callovian(?) to Bathonian(?) and Tithonian to Kimmeridgian, respectively), but marine conditions were even more widespread earlier (Aalenian(?) to Sinemurian(?)), during deposition of the Iroquois Formation.

During the Late Jurassic on the Scotian shelf, carbonate deposition was concentrated along the stable shelf edge in a discontinuous series of banks of the Baccaro Limestone Member. The shelf-edge facies is a skeletal-reef association, while the bank interior is a nonskeletal, highly terrigenous, oolitic, muddy limestone association (Eliuk, 1978). A broad "moat" of calcareous shales developed in a depression behind the shelf-edge banks, and farther updip the siliciclastic Mohawk sands and Mic Mac shales were deposited as fluvial and nearshore facies (Eliuk, 1978). Periodic subaerial exposure and development of a freshwater lens on the emergent banks altered much of the Baccaro from limestone to dolomite.

The same general facies patterns developed in the Georges Bank basin. The equivalent of the Baccaro Limestone Member accumulated in shelf-edge banks (presumably including reef facies), and a broad back-bank platform of oolitic, pelletal, and micritic limestones extended to the G-2 well site (figs. 20, 21). From there, the Baccaro was split into two parts by a thick siliciclastic tongue of Mohawk-Mic Mac facies. The lower Baccaro unit extended only a few tens of kilometers updip from G-2, but the upper Baccaro unit extended shoreward of the strike position of the G-1.

On the Scotian shelf, the widespread Late Jurassic carbonate deposition ended abruptly

during the Hauterivian, and the sediments were buried under the siliciclastic deltaic deposits of the Missisauga Formation near the Sable Island delta. A rapid sea-level rise influenced deposition of the marine shales of the Verrill Canyon Formation in locations away from the Sable Island delta, such as at the Mohican I-100 site (Eliuk, 1978).

Slightly earlier in the Georges Bank basin, during the Berriasian, the coarse siliciclastics of the Missisauga Formation began to cover the Baccaro shelf carbonates at G-2 (figs. 20, 21). During the early Valanginian to early Hauterivian, siliciclastic deposition progressed seaward to the shelf-edge reefs and began to spill onto the ancient slope.

The Missisauga siliciclastic deposition was interrupted briefly in both regions by carbonate deposition of the "0" limestone marker. The interruption occurred in the early Barremian on the Scotian shelf, and in the late Hauterivian to early Barremian in the Georges Bank basin; however, the resolution of faunal zones and stage boundaries in this time interval is not precise, and deposition of the "0" marker may have been essentially isochronous over the entire region.

Progressively deeper marine paleoenvironments encroached upon both the Nova Scotian and New England shelves during the Late Cretaceous, depositing sandstones, shales, and mudstones (figs. 20, 21). On the Scotian shelf, the Upper Cretaceous deep-water deposits culminated in the chalks of the Wyandot Formation, but contemporaneous deposits appear to have been eroded from the old shelf of the Georges Bank basin. However, a thick, slope-fill unit of Wyandot age (Campanian-Maestrichtian) appears to be present on the continental slope.

Deep-water carbonate deposition continued into the Paleogene in both regions as bioclastic, middle Eocene chalky limestones accumulated in the Georges Bank basin. The Neogene sedimentation returned to a shallower water siliciclastic depositional mode, which continued into and through the Pleistocene.

SEA-LEVEL FLUCTUATIONS AND DEPOSITIONAL CYCLES

Relative changes in sea level have a direct effect on the lithology and fauna and flora of rock sequences and on their vertical and lateral facies relationships. Conversely, the interpretations of microfaunas and seismic facies leads to the recognition of ancient sea-level fluctuations.

A curve illustrating changing paleobathymetry in the G-1 and G-2 wells is shown in figure 27. In both wells the Lower to Middle Jurassic carbonate rocks are highly indurated, and microfossils were rare or absent in the cuttings. Several shale samples from conventional cores were also processed, but they yielded no calcareous microfossils or palynomorphs. Only broad depositional cycles could be inferred from lithologic and seismic data. These suggest nonmarine fluvial to shallow, nearshore marine conditions in the Early to Middle Jurassic.

Inner shelf marine foraminiferal faunas begin to appear in the upper Callovian-lower Oxfordian rocks. The first sustained Jurassic middle shelf faunas occur in the Tithonian.

The early parts of supercycle Ka (Valanginian through Albian) are represented by inner shelf to nonmarine paleoenvironments, but the Albian is poorly represented in the two G wells. The earliest part of cycle Kb is not represented, but deep waters (outer shelf conditions) were present throughout the late Cenomanian to Santonian interval at G-2. G-1 shows a peak transgression during the late Cenomanian, a regression during the Coniacian, and a minor transgression during the Santonian. The peak of cycle Kb (Campanian and Maestrichtian) is not represented in either well.

Tertiary supercycles are poorly represented. However, the outer shelf and slope environments of the late middle Eocene reflect the major transgression postulated by Vail and others (1977) and shown in the other Atlantic COST wells (GE-1, Poag and Hall, 1979; B-2 and B-3, Poag, 1980b). Miocene, Pliocene, and Pleistocene intervals contain outer, middle, and inner shelf deposits.

In general, the pattern of transgression and regression coincides with the patterns seen in the other Atlantic COST wells and those published by Vail and others (1977; fig. 27).

COMPARISON WITH DEEP-SEA SEDIMENTARY SEQUENCES

The western part of the North American Basin, which borders the Georges Bank basin to the

south and east, has now been penetrated by 25 Deep Sea Drilling Project (DSDP) coreholes from Legs 1, 2, 11, 43, and 44 and has been crisscrossed with thousands of kilometers of seismic reflection profiles. Tucholke (1979), Tucholke and Vogt (1979), Tucholke and Mountain (1979) and Jansa and others (1979) have summarized the sedimentary evolution and stratigraphy of this vast deep-sea region. Six widespread formations of Mesozoic and Cenozoic age have been formally recognized at the core sites, and a series of eight major seismic reflectors have made possible extrapolation of the core data across the abyssal plain and under the lower continental rise of North America (fig. 28). Some of these reflectors have been traced beneath the continental rise adjoining Georges Bank (see Schlee and others, 1979; Klitgord and Grow, 1980) and provide a few tie points through which slope and upper rise sequences can be correlated with those of the deep sea.

The seismic sequences and inferred lithologic facies are more complex beneath the slope and upper rise than at those deep-sea basin localities that serve as stratotypes for the oceanic formations. For this reason, and because we have very little direct evidence of their composition, the slope and rise strata are referred to as "updip equivalents" of the oceanic formations.

Line 19 provides a typical example of the seismic sequences beneath the slope and upper rise off Georges Bank. Six high-amplitude, unconformable reflectors or series of reflectors and several of lesser amplitude permit tentative subdivision of the slope-rise wedge into the chronostratigraphic section shown in figure 21. The oldest seismic sequence overlying the oceanic basement comprises a series of steeply dipping, nonparallel, discontinuous, variable-amplitude reflectors that form a slope-front fill facies and onlap the seaward base of the shelf-edge reefal bank between s.p. 4140 and 4280. At s.p. 4280, the reflectors become flatter, parallel, and continuous and remain so to the end of line 19. The very high amplitudes of these reflections suggest that they represent carbonate strata. The slope-front fill facies can probably be classified as an olistostrome, formed by debris flows that incorporated eroded fragments of the shelf-edge reefal bank, whereas the more flat-lying, basin-fill facies probably contains finer-grained strata deposited by turbidity currents. Some terrigenous detritus may have reached the reef front as well, through breaks in the barrier (indicated by the lack of a reefal bank on some dip lines). These strata constitute the second major seismic sequence below the β horizon (fig. 28), and as such are believed to represent Middle and Upper Jurassic and lowest Cretaceous rocks. The presence of carbonate strata of this age behind the reefal bank and in the DSDP sites (site 105, for example) supports the conclusion that carbonate rocks should be abundant on the ancient slope too. Lithostratigraphically, this unit appears to include an equivalent of the Cat Gap Formation (fig. 28); its equivalents farther updip beneath the shelf are the Abenaki, Mohawk, and Mic Mac Formations. The old slope sequence may, however, include older formations not yet sampled in the North Atlantic Basin, because Tucholke and Mountain (1979) have recognized a thick (10,469-ft; 3,200-m) series of reflectors older than the β sequence, which they estimated may be as old as Pliensbachian. They interpreted these strata to be coarse terrigenous and calcareous debris.

The next seismic sequence is bounded at the top by what is believed to be reflector β (figs. 20, 21, 28). At least two facies (slope-front fill and basin fill) can be recognized in this unit, and they appear to be similar in origin and composition to the underlying sequence. However, the amplitudes of the reflectors are not as high as those of the underlying unit suggesting, perhaps, a greater proportion of siliciclastic turbidites and fewer carbonates. These strata appear to be of Valanginian to Barremian Age and are updip equivalents of the Blake-Bahama Formations, a pelagic limestone known from the basin. Shelf equivalents are the upper part of the Abenaki Formation, the "0" marker limestone, and the Missisauga Formation.

The seismic sequence immediately above β also consists of a slope-front fill facies and a basin-fill facies (figs. 20, 21). The slope-front fill facies has the same intermittent, variable-amplitude, divergent reflectors as the underlying slope-front fill facies, but the amplitudes are not as high, which suggests a change to predominantly siliciclastic debris flows. The basin-fill facies also contains lower amplitude reflectors than the underlying facies, and its reflectors are fairly continuous. These basin-fill rocks are interpreted to be siltstones and clays that are updip equivalents of the organic-rich black clays of the Hatteras Forma-

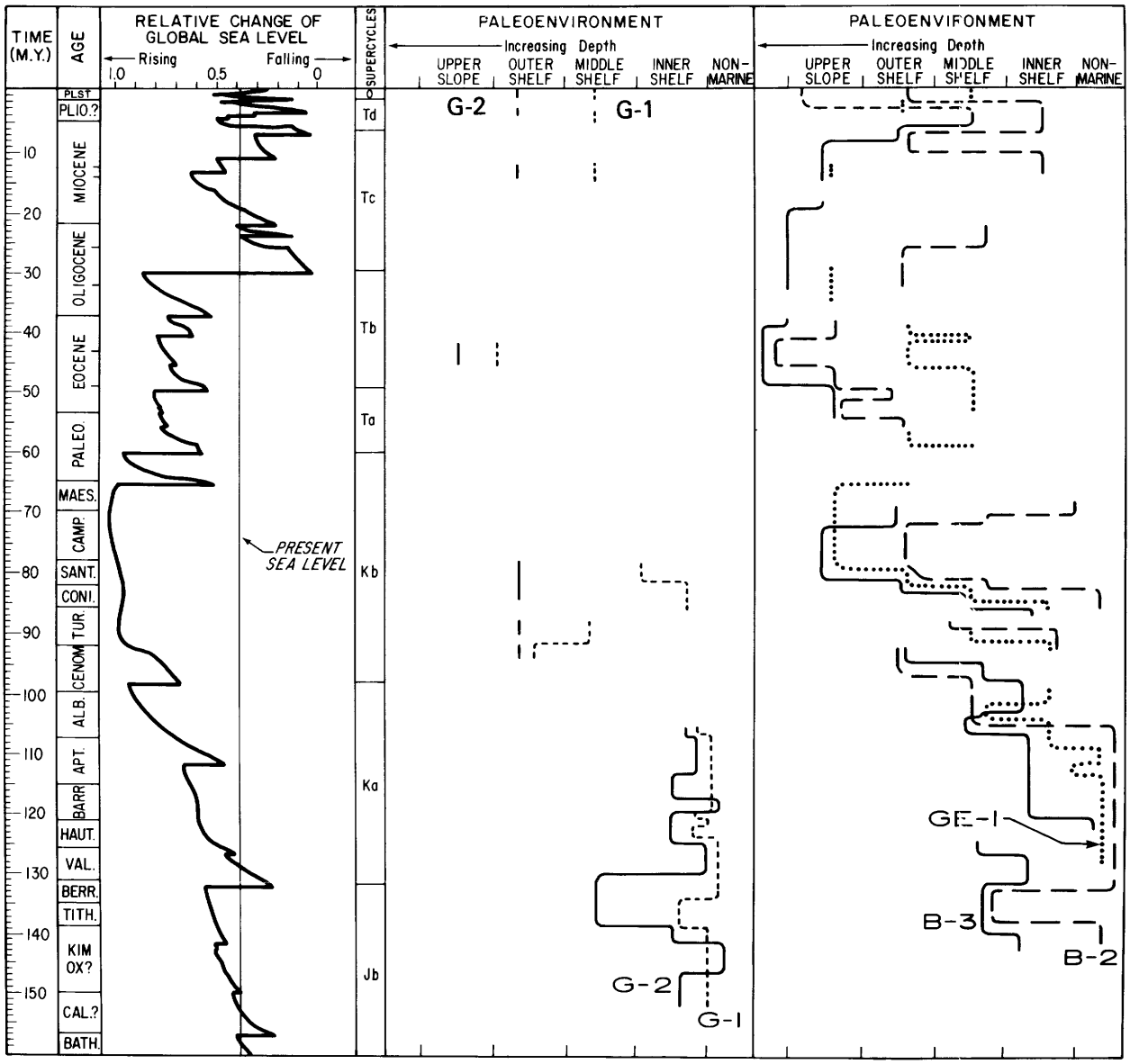

FIGURE 27.—Paleoenvironments of the COST Nos. G-1 and G-2 wells, compared with those of previous COST wells, the relative sea-level curve of Vail and others (1977), and global supercycles. Gaps in paleoenvironmental curves are hiatuses. The age terms abbreviated in the left side column are spelled out on figures 17 and 22.

tion. The inferred coarseness of the slope-front fill facies, however, probably makes it similar to the equivalent lower siltstones of the Dawson Canyon Formation.

The next seismic sequence is a basin-fill facies bounded above by high-amplitude reflectors that are believed to represent reflector A^* of the deep sea (approximately the Cretaceous-Tertiary contact) (figs. 20, 21, 28). The reflectors are subparallel in the upper and outer parts of the sequence, but divergent and intermittent in the basal part beneath s.p. 4300. This sequence is interpreted to be terrigenous turbidites of Late Cretaceous age. It is the updip equivalent of the Plantagenet Formation, and its shelf equivalents are the upper parts of the Dawson Canyon and Logan Canyon Formations.

Above the Plantagenet Formation equivalent and onlapping the Dawson Canyon(?) equivalent are a series of intermittent, very high amplitude

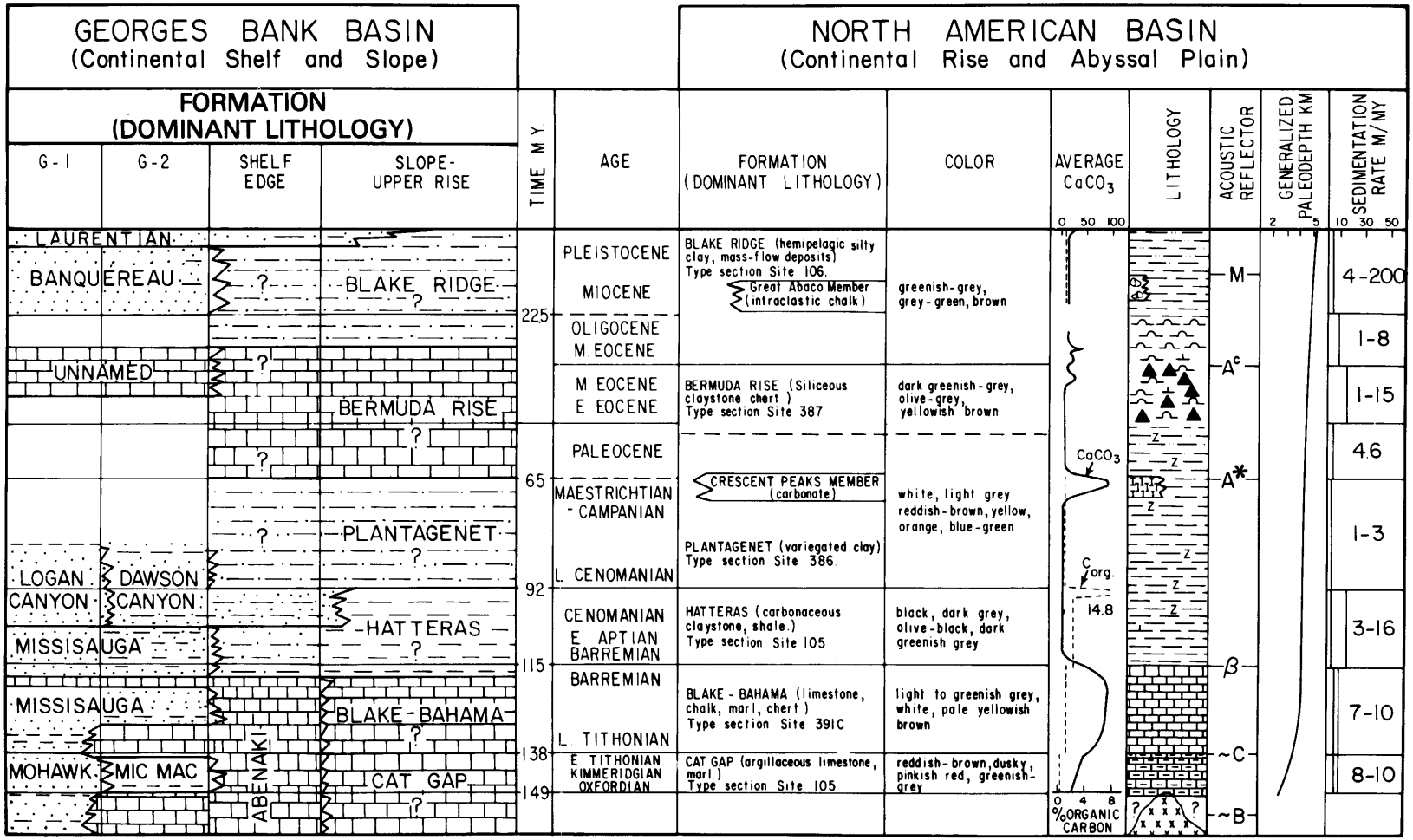

FIGURE 28.—Comparison of stratigraphy of Georges Bank basin with that of the adjacent North American Basin. Data for North American Basin after Jansa and others (1979).

reflectors thought to represent the cherty Paleocene and Eocene carbonate strata equivalent to the Bermuda Rise Formation (figs. 20, 21). The shelf equivalents are unnamed Paleocene and Eocene limestones. Some of the high amplitudes may be caused by cherty horizons known from deep-sea sites to cause the well-known reflector A^c (fig. 28).

Above the Bermuda Rise equivalent is a thick sequence of slope-front fill and basin-fill facies. The slope-front fill extends from s.p. 4080 to 4300 and contains steeply dipping, divergent, variable-amplitude, intermittent reflectors, indicative of an olistostrome. The basin-fill facies contains horizontal, chaotic reflectors with some arcuate, high-amplitude reflectors in the middle of the sequence. These probably represent siliciclastic turbidites deposited during the Miocene and Oligocene and constitute part of the updip equivalent of the Blake Ridge Formation. Under the shelf, equivalent beds belong to the Banquereau Formation.

The next younger sequence is a narrow band of faint reflectors below a moderately high-amplitude, discontinuous reflector, believed to be a turbidite sequence of Pliocene age (figs. 20, 21). Above the Pliocene is another seismic facies representing slope-front fill and basin fill. The dipping, divergent, high-amplitude, slope-front facies is believed to be an olistostrome of Pleistocene age that includes older clastic fragments and blocks derived from outcropping Tertiary and Upper Cretaceous beds, such as were observed by Ryan and others (1978) in Heezen Canyon. The basin-fill facies probably is composed of finer grained Pleistocene turbidite sequences, but older (Eocene, Cretaceous) debris is also present much farther seaward (for example DSDP Site 107; Hollister, Ewing and others, 1972). The slope-front fill facies can be correlated with the Laurentian Formation of the shelf, and the basin-fill facies and the underlying Pliocene beds form the upper part of the updip equivalent of the Blake Ridge Formation (figs. 20, 21, 28).

These sequences show that depositional cycles on the shelf have been coupled with and have affected depositional cycles in the deep sea. Carbonate deposition was predominant on the shelf and in the deep sea in the Jurassic and Early Cretaceous. The shelf-edge reefal bank and the broad carbonate platform behind it served as barriers that prevented terrigenous sediments from reaching the deep basin in significant quantities, except in a few areas where the reefal bank system was breached or absent. Carbonate olistostromes and turbidites buried the basinward flank of the reefal bank and built the protocontinental slope and rise, while pelagic limestones accumulated on the oceanic basement.

Sometime during Hauterivian to Barremian time the terrigenous constituents of the Missisauga Formation began to cover the reefal bank, spilling down the seaward flank and extending the terrigenous depositional regime to the deep sea. At the same time, the rising carbonate compensation depth (CCD) and widespread oxygen-deficient conditions over the abyssal plain allowed preservation of layers enriched in terrestrial organic matter, which became the distinctive black clays of the Hatteras Formation (Tucholke and Mountain, 1979; Tissot and others, 1979, 1980).

Hemipelagic deposition prevailed until the Paleocene and Eocene, when carbonates again dominated both the shelf and parts of the deep sea. Then the rapidly deposited siliciclastics of the Oligocene and Miocene began to build a thick slope-rise wedge that included eroded blocks and fragments of the Upper Cretaceous to Eocene beds that cropped out along the edge of Georges Bank.

During the Pleistocene, glaciofluvial and glaciomarine deposition took place on the bank, and during glacial intervals the Laurentian ice sheets scoured large volumes of sediment off the bank, forming a thick slope-front fill and basin fill beneath the upper continental rise. Even now, bank-edge erosion continues to contribute Cretaceous and lower Tertiary debris to the slope-rise wedge.

SUMMARY

The COST Nos. G-1 and G-2 wells in the Georges Bank basin penetrated 15,257 ft (4,650 m) and 21,490 ft (6,550 m), respectively, of marine and nonmarine sedimentary rocks ranging in age from Late Triassic to Pleistocene and Holocene(?). The lithologic, faunal, and floral records from these wells and from auxiliary short cores and dredgings, and the analyses of seismic sequences and facies show that the geologic development of the Georges Bank basin generally

paralleled that of the neighboring Scotian basin.

The initial rifting of the Triassic was characterized by terrigenous graben-fill deposits (Eurydice(?) Formation) interspersed with occasional marine beds and followed by accumulation of thick evaporitic strata (Argo Formation). In the Late Triassic and Early Jurassic, as much as 8,200 ft (2,500 m) of shallow-marine limestones, dolomites and evaporites (Iroquois Formation) accumulated in the outer part of the basin as elongate carbonate mounds and widespread platform facies behind a bordering shelf-edge complex of reefal banks. Concurrently, the inner part of the basin was the site of coarse terrigenous deposition (Mohican Formation). The Mohican sandstones and mudstones prograded far out onto the carbonate platform during the early Middle Jurassic(?) (early Bathonian(?)), but did not reach the shelf edge.

A major marine transgression during the late Bathonian(?) reestablished a carbonate regime nearly as far updip as the G-1 well site, depositing the oolitic and pelletal strata of the Abenaki Formation. Another pulse of terrigenous deposition spread thick sandstones and shales of the Mohawk and Mic Mac Formations as far downdip as the G-2 well site during the Oxfordian(?) to late Kimmeridgian interval. Carbonates were dominant for the last time in the late Kimmeridgian to early Berriasian as Abenaki facies once more nearly reached as far updip as the G-1 well site.

During the Early Cretaceous (Berriasian and Valanginian) a sustained influx of coarse-grained, lignitic terrestrial sediments (Missisauga Formation) replaced the carbonate regime over the entire shelf, and during the early Hauterivian the terrigenous sediment spilled over the shelf edge into the North American Basin. A short-lived but widespread interruption of this influx by the thin, calcareous "0" marker took place in the late Hauterivian.

During the rest of the Cretaceous, sandstones, claystones, and mudstones of the Missisauga and Dawson Canyon Formations spread across the shelf and down onto the shelf and rise.

The sparsely sampled record of Tertiary deposition shows that during the Paleogene, an unnamed, white chalk, carbonate unit, prominent as far south as the southeast Georgia embayment, extended across the Georges Bank basin as well. Terrigenous marine deposition resumed during the Neogene (Banquereau Formation) and was replaced by glaciofluvial and glaciomarine deposition in the Pleistocene (Laurentian Formation).

The depositional sequences, hiatuses, sediment accumulation rates, and paleoenvironmental changes at the COST Nos. G-1 and G-2 well sites suggest that the continental shelf of the Georges Bank area was created by changing sea level, changing volumes of terrigenous and carbonate sediments, and episodic subsidence of the basin.

Deposition on the adjacent slope and rise was affected by sedimentation on the shelf, and throughout the Jurassic and Early Cretaceous by the intervening shelf-edge reefal banks. Shelf, slope, and rise deposition was significantly altered in the middle Cretaceous (Hauterivian-Barremian), when the carbonate platform and its bordering reefal bank were buried, allowing terrestrial debris to reach the deep sea.

Terrestrial organic matter was preserved in the black shales of the Hatteras Formation on the oxygen-deficient, carbonate-free abyssal plain.

Significance of the Mesozoic Carbonate Bank-Reef Sequence for the Petroleum Geology of the Georges Bank Basin

Robert E. Mattick

Analyses of rock cuttings and cores from the Jurassic section in the COST No. G-2 well indicate the following: above 10,500 ft (3,200 m) the predominantly clastic rocks have high porosities and permeabilities and are too thermally immature for the generation of liquid petroleum (Smith, 1980, p. 98). Between 10,500 ft (3,200 m) and 14,000 ft (4,300 m) there are moderately porous (10–15 percent) limestones which contain little organic material. Below 14,000 ft (4,300 m), the carbonate rocks show minimal to moderate amounts of organic matter, and many rock samples near the bottom of the well contain "amorphous-sapropelic" organic matter (Smith, 1980, p. 98). These deeper rocks, however, have porosities below 10 percent and permeabilities of about 0.1 millidarcy (Malinowski, 1980, figs. 12 and 13).

These results suggest that on the North Atlantic Outer Continental Shelf potential source rocks are generally not in close contact with potential reservoir rocks. High-porosity sandstones occur at shallow depths where the potential source rocks are immature; at greater depths where mature potential source rocks occur, porosities and permeabilities of potential reservoir beds are low. Without proximity of source and reservoir beds, petroleum can accumulate in significant amounts only through long distance lateral migration or through vertical migration along faults. There is little possibility that significant amounts of petroleum have accumulated on the U.S. Atlantic shelf by long distance migration, because of the probable absence of laterally continuous, porous Jurassic sandstone beds and the absence of major post-Triassic tectonic events that might have provided major fluid migration paths along fault and fracture systems. However, there may have been some migration at the shelf margin along faults related to mass movement of sediment rather than tectonic events (Mattick and others, 1981).

Preliminary analyses of seismic data recorded farther seaward on the continental slope than the COST No. G-2 well suggest that potential source rocks may be in close contact with potential reservoir rocks. According to Mattick and others (1978), Jurassic forereef and reef facies could interfinger with basinal facies on the continental slope. Although the seismic evidence for the interfingering of these facies is strong, neither the source-rock potential of the basinal facies nor the porosity and permeability potential of the possible reef and associated facies has been established. Evidence from the COST No. G-2 well in the Georges Bank basin indicates that the sedimentary rocks of Jurassic age at this site were deposited at or near sea level; thus, reef and associated carbonate facies deposited at the edge of the ancient shelf margin possibly were intermittently exposed to subaerial weathering and, as a result of leaching by freshwater and perhaps dolomitization, secondary porosity may have developed. The basinal facies of the ancient slope environment may have been deposited in a zone of low oxygen concentration (comparable to the oxygen minimum zone that intersects the present continental slope), enhancing the preservation of organic matter and making these sedimentary rocks a potential source for petroleum if subjected to deep burial. Under these conditions the organic content of the basinal shales is likely to contain a higher percentage of marine-derived organic matter than shales formed on the shelf and hence should have a greater capacity for generating liquid instead of gaseous hydrocarbons.

The purpose of this paper is to analyze the development of the shelf margin during Jurassic time and to show the relationship between carbonate facies, which may or may not be significantly porous, and basinal facies, which may contain large amounts of marine-derived organic carbon. Areas in which these facies are in proximity may prove to be areas where significant amounts of petroleum have accumulated in stratigraphic traps. Although this work is based chiefly on the interpretation of seismic data and is therefore speculative, a proposed well to test these interpretations (COST No. B-4) may be drilled in about 4,300 ft (1,300 m) of water in the Baltimore Canyon trough area. It should penetrate an area where, based on the interpretation of seismic data, Jurassic forereef facies interfinger with basinal facies of the same age.

SEISMIC DATA

Figure 29 shows the U.S. Geological Survey common depth point (CDP) seismic profiles recorded on the northern and central U.S. Atlantic margin. The parts of the record discussed in this paper are marked, and each is about 30 mi (50 km) long.

In order to correlate reflection events with stratigraphy and lithology, the seismic grid was tied to the COST No. G-2 well. In figure 30 the data from the well (Judkins and others, 1980) is plotted alongside a segment of seismic profile 15 that crosses over the well site. The well bottomed in salt at 21,851 ft (6,660 m). Between 13,571 ft (4,136 m) and the top of the salt, the dominant lithology is dolomite, anhydrite, and limestone of Early and Middle Jurassic(?) age. Because of the similarity in age and lithology, Judkins and others (1980) correlated this part of the Jurassic section with the upper part of the Iroquois Formation of the Scotian shelf. If the correlation is correct, these rocks represent deposition during a rift valley stage in the development of the Atlantic Ocean basin (Given, 1977). From 13,306 ft (4,056 m) to the top of the Jurassic section, the rocks are chiefly limestone and sandstone. Judkins and others (1980) correlated the thick

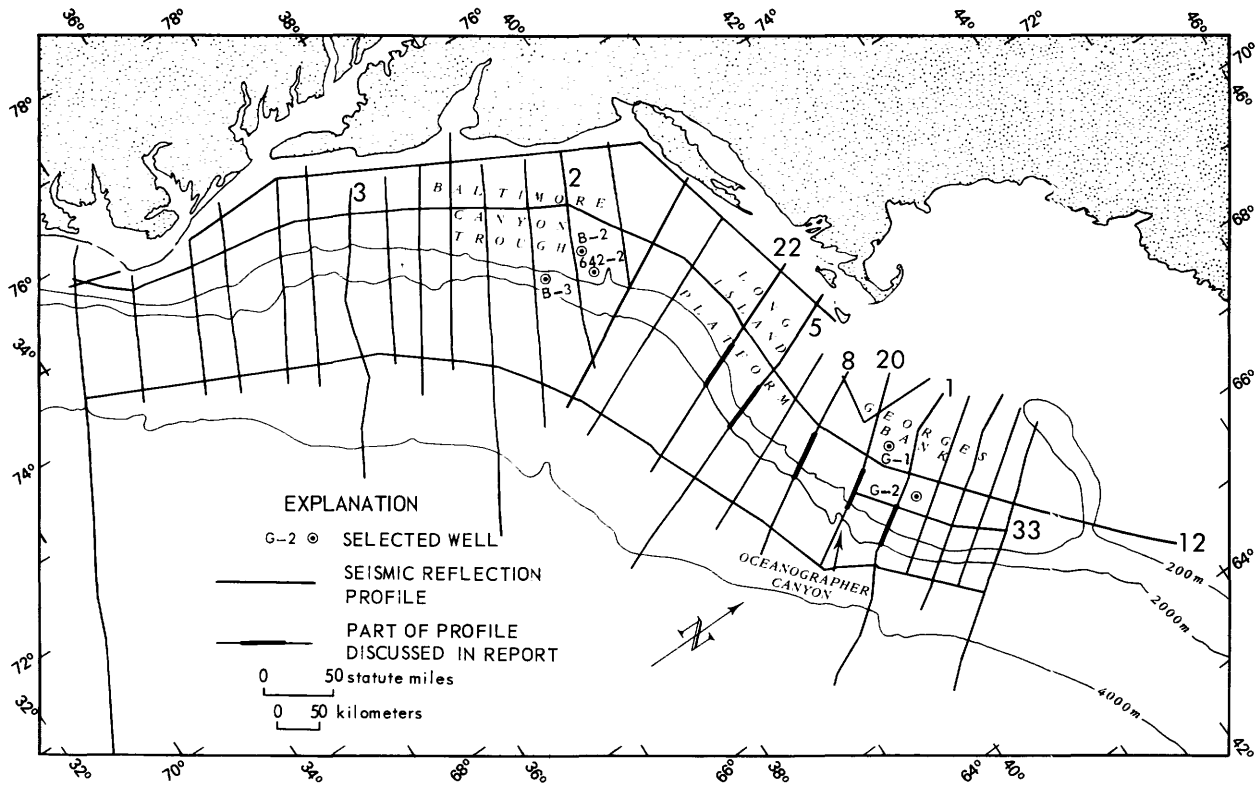

FIGURE 29.—U.S. Geological Survey common depth point (CDP) seismic reflection profiles recorded on the northern and central U.S. Atlantic margin. The parts of the profiles displayed in other figures are shown by heavy lines and those discussed in the text are numbered.

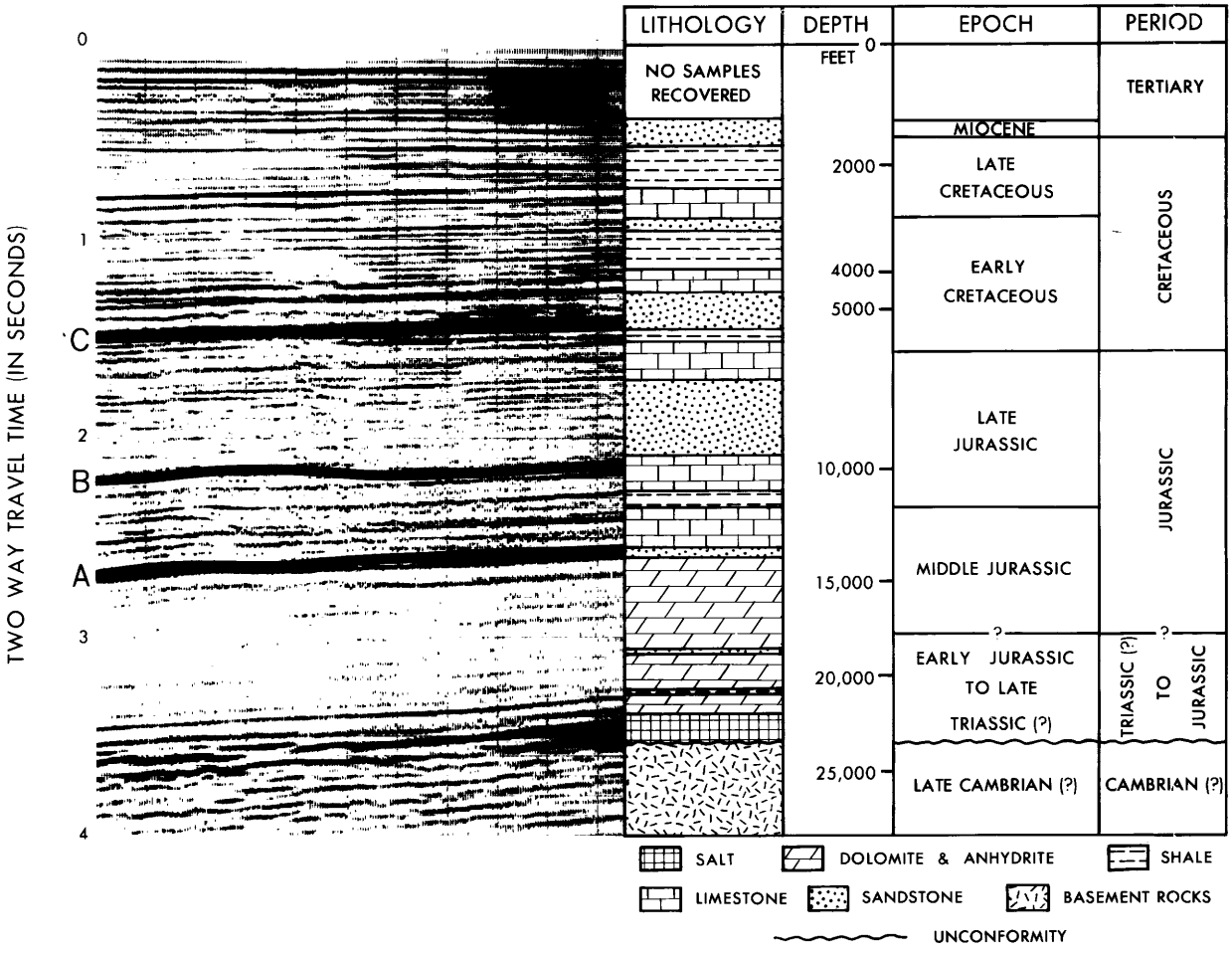

FIGURE 30.—Data from the COST No. G-2 well plotted alongside a part of seismic reflection profile 15 that crosses the well site. The vertical scale is two-way reflection time, and depths (not to scale) are annotated on the right. Three prominent reflectors (A, B, and C) can be mapped throughout much of the Georges Bank basin. The top of basement rocks is estimated from interpretation of seismic data. Evidence from the COST No. G-1 well indicates that the basement consists of highly metamorphosed rocks of Cambrian(?) age.

limestone unit with the Abenaki Formation of the Scotian Shelf and the thick sandstone unit with a tongue of the Mohawk and Mic Mac Formations. On the Scotian shelf these formations represent deposition during the post-breakup transgression of the early Atlantic (Given, 1977).

Three prominent reflectors were noted and labeled from deep to shallow as A, B, and C. The deepest reflector (A) can be correlated with the contact between the dolomite-anhydrite unit of Early-Middle Jurassic(?) age and the overlying limestone unit, and marks the continental breakup. Reflector A can be mapped throughout the Georges Bank basin except in areas where it terminates against basement in a shoreward direction and in the vicinity of the Long Island platform. Reflector B was picked at a depth of about 10,000 ft (3,000 m), near the contact between a thick Upper Jurassic sandstone unit and an underlying Upper Jurassic limestone unit. Reflector C, at a depth of about 5,300 ft (1,600 m), correlates with Lower Cretaceous strata located near the top of the Jurassic section. Throughout this paper, these reflectors are assumed to be time correlative rather than lithologic markers. This assumption, although probably not completely valid, results in good correlation between seismic events recorded on the shelf margin and slope.

Reflector A at the G-2 site is correlated with

the "breakup unconformity," which refers to the erosional surface developed between the rift valley stage of development and the onset of seafloor spreading. According to Falvey (1974), the rift valley stage of development is a protracted event that involves hogback uplift due to extensive thermal expansion and later, as a result of block collapse, results in the accumulation of considerable volumes of clastic sediments in the rift valley. However, the process of continental breakup and the onset of seafloor spreading was not instantaneous. Following block collapse and accumulation of clastic rocks in grabens, a shallow sea apparently occupied the site of the present Atlantic Continental Shelf. This event is reflected by the salt layer and the dolomite-anhydrite sequence penetrated in the bottom of the COST No. G-2 well. Klitgord and others (this volume) seem to suggest, by their placement of the breakup unconformity between the salt interval and the dolomite-anhydrite sequence, that the onset of seafloor spreading immediately followed deposition of the salt unit. This author infers that seafloor spreading coincided with a deepening of the early Atlantic and places the breakup unconformity between the dolomite-anhydrite sequence and the overlying limestone unit. According to Falvey (1974), the onset of seafloor spreading should involve a secondary heating event that leads to a short period of emergence just prior to breakup. This short period of uplift, resulting in a regression of the sea, may be reflected by the thin sandstone interval that separates the dolomite-anhydrite sequence from the overlying limestone unit at a depth of about 13,450 ft (4,100 m) in the COST No. G-2 well. Accurate placement of the breakup unconformity requires better time correlation between the Jurassic sedimentary rock units deposited on the continental rise and those deposited on the continental shelf.

Figure 31 shows the part of seismic profile 1 that crosses the shelf margin in the central Georges Bank area. The profile is typical of those recorded across the northeastern end of the Georges Bank basin. Reflectors can be traced from the central basinal area to the outer part of the shelf, where they become faint and disappear in a poorly defined structureless mass, which Mattick and others (1978) and Schlee and others (1979) have interpreted to be a Jurassic-Lower Cretaceous limestone platform. On seismic lines to the southwest, details of the platform complex become distinguishable.

Figure 32 shows part of seismic reflection profile 20 located about 25 mi (40 km) southwest of the previously discussed seismic section. On a shelf margin of Late Jurassic age, represented by reflections between reflectors B and C, Mattick and others (1978) and Schlee and others (1979) mapped a possible reef sequence. The sequence is not well developed on this profile, and it appears on other sections as a loss of reflections. Two distinct facies can be mapped: an oblique-progradational seismic facies between reflectors as A and B, and a sigmoid-progradational seismic facies between reflectors B and C. According to Vail and others (1977) the distinction between the two facies is as follows: in the oblique-progradational seismic facies, reflections terminate by toplap truncation at or near the upper surface and by downlap at the base. The sigmoid-progradational seismic units are characterized by gentle S-shaped reflections along depositional dip. On seismic lines parallel to depositional strike, the sigmoid-progradational reflections are usually parallel and concordant with unit boundaries. In figure 32 only the upper parts of the sigmoid reflections are seen: the lower parts of the reflections are lost under the slope where reflections become faint and chaotic.

As can be seen on figure 32, the oblique-progradational seismic facies appear to be associated primarily with shelf outbuilding; the sigmoid-progradational seismic facies appear to be associated primarily with upbuilding of the shelf and a lesser amount of seaward progradation. These two types of progradational seismic facies can be mapped throughout much of the Georges Bank basin.

Oblique-progradational seismic facies on shelf margins are characteristic of fluvial deltas and associated coastal-plain sediments and contain high-energy deposits (Vail and others, 1977). The undaform zone, corresponding to a delta-plain environment, and the upper part of the clinoform zone, corresponding to a delta-front environment, are likely to contain sand. The lower clinoform and fondoform zones, corresponding to a prodelta environment, are typically shale prone. In addition, the fondoform part of the oblique seismic facies may contain turbidite deposits of sands interbedded with marine shales.

In their discussion of sigmoid-progradational facies, Vail and others (1977) suggest that the corresponding sedimentary rocks are usually deposited on the slope along continental margins

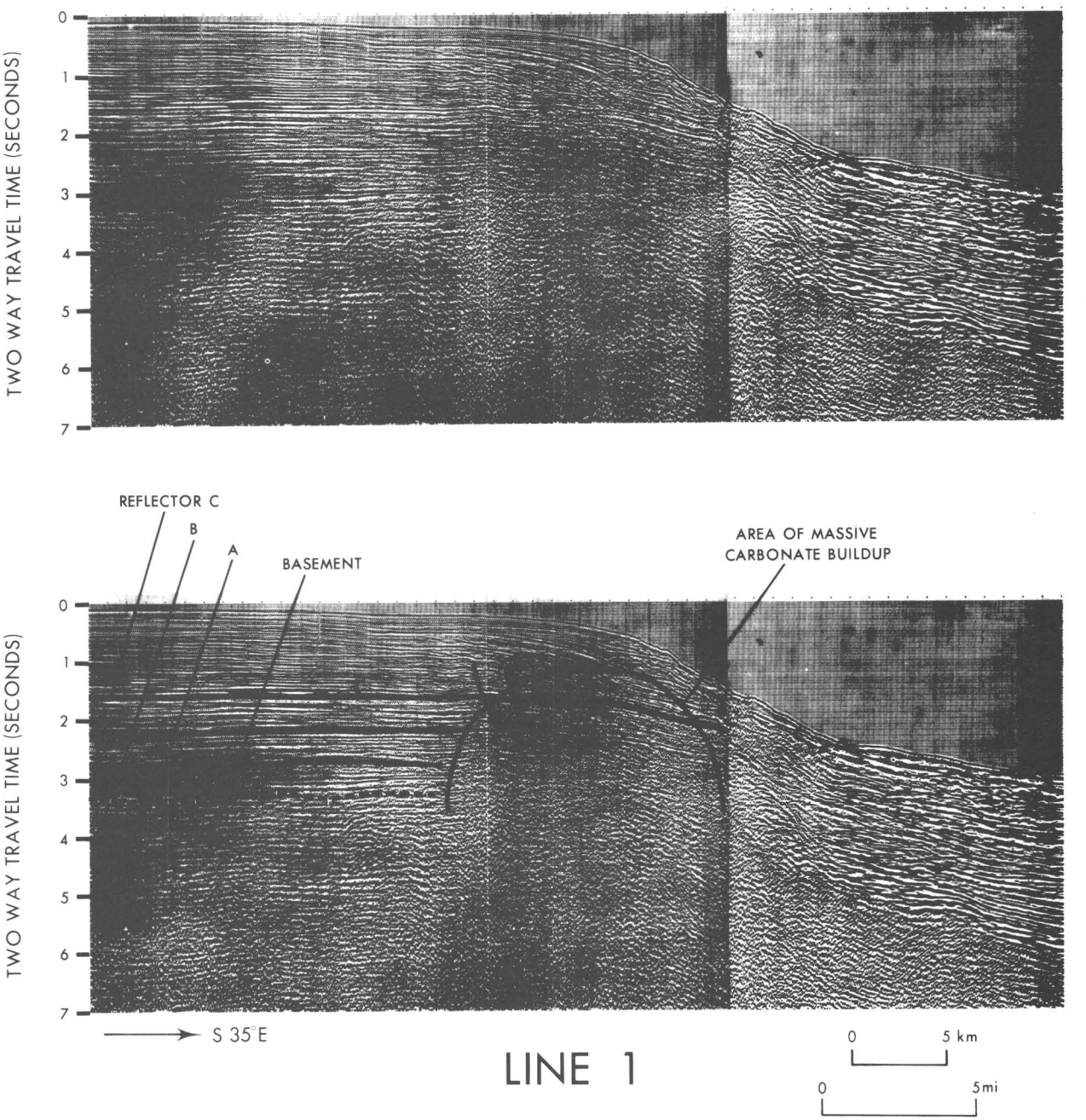

FIGURE 31.—Part of seismic reflection profile 1 recorded across the outer shelf and slope in the central part of the Georges Bank basin. Location of profile is shown in figure 29. Uninterpreted section is shown above and interpretive lines have been added below.

and that the undaform part of the reflection event extends into shelf margin facies. Shelf upbuilding produces thick deposits corresponding to the undaform parts of the reflections. Clinoform facies represent dominantly fine-grained clastics that were most likely deposited from low-energy turbidity currents and from low-velocity currents as hemipelagic deposits. Sedimentary rocks represented by the undaform facies may result from wave or fluvial transport, hence there is some possibility of coarse reservoir clastics in the undaform environment.

These interpretations suggest that the oblique facies between reflectors A and B represent more sand-prone sedimentary rocks than do the sigmoid facies between reflectors B and C. At the COST No. G-2 well there are predominantly limestone facies below reflector B and predominantly

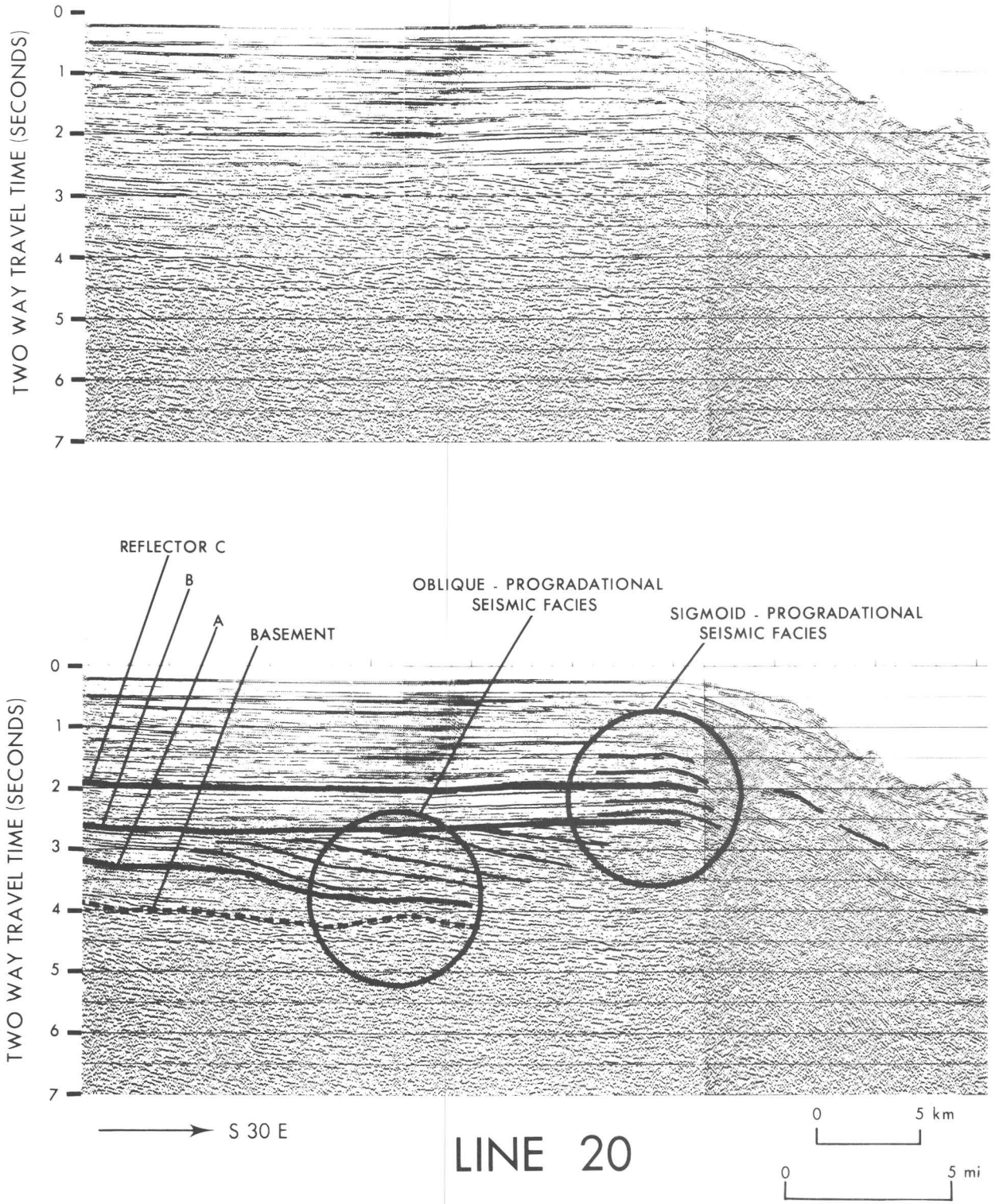

FIGURE 32.—Part of seismic reflection profile 20 recorded across the outer shelf and slope in the central part of the Georges Bank basin. Location of profile is shown in figure 29. Uninterpreted section is shown above and interpretive lines have been added below. The reflections between reflectors A and B are classified as oblique-progradational seismic facies and those between reflectors B and C are classified as sigmoid-progradational seismic facies.

sandstone facies above. This pattern suggests that the oblique seismic facies represent limestone beds deposited in a high-energy environment, perhaps an oolitic limestone. In this case, termination of reflections by toplap near the upper surface suggests that the limestone was derived at or near a shelf edge and deposited on the slope by wave action. Upbuilding of the shelf did not occur during this time because there was little influx of clastics to the shelf. As the influx of clastic material increased after the time represented by reflector B, the shelf began to build upwards.

Seismic profiles 8, 5, and 22 are shown in figures 33, 34, and 35 respectively. The reflecting horizons noted in these figures were carried from profile to profile by additional mapping on seismic profile 12 (fig. 29), which intersected all of the seismic lines discussed in this paper. Although they differ in detail, all of the profiles reveal the same overall structure of the shelf margin during the Jurassic: oblique-progradational seismic

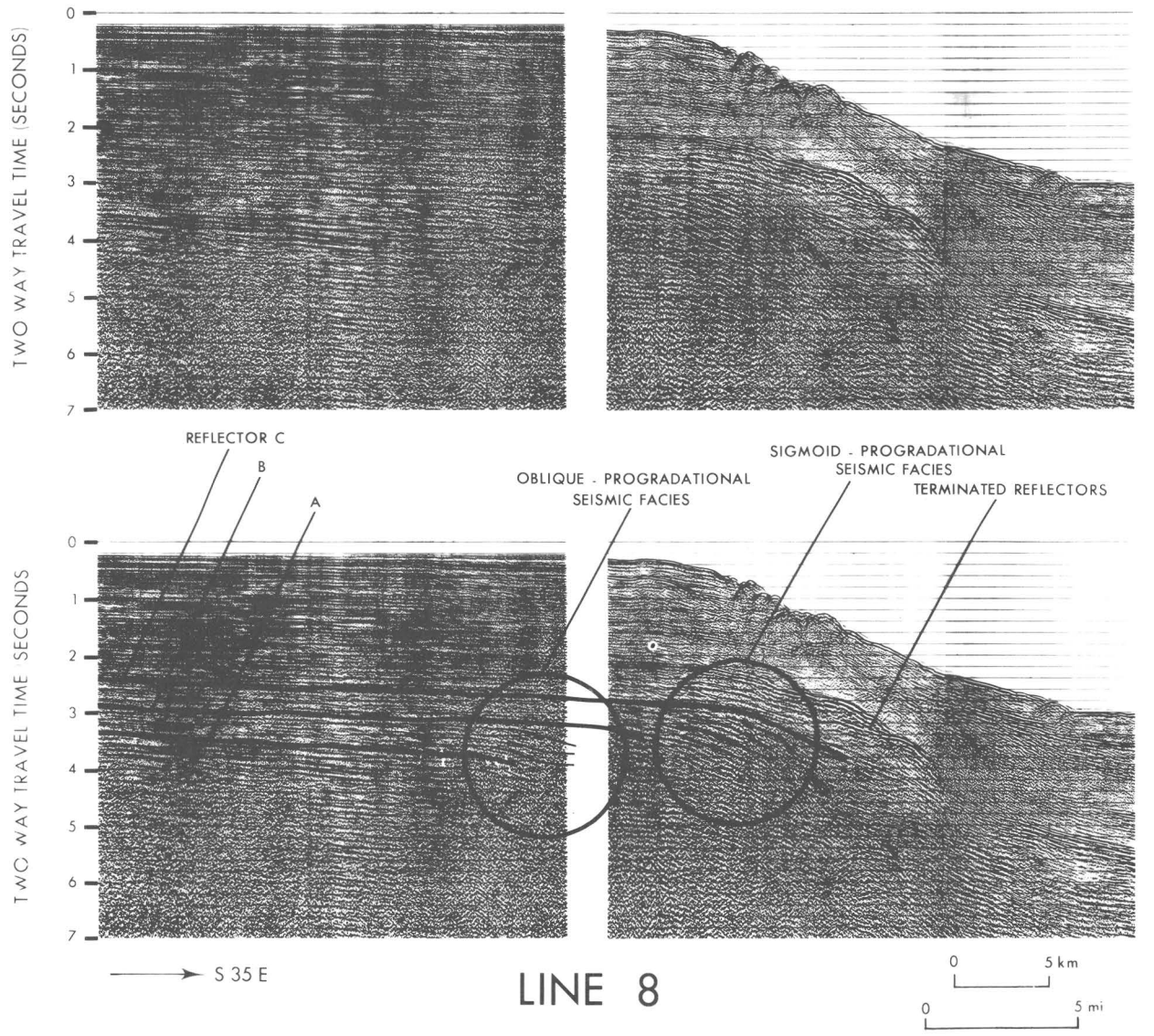

FIGURE 33.—Part of seismic reflection profile 8 recorded across the outer shelf and slope in the southwestern part of the Georges Bank basin. Location of profile is shown in figure 29. Uninterpreted section is shown above and interpretive lines have been added below.

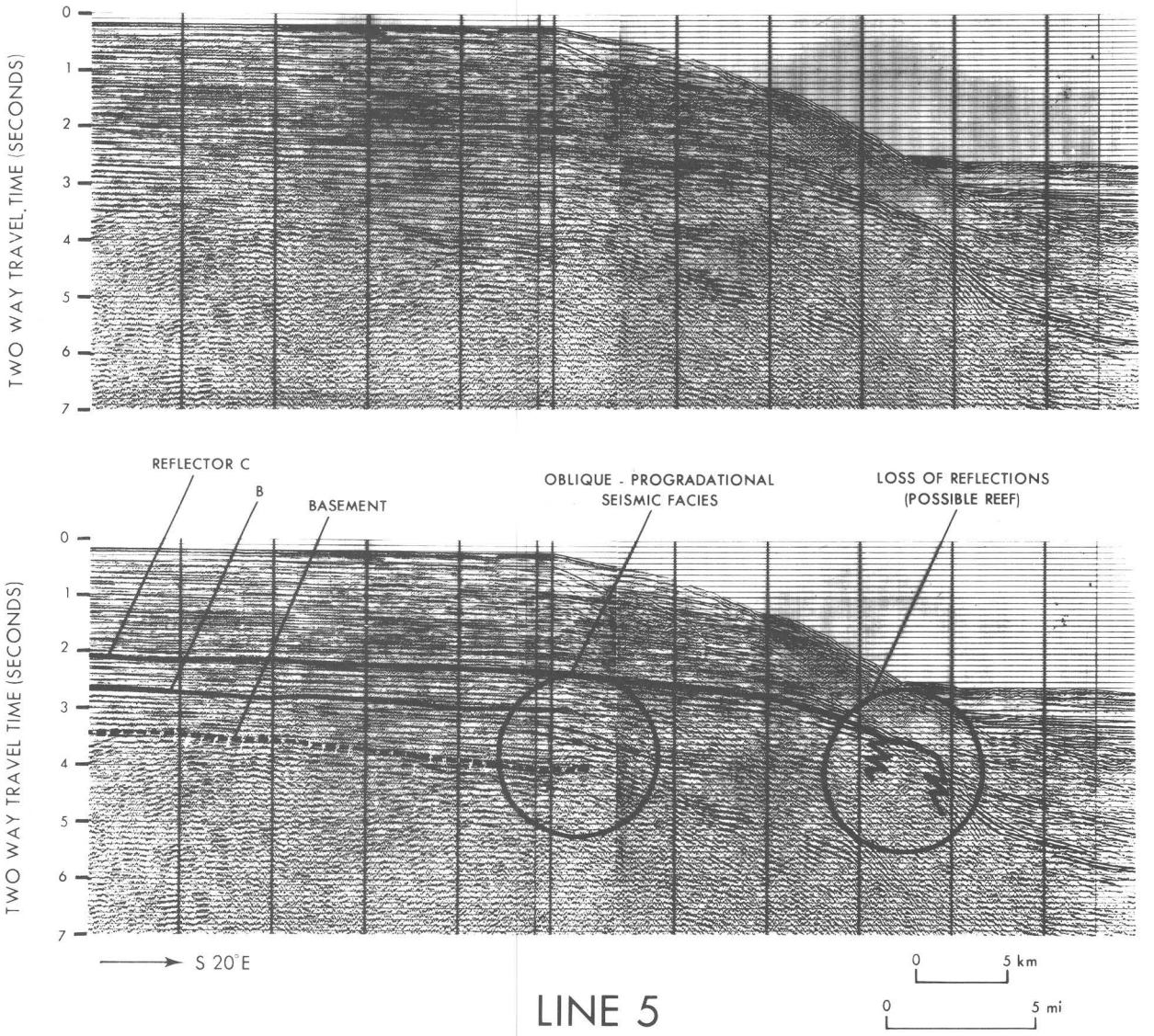

FIGURE 34.—Part of seismic reflection profile 5 recorded across the outer shelf and slope in the southwestern part of the Georges Bank basin. Location of profile is shown in figure 29. Uninterpreted section is shown above and interpretive lines have been added below.

facies, which represent outbuilding of the shelf margin during Middle and Late Jurassic time, and sigmoid-progradational seismic facies, which represent upbuilding of shelf margin during Late Jurassic time. On profile 8 (fig. 33) the reflectors immediately above reflector A suggest that a carbonate ramp began to build seaward following continental breakup. Later, during the Cretaceous, the shelf margin apparently prograded seaward over the Upper Jurassic shelf edge for some undetermined distance. The truncation of reflectors that represent Cretaceous strata suggests that the Cretaceous shelf edge has retreated shoreward because of erosion.

Profile 5 (fig. 34) is located just northeast of the Long Island platform and profile 22 (fig. 35) crosses the platform. On the shoreward ends of these profiles reflector A, which terminates against the basement surface in the shallower parts of Georges Bank basin, was absent. Oblique seismic facies can be seen at a depth of about 3.4 seconds (two-way traveltime) on profile 5; the base of this seismic facies probably correlates with reflector A. Near the southeast end of profile

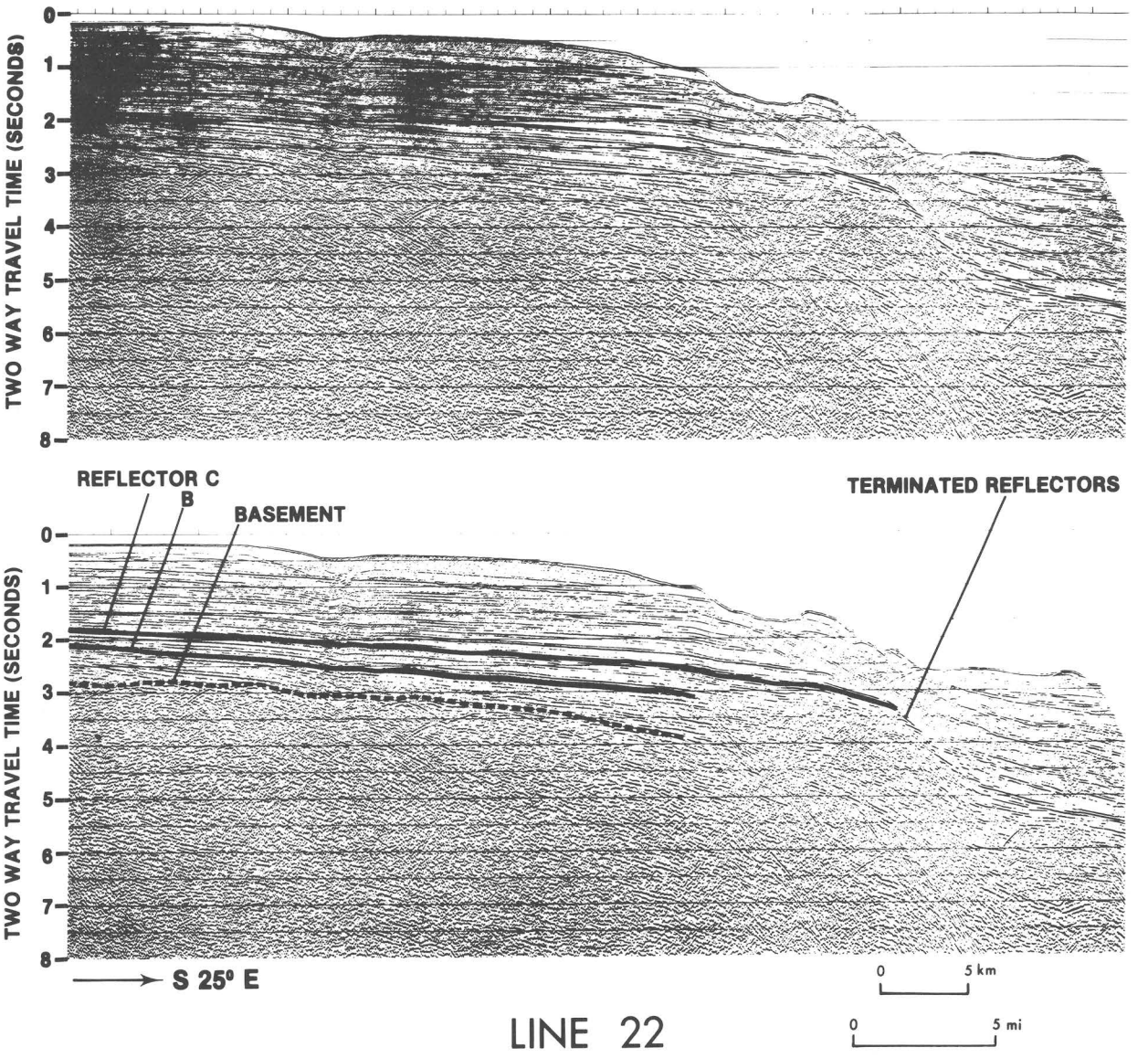

FIGURE 35.—Part of seismic reflection profile 22 recorded across the Long Island platform immediately south of the Georges Bank basin. The location of profile is shown in figure 29. Uninterpreted section is shown above and interpretive lines have been added below.

5, a zone of weak reflections is interpreted as a reef facies of Late Jurassic to Early Cretaceous age that grew along the shelf margin during that time. Along profile 22 (fig. 35), the sedimentary section is substantially thinner than that shown on previous profiles. On the Long Island platform this thinness results from the absence of the rocks correlating to the basal part of the oblique-progradational seismic facies below reflector B. In this area the location of the Middle Jurassic shelf edge probably coincides with that of the Upper Jurassic-Lower Cretaceous shelf edge. Terminated reflectors appear to mark that location.

GEOLOGIC IMPLICATIONS

The interpretation of seismic data recorded along the central and northern part of the U.S. Atlantic margin indicates two styles of shelf construction during the Jurassic and Early Cretaceous (fig. 36). Middle Jurassic time, following

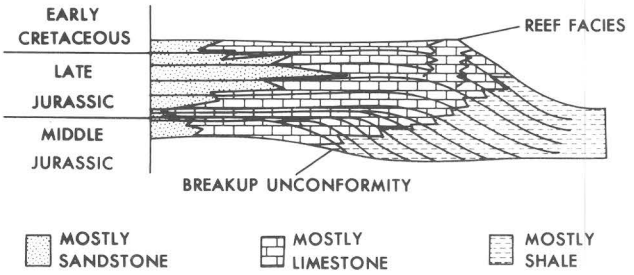

FIGURE 36.—Construction of continental shelf during Jurassic time. In this period, the shelf margin was marked by two primary styles of shelf construction—outbuilding during Middle Jurassic time and upbuilding during Late Jurassic-Early Cretacous time.

continental breakup, was marked primarily by out-building of the shelf. Late Jurassic-Early Cretaceous time was a period of shelf upbuilding with reef growth along the shelf margin. Correlation with the COST No. G-2 well on Georges Bank suggests that the change from outbuilding to upbuilding correlates with a Late Jurassic influx of clastic material.

The locations of the Middle Jurassic and Late Jurassic-Early Cretaceous shelf margins can be mapped using differing seismic facies. These locations and the location of the present shelf margin are shown in figure 37. The present shelf margin follows the 600-ft (200-m) bathymetric contour. The Late Jurassic-Early Cretaceous shelf margin was mapped by following the main mass of suspected reef trend on seismic records. The Middle Jurassic shelf margin was delineated by following the onset of oblique seismic facies nearest the shore.

In the Baltimore Canyon trough area southeast of line 2, the age correlations of the shelf margin are tentative because the oldest strata penetrated in that area is of Late Jurassic age (Poag, 1980b). It was assumed, for purposes of interpretation in the Baltimore Canyon trough area, that the change from oblique to sigmoid seismic facies is

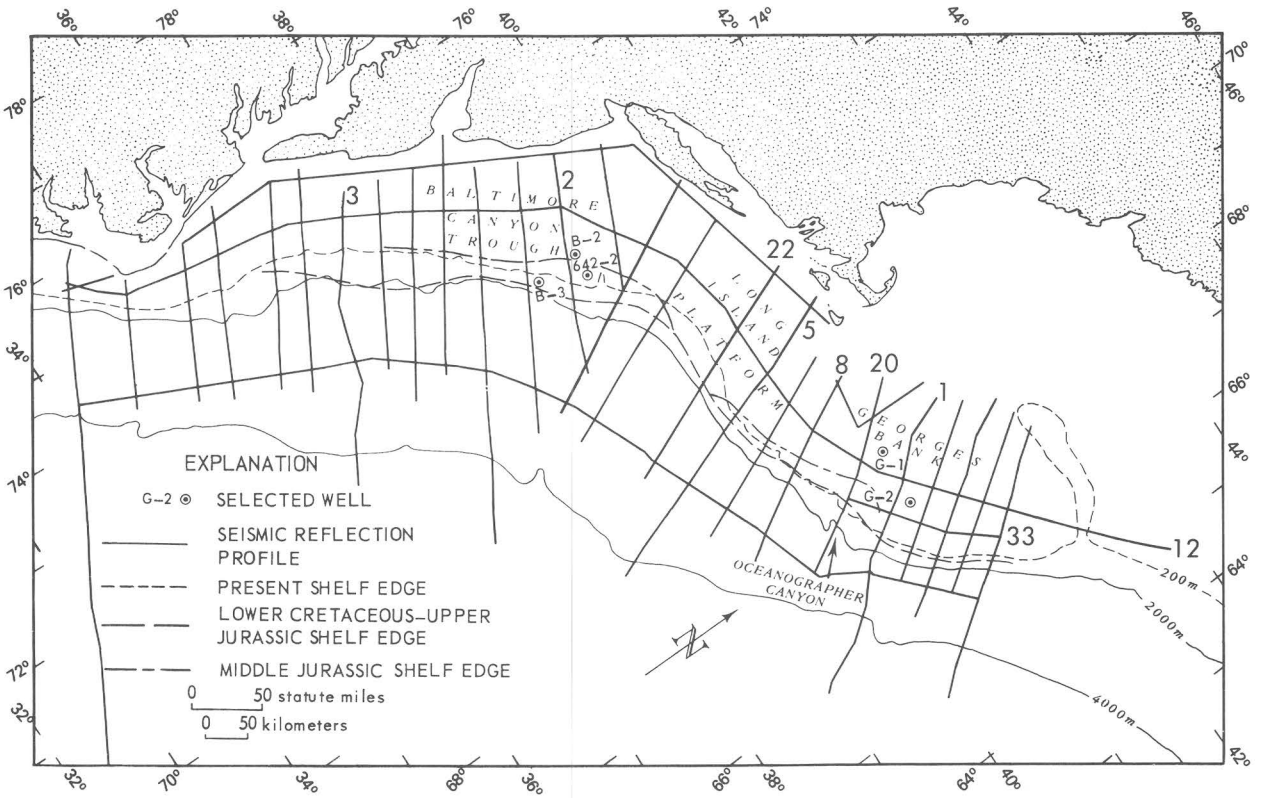

FIGURE 37.—Locations of the continental shelf margin during Middle Jurassic, Late Jurassic-Early Cretaceous, and present times. This mapping suggests that basinal shales (possibly containing oil-prone source rocks) underlie the present continental shelf in two areas—one in the vicinity of the Tenneco 642-2 well (the only well on the U.S. Atlantic margin reported to have flowed significant amounts of oil) and the other in the vicinity of Oceanographer Canyon on Georges Bank. The numbered seismic profiles are those that are discussed in the report.

the same age as Reflector B mapped in the Georges Bank area. As in the Georges Bank area, the top of the Jurassic section occurs slightly below the top of the sigmoid facies representing the Upper Jurassic-Lower Cretaceous shelf edge.

In the Georges Bank basin, the Late Jurassic-Early Cretaceous shelf margin lies just seaward of the present shelf margin except in vicinity of line 20 (fig. 37). In the Baltimore Canyon trough area, the Late Jurassic-Early Cretaceous shelf margin lies almost 30 mi (50 km) seaward of the present shelf-slope break. At the southern end of the Baltimore Canyon trough, along line 3, deep-water multiple reflections obscured most of the seismic data and prevented interpretation. The Middle Jurassic shelf margin lies shoreward of the present shelf-slope break except in the vicinity of the Long Island platform, where it is assumed to coincide with the Late Jurassic margin.

SUMMARY

Several generalizations about the petroleum geology of the shelf margin can be made from the foregoing discussion. Promising areas for petroleum accumulation occur on the continental shelf and especially on the continental slope. On the present continental shelf, petroleum may have accumulated in porous limestone or sandstone beds of Late Jurassic and Early Cretaceous age by upward migration along faults from possible organic-rich sinal shales of Middle Jurassic age. The most likely areas for such accumulations would be where Jurassic shales extend under the present shelf. As shown in figure 36, the maximum shoreward deposition of basinal shales occurred in Middle Jurassic time after continental breakup. The shoreward extent of these shales is represented by the Middle Jurassic shelf edge shown in figure 37. The maximum displacements between the Middle Jurassic and present shelf margins occur in the vicinity of line 2 in the Baltimore Canyon trough and in the vicinity of line 20 in the Georges Bank basin (fig. 37). These two areas are especially attractive for petroleum exploration because the only wildcat well on the U.S. Atlantic margin reported to date to have flowed significant amounts of oil is Tenneco 642-2, located at the shelf margin in the vicinity of line 2.

The oil (48.4 API gravity) from the Tenneco 642-2 well flowed at a rate of 630 barrels per day from a thin Lower Cretaceous sandstone bed at a depth of 8,315 ft (2,535 m) (Mattick and Bayer, 1980). According to these authors, the shallow depth of the discovery, together with geochemical and temperature data from the COST Nos. B-2 and B-3 wells (Scholle, 1977a, 1980), preclude the possibility that the oil was generated in proximate strata. Whether the 642-2 reservoir was charged with liquid hydrocarbons generated in more deeply buried basin facies is not known, but normal faults mapped in the vicinity of the Tenneco 642-2 well (Mattick and others, 1981) could have provided the necessary avenues for upward migration to Lower Cretaceous beds.

On the Atlantic continental slope of the United States, a primary task of petroleum exploration will be to locate possible hydrocarbon traps in forereef, reef, and backreef facies (fig. 38). Although not yet tested, the basinal shales that interfinger with carbonate rocks of the forereef facies may be some of the best potential source rocks on the continental slope in this area. Data from the COST wells drilled on the continental shelf (Scholle, 1977b, 1979, 1980; Amato and Bebout, 1980; Amato and Simonis, 1980) indicate that rocks deposited in the backreef environment have poor potential to generate liquid hydrocarbons.

If these basinal shales prove to have had the capacity to generate large amounts of petroleum, the key to hydrocarbon production will be locating strata with high porosity and permeability,

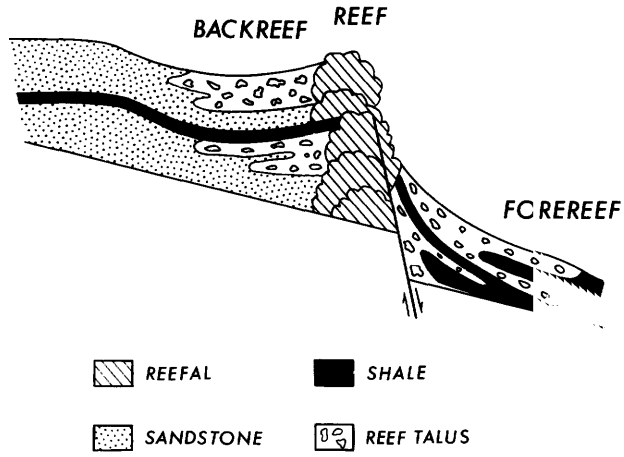

FIGURE 38.—Forereef, reef, and backreef facies of a carbonate bank. Basinal shales deposited in the forereef area could prove to be good source rocks for the generation of liquid hydrocarbons.

which formed as a result of subaerial exposure during periods of relatively low sea level. According to Benson and others (1976), Lower Cretaceous reef, bank, and backreef facies in DSDP holes 390, 392, and 392A all showed "evidence of subaerial weathering and leaching by fresh water." Although Mattick and others (1978) considered the Mesozoic shelf margin complex of the U.S. Atlantic comparable to the reef and forereef trend of the El Abra-Tamaulipas Formation of the Golden Lane and Poza Rica trends of Mexico, Simonis (1979, p. 105) points out that there have been no discoveries of hydrocarbons in the Upper and Middle Jurassic Abenaki Formation (carbonate unit) of the Scotian shelf, offshore eastern Canada, and that oolitic limestone penetrated in the COST No. B-3 well had porosities of less than 8 percent and permeabilities of less than 0.1 mD.

Although comparison with the Abenaki Formation (Middle to Late Jurassic age) of the Scotian shelf would suggest that carbonate units of the same age on the U.S. Atlantic margin are usually tight, the Shell Demascota G-32 well, drilled as a shelf edge test on the Scotian shelf, penetrated 551 ft (168 m) of porous dolomite and limestone (including reef carbonates) that have porosities as high as 14 percent in the limestone and fracture porosities of unknown magnitude in the dolomite (Given, 1977, p. 74). The dolomite in the Iroquois Formation (Upper Triassic, Early to Middle Jurassic) on the Scotian shelf has porosities as high as 15 percent and oil staining has been reported in several wells (Given, 1977, p. 71). It is not known whether such potential reservoirs exist on the old shelf margin (the present continental slope) in the Georges Bank area, or whether these reservoirs have been charged with sufficient amounts of liquid hydrocarbons generated in the nearby basin facies.

As can be seen from figure 37, in the Georges Bank area the Upper Jurassic-Lower Cretaceous reef trend underlies relatively shallow waters of the upper slope. In other areas of the U.S. Atlantic margin, this feature is under deeper water on the lower slope. Therefore, the Georges Bank should be one of the first areas targeted for the exploration of potential reservoirs in Mesozoic reef trends on the Atlantic margin.

Organic Geochemistry of the Georges Bank Basin COST Nos. G–1 and G–2 Wells

R. E. Miller, H. E. Lerch, G. E. Claypool, M. A. Smith,
D. K. Owings, D. T. Ligon, and S. B. Eisner

PURPOSE AND SCOPE

The objectives of this petroleum geochemistry study were to (1) compare the source-rock characteristics of the stratigraphic intervals that may be considered prospects for the generation of oil or natural gas in the COST Nos. G-1 and G–2 wells from the Georges Bank basin; (2) assess the depth of burial required for the onset of thermal maturation processes; and (3) evaluate the geochemical effects that mud additives may have on the source-rock interpretations.

CONCEPTS AND TERMS

The basic concepts of petroleum generation and source rock geochemistry used in this study are those established by Vassoyevich and others (1970), Dow (1977), Tissot and Welte (1978), and Hunt (1974, 1978, 1979). The terms used to describe source-rock richness, maturity, and potential are consistent with the definitions and concepts reported by Claypool and others (1977) and Miller and others (1979, 1980).

The quality or organic richness of a source shale and the source potential of such a bed to provide petroleum hydrocarbons may be indicated by (1) a minimum amount of total organic carbon (0.7 to 1.0 weight percent for argillaceous rocks); (2) pyrolytic oil yields greater than 0.2 to 0.3 percent, and (3) solvent extractable hydrocarbon concentrations in excess of 100 to 500 ppm. It is important to note that the weight percent of total organic carbon necessary to constitute an excellent, good, or poor source rock is not as well defined for fine-grained, medium- to dark-gray limestones and dolomites. Hunt (1979) points out that because of the amorphous nature of the organic matter derived from hydrogen-rich marine algae, dark-gray carbonates may have the potential to generate more hydrocarbons than shales with equivalent amounts of total organic matter. Thus, medium- to fine-grained, dark-gray to dull-brown limestones and dolomites with a total organic carbon content as low as 0.3 weight percent may have sufficient richness to be classified as source rocks (Hunt, 1967).

The definitions of the terms thermally immature and thermally mature are those established by Claypool and others (1977) and Miller and others (1979, 1980). If sedimentary rocks that contain an abundance of organic matter are subjected to thermal pyrolysis and are shown to be capable of generating petroleum hydrocarbons, and yet these organic-rich sedimentary rocks have not been altered by thermochemical petroleum-generating reactions to the degree that a minimum amount of petroleum has been generated and physically expelled, then the source rock is defined as "immature." A source rock is "mature" when thermochemical processes have converted the indigenous extractable hydrocarbons to a molecular composition and concentration that is identical to that of petroleum, and the extractable hydrocarbons are present in quantities of about 1 to 2 percent of the total organic carbon.

"Possible" or "potential" source rock refers to the degree of thermal maturity of the organic-rich rock. An immature organic-rich rock is defined as a "potential source rock," whereas a thermally mature organic-rich rock is designated a "possible source rock" (Claypool and others, 1977; Miller and others, 1979, 1980).

ANALYTICAL METHODS AND PROCEDURES

The USGS analyzed 23 well-cutting samples from the COST No. G-1 well from 1,090 to 16,070 ft (332 to 4,898 m) and 26 well-cutting samples from the COST No. G-2 (1,190 to 21,540 ft; 363 to 6,565 m). The unwashed well cuttings were removed from their plastic storage bags, and the drilling mud was carefully removed from each rock chip by thoroughly washing each chip under running water on a Tyler 100-mesh (150-μm) screen. The washed rock chips were oven dried at 95° to 104° F (35° to 40° C). Each sample was examined under a binocular microscope, the lithology was described, and all of the foreign substances were removed, including string, plastic, rubber, and mica. The lithologic descriptions of the samples analyzed for the COST Nos. G-1 and G-2 wells are shown in tables 1 and 2, respectively. Only those rock chips larger than 10 to 20 mesh (2.0 to 0.85 mm) were used for the C_{15+} hydrocarbon analyses. Each sample was ground, using mortar and pestle, to smaller than 60 mesh (250 μm) and weighed. Aliquots of the ground sample were taken for total-organic-carbon determinations. Thermal pyrolysis analyses were determined on a separate set of washed and ground samples from depths of burial that were similar to those used for the extractable C_{15+} hydrocarbon studies.

The details of the solvent-extraction methods, liquid-column chromatography, and gas chromatography procedures employed for the C_{15+} liquid-hydrocarbon analyses have been described previously (Miller and others, 1979, 1980). The major steps involved are Soxhlet-solvent extraction in chloroform, followed by removal of sulfur by passing the sample over activated copper, then elution-column chromatography (gravimetrics) on silica gel. The saturated paraffin-naphthene fractions were analyzed both qualitatively and quantitatively on Perkin-Elmer Sigma 2-B and 3920 gas chromatographs, respectively. Both systems were supported by Sigma 10 data microprocessors. The qualitative gas chromatographic analyses were performed on 8 ft × 0.125 in. (2.4 m × 0.318 cm) stainless steel columns packed with 3 percent OV-101, 100- to 200-mesh (150- to 75-μm) GCQ. The column temperature was 176° F (80° C) at injection and was programmed to increase initially at a rate of 29° F/min (16° C/min) for 8 minutes and then at a rate of 14° F/min (8° C/min) to a final temperature of 572° F (300° C). Quantitative analyses were performed on an OV-1 50-ft (15-m) SCOT column. The column was held for one minute at an injection temperature of 212° F (100° C); it was then programmed to increase at 7° F/min (4° C/min) to a final temperature of 473° F (245° C) and held at the final temperature until $n\text{-}C_{32}$ eluted. The following expression, modified from Hunt (1974), was used to calculate the Carbon Preference Index (CPI):

$$CPI = \frac{\frac{(\%nC_{25} + \%nC_{27} + \%nC_{29} + \%nC_{31})}{(\%nC_{24} + \%nC_{26} + \%nC_{28} + \%nC_{30})} + \frac{(\%nC_{25} + \%nC_{27} + \%nC_{29} + \%nC_{31})}{(\%nC_{26} + \%nC_{28} + \%nC_{30} + \%nC_{32})}}{2}$$

Total organic carbon is a measure of the organic richness of a source rock. Triplicate total organic carbon analyses were performed by the USGS on dried, weighed aliquots of the carbonate-free residue produced by leaching with hot, 6-normal hydrochloric acid of approximately 0.07 oz avdp (0.2 g) of ground sample smaller than 60 mesh (250 μm). The samples were combusted in a Perkin-Elmer model 240 Carbon, Hydrogen, Nitrogen Analyzer. The organic carbon analyses for the thermal pyrolysis studies were performed by Rhinehart Laboratories, Arvada, Colo., on sample aliquots using the chromic oxidation method outlined by Bush (1970).

The thermal pyrolysis analyses performed in this study were carried out by the USGS on a Rock-Eval system following the basic principles of source-rock characterization of Espitalie and others (1977). The terms used to describe the thermal pyrolysis measurements are those of Claypool and Reed (1976), Claypool and others (1977), Tissot and Welte (1978), and Miller and others (1979, 1980). The free or indigenous hydrocarbon component (expressed as mg HC/gC (ppt)) already present in the rock and volatilized when the rock is heated at 481° F (250° C) for five minutes is the original generation potential of the source rock, S_1. Those hydrocarbons and related compounds generated by pyrolysis at temperatures from about 480° to 1,020° F (250° to 550° C) from the nonvolatile organic matter are referred to as the residual generation potential, expressed by

the term S_2. S_1 and S_2 are expressed in units of mgHC/gC (ppt). The sum ($S_1 + S_2$) is expressed on a weight percent basis and is a measure of the generation potential of the rock when expressed in kgHC/ton rock (Tissot and Welte, 1978). The carbon dioxide generated from the kerogen, S_3, was not determined for the kerogens in this study.

The ratio of pyrolytic hydrocarbon yield ($S_1 + S_2$) to percent total organic carbon is a measure of the thermal maturation of the organic matter. The maximum temperature at which the yield of volatile organic components is produced by pyrolysis of the solid organic matter (T_{S_2} °C) is also used as an indicator of thermal maturation (Tissot and Welte, 1978). The ratio S_2/Org. C is the hydrogen index, whereas S_3/Org. C (not determined) is a measure of the oxygen content of a kerogen (Tissot and Welte, 1978). Atomic (hydrogen/carbon) ratios, carbon isotopic compositions ($\delta^{13}C$ PDB), and classes of relative percent of kerogen are also used to evaluate the kerogen types.

RESULTS AND DISCUSSION

This study compares the source-rock potential of the sedimentary rocks in the Georges Bank COST wells No. 1 and No. 2. The interpretations of source-rock richness, maturity, and type based on the results of different geochemical techniques have been assessed and evaluated.

The amount and molecular composition of the solvent-extractable organic matter in shales is considered to be indicative of the quality (richness), degree of thermal maturation, and type of original organic matter, assuming that the extractable organic matter is indigenous to the sedimentary rocks (Tissot and Welte, 1978; Miller and others, 1979, 1980). Lithologic descriptions, extractable organic matter data, and paraffin-naphthene hydrocarbon gas chromatograms for the Georges Bank COST Nos. 1 and 2 wells are given in tables 1–4 and figures 39–51. Thermal pyrolysis-FID analyses of selected well cuttings for determination of the original genetic (S_1) and residual (S_2) source-rock potential were carried out on sample suites different from those used for the extractable-organic-matter analyses. The whole-rock thermal evolution (pyrolysis) data are reported in tables 5 and 6.

Geochemical analyses on different sample sets collected from the COST Nos. G–1 and G–2 wells were performed for the drilling participants by several commercial laboratories. These data have been summarized by Smith (1980) and Smith and Shaw (1980). Measurements of relative kerogen types and abundances (percent) and thermal alteration indices (TAI) determined by optical methods were made by GeoChem Laboratories, Inc., for both wells; vitrinite reflectance measurements were conducted by Superior Oil Company for the COST No. G–1 well and by Core Laboratories, Inc., for the G–2 well; hydrogen-carbon ratios were provided by Amoco Production Company for the COST No. G–1 and by Core Laboratories, Inc., for the COST No. G–2; stable carbon isotope ratios of the saturated paraffin-naphthene and aromatic hydrocarbons, as well as the total extractables and kerogens were determined by Phillips Petroleum Company for both COST wells (J. G. Erdman, written commun., 1978). The concentrations and distributions of the light hydrocarbons (C_1 to C_4) and gasoline-range hydrocarbons (C_5 to C_7) were determined by GeoChem Laboratories, Inc., for both wells. These data are shown in summary depth profiles in figures 53–56.

Drilling mud additives may influence the molecular composition and distribution of the C_{15+} saturated paraffin-naphthene hydrocarbons and as a consequence can affect interpretations of the maturity and type of the indigenous, extractable organic matter (K. F. Thompson, Atlantic Richfield, written commun., 1977; Miller and others, 1979, 1980). Mud additive effects are believed to be of particular importance in limestones that have less than 0.3 percent organic matter, especially if the organic matter is not all liptinitic (J. M. Hunt, written commun., 1981). Aliquots of the major mud additive components used in drilling the COST G–1 and G–2 wells were not made available to the USGS for direct comparative analysis. However, previously analyzed mud additives similar in type and composition to those used in drilling both wells were compared to make a first-order assessment of the possible influence such additives may have had on the distribution and composition of the extractable hydrocarbons (Miller and others, 1979, 1980). The cutting samples used in this study were thoroughly washed,

TABLE 1.—*Lithologic descriptions of COST No. G-1 well cuttings used for organic geochemical analyses*
[Lithologic descriptions by F. Adinolfi and D. Shaw]

Depth		Lithology
Feet	Meters	
1,090- 1,130	332- 344	95% coarse- to very coarse-grained quartz sand; 3% coarse, golden-brown feldspar fragments; 1% fossil fragments, mostly pelecypods; 1% coarse muscovite flakes, green chlorite, traces of medium- to fine-grained glauconite pellets, lignite, chert, igneous rock fragments, coarse-grained feldspathic sandstone, brown glauconitic siltstone, hematite, phosphate, mica schist, fine-grained quartz fragments and quartz pebbles, and aragonite.
2,080- 2,110	634- 643	80% white, very coarse- to coarse-grained quartz sand; 10% gray to buff quartz and feldspar gravel, subrounded to well rounded; 6% light-gray, sandy, silty, micaceous, and calcareous mudstone; 3% tan mud and claystone; 1% mica flakes, lignite, pyrite, clay, and fine-grained quartz sand and sandstone.
3,190- 3,220	972- 981	97% white to clear, very coarse- to medium-grained quartz sand with minor pebbles; 3% tan to brownish-red sandy mudstone; traces of lignite, chert, large feldspar fragments, pyrite, muscovite, hematite, and glauconite.
4,000- 4,030	1,219-1,228	95% coarse- to very coarse-grained quartz sand; 2% white to buff feldspar sand and gravel; 2% gray coarse-grained quartz sandstone with buff mud matrix; 1% tan, hard mudstone; traces of lignite, glauconite, calcite, pyrite, and very fine-grained silica-cemented quartz sandstone.
5,140- 5,170	1,567-1,576	96% white, coarse- to medium-grained quartz sand; 3% black to dark-gray lignite; 1% light-brown mudstone; traces of feldspar, hematite, muscovite, pyrite, calcareous siltstone, and peat.
5,940- 5,950	1,811-1,814	30% white medium- to very fine-grained calcite-cemented sandstone; 30% medium-gray, calcareous fissile shale; 25% hard tan mudstone with minor sandy mudstone; 5% medium- to fine- grained angular quartz fragments; 5% light-gray siltstone; 1% black to dark-gray lignite; traces of calcite, aragonite, pyrite, and muscovite.
7,020- 7,060	2,140-2,152	60% very coarse- to medium-grained sub-arkosic sand (15% feldspar); 10% red calcareous mudstone; 5% feldspar gravels; 5% white calcite-cemented sandstone; 5% red siltstone; 5% green siltstone; 4% quartz gravel; 3% medium-grained arkosic sandstone with red hematite cement; 3% light- to medium-gray, slightly calcareous siltstone; traces of calcite, chalk, black coal, and mica.
8,040- 8,080	2,451-2,463	45% very coarse- to medium-grained feldspathic sand; 30% reddish-brown sandstone; 10% red calcareous siltstone; 5% feldspar gravel; 4% quartz gravel; 2% white calcite-cemented, medium-grained quartz sandstone; 2% light-gray calcareous shale; 2% medium- to very fine-grained, green, purple, and red arkosic sandstone; traces of coal, calcite, and mica.
9,030- 9,070	2,752-2,765	35% reddish-brown mudstone; 30% medium- to dark-gray shale; 20% white, calcite-cemented sandstone; 5% brown siltstone; 5% light-brown, very fine-grained arkosic sandstone; 5% medium- to coarse-grained quartz sand; traces of coal, feldspar, buff mudstone, and mica.
9,540- 9,580	2,908-2,920	40% white, coarse- to fine-grained quartzarenite; 40% red to reddish-brown mudstone; 8% coarse- to medium-grained quartz sand having angular grains, generally white; 5% arkosic, red, very fine grained sandstone and siltstone; 5% gray siltstone; 2% coarse to very coarse feldspar fragments; traces of feldspar and quartz pebbles.
10,020-10,060	3,054-3,066	25% oolitic quartz sandstone (medium-gray oolites in a very fine-grained quartz sandstone matrix); 25% dark-brown to reddish-brown mudstone; 25% gray, soft, fissile, somewhat silty shale; 10% slightly oolitic quartzarenite, oolitic sandstone, sandy oolite, and oolitic limestone; 10% white, calcite-cemented, very fine-grained sandstone; 5% brown dolomitic limestone; traces of coal, mica, medium- to fine-grained quartz fragments and feldspar pebbles.
10,440-10,480	3,182-3,194	40% buff limestone with micritic matrix; 20% medium-gray shale; 10% oolitic limestone; 10% brownish-gray, slightly dolomitic limestone; 10% light-gray calcareous shale; 5% white, medium- to fine-grained, calcite-cemented sandstone (quartzarenite); 2% white to tan, slightly calcareous anhydrite; 1% brownish-red mudstone; 1% red shale; 1% brown, arkosic, medium-grained sandstone; traces of sandy anhydrite, quartz grains, pyrite, and green shale.
10,950-10,970	3,338-3,344	38% buff to white anhydritic sandstone, very fine-grained to fine-grained; 30% greenish-gray to medium-gray fissile shale; 10% brown to buff limestone; 10% light to reddish-brown shale; 5% white to buff anhydrite; 5% buff siltstone and sandy anhydrite; 2% very fine-grained quartzarenite; traces of calcite, coarse quartz grains, and oolitic limestone.

TABLE 1.—*Lithologic descriptions of COST No. G-1 well cuttings used for organic geochemical analyses*—Continued
[Lithologic descriptions by F. Adinolfi and D. Shaw]

Depth		Lithology
Feet	Meters	
11,220–11,260	3,420–3,432	45% brown micritic limestone; 30% slightly siliceous, light- to medium-gray hard shale; 10% buff, slightly sandy siltstone; 5% white to buff, finely crystalline limestone; 5% reddish-brown shale; 2% green shale; 2% dark-gray laminated micaceous shale; 1% red siltstone and fine-grained white slightly micaceous sandstone with subangular to angular grains; traces of orange hematite staining, anhydrite, and coal.
11,850–11,890	3,612–3,624	40% medium- to very fine-grained, white to light-pink quartz sandstone; 20% medium- to dark-gray shale, somewhat fissile; 15% reddish-brown shale with minor silty shale; 10% medium-grained, tan arkosic sandstone, tightly cemented; 5% medium to coarse quartz fragments; 5% red and gray siltstone; 5% brown micritic limestone; traces of black coal, biotite, and white anhydrite.
12,360–12,400	3,767–3,780	25% white, pink, and light-gray, fine-grained feldspathic sandstone, silica-cemented; 18% red silty mudstone; 18% gray and buff dolomite, some coated with white anhydrite; 15% pink to white, transparent anhydrite, some sucrosic; 7% medium- to dark-gray, fissile and carbonaceous shale; 5% hard, red shale; 5% brown, micritic, dolomitic limestone; 5% white to buff sparry limestone; 2% red, micaceous siltstone; traces of coal, biotite, calcite, hematite, purple sandstone, green siltstone, and laminated gray siltstone.
12,960–13,000	3,950–3,962	55% anhydrite; 25% reddish-brown mudstone (coated with yellow anhydrite); 10% dark- to medium-gray, slightly carbonaceous shale (coated with anhydrite) and minor light-green shale; 10% medium- and light-gray dolomite; trace of very fine-grained sandstone.
13,530–13,570	4,124–4,136	40% light- to medium-gray and brown, micritic to vuggy dolomite, some porous; 17% anhydrite, some yellowish brown and microcrystalline, some white, sucrosic, and cryptocrystalline; 15% sandstone, some quartzitic (white with anhydrite and silica cement, very fine-grained to fine-grained); 10% medium- to dark-gray shale, 8% reddish-brown mudstone and minor muddy siltstone; 5% light-gray dolomite with clear anhydrite nodules; 3% white crystalline limestone with sparry calcite cement; 2% pelletal dolomite; traces of coal, pyrite, hematite, and large quartz grains.
14,040–14,080	4,279–4,292	30% light-gray to buff micritic dolomite; 20% tan, white, buff and light-gray anhydrite; 15% red mudstone; 10% buff to white anhydritic dolomite; 10% red micaceous siltstone; 10% dark-gray carbonaceous shale and medium-gray, slightly micaceous shale; 5% very fine-grained, pink and reddish-brown sandstone; traces of coal, and calcite.
14,550–14,590	4,435–4,446	35% red medium- to very fine-grained sandstone, some with anhydrite cement; 20% medium-hard, red shale, some with anhydrite streaks; 20% white, tan, pink, and buff anhydrite; 5% white anhydritic sandstone with red hematite cement; 5% large quartz fragments; 5% sandy anhydrite; 5% very fine- grained white and gray sandstone; 4% micaceous dark- and medium-gray shale; 1% angular feldspar fragments; traces of mica, and hematite.
15,040–15,080	4,584–4,596	35% white, coarse- to very coarse-grained quartz sandstone, some coated with red hematite; 25% white anhydrite coated with red hematite; 25% red, slightly micaceous mudstone; 8% red to tan dolomite; 5% very fine-grained to medium-grained red quartzitic sandstone; 2% light-gray to buff feldspar pebbles; traces of gray shale and hematite.
15,640–15,670	4,767–4,776	65% red, tan, white, and light-gray anhydrite, some sucrosic, some transparent, some slightly dolomitic; 23% tan, light-gray, and buff dolomite; 7% brownish-red mudstone; 5% angular, white, coarse quartz grains; traces of gray shale, coal, brown and green pebbly mudstone (green feldspar in brown clay matrix), light-green feldspar pebbles, fine-grained anhydrite, and light-green lithic sandstone.
16,030–16,070	4,886–4,898	69% dark-gray to black, schistose, slaty, shiny, micaceous shale; 12% red to brownish-red silty mudstone; 8% brown to light-gray, very fine-grained sandstone; 7% brown to brownish-gray micritic dolomite; 2% buff to light-gray anhydrite; 2% brown and buff siltstone; traces of angular quartz pebbles, microbreccia of green sanidine in red mud matrix, coal, and white calcareous mudstone.

sieved, and picked to eliminate the effects of mud additives, but very low levels of drilling mud contamination may have occurred in several intervals in the Jurassic section. Results for those intervals that are thought to be influenced by mud additives have been marked on table 4. Figure 39 is the saturated paraffin-naphthene hydrocarbon gas chromatogram of leonardite

TABLE 2.—*Lithologic descriptions of COST No. G-2 well cuttings used for organic geochemical analyses*
[Descriptions by F. Adinolfi and D. Shaw]

Depth		Lithology
Feet	Meters	
1,190–12,220	363– 372	90% buff to light-yellow calcareous mud, slightly micaceous, with about 1% limonitic siltstone; 9% white to buff mud; traces of hematite and calcite.
2,180– 2,210	664– 674	95% light-gray mud, slightly micaceous, moderately calcareous; 5% white mud; trace white calcite, angular to round quartz grains, glauconite, chert, and hematite.
3,020– 3,050	920– 930	90% grayish-brown calcareous mud; 4% fossil fragments; 5% white, rounded, coarse quartz grains; 1% drilling mud (buff); trace hematite, mica, calcite, coal, and possible pipe dope.
4,130– 4,160	1,259–1,268	90% gray, soft to firm, partly silty and sandy mudstone, contains spots of white, chalky limestone, abundant fossils, and shell fragments; 10% loose, very coarse quartz sand grains and tan, medium-grained, medium to well sorted sandstone with calcite cement and subangular glauconite.
6,070– 6,100	1,850–1,859	80% tan to tan-gray, argillaceous, firm (some hard) micrite limestone; 20% gray, partly fissile, calcareous, silty shale.
7,000– 7,030	2,134–2,143	70% medium-gray shaley limestone; 25% gray to buff limestone; 2% tan, silty mudstone, 1% quartz grains, 2% gray shale; trace pipe dope, drilling mud, threads, gastropod fragments, and mica.
7,990– 8,020	2,435–2,444	80% white, very fine-grained, calcite-cemented quartz sandstone; 14% medium-gray, slightly calcareous shale; 4% red mudstone; 1% muscovite flakes; 1% oolitic limestone (brown pellets in gray matrix); trace brown lignite, and asphalt.
9,010– 9,040	2,746–2,755	40% silty, reddish-brown, micaceous shale with streaks of yellow-brown and gray mottling; 25% micaceous quartz sandstone with detrital coal and calcite cement; 20% dark-brown, fissile, waxy, noncalcareous shale; 10% dark-gray, micaceous, noncalcareous shale; 2% light-pink to reddish sandstone and buff-white and brown pelletal limestone; 1% rounded coal grains; trace glauconite and foraminifers.
10,490–10,510	3,197–3,203	30% microcrystalline, tan to light-brownish-gray limestone; 20% oolitic, buff-white, tan, and dark-brown limestone; 30% gray, silty shale with detrital coal; 15% yellow-brown to dark-reddish-brown micaceous, silty, shale; 5% fine-grained, sub-rounded white to light reddish-brown sandstone, well-cemented with calcite cements and containing detrital coal; traces of coal and yellow mudstone.
11,500–11,510	3,505–3,508	90% microcrystalline, brown, gray, and buff-tan pelletal limestone; 8% dark-gray shale with traces of coal; 2% very fine-grained, green and white glauconitic quartzite sandstone.
12,520–12,540	3,816–3,822	75% microcrystalline, blocky, light grayish-brown and buff-white limestone; 15% white and grayish-brown pelletal limestone; 3–5% light-gray, slightly micaceous, noncalcareous shale with disseminated organic material; 2% very fine-grained, light- to dark-green, hard glauconitic sandstone; 3% silty, micaceous, reddish-brown shale; 2% fine-grained, calcite-cemented, glauconitic, light-green, clear, and white sandstone; trace quartz grains, coarse-grained pyrite, coal, and orange rust staining.
13,500–13,520	4,115–4,121	80% fine-grained to medium-grained, well-sorted, subrounded, pink to red, clear, and white sandstone containing quartz, feldspar, biotite, and glauconite; 15% gray to grayish-brown limestone; 3% dark-gray, fissile, carbonaceous shale; 2% silty, micaceous, reddish-brown shale; trace pelletal limestone, green, hard shale, and coal.
14,480–14,500	4,414–4,420	40% yellow-brown, translucent dolomite; 40% white, light-gray and grayish-brown limestone with larger grains than the dolomite; 20% conglomeratic, well-cemented rock fragments of grayish-brown limestone and dark-brown, medium-crystalline dolomite in a matrix of yellow-brown, clear, to white anhydrite and calcite cement; trace gray shale, reddish-brown silty shale, and coal.
15,490–15,510	4,721–4,727	45% light-gray, tan to brownish-gray micritic, partly dolomitized limestone; 45% brown-gray, dark-brownish-gray, and gray, very finely crystalline, partly argillaceous dolomite; 10% dark-reddish hard shale and coal.
15,900–15,920	4,846–4,852	40% buff micritic limestone; 29% medium-gray micrite limestone; 20% dark-gray, slightly shaley limestone; 9% sparry white limestone; 2% buff mudstone and gray-white mud; trace pyrite, red mudstone, and hematite staining.
16,450–16,470	5,014–5,020	40% light-gray to brownish-gray, partly pelletal, partly recrystallized micrite limestone; 30% soft, white, chalky, limestone with sugary texture; 30% dark gray, argillaceous, dolomitic limestone.
17,020–17,540	5,188–5,346	Composite.[1]

TABLE 2.—*Lithologic descriptions of COST No. G-2 well cuttings used for organic geochemical analyses*—Continued
[Descriptions by F. Adinolfi and D. Shaw]

Depth		Lithology
Feet	Meters	
17,020–17,040	5,188–5,194	70% buff to cream, loosely consolidated limestone, mostly sparry calcite, sugary textured; 25% medium- to dark-gray limey dolomite; 5% buff, crystalline, sparry limestone; trace tan mudstone, black bituminous limestone, and coal.
17,520–17,540	5,340–5,346	40% buff limestone, micritic; 30% medium-gray shaley limestone; 10% light-gray calcareous mudstone; 10% limey, dark dolomite, slightly shaley; 5% black, fibrous soft coal, most in fine fragments; 5% white, sparry limestone, sugary textured; traces of hematite and asphaltite.
17,470–17,520	5,325–5,340	60% tan, grayish-brown, and brown, micritic, blocky, dense, slightly dolomitic limestone; 10% white, chalky micrite limestone; 20% white, clear, coarsely crystalline anhydrite with layers of dark-brown dolomite; 10% dark-gray and black, carbonaceous, slightly calcareous shale; trace of a white, soft substance.
17,980–18,000	5,480–5,486	55% buff micritic limestone; 15% white sucrosic, crystalline, sparry limestone; 30% shaley, dark- to medium-gray micritic limestone; trace dolomite, coal, hematite, limonite, and oolitic limestone.
18,470–18,500	5,630–5,639	35% brownish-gray, micritic, sparry limestone; 35% buff sparry limestone, slightly anhydritic; 15% medium-gray micritic, argillaceous limestone; 12% dark-gray, shaley and calcareous dolomite; 3% buff anhydrite; trace coal, tan limonite, bituminous limestone, and oolitic limestone.
18,980–19,030	5,785–5,800	95% dark-gray to black bituminous limestone, micritic; 2% white to buff powdery anhydrite; 2% dark-gray calcareous sandstone containing fine-grained angular fragments; 1% medium- to light-gray limestone (micrite with sparry calcite cement).
19,500–19,530	5,944–5,953	65% brownish-gray to medium-gray micrite limestone with minor sparry calcite cement; 10% buff to light-gray anhydritic dolomite with sucrosic texture; 15% buff to white calcareous anhydrite, some chalky, some clear and microcrystalline; 10% dark-gray, micritic, bituminous limestone.
19,950–20,010	6,081–6,099	25% light-gray micritic dolomite; 25% brownish-gray micritic dolomite; 25% dark-gray shaley dolomite; 8% brown micritic limestone; 8% dark-gray dolomitic shale; 8% white and buff anhydrite, some powdery and cryptocrystalline, some sucrosic and microcrystalline; 1% brownish-gray calcareous dolomite; trace quartz grains and gypsum.
20,480–20,520	6,242–6,254	75% brownish-gray to medium-gray micritic limestone; 10% dark-gray, shaly bituminous limestone; 10% powdery white anhydrite; 5% light-gray, sucrosic, calcareous dolomite with sparry calcite cement; trace white microcrystalline anhydrite and quartz fragments.
20,970–21,030	6,392–6,410	50% brownish-gray to medium-gray anhydritic micrite dolomite with sucrosic dolomite rhombs; 10% buff to white, anhydritic, powdery, chalky limestone; 40% tan, light- to medium-brown clear, and white anhydrite with greasy luster; trace dark-gray shale, quartz sandstone, red mudstone, hematite, and calcite.
21,460–21,540	6,541–6,565	35% light brown to brownish-gray dolomite, micritic greasy texture; 20% dark- to medium-gray dolomitic shale; 20% buff to light-brown micritic limestone; 20% buff, tan, and white anhydrite; 5% light- to medium-gray anhydritic dolomite; trace coal, red mudstone, micaceous siltstone, and white sandstone.

[1]The 17,020- to 17,540-ft sample is a composite of two samples from 17,020–17,040 and 17,520–17,540 ft.

used in the commercial preparation of the mud additive lignosulfonate. Except for the specific intervals designated, the influence of this component on the saturated hydrocarbon fraction appears to be minimal because of the dissimilarity in the molecular distribution and concentration. The effects of drilling mud additives on the deeper stratigraphic samples are believed to be restricted to specific zones, because there is no constant, pervasive mud-additive fingerprint on the entire suite of C_{15+} extractable hydrocarbons. In USGS samples from the COST No. G-2 well, from 17,500 to 18,000 ft (5,330 to 5,480 m), traces of an asphalt-like substance were found. The gas chromatogram revealed only an unresolved envelope and had no resolved normal aliphatics. GeoChem Laboratories, Inc., observed a similar substance below 14,000 ft (4,267 m), and a gas chromatogram of their paraffin- naphthene fraction is shown in figure 39. This asphalt-like substance was not found in the matrix of the rock fragments but appeared to be coating only a part of the individual rock chips and thus acted as a cement to hold several rock fragments together.

TABLE 3.—*Organic carbon and extractable organic matter, COST No. G-1 well*

Depth		Organic carbon (percent)	Total hydrocarbon (ppm)	Ratio of total hydrocarbon to total organic carbon (percent)	Ratio of total hydrocarbon to extractable organic matter	Ratio of saturated hydrocarbon to aromatic hydrocarbon	Carbon Preference Index (CPI)
Feet	Meters						
Upper Cretaceous							
1,090- 1,130	332- 344	0.05	5.9	1.18	0.57	0.42	1.29
2,080- 2,110	634- 643	.12	9.2	0.76	.98	.65	1.10
Lower Cretaceous							
3,190- 3,220	972- 981	0.04	8.0	2.00	0.53	1.85	1.38
4,000- 4,030	1,219-1,228	0.12	6.6	0.55	0.38	1.39	1.69
5,140- 5,170	1,567-1,576	1.97	133.0	0.68	0.63	1.55	5.56
Upper Jurassic							
5,940- 5,950	1,811-1,814	2.70	110.7	0.41	0.31	0.52	2.55
7,020- 7,060	2,140-2,152	0.12	8.8	.73	.19	.98	2.59
8,040- 8,080	2,451-2,463	.21	70.9	3.37	.64	1.97	1.57
9,030- 9,070	2,752-2,765	.69	26.3	.38	.34	1.55	2.17
9,540- 9,580	2,908-2,920	.28	4.0	.14	.16	15.03	0.88
10,020-10,060	3,054-3,066	.37	10.2	.28	.19	1.79	1.54
Middle Jurassic							
10,440-10,480	3,182-3,194	0.30	19.1	0.63	0.69	1.58	0.94
10,950-10,970	3,338-3,344	.28	62.1	2.21	.77	1.92	1.22
11,220-11,260	3,420-3,432	.22	40.5	1.84	.65	2.50	1.11
11,850-11,890	3,612-3,624	.53	21.6	.40	.32	1.42	1.31
12,360-12,400	3,767-3,780	.18	25.21	1.40	.33	.86	1.42
12,960-13,000	3,950-3,962	.14	47.9	3.42	.61	3.21	1.16
13,530-13,570	4,124-4,136	.11	37.4	3.40	.69	1.36	1.20
Lower Jurassic							
14,040-14,080	4,279-4,292	0.18	12.3	0.68	0.29	1.16	1.02
14,550-14,590	4,435-4,447	.12	87.3	7.27	.59	4.21	.95
15,040-15,080	4,584-4,596	.02	16.3	8.15	.40	2.08	.68
Cambrian							
15,640-15,670	4,767-4,776	0.05	36.3	7.26	0.52	2.36	1.30
16,030-16,070	4,886-4,898	.23	40.9	1.77	.70	1.64	.91

The origin of this heavy hydrocarbon substance is unknown; it may be a well-cutting contaminant, but an indigenous source cannot be discounted.

COMPARISON AND EVALUATION OF SOURCE-ROCK RICHNESS AND OF THE TYPE AND MATURITY CHARACTERISTICS OF THE ORGANIC MATTER IN THE COST NOS. G-1 AND G-2 WELLS

TERTIARY

The thin Tertiary strata recovered in the G-1 and G-2 wells ranged in depth from 1,013 to 1,030 ft (309 to 314 m) and from 1,100 to 1,310 ft (335 to 399 m), respectively. The Tertiary sediments in G-1 consisted of unconsolidated, coarse- to very coarse-grained quartz sand with traces of glauconite, lignite, chert, mica schists, and phosphate. The G-2 Tertiary sediments are calcareous muds with subordinate limonitic siltstone. Because of the lack of available Tertiary cuttings, only one interval representing the Tertiary in the COST G-2 (1,190 to 1,220 ft; 363 to 372 m) underwent solvent extraction for determination of the total extractable hydrocarbons (153 ppm) and analysis for total organic carbon (0.95 percent by weight) (tables 3 and 4). The saturated paraffin-naphthene hydrocarbon gas chromatogram (fig. 43) shows an unresolved, bimodal complex mixture that is equal to or that predominates over the resolved aliphatics, a characteristic signature that suggests thermal immaturity.

UPPER CRETACEOUS

The Upper Cretaceous strata range from 1,030 to 2,680 ft (314 to 817 m) and 1,310 to 2,600 ft (399 to 792 m) in the COST Nos. G-1 and G-2 wells, respectively. The G-1 Upper Cretaceous

TABLE 4.—*Organic carbon and extractable organic matter, COST No. G-2 well*

Depth		Organic carbon (percent)	Total hydrocarbon (ppm)	Ratio of total hydrocarbon to total organic carbon (percent)	Ratio of total hydrocarbon to extractable organic matter	Ratio of saturated hydrocarbon to aromatic hydrocarbon	Carbon Preference Index (CPI)
Feet	Meters						
Tertiary							
1,190- 1,220	363- 372	0.95	153.1	16.61	0.51	4.01	1.75
Upper Cretaceous							
2,180- 2,210	664- 674	1.06	74.0	0.69	0.34	2.94	2.36
Lower Cretaceous							
3,020- 3,050	920- 930	1.06	162.7	1.53	0.69	4.10	2.17
4,130- 4,160	1,259-1,268	0.42	42.9	1.02	0.42	2.09	1.79
Upper Jurassic							
6,070- 6,100	1,850-1,859	0.55	154.3	2.80	0.54	4.35	1.73
7,000- 7,030	2,134-2,143	0.86	74.5	.87	.58	1.73	1.23
7,990- 8,020	2,435-2,444	.66	60.2	.91	.43	2.73	1.32
9,010- 9,040	2,746-2,755	.72	344.7	4.65	.67	2.91	1.76
10,490-10,510	3,197-3,203	.62	186.8	3.01	.83	3.44	1.44
11,500-11,510	3,505-3,508	.31	109.4	3.51	.55	2.29	1.81
Middle Jurassic							
[1]12,520-12,540	3,816-3,822	0.33	74.6	2.27	0.58	1.71	1.44
13,500-13,520	4,115-4,121	.05	31.5	6.30	.58	1.84	1.27
14,480-14,500	4,414-4,420	.19	225.6	11.89	.43	3.52	1.07
[1]15,490-15,510	4,721-4,727	.29	792.3	27.31	.44	2.18	1.41
15,900-15,920	4,846-4,852	.14	65.2	4.65	.68	2.01	1.13
[1]16,450-16,470	5,014-5,020	.15	363.8	24.26	.51	3.92	2.26
[2]17,020-17,540	5,188-5,346	.24	179.0	7.45	.50	2.07	1.38
17,470-17,520	5,325-5,340	0.14	131.9	9.42	0.41	3.07	1.15
[1]17,980-18,000	5,480-5,486	.17	93.9	5.52	.42	2.67	1.53
18,470-18,500	5,630-5,639	.12	32.0	2.66	.47	1.91	1.07
18,980-19,030	5,785-5,800	0.29	117.9	4.06	0.62	1.85	1.14
19,500-19,530	5,944-5,953	.18	125.4	6.96	.52	1.67	1.01
19,950-20,010	6,081-6,099	.15	75.8	5.05	.80	2.07	1.02
20,480-20,520	6,242-6,254	.10	42.0	4.20	1.41	1.58	1.77
[1]20,970-21,030	6,392-6,410	.18	152.4	8.46	.52	1.26	.75
21,460-21,540	6,541-6,565	.42	210.0	5.00	.42	1.58	1.01

[1]Possible mud additive contamination.
[2]17,020-17,540 is a composite interval of 17,020-17,040 and 17,520-17,540.

strata are characterized by calcareous shales, coarse quartz sands, and gray sticky shales that contain trace amounts of glauconite, biotite, pyrite, lignite, feldspar, and calcite. In comparison, the Upper Cretaceous rocks of the G-2 well are represented by light-gray calcareous shales, claystones, and chalky limestones with varying quantities of glauconite, fossil fragments, plant fragments, ostracods, foraminifers, mica, and pyrite (Lachance, 1980; Simonis, 1980).

The Upper Cretaceous strata of the COST No. G-1 well contain significantly less total organic carbon than the Upper Cretaceous calcareous shales and fine to medium sands present in G-2. The total extractable hydrocarbons in the Upper Cretaceous of the G-1 are very low, averaging 8.0 ppm, whereas the single Upper Cretaceous sample analyzed from G-2 contains 74.0 ppm of total extractable hydrocarbons. The nitrogen, sulfur, and oxygen contents of the Upper Cretaceous interval in the COST No. G-1 well are about five times greater than in the Upper Cretaceous of the COST No. G-2 well (tables 1-4, figs. 40 and 41).

The gas chromatograms of the saturated paraffin-naphthene hydrocarbons of the Upper Cretaceous from the two wells are shown in figures 42 and 43. The resolved alkanes in the Upper Cretaceous strata from the G-1 (1,090-1,130 and 2,080-2,110 ft; 332-344 and 634-643 m) have a molecular composition and boiling-point range that extends from about n-C_{15} to n-C_{32} and a CPI ratio that averages 1.20. The resolved aliphatic components are dominated by a broad, bimodal,

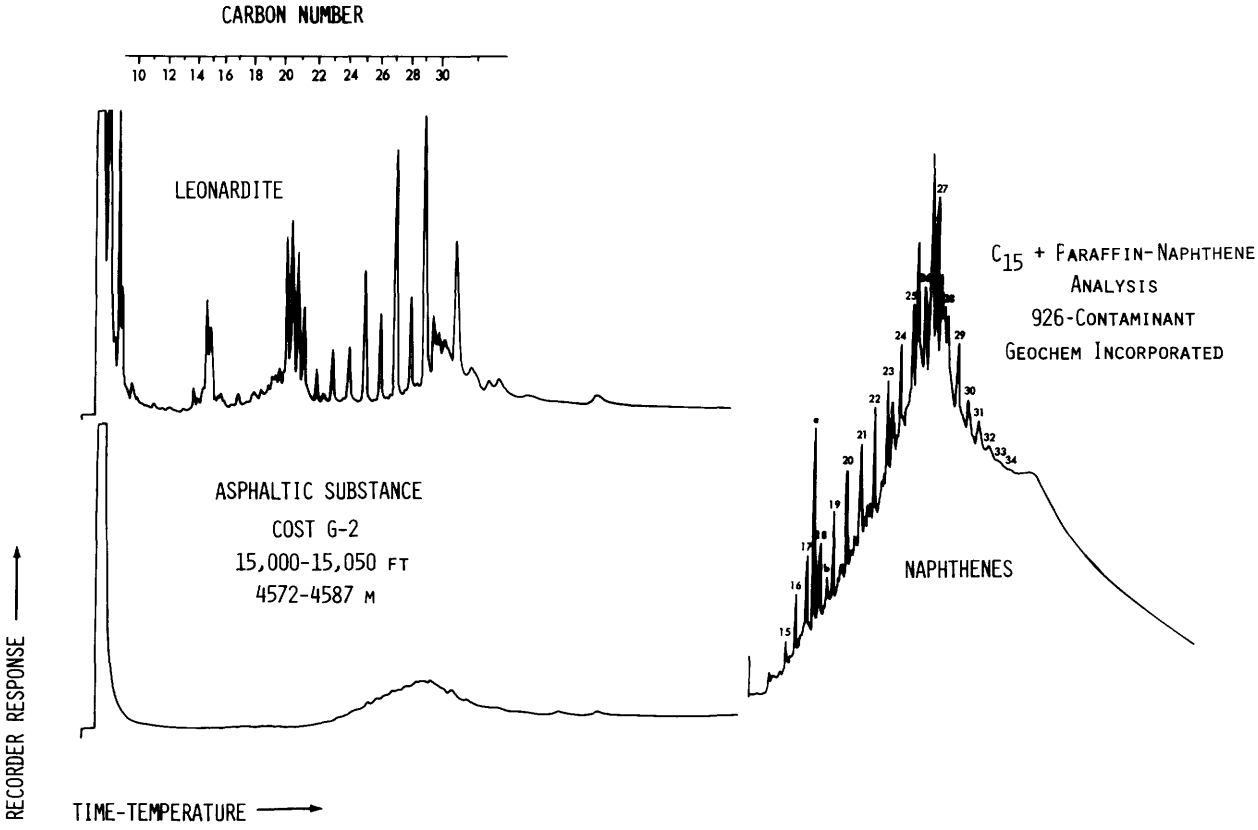

FIGURE 39.—Gas chromatographic analyses of (upper left) saturated paraffin-naphthene hydrocarbons in lignosulfonate (leonardite), (lower left) an asphalt-like substance isolated from the 15,000- to 15,050-ft (4,572- to 4,587-m) interval of the COST No. G-2 well by the USGS, and (at right) a solid black hydrocarbon substance isolated by GeoChem Laboratories, Inc., from the COST No. G-2 well at about 14,000 ft (4,267 m).

unresolved complex mixture. In contrast, the extractable paraffin-naphthene hydrocarbons from the Upper Cretaceous rocks of G-2 (2,180-2,210 ft; 664-674 m) are characterized by highly resolved alkanes that range from n-C_{15} to n-C_{28} and dominate over the much less pronounced bimodal, unresolved complex mixture. The predominant normal aliphatic species occur in the n-C_{15} to n-C_20 range and have a CPI ratio of 2.36 (tables 3 and 4; figs. 42 and 43). The narrow range of the resolved alkanes (n-C_{15} to n-C_20) is consistent with a thermally mature hydrocarbon assemblage and is similar to molecular distribution of diesel fuel. The pristane and phytane isoprenoid hydrocarbons are dominated by the resolved normal alkanes, a signature that is usually associated with mature saturated hydrocarbons. However, the shallow burial depth and the thermal-pyrolysis maximum yield temperatures that range from 837° to 860° F (447° to 460° C) (tables 3-6) are inconsistent with the extractable hydrocarbon chemical maturity signatures. The degree of convertibility of the sedimentary organic matter to petroleum hydrocarbons may be expressed by the ratio of the total pyrolytic hydrocarbons ($S_1 + S_2$) to total organic carbon (Claypool and others, 1977; Miller and others, 1979, 1980). This convertibility ratio for the Upper Cretaceous strata averages 8.9 percent for G-1 and 7.6 percent for G-2. Such values imply a strong influence of hydrogen-poor kerogens. The thermal pyrolytic measurements and geochemical source-rock parameters indicate that the organic matter in the Upper Cretaceous strata is thermally immature and would be a poor source for liquid petroleum hydrocarbons in both wells of the Georges Bank basin.

LOWER CRETACEOUS

The Lower Cretaceous strata in the COST Nos. G-1 and G-2 wells range from 2,680 to 5,290 ft

(817 to 1,612 m) and from 2,600 to 5,960 ft (792 to 1,817 m), respectively. Alternating units of glauconitic, unfossiliferous sandstones and shales containing trace amounts of coal, pyrite, and plant fragments (with small amounts of silty dolomite near the base of the interval) characterize the Lower Cretaceous of the G-1. In contrast, the Albian sandstones of G-2 (2,500 to 3,950 ft; 762 to 1,204 m) contain glauconitic pellets and shell fragments, plant debris, thin coal streaks, and carbonaceous dark-gray shales. Underlying these units is a bioclastic limestone intercalated with argillaceous micrites, calcareous claystones, and silty mudstones (3,950 to 4,500 ft; 1,204 to 1,372 m). From 4,500 ft to 5,320 ft (1,372 m to 1,622 m) are thickly bedded, poorly consolidated sandstones with thin beds of coal and lignitic shales (tables 1 and 2) (Lachance, 1980; Simonis, 1980).

Based on the combustion oxidation method, the Lower Cretaceous strata of the G-1 well contain very low amounts of total organic carbon: 0.04 weight percent between 3,190 and 3,220 ft (972 and 981 m), and 0.12 weight percent between 4,000 and 4,030 ft (1,219 and 1,228 m). The exception is the interval from 5,140 to 5,170 ft (1,567 to 1,576 m), which contains 1.97 weight percent total organic carbon. In comparison, the Lower Cretaceous strata from the COST No. G-2 well contain total organic carbon ranging from 0.42 to 1.06 weight percent (tables 3 and 4). The total extractable hydrocarbon content for the Lower Cretaceous in the G-1 and G-2 averages 49 and 103 ppm, respectively. The total organic carbon and total extractable hydrocarbon values indicate that the Lower Cretaceous strata of the Georges Bank basin have comparatively low source-rock quality and richness. The average total hydrocarbon to total organic carbon values are 1.07 percent for G-1 and 1.3 percent for G-2; total hydrocarbon to extractable organic matter ratios average 0.51 and 0.56 for G-1 and G-2 respectively; and saturated paraffin-naphthene to aromatic hydrocarbon ratios average 1.60 and 3.10, respectively, for the Lower Cretaceous of G-1 and G-2 (tables 3 and 4). The saturated paraffin-naphthene to aromatic hydrocarbon ratio is unusually high, but may reflect the thermal history of the rocks as well as the type and amount of the organic matter and the preferential destruction of aromatic hydrocarbons (Baker, 1972; Baker and Claypool, 1970; Louis and Tissot, 1967). The low hydrocarbon to total organic carbon and total hydrocarbon to extractable organic matter ratios, and the average CPI values of 2.88 for the G-1 and 1.98 for the G-2 well suggest that the organic matter in the Lower Cretaceous strata is thermally immature with regard to liquid hydrocarbon generation (tables 3 and 4).

The saturated paraffin-naphthene hydrocarbon gas chromatograms for the Lower Cretaceous from the No. COST G-1 well are characterized by a moderately strong bimodal, unresolved complex mixture (fig. 42). The resolved aliphatic hydrocarbons have a molecular composition and distribution that ranges from $n\text{-}C_{15}$ to $n\text{-}C_{30}$. With the exception of those in the 4,000- to 4,030-ft (1,219- to 1,228-m) interval, the resolved normal alkanes are equal to or dominant over the unresolved branched and cyclic paraffin envelope. The resolved aliphatics also show significant concentrations of the $n\text{-}C_{22}$ to $n\text{-}C_{30}$ plant-wax hydrocarbons probably associated with terrestrially derived organic matter. In comparison, saturated paraffin-naphthene hydrocarbon gas chromatograms for Lower Cretaceous strata from the COST No. G-2 well show a well resolved, strong predominance of the normal aliphatics over the unimodal unresolved complex envelope (fig. 43). The narrow range of molecular composition and distribution of the normal alkanes ($n\text{-}C_{15}$ to $n\text{-}C_{22}$) in these Lower Cretaceous strata tend to resemble those of thermally mature hydrocarbon assemblages, whose presence may also be indicated by the predominance of the normal alkanes over the isoprenoid hydrocarbons pristane and phytane. Inconsistent with an interpretation of maturity, however, is the odd-carbon predominance indicated by an average CPI ratio of 1.98, which suggests thermal immaturity (table 4). However, because of the restricted range of the resolved normal alkanes the CPI ratio of 1.98 is considered to be of limited use as an indicator of thermal maturity (Swetland and others, 1978; Miller and others, 1979, 1980; figs. 42 and 43; tables 3 and 4). Although the influence of diesel fuel cannot be totally disregarded, the narrow molecular range and distribution of the resolved aliphatics probably reflects a marine algal source of the aliphatics (Hunt, 1979).

The thermal pyrolysis convertibility parameter (S_1+S_2)/Org. C of the Lower Cretaceous rocks

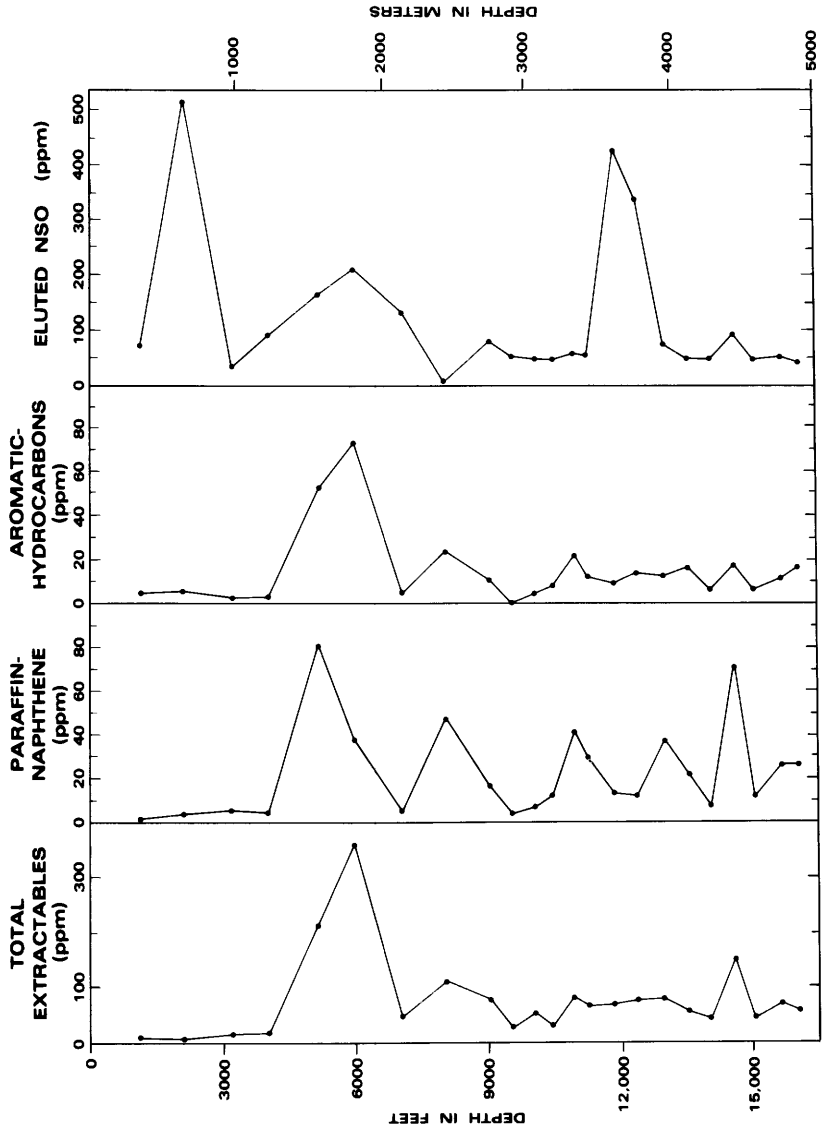
DEPTH IN METERS
1000
2000
3000
4000
5000
ELUTED NSO (ppm)
0
100
200
300
400
500
AROMATIC-HYDROCARBONS (ppm)
0
20
40
60
80
PARAFFIN-NAPHTHENE (ppm)
0
20
40
60
80
TOTAL EXTRACTABLES (ppm)
0
100
300
0
3000
6000
9000
12,000
15,000
DEPTH IN FEET

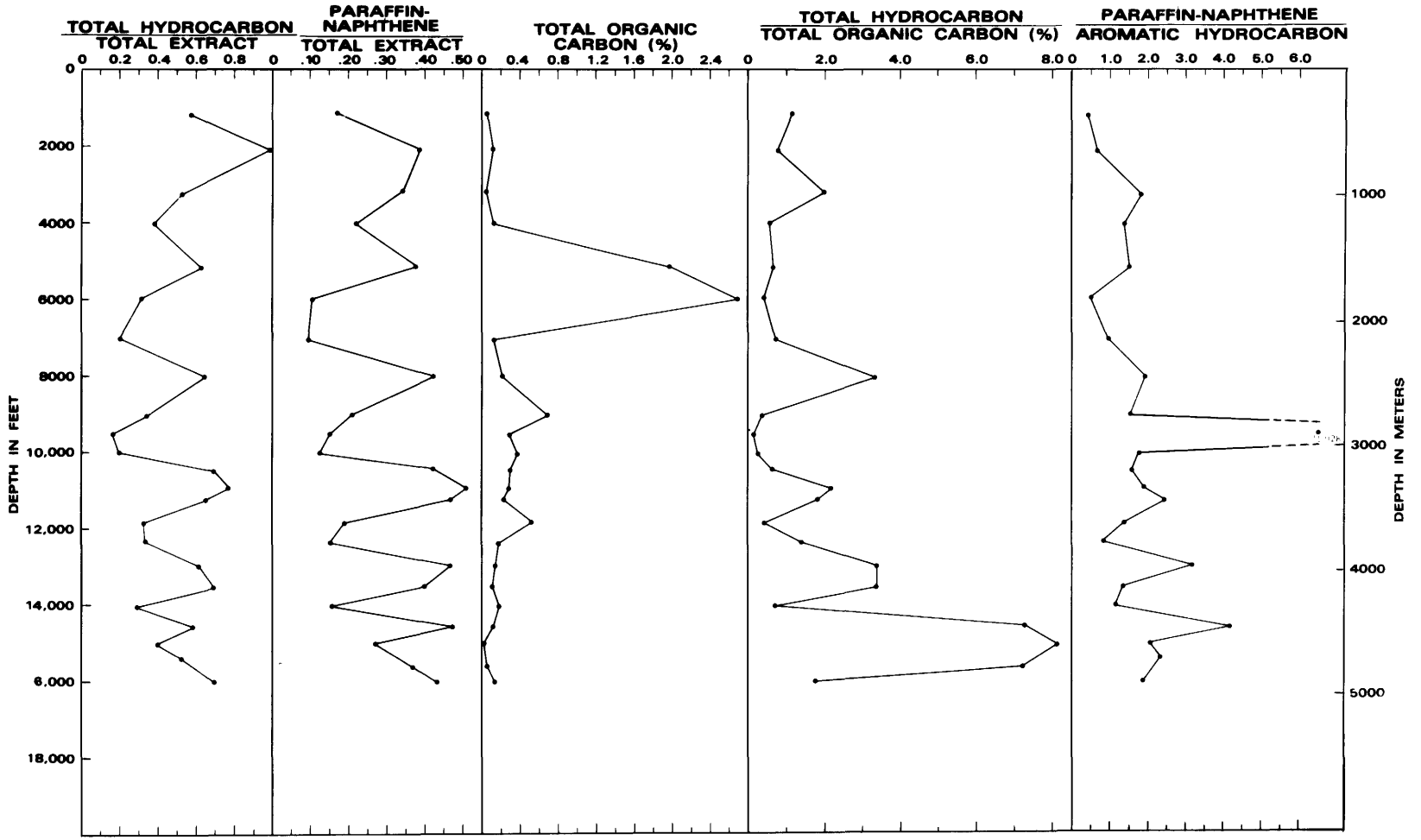

FIGURE 40.—Summary of organic-richness analyses on C_{15+} hydrocarbon extractables of samples from the COST No. G-1 well.

TOTAL EXTRACTABLES (ppm)
0 200 800 1200 1600
PARAFFIN-NAPHTHENE (ppm)
0 200 400 600
AROMATIC-HYDROCARBONS (ppm)
0 80 160 240 320
ELUTED NSO (ppm)
0 200 400 600 800
DEPTH IN FEET
0
3000
6000
9000
12,000
15,000
18,000
21,000
DEPTH IN METERS
1000
2000
3000
4000
5000
6000

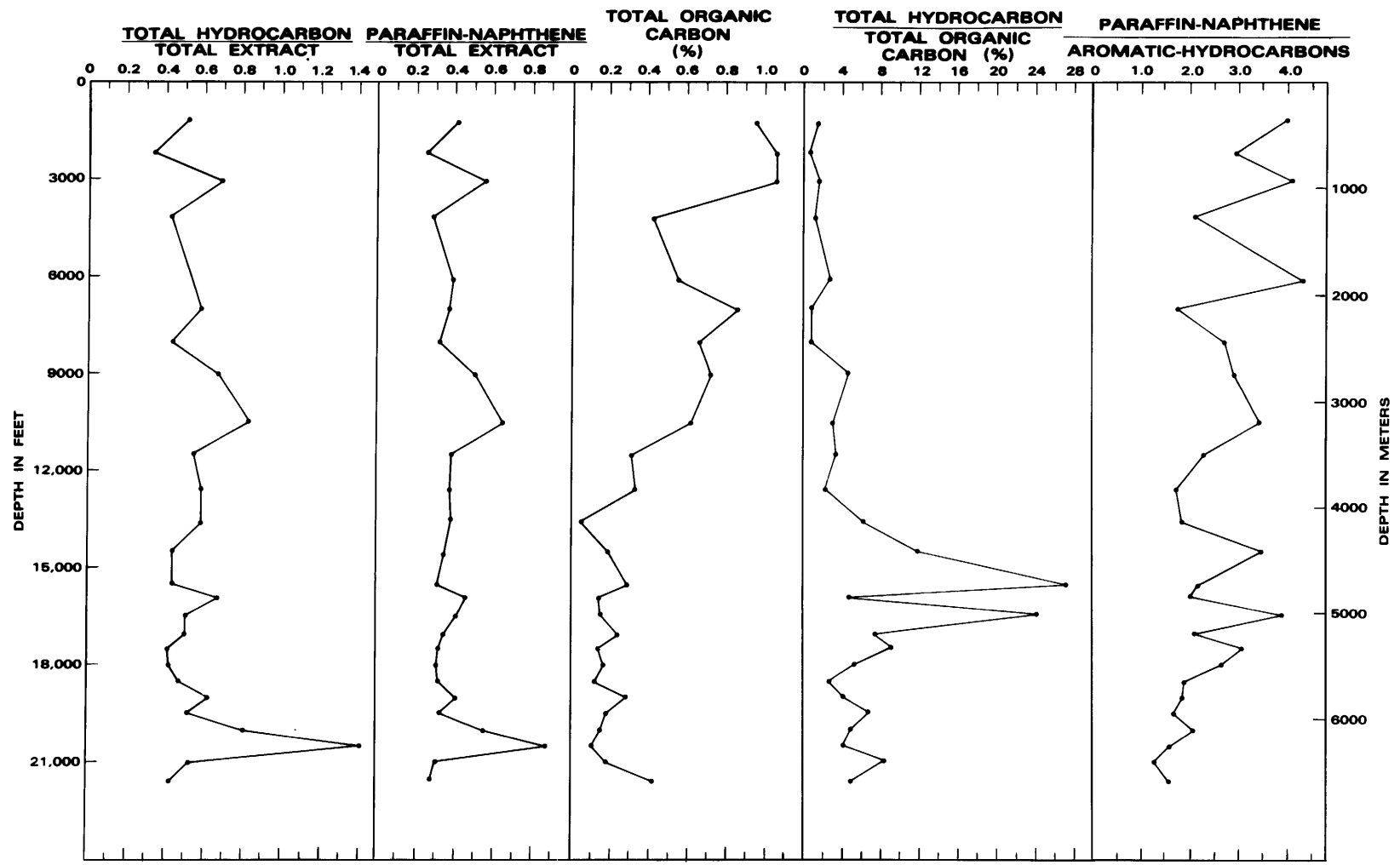

FIGURE 41.—Summary of organic-richness analyses on C_{15+} hydrocarbon extractables of samples from the COST No. G-2 well.

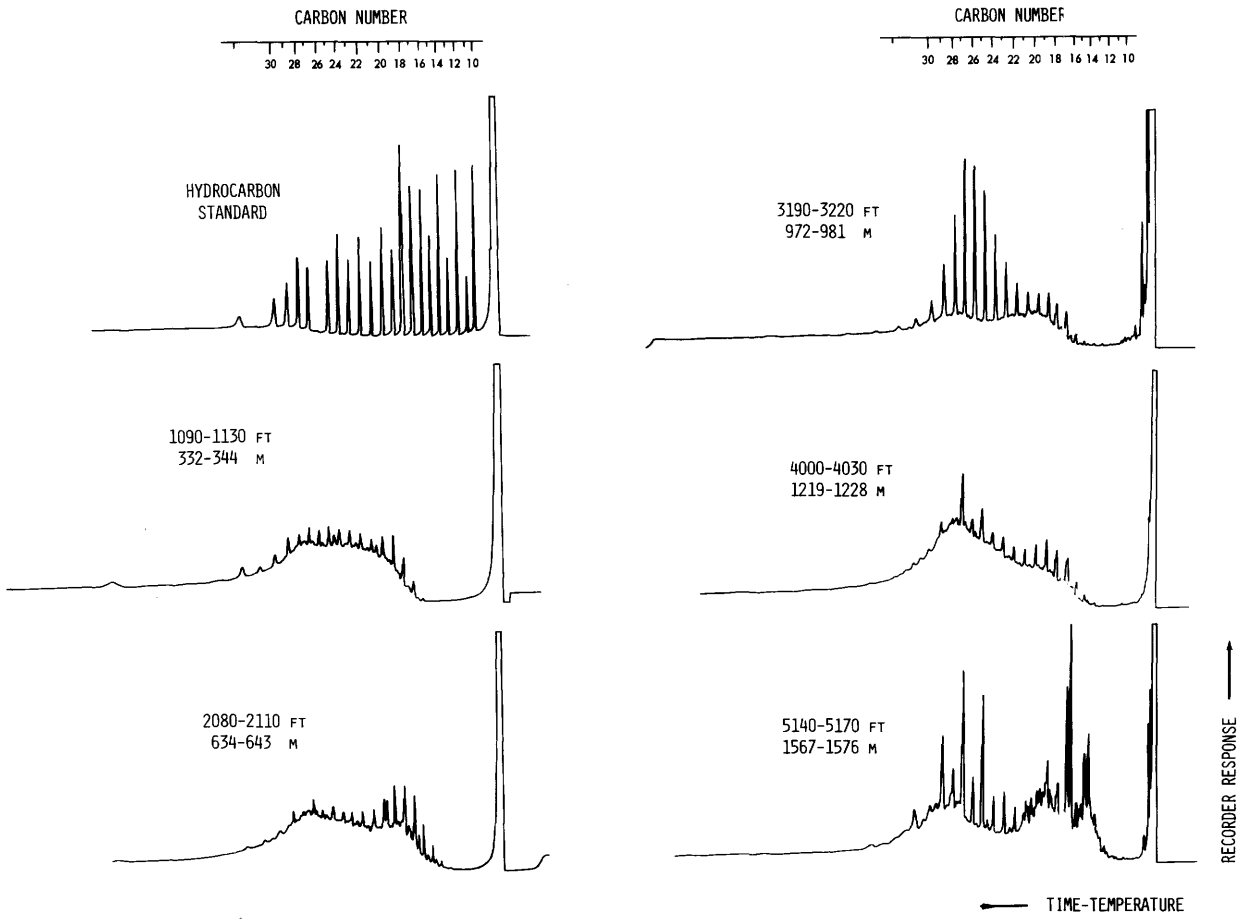

FIGURE 42.—Gas chromatographic analyses of saturated paraffin-naphthene hydrocarbons of Upper to Lower Cretaceous rock above 5,290 ft (1,612 m), COST No. G-1 well.

from the COST No. G-1 well averages 11.7 percent, indicating that the most common type of kerogens present are predominantly of the hydrogen-poor variety, with a temperature of maximum pyrolysis (T_{S_2}) ranging from 828° to 878° F (442° to 470° C). In comparison, the Lower Cretaceous rocks of the COST No. G-2 well have thermal pyrolytic convertibility ratios that average 7.4 percent. From 4,510 to 4,600 ft (1,375 to 1,402 m) and 5,050 to 5,080 ft (1,539 to 1,548 m) the convertibility ratios average 90.5 percent, suggesting the presence of a zone of hydrogen-rich kerogens. The temperature of maximum pyrolysis (T_{S_2}) for the solid organic matter ranges from 851° to 869° F (455° to 465° C) and is in the submature to immature temperature range (tables 5 and 6). The richness, type, and maturity characteristics of the extractable organic matter and the thermal pyrolysis measurements of the solid organic matter suggest that the potential for generation of liquid or gaseous hydrocarbons in the Lower Cretaceous strata is very poor.

UPPER JURASSIC

The Upper Jurassic stata of the COST No. G-1 well are characterized by alternating very fine- to coarse-grained sandstone, slightly calcareous shales with thin beds of silty dolomite, traces of coal, pyrite, muscovite, shell fragments, and rare glauconite. The carbonate content of the Upper Jurassic section increases towards the Upper-Middle Jurassic boundary. The Upper Jurassic lithologies of the COST No. G-2 well are, in general, similar to those of the G-1. The G-2, however, contains a larger percentage of brown oolitic and algal carbonate rocks from 6,000 to

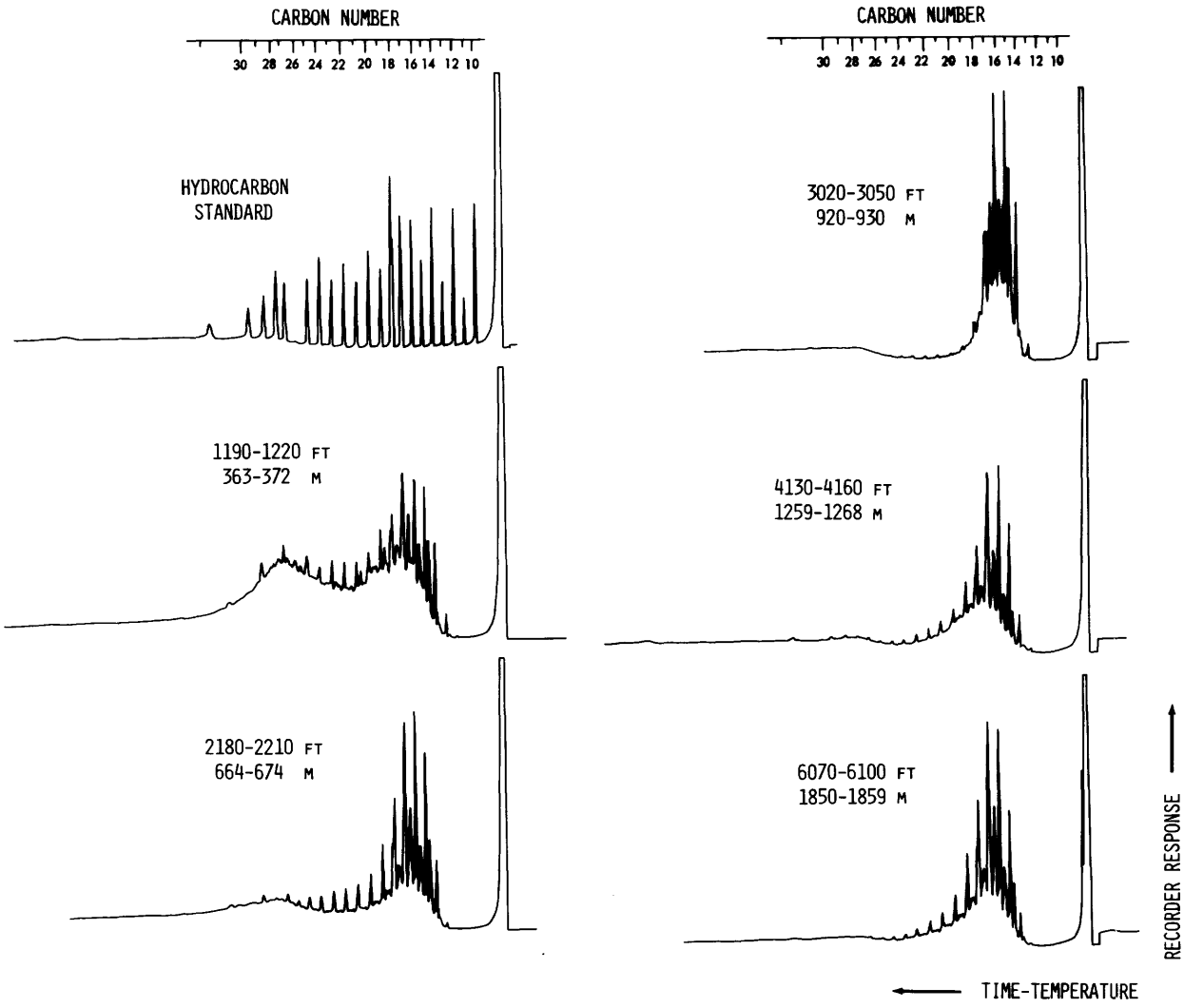

FIGURE 43.—Gas chromatographic analyses of saturated paraffin-naphthene hydrocarbons of Tertiary (1,190 to 1,220 ft; 363 to 372 m), Upper Cretaceous (2,180 to 2,210 ft; 664 to 674 m), Lower Cretaceous (3,020 to 4,160 ft; 920 to 1,268 m), and Upper Jurassic (6,070 to 6,100 ft; 1,850 to 1,859 m) samples, COST No. G-2 well.

7,000 ft (1,829 to 2,134 m) (tables 1 and 2) (Lachance, 1980; Simonis, 1980).

The Upper Jurassic strata in the two wells have similar average total organic carbon values of 0.73 percent (G-1) and 0.62 percent (G-2). The average hydrocarbon to total organic carbon ratios of 0.88 percent (G-1) and 2.62 percent (G-2) suggest that the extractable organic matter of the Upper Jurassic units is approaching thermal maturity in the G-2. However, because of the effect that small absolute concentrations may have on a specific geochemical ratio, the interpretation of maturity must be viewed with caution (Claypool and others, 1978; Swetland and others, 1978; Miller and others, 1979, 1980). The Upper Jurassic rocks of the COST No. G-2 well have an average total extractable hydrocarbon content of 155 ppm and a total hydrocarbon to extractable organic matter ratio of 0.60. These values are higher than those for equivalent COST No. G-1 well strata, which average 39.0 ppm total extractable hydrocarbons and 0.31 total hydrocarbon to extractable organic matter (tables 3 and 4). The polar nitrogen, sulfur, and oxygen concentrations range from 10 to 200 ppm for Upper Jurassic units in the COST No. G-1 well and are usually less than 150 ppm in the COST No. G-2 well. Although G-2 contains more

TABLE 5.—*Organic carbon and thermal analysis (Rock-Eval pyrolysis) data for samples from the COST No. G-1 well*

[Organic carbon analyses, wet oxidation method by Rhinehart Laboratories, Inc., Arvada, Colo. Rock-Eval pyrolysis by Jeff Baysinger, U.S. Geological Survey. The parameter S_3 (CO_2 derived from kerogen) was not determined in this study]

Depth		Total organic carbon (weight percent)	S_1 (mgHC/g) (ppt)	S_2 (mgHC/g) (ppt)	S_1+S_2 (weight percent)	S_2/Org. C $\left(\frac{\text{mgHC}}{\text{g Org. C}}\right)$	T_{S_2} (°C)	$\frac{S_1}{S_1+S_2}$	$\frac{S_1+S_2}{\text{Org. C}}$ (percent)
Feet	Meters								
Upper Cretaceous									
1,090- 1,120	332- 341	0.10	0.045	0.11	0.016	110	470	0.29	15.5
2,080- 2,110	634- 643	.88	.014	.41	.042	46	450	.03	4.8
2,350- 2,380	716- 725	.59	.012	.36	.037	61	452	.03	6.3
Lower Cretaceous									
2,920- 2,950	890- 899	0.34	0.019	0.16	0.018	47	442	0.11	5.3
3,280- 3,310	1,000-1,009	.10	.044	.15	.019	150	447	.23	19.4
4,180- 4,210	1,274-1,283	.12	.013	.07	.008	58	455	.16	6.9
4,870- 4,900	1,484-1,494	4.22	.066	4.40	.447	104	452	.01	10.6
5,140- 5,170	1,567-1,576	2.18	.056	2.97	.303	136	470	.02	13.9
5,050- 5,080	1,539-1,548	4.66	.057	6.54	.660	140	455	.01	14.2
Upper Jurassic									
6,030- 6,040	1,838-1,841	1.45	0.015	0.89	0.091	61	457	0.02	6.2
6,210- 6,220	1,893-1,896	.39	.012	.20	.021	51	460	.06	5.4
6,960- 6,970	2,121-2,124	.28	.008	.14	.016	50	458	.05	5.3
7,050- 7,060	2,149-2,152	.20	.012	.08	.009	40	452	.13	4.6
7,140- 7,150	2,176-2,179	.32	.023	.12	.014	38	456	.16	4.5
7,650- 7,660	2,332-2,335	.38	.008	.09	.010	24	464	.08	2.6
7,740- 7,750	2,359-2,362	.26	.015	.09	.011	35	442	.14	4.0
8,550- 8,560	2,606-2,609	.26	.013	.07	.008	27	462	.16	3.2
9,540- 9,550	2,908-2,911	.18	.011	.05	.006	28	465	.18	3.4
Middle Jurassic									
10,530-10,540	3,210-3,213	0.33	0.015	0.19	0.021	58	460	0.07	6.2
11,250-11,260	3,429-3,432	.24	.016	.12	.014	50	462	.12	5.7
11,850-11,860	3,612-3,615	.62	.018	.31	.033	50	485	.05	5.3
12,210-12,220	3,722-3,725	.26	.021	.14	.016	54	456	.13	6.2
12,480-12,490	3,804-3,807	.23	.026	.12	.015	52	[1](375)	.18	6.4
12,790-12,800	3,898-3,901	.17	.020	.09	.011	53	468	.18	6.5
12,960-12,970	3,950-3,953	.18	.018	.12	.014	67	[1](392)	.13	7.7
13,020-13,030	3,968-3,972	.17	.016	.07	.009	41	460	.19	5.1
13,440-13,450	4,097-4,100	.18	.021	.08	.010	44	460	.21	5.6
Lower Jurassic									
14,040-14,050	4,279-4,282	0.32	0.026	0.16	0.019	50	[1](400)	0.14	5.8
14,340-14,350	4,371-4,374	.21	.030	.16	.019	76	450	.16	9.1
15,040-15,050	4,584-4,587	.19	.040	.15	.019	79	460	.21	10.0
15,100-15,110	4,602-4,606	.17	.032	.13	.016	77	[1](379)	.20	9.5
Cambrian									
15,640-15,650	4,767-4,770	0.21	0.26	0.10	0.013	48	450	0.21	6.0
16,010-16,020	4,880-4,883	.31	.32	.09	.012	29	[1](380)	.26	3.9

[1]No definite pyrolysis peak.

organic-rich sediment than G-1, the organic-richness properties of total organic carbon and total extractable hydrocarbons suggest that the Upper Jurassic rocks of the Georges Bank basin area have very poor source-rock quality (tables 3 and 4; figs. 40 and 41).

The saturated paraffin-naphthene hydrocarbon gas chromatograms for the Upper Jurassic rocks in the COST No. G-1 well, with the exception of the 9,030- to 9,070-ft (2,752- to 2,765-m) interval, show a strong unresolved bimodal envelope of branched and cyclic paraffins. The resolved aliphatics range from n-C_{15} to n-C_{30} and have an average CPI of 1.88. The isoprenoid pristane continues to predominate over both the isoprenoid phytane and n-C_{17}. There is no consistent change in the molecular composition and distribution of the resolved aliphatics or in the character of the unresolved complex envelope with increasing depth of burial in the Upper Jurassic strata of the COST No. G-1 well (fig. 44). In comparison, the resolved aliphatics of the Upper Jurassic strata from the COST No. G-2 well continue to dominate the unresolved envelope and are character-

TABLE 6.—*Organic carbon and thermal analysis (Rock-Eval pyrolysis) data for samples from the COST No. G-2 well*

[Organic carbon analyses, wet oxidation method by Rhinehart Laboratories, Inc., Arvada, Colo. Rock-Eval pyrolysis by Jeff Baysinger, U.S. Geological Survey. The parameter S_3 (CO_2 derived from kerogen) was not determined in this study]

Depth (Feet)	Depth (Meters)	Total organic carbon (weight percent	S_1 (mgHC/g) (ppt)	S_2 (mgHC/g) (ppt)	S_1+S_2 (weight percent)	S_2/Org. C ($\frac{\text{mgHC}}{\text{g Org. C}}$)	T_{S_2} (°C)	$\frac{S_1}{S_1+S_2}$	$\frac{S_1+S_2}{\text{Org. C}}$ (percent)
Tertiary									
1,130- 1,160	344- 354	0.65	0.310	1.20	0.151	185	460	0.205	23.2
Upper Cretaceous									
1,550- 1,580	472- 482	1.04	0.090	0.42	0.051	40	447	0.176	4.9
2,150- 2,180	655- 664	.83	.100	.81	.091	98	ND	.110	11.0
2,510- 2,540	765- 774	.65	.045	.41	.046	63	451	.099	7.0
Lower Cretaceous									
3,110- 3,140	948- 957	0.83	0.045	0.33	0.038	40	465	0.120	4.5
3,530- 3,560	1,076-1,085	.74	.045	.43	.048	58	460	.095	6.4
4,130- 4,160	1,259-1,268	.54	.090	.47	.056	87	456	.161	10.4
4,510- 4,600	1,375-1,402	.37	2.000	2.10	.410	568	455	.488	110.8
5,050- 5,080	1,539-1,548	3.09	8.000	13.70	2.170	443	465	.369	70.2
5,560- 5,590	1,695-1,704	1.73	6.600	8.00	1.460	462	460	.452	8.4
Upper Jurassic									
6,010- 6,040	1,832-1,841	0.84	1.000	1.80	0.280	214	482	0.357	33.3
6,550- 6,580	1,996-2,006	.71	.660	1.00	.166	141	457	.398	23.4
9,730- 9,740	2,966-2,969	.48	.630	.87	.150	181	470	.420	31.3
10,230-10,240	3,118-3,121	.72	.550	1.02	.157	142	452	.350	21.8
10,730-10,740	3,271-3,274	.42	.390	.64	.103	152	472	.379	24.5
11,230-11,240	3,423-3,426	.53	.340	.68	.102	128	462	.333	19.2
11,730-11,740	3,575-3,578	.33	.290	.56	.085	170	464	.341	25.8
Middle Jurassic									
12,230-12,240	3,728-3,731	0.38	0.320	0.49	0.081	129	462	0.395	21.3
12,740-12,750	3,883-3,886	.267	.170	.31	.048	119	446	.354	18.5
13,230-13,240	4,033-4,036	.33	.530	1.01	.154	306	448	.344	46.7
13,250-13,260	4,039-4,042	.29	.240	.61	.085	210	454	.282	29.3
13,750-13,760	4,191-4,194	.20	.160	.30	.046	150	ND	.348	23.0
14,250-14,260	4,343-4,346	.50	.310	1.66	.197	332	464	.157	39.4
14,740-14,750	4,493-4,496	.43	.230	.58	.081	135	468	.284	18.8
15,250-15,260	4,648-4,651	.51	.200	.66	.086	129	456	.233	16.9
15,750-15,760	4,801-4,804	.46	.460	1.22	.168	256	460	.274	36.5
16,240-16,250	4,950-4,953	.27	.151	.38	.053	141	448	.284	20.0
16,740-16,750	5,102-5,105	.22	.110	.29	.040	132	446	.275	18.2
17,250-17,260	5,358-5,361	.41	.150	.51	.066	124	456	.227	16.1
17,750-17,760	5,410-5,413	.29	.074	.27	.034	93	436	.215	11.9
18,250-18,260	5,563-5,566	.53	.175	.85	.103	160	450	.171	19.3
18,750-18,760	5,715-5,718	1.10	1.700	5.24	.694	476	460	.245	63.1

ized by a rather narrow range of normal alkanes with an average CPI of 1.54 extending from n-C_{15} to n-C_{22}, which are probably of a marine algal origin (figs. 43 and 45).

The average thermal pyrolysis convertibility of the Upper Jurassic strata from the COST No. G-2 well is 25.6 percent, which is significantly higher than the 4.4 percent of the COST No. G-1 well. This difference is thought to reflect the hydrogen-rich nature of the Upper Jurassic kerogens in the G-2, associated with shallow-water marine algal carbonates, as opposed to the predominance of hydrogen-poor humic-type kerogens present in the G-1. The transformation ratios ($S_1/(S_1+S_2)$) for the Upper Jurassic strata can be grouped into two distinct populations with the higher ratios predominating in the COST No. G-2 well samples. This difference may indicate greater thermal evolution of the more hydrogen-rich Upper Jurassic kerogens in the COST No. G-2 well. The temperature of maximum pyrolysis yield (T_{S_2}) for the solid organic matter in the Upper Jurassic rocks ranges from 828° to 869° F (442° to 465° C) for the COST No. G-1 well. With the exception of the 6,010- to 6,040-ft (1,832- to 1,841-m) interval, which is 900° F (482° C), the

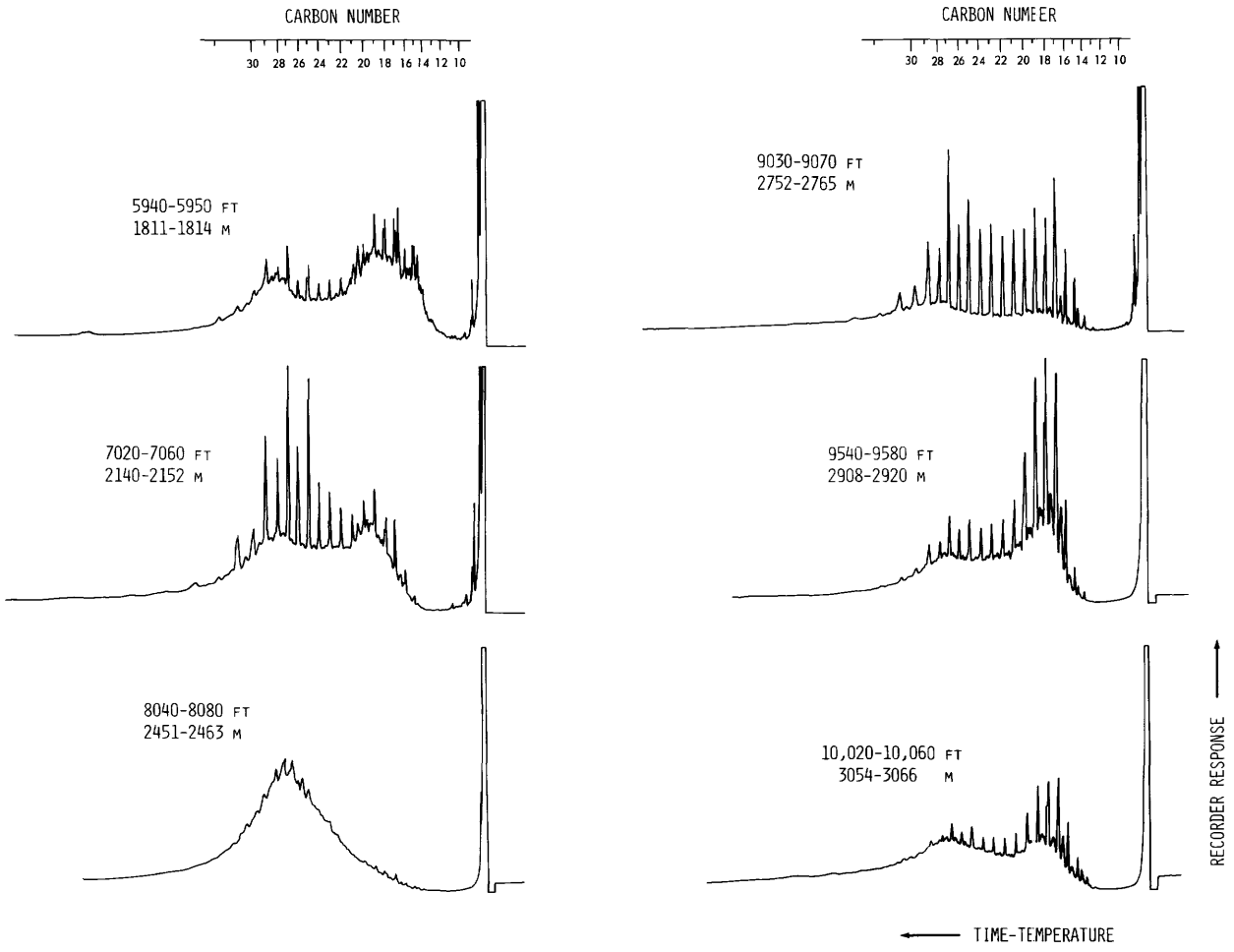

FIGURE 44.—Gas chromatographic analyses of saturated paraffin-naphthene hydrocarbons of Upper Jurassic rocks between 5,290 ft (1,612 m) and 10,100 ft (3,078 m), COST No. G-1 well.

temperature of maximum pyrolysis yield ranges from 846° to 882° F (452° to 472° C) for the Upper Jurassic strata of the COST No. G-2 well (tables 5 and 6). A maximum pyrolysis temperature of 878° F (470° C) is believed to be the critical temperature required to indicate the onset of maturation (Claypool and Baysinger, 1978). This temperature is also influenced by kerogen type, lithology, and design of the pyrolysis system (Hunt, 1979). For the COST No. G-2 well, the Upper Jurassic rocks appear to be slightly below the critical temperature threshold.

MIDDLE JURASSIC

The Middle Jurassic strata of the COST No. G-1 well occur from 10,100 to 14,000 ft (3,078 to 4,267 m) and are characterized by interbedded pelletal carbonates, siltstones, sandstones, and gray shales that grade downward into dolomites, anhydrites, and thin shales. Traces of coal and pyrite occur from about 10,000 to 13,000 ft (3,048 to 3,962 m). The Middle Jurassic strata from the COST No. G-2 well range from 11,800 ft (3,597 m) down to at least 18,000 ft (5,486 m). Below 18,000 ft (5,486 m) and to the total well depth of 21,874 ft (6,667 m) it is possible that Lower Jurassic or Triassic strata may be present; however, because of the lack of micropaleontological control, the exact age of these older rock units cannot be determined (Behout, 1980). The Middle Jurassic interval in the G-2 well contains a much thicker section of brown to gray micritic and oolitic limestones, microcrystalline to fine crystalline dolomites, and anhydrites with considerably less shale and sandstone than occurs in

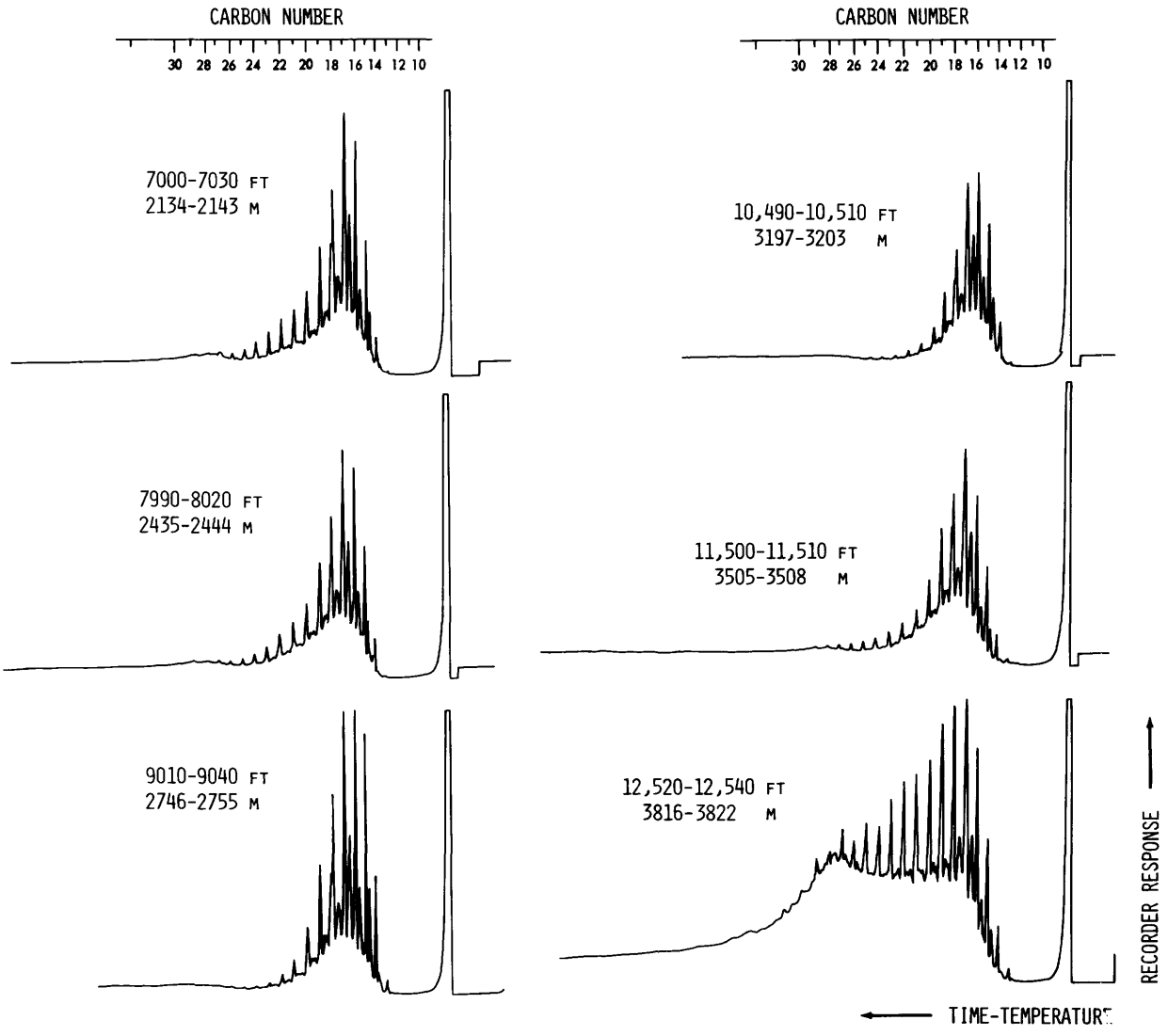

FIGURE 45.—Gas chromatographic analyses of saturated paraffin-naphthene hydrocarbons of Upper Jurassic (7,000 to 9,040 ft; 2,134 to 2,755 m), and Middle Jurassic rocks down to 12,540 ft (3,822 m), COST No. G-2 well.

the G-1 well (tables 1 and 2). The Middle Jurassic strata probably were deposited in a shallow-water, restricted (supratidal to subtidal) environment (Lachance, 1980; Simonis, 1980).

The total organic carbon contents of the Middle Jurassic rocks from the COST Nos. G-1 and G-2 wells average 0.25 and 0.20 weight percent, respectively (tables 3 and 4). These values are slightly below the 0.3 percent considered adequate for some carbonate strata to be termed source rocks (Hunt, 1967). However, fine-grained, dark-colored carbonate rocks may be capable of generating more hydrocarbons than some shales that contain the same amount of total organic matter. Carbonate rocks commonly contain only amorphous organic matter derived from algae. This kind of organic matter has the highest yield of petroleum among the kerogen types, which may explain why dark-gray to medium-gray carbonate rocks commonly yield more oil than shales that have the same total organic-carbon content (Hunt, 1979). The question of how much organic carbon is needed to make an excellent, good, or poor carbonate source rock is highly controversial. From a qualitative point of view, however, limestones and dolomites that are predominantly gray to dull brown or black commonly have an extractable hydrocarbon content equivalent to that

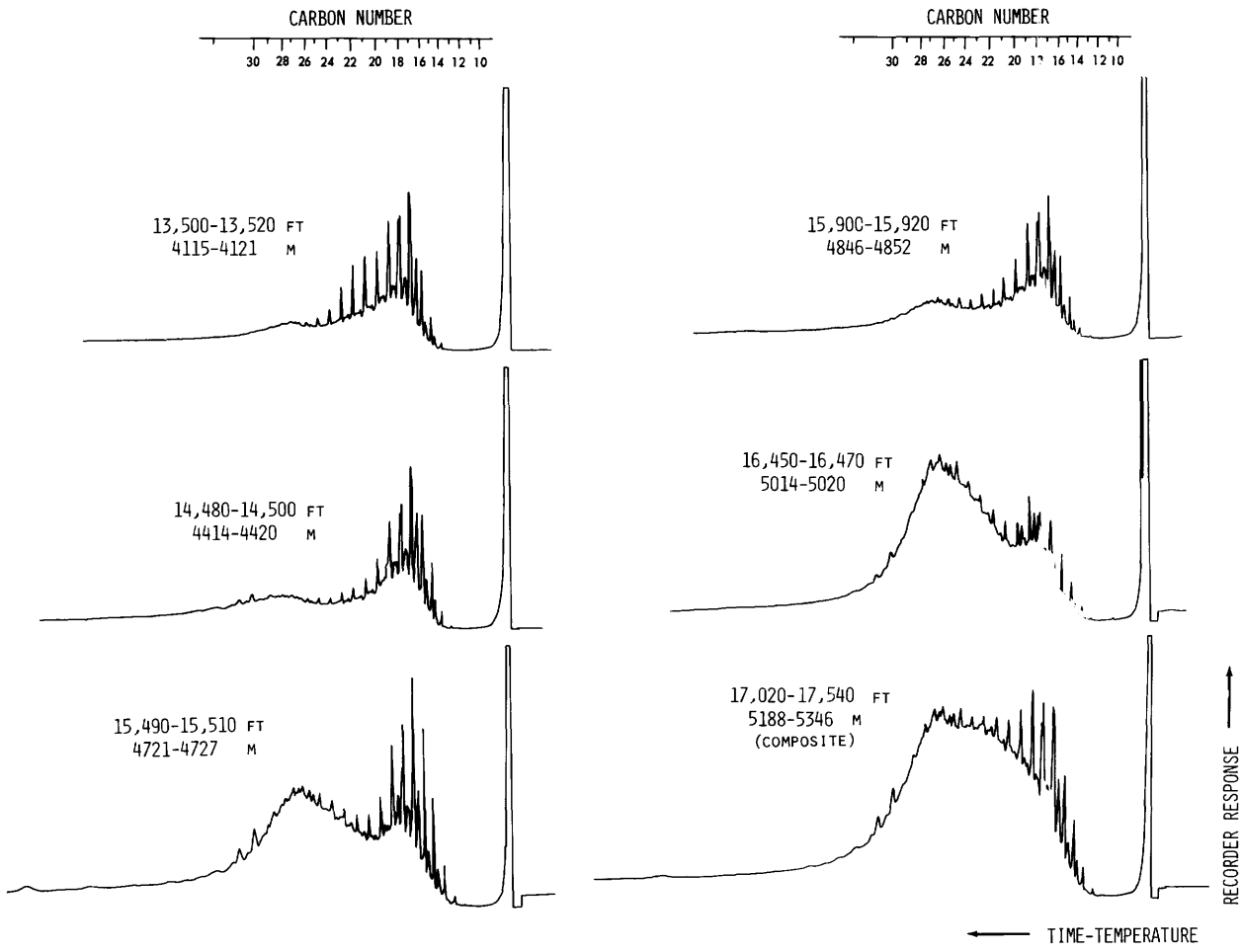

FIGURE 46.—Gas chromatographic analyses of saturated paraffin-naphthene hydrocarbons of Middle Jurassic rocks from 13,500 to 17,540 ft (4,115 to 5,346 m), COST No. G-2 well. The 17,020- to 17,540-ft sample is a composite of two samples from 17,020–17,040 and 17,520–17,540 ft (5,188–5,194 and 5,340–5,346 m).

associated with good source rocks, whereas light-colored, recrystallized carbonate rocks generally have very few, if any, indigenous hydrocarbons (Hunt, 1979). In addition, it has been demonstrated that organic matter and bitumen content increases with an increase in the clay content of carbonate strata (Hunt, 1967). Thus, the light-gray to black, argillaceous, fine-grained carbonate rocks of the Middle Jurassic section could be considered as potential source rocks.

A major difference exists between the average total extractable hydrocarbons of the Middle Jurassic sediments from the COST Nos. G-1 and G-2 wells. The G-1 rocks contain an average of 36 ppm, whereas the G-2 strata average 170 ppm. Although these values are both low in terms of source-rock richness, the difference in quality may be related to the nearshore character of the Middle Jurassic in the COST No. G-1 well. The Middle Jurassic section of the G-2 contains a much larger percentage of marine carbonate rocks and anhydrites. The average total hydrocarbon to total organic carbon ratios may signal the begining of the intense oil generation process below 10,000 ft (3,050 m) in the Middle Jurassic (table 3 and 4). Between 15,000 and 18,000 ft (4,572 and 5,486 m) in the COST No. G-2 well, the Middle Jurassic rocks contain a higher concentration of nitrogen, sulfur, and oxygen compounds than occurs in the Upper Jurassic or Cretaceous rocks (fig. 41). This higher concentration of the polar compounds is believed to reflect the nature and type of organic matter present in this interval. Traces of a black, asphalt-like substance, soluble in carbon disulfide, was present in several of the cutting samples between 15,500 and 18,000 ft

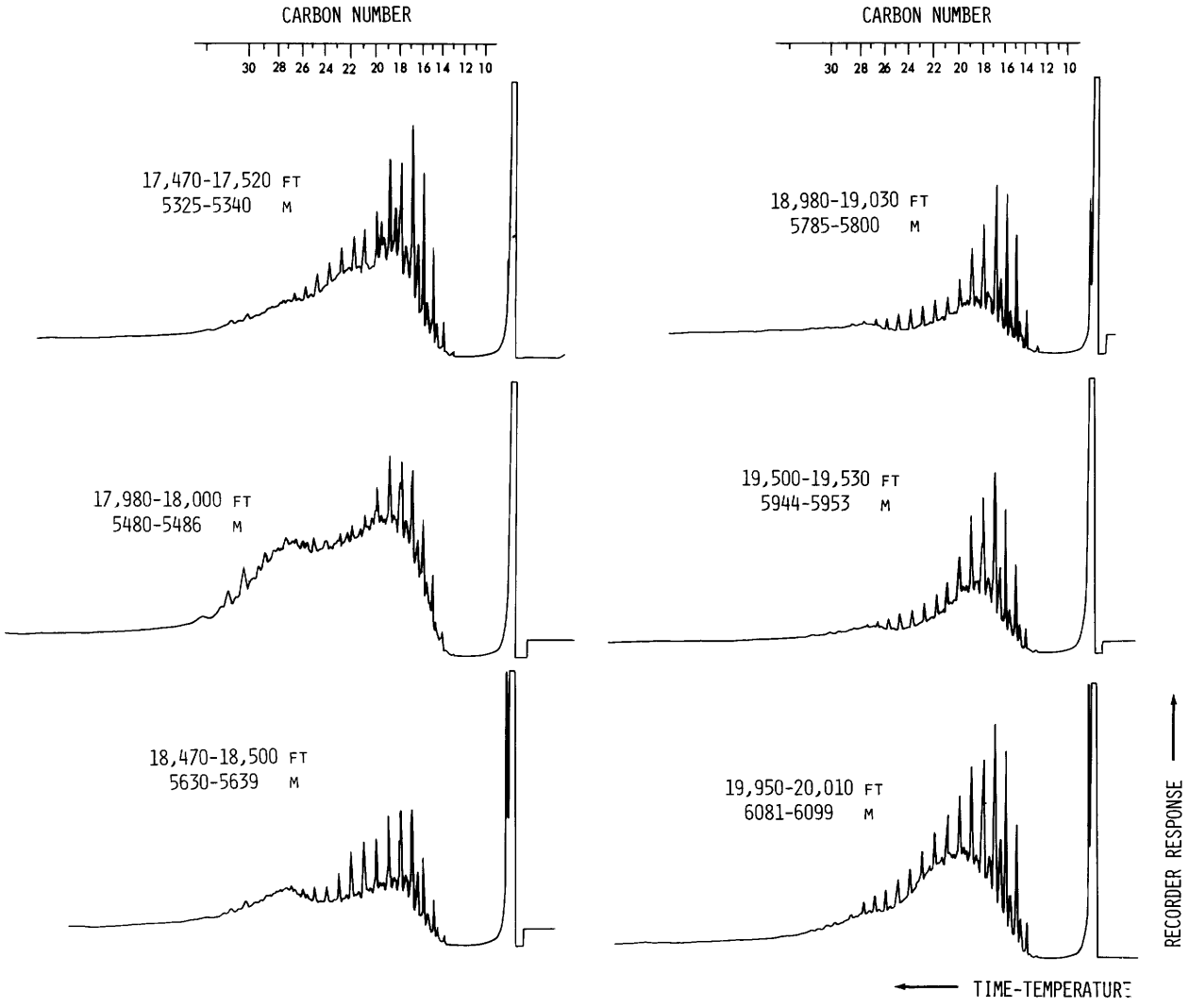

FIGURE 47.—Gas chromatographic analyses of saturated paraffin-naphthene hydrocarbons of Middle Jurassic rocks from 17,470 to 20,010 ft (5,325 to 6,099 m), COST No. G-2 well.

(4,724 and 5,486 m). A gas chromatogram of the saturated paraffin-naphthene hydrocarbons from a similar substance isolated by GeoChem Laboratories, Inc., in samples from below 14,000 ft (4,267 m) is shown in figure 39. If this substance is indigenous, it supports the interpretation of low thermal maturity; however, the possibility is equally good that the substance may be a mud contaminant. Because this substance was present only in a few samples from a limited interval, its interference with the paraffin-naphthene signatures of this interval is believed to be minimal except where noted.

The saturated paraffin-naphthene hydrocarbon gas chromatograms for the Middle Jurassic strata from 12,520 to 21,540 ft (3,816 to 6,565 m) in the COST No. G-2 well show an irregular and inconsistent change in the magnitude of the unresolved bimodal branched and cyclic paraffins relative to the resolved aliphatics (figs. 46, 47, 48). This inconsistent change may be due in part to possible background interference by mud additives. Except in the 12,520- to 12,540-ft (3,816-to 3,822-m) interval, the major portion of the resolved aliphatic hydrocarbons are the n-C_{15} to n-C_{22} molecular species, which predominate over the isoprenoid hydrocarbons pristane and phytane. Although not completely source-specific because of the masking effects of catagensis, the pristane/phytane ratio varies throughout the Middle Jurassic between 1.1 and 2.0, probably indicating the influence of mixed marine-algal,

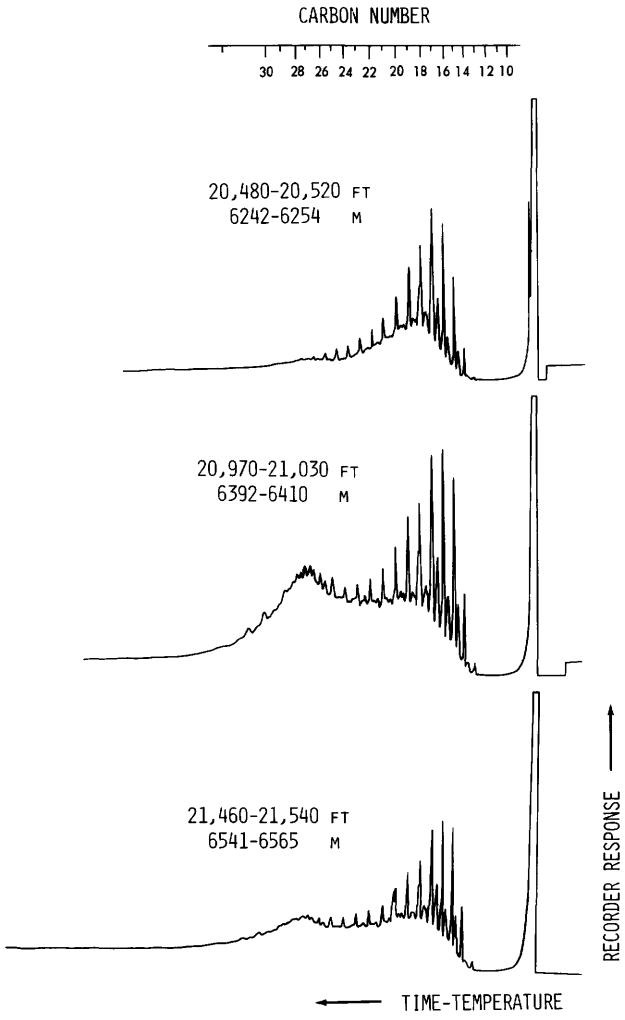

FIGURE 48.—Gas chromatographic analyses of saturated paraffin-naphthene hydrocarbons of Middle Jurassic rocks from 20,480 to 21,540 ft (6,242 to 6,565 m), COST No. G-2 well.

herbaceous, and woody organic matter. At about 18,500 ft (5,639 m), the resolved normal alkanes begin to predominate over the unresolved complex envelope and shift toward the lower molecular weight ranges, and the CPI ratio approaches unity (figs. 47 and 48). Such characteristics indicate that thermal maturation processes have been active. However, at a depth of 21,460 to 21,540 ft (6,541 to 6,565 m), the resolved normal aliphatics, the molecular distribution and composition, and the unresolved napthenic envelope still do not resemble those of thermally mature petroleum hydrocarbons and may be influenced by mud additives (fig. 48).

In the COST No. G-1 well, the Middle Jurassic section is much thinner than in the COST No. G-2 well, extending from 10,100 to 14,000 ft (3,078 to 4,267 m). The resolved normal aliphatics occur predominantly in the n-C_{14} to n-C_{22} range, except for the 12,360- to 12,400-ft (3,767- to 3,780-m) sample, and generally are dominated by a strongly bimodal, unresolved, complex mixture, a signature that usually indicates a low-temperature thermal history for the liquid C_{15+} hydrocarbons (figs. 49 and 50). Throughout the Middle Jurassic section, the resolved normal aliphatic hydrocarbons dominate over the isoprenoids pristane and phytane. The generally low concentration of the aliphatics in the n-C_{27} to n-C_{35} range, the predominance of the resolved normal aliphatics from n-C_{14} to n-C_{22}, and an average CPI ratio of 1.2 are characteristics of hydrocarbons that are considered to have a marine origin.

The temperatures of maximum thermal pyrolysis yield for the Middle Jurassic strata in the COST Nos. G-1 and G-2 wells average 867° F (464° C) and 849° F (454° C), respectively. These temperatures are consistent with the interpretation of a relatively low degree of thermal maturation, which is in general agreement with the low-thermal-maturity signatures of the saturated paraffin-naphthene hydrocarbon gas chromatograms (tables 5 and 6; figs. 45-50).

LOWER JURASSIC AND CAMBRIAN

Lower Jurassic and Cambrian rocks were penetrated in the COST No. G-1 well. The Lower Jurassic rocks extend from 14,000 to 15,630 ft (4,267 to 4,764 m), and the Cambrian from 15,630 to 16,061 ft (4,764 to 4,895 m). The Lower Jurassic is characterized by light-gray to buff dolomites, anhydrites, and micaceous siltstones that grade downward into coarse-grained sandstones and red hematitic mudstones (table 1). Only traces of dolomite are present below a depth of about 15,000 ft (4,572 m). Chips of black, graphitic schist, present from 16,056 to 16,061 ft (4,894 to 4,895 m), yielded K-Ar ages of 450 to 550 million years (Steinkraus, 1980).

The total extractable hydrocarbons for the Lower Jurassic and Cambrian rocks averaged 39 ppm, and these intervals have average total organic carbon values of 0.11 and 0.14 weight percent, respectively. The ratio of total hydrocarbon

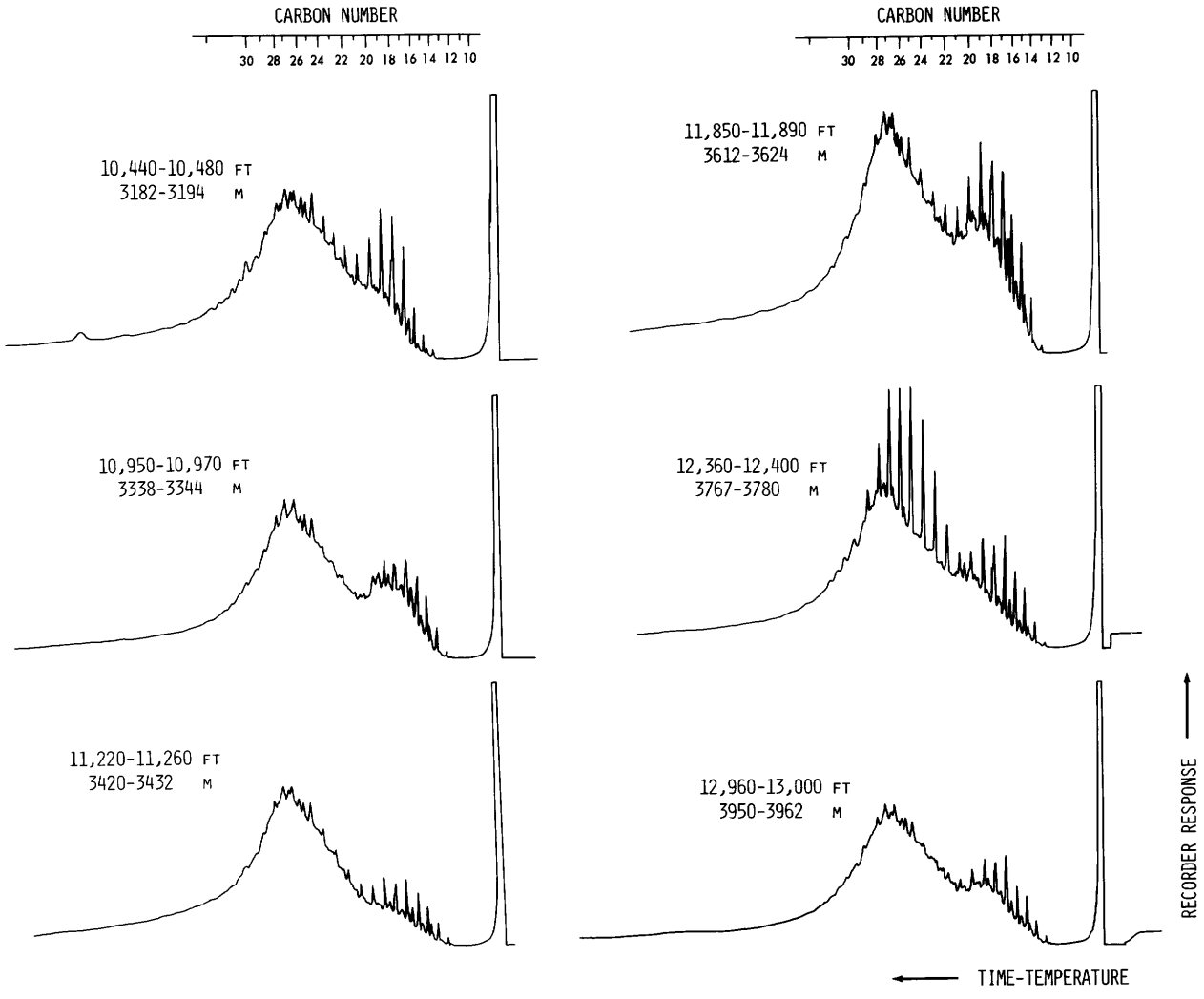

FIGURE 49.—Gas chromatographic analyses of saturated paraffin-naphthene hydrocarbons of Middle Jurassic rocks above 13,000 ft (3,962 m), COST No. G-1 well.

to total organic carbon averages 5.37 percent for the Lower Jurassic and 4.52 percent for the Cambrian rocks. The average ratios of total hydrocarbon to extractable organic matter are 0.43 and 0.61, saturated hydrocarbon to aromatic hydrocarbon ratios are 2.48 and 2.00, and Carbon Preference Indices (CPI) are 0.88 and 1.10 for the G-1 Lower Jurassic and Cambrian, respectively (table 3). The progressive increase in the average values from the Upper through Lower Jurassic strata indicates progressively increasing thermal maturation. The saturated paraffin-napthene hydrocarbon gas chromatograms, however, continue to show a strong bimodal distribution of the unresolved complex mixture with a predominance of the naphthenes over the resolved n-alkanes, a signature that may indicate mud additive effects (fig. 50). These gas chromatographic characteristics of thermal immaturity are inconsistent with the extractable hydrocarbon ratios that indicate a time-temperature history characteristic of mature sources. The low average convertibility ((S_1+S_2)/Org. C) of 8.6 indicates the predominance of hydrogen-poor organic matter. The average thermal-pyrolysis maximum-yield temperature for the Lower Jurassic and Cambrian rocks was calculated to be 847° F (453° C) where definite thermal peaks were present (table 5). This temperature of maximum yield indicates that the solid organic matter in the Lower Jurassic and

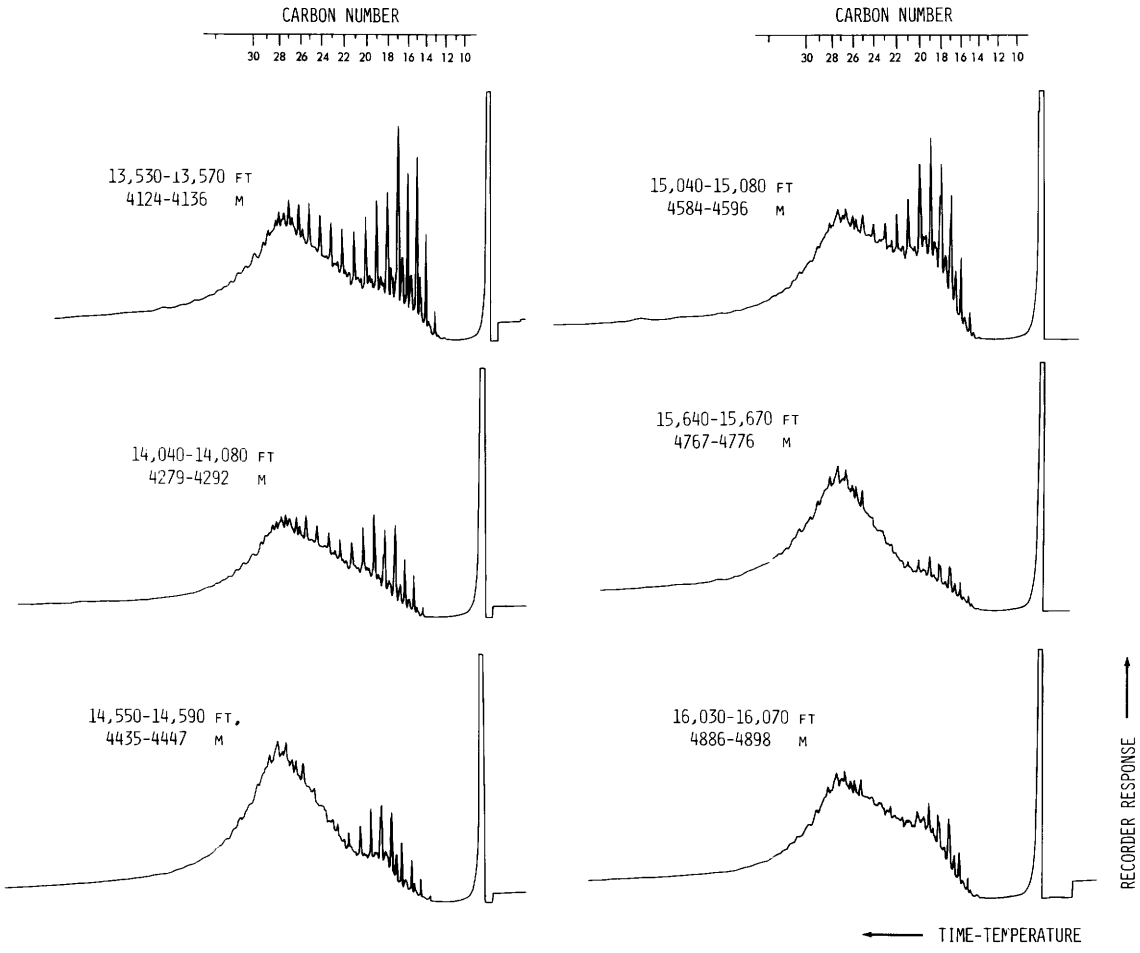

FIGURE 50.—Gas chromatographic analyses of saturated paraffin-naphthene hydrocarbons of Middle Jurassic (13,530 to 13,570 ft; 4,124 to 4,136 m), Lower Jurassic (14,040 to 15,080 ft; 4,279 to 4,596 m), and Cambrian (15,640 to 16,070 ft; 4,767 to 4,898 m) rocks, COST No. G-1 well.

Cambrian rocks are apparently still thermally immature with respect to the generation of liquid hydrocarbons. This temperature of maximum yield may be influenced by the low total organic matter content of the rocks. The $S_1/(S_1+S_2)$ production index ratio, which is a measure of maturation, does however, show a consistent increase from 0.14 at 14,040 to 14,050 ft (4,279 to 4,282 m) to 0.26 at 16,010 to 16,020 ft (4,880 to 4,883 m) and indicates significant thermal maturity.

The low total organic carbon (average 0.12 weight percent) and the thermal-pyrolysis and gas chromatographic maturity characteristics of the organic matter in the Lower Jurassic and Cambrian rocks suggest that this interval in the COST No. G-1 has a very poor oil and gas source-rock potential.

KEROGEN TYPES AND THERMAL MATURATION FOR THE COST NO. G-1 WELL

The geochemical parameters used to classify the kerogens in the COST No. G-1 well are relative type and abundance, hydrogen to carbon ratios, stable carbon isotope compositions ($\delta^{13}C$), and thermal pyrolysis hydrogen index (S_2/Org. C), (fig. 51). The sediments of the COST No. G-1 down to a burial depth of about 6,000 ft (1,820 m) contain mainly amorphous and herbaceous, hydrogen-rich kerogens (fig. 51). Below 6,000 ft (1,829 m), there is a considerable decrease in the abundance of amorphous kerogen and a significant increase in the herbaceous, woody, and coaly types. This predominance of hydrogen-poor kerogen extends into the Lower Jurassic and Cambrian rocks below 14,000 ft (4,267 m) and is be-

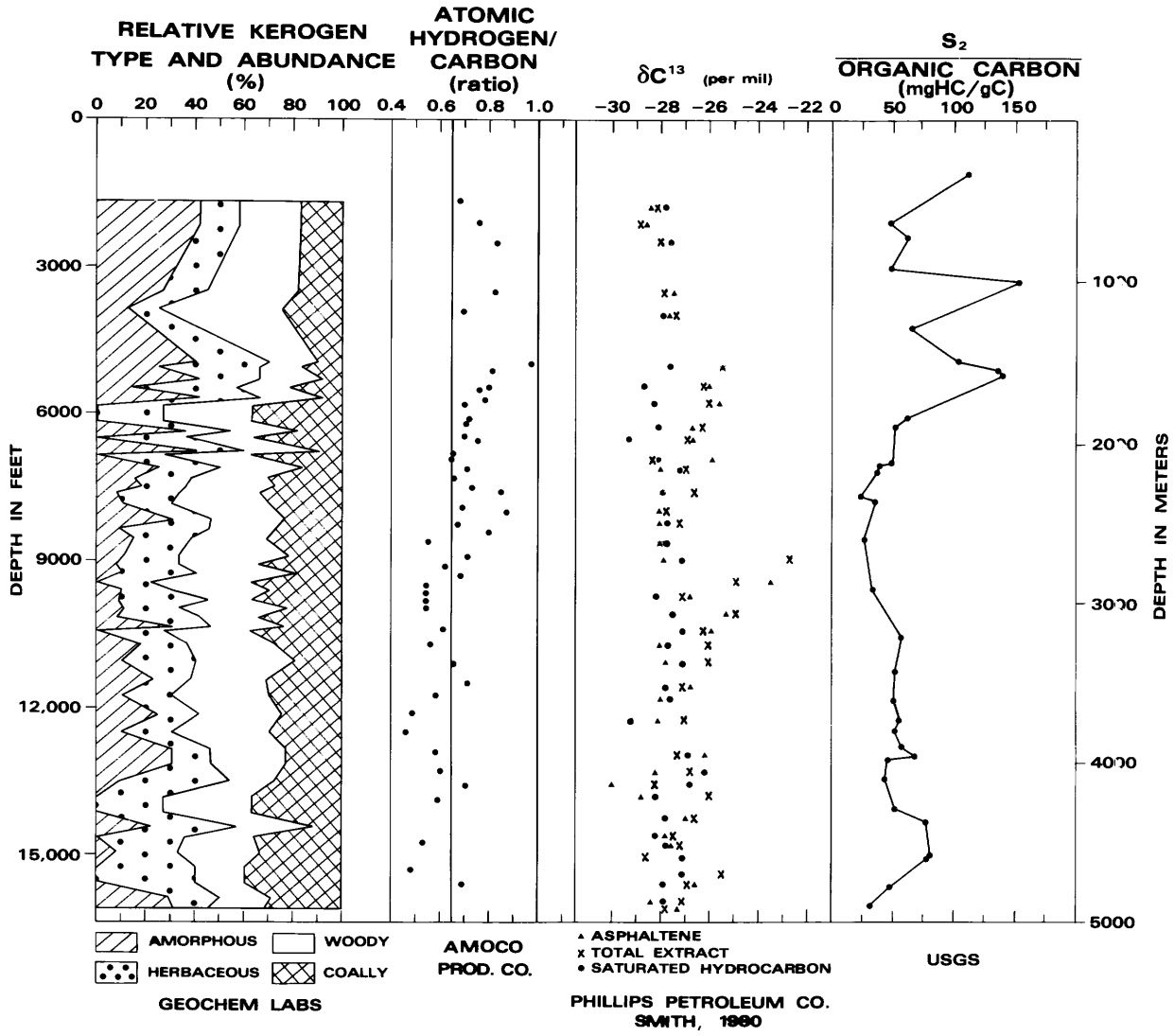

FIGURE 51.—Summary profile of indicators of types of organic matter present in the COST No. G-1 well as a function of depth of burial.

lieved to reflect the influence of the terrestrially derived organic matter associated with nearshore sedimentary facies.

In the COST No. G-1 well, the hydrogen to carbon ratios of the kerogens range from 0.5 to 0.9. The hydrogen-poor character of these kerogens is also indicated by their average thermal pyrolysis hydrogen indices (S_2/Org. C), which range from 38 in the Cambrian to 118 in the Lower Cretaceous (table 5). Such values are generally consistent with poor-quality source rocks that contain predominantly hydrogen-lean, type III, gas-prone kerogens. The stable carbon isotopic compositions of the asphaltene, total extracts, and saturated paraffin-naphthene fractions are shown in figure 51. Yen (1972) has reported that the asphaltene fraction of an oil should have a $\delta^{13}C$ value similar to that of the kerogen from which it was derived. This isotopic relationship is due to the structural and chemical similarities between the asphaltene and kerogen. Stahl (1978) confirmed the isotopic similarity between genetically associated kerogens and asphaltenes from crude oils. In the COST No. G- well, no $\delta^{13}C$ values of the kerogens were available for comparison with those of the asphaltenes. However, if it is assumed that a genetic asphaltene-kerogen chemical structure relationship does exist (Yen, 1972;

Stahl, 1978) and that this relationship can be extended to include the asphaltene fractions associated with the total bitumen extractables of the source shales (believed to represent that portion of the generated hydrocarbons remaining at the place of origin), then the $\delta^{13}C$ values of the asphaltene fraction of the source shales may be interpreted as being representative of the $\delta^{13}C$ ratio of the source kerogens. The $\delta^{13}C$ values for the asphaltene fractions of the COST No. G-1 well are predominatly between −26 and −28 permil. Such $\delta^{13}C$ values are, however, inconsistent with the $\delta^{13}C$ values of the predominantly terrestrial kerogen types described from well cuttings. With the exception of those from the Cretaceous strata, the kerogens of G-1 are considered to have a predominantly terrestrial source, as indicated by their relative abundances determined by optical microscopy methods (fig. 51).

The distribution and concentration of the C_1 to C_7 hydrocarbons, the percent gas wetness, and the n-C_4 to n-C_7 ratios for the COST No. G-1 well are shown in figure 52, and the thermal maturation geochemical characteristics for G-1 are shown in figure 53. The maximum C_1 to C_4 light hydrocarbon concentrations range from 15,000 to 27,000 ppm in the 4,500- to 6,500-ft (1,372- to 1,981-m) Cretaceous-Jurassic interval, and generally the strata have less than 10 percent gas wetness. These Cretaceous-Jurassic rocks contain lignitic and peaty types of organic matter. The extractable organic matter from this interval is characterized by the highest total organic carbon, total extractable saturated paraffin-naphthene, and aromatic hydrocarbons. The nitrogen, sulfur, and oxygen compound concentrations in this interval range from 50 to 200 ppm. The apparently low thermal maturity of the extractable organic matter, and low gas wetness, as well as the presence of terrestrial organic matter associated with these Cretaceous-Jurassic sandstones and shales, suggest that the light hydrocarbons in this interval are probably unrelated to indigenous, thermally produced, mature liquid petroleum hydrocarbons. This interpretation is consistent with the bimodal distributions of the saturated paraffin-naphthene hydrocarbon gas chromatograms, the CPI ratios that show a predominance of odd-carbon chain hydrocarbons, the moderately low temperatures of maximum thermal pyrolysis yield (846° to 878° F; 452° to 470° C), and TAI values that range from 1.5 to 1.8 (figs. 41, 43, 44, and 49-53).

Where the n-C_4/n-C_7 profile shows values that are less than unity, the possibility exists that diesel fuel contamination may be present (7,000-10,000 ft, 2,134-3,048 m; 12,000-13,000 ft, 3,658-3,962 m; and 14,000-15,000 ft; 4,267-4,572 m) (fig. 52). However, the n-C_4/n-C_7 ratio compares molecular species that are in gaseous and liquid physical states. Because of the possibility of preferential loss of the lower molecular weight species due to the difference in vapor pressures, this ratio may be misleading and should be used with caution; the presence of diesel fuel should not be inferred on the basis of this ratio alone. The molecular distribution and concentrations of the saturated paraffin-naphthene hydrocarbons do not reflect the presence of diesel fuel in the lithologic units below 6,500 ft (1,981 m). Although an inconsistency exists with the n-C_4/n-C_7 ratios, the normal saturated paraffin-naphthene hydrocarbon distributions and the thermal-maturation interpretations are not believed to be influenced by diesel fuel effects.

If vitrinite reflectance (R_o) values are determined on primary (first-cycle) vitrinite macerals and the geothermal gradient is assumed to be constant, then for a sedimentary basin with a simple burial history involving no loss of overburden by erosion, vitrinite reflectance is the only thermal maturation parameter that is believed to increase exponentially with thermal maturity and to be unaffected by kerogen composition (Dow, 1977). The slope of the vitrinite reflectance profile is a function of the maximum geothermal gradient and the age of the lithologic units or, more specifically, the length of the time of heating. In those instances where sedimentary units have experienced varying geothermal gradients, segmented maturation gradients may occur. If the R_o values are plotted on a log scale and depth on a linear scale, the relationship between the two parameters for each segment will usually be a straight line (Dow, 1977). Vitrinite reflectance values determined on well cuttings, however, may give anomalous results. Such factors as the presence of oxidized vitrinite or recycled material, natural variations, and statistical and technical errors in not selecting first-cycle vitrinite, can produce abnormally high R_o values,

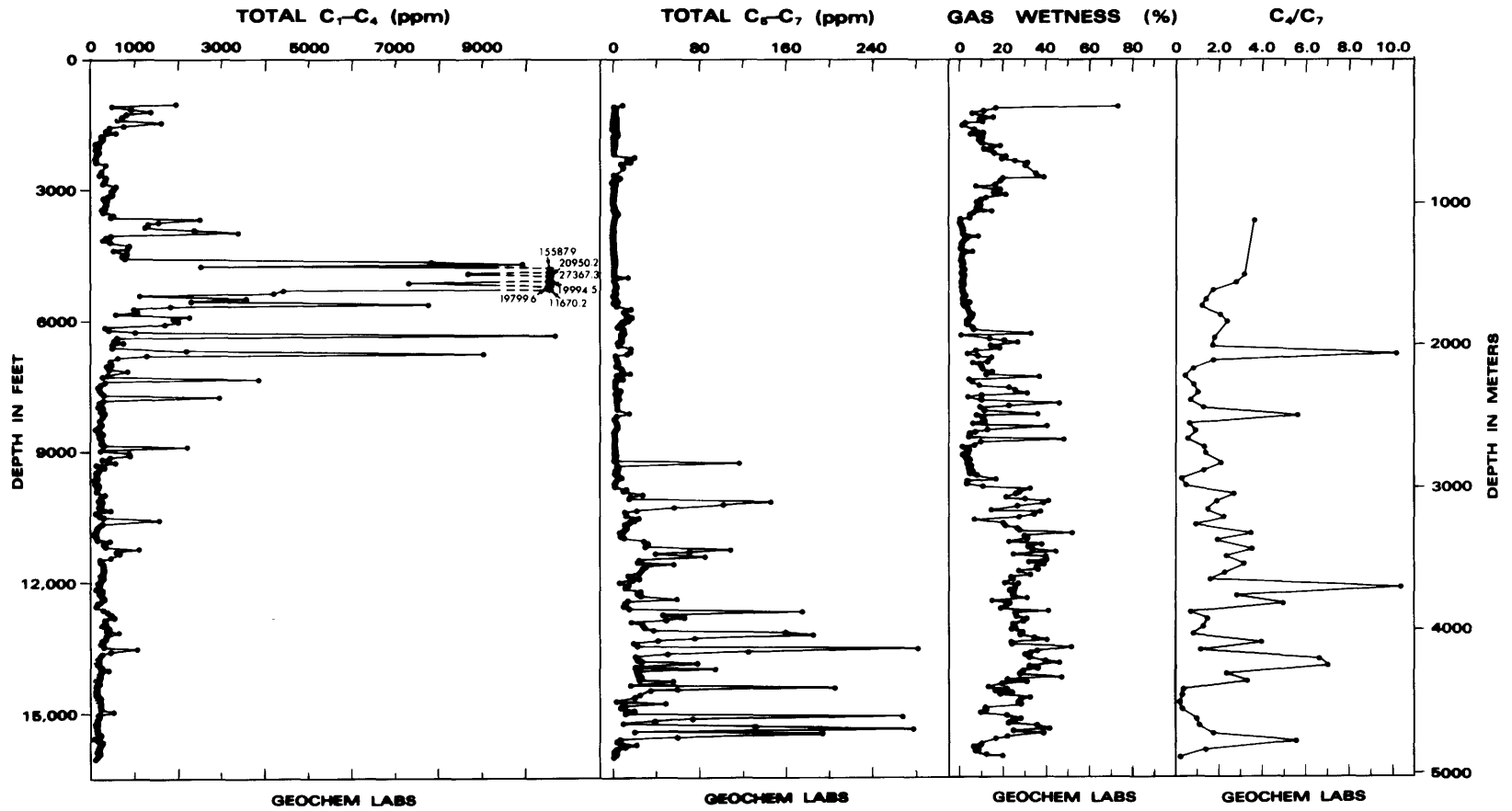

FIGURE 52.—Summary of C_1 to C_7 hydrocarbon analyses of samples from the COST No. G-1 well.

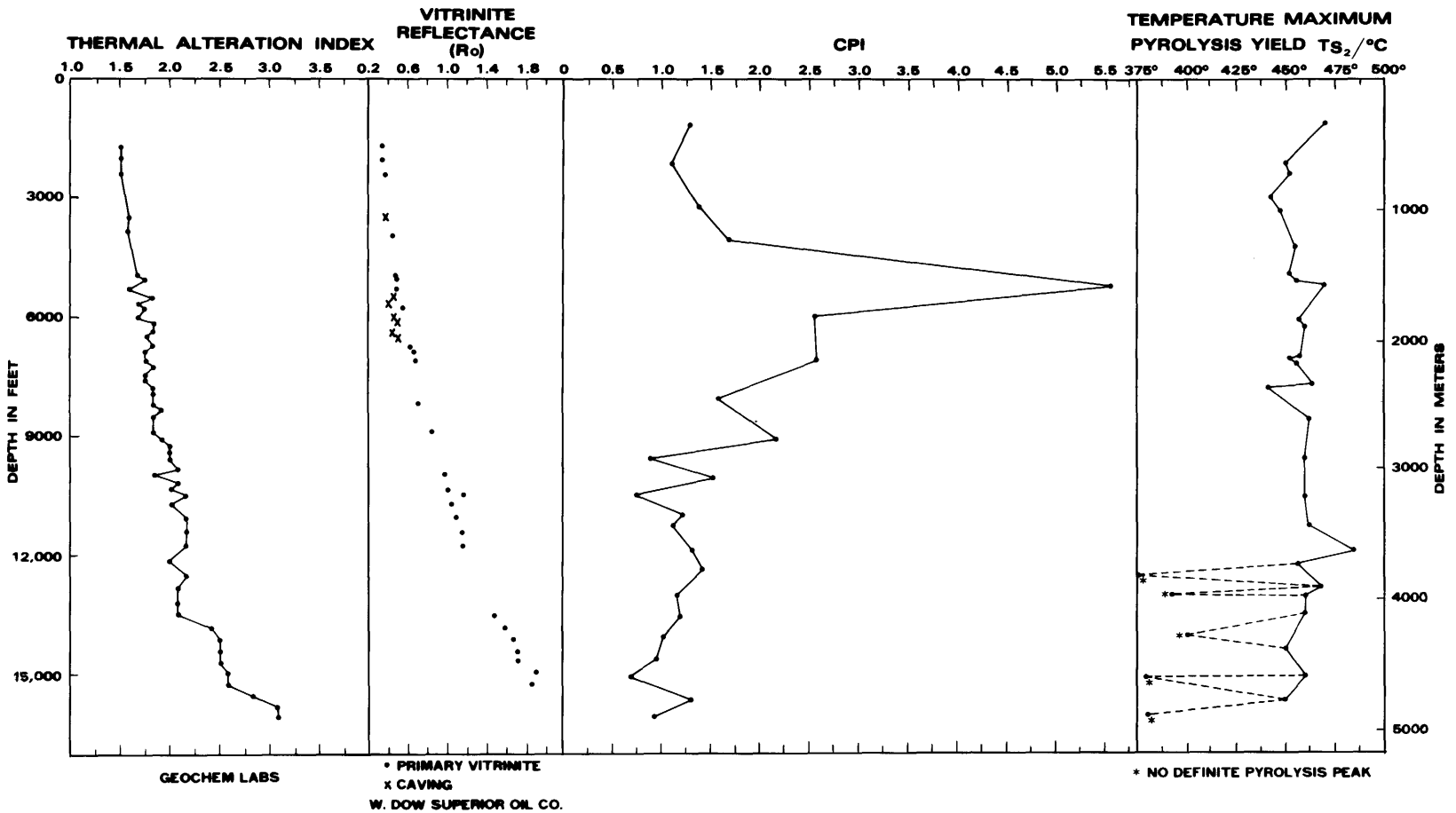

FIGURE 53.—Maturity profiles of organic matter as a function of depth of burial for samples from the COST No. G-1 well.

whereas cavings, rough vitrinite, and mud contamination can result in abnormally low R_o values (Dow, 1977; Bostick and others, 1978).

The R_o values from the COST No. G-1 well were reported as having been determined on primary vitrinite except in the 5,500- to 6,500-ft (1,676- to 1,981-m) interval, where cavings from overlying coals may have given abnormally low R_o values (Smith and Shaw, 1980). The slope of the R_o profile for the sedimentary section from about 6,500 ft (1,981 m) to the bottom of the well (16,071 ft; 4,898 m) is less steep than the profile from 2,000 ft (610 m) down to 6,500 ft (1,981 m) (fig. 53). The change in slope of the R_o profile at about 6,500 ft (1,981 m) suggests a cooler thermal history for the overlying Cretaceous-Jurassic rocks and a higher geothermal gradient for the older Jurassic rocks below this depth. These vitrinite data suggest that a complex thermal and burial history may have existed for the Cretaceous and Jurassic. The effect of possible removal of overburden on the vitrinite profile is open to question. The degree of thermal maturity indicated by the vitrinite reflectance values below 6,500 ft (1,981 m) is also not consistent with the TAI values, odd-even carbon preference indices (CPI), or temperature of maximum pyrolysis yield (T_{S_2}). If the range of R_o values (0.62 to 1.8) below 6,500 ft (1,981 m) is representative of indigenous, first-cycle vitrinite, then the existence of a higher thermal gradient is suggested for the more deeply buried Jurassic rocks.

This history of higher temperatures is not totally corroborated, however, by the other comparative thermal maturation parameters. The vitrinite reflectance data suggest paleotemperatures have already exceeded those needed for the first-order chemical reactions that are responsible for the formation of petroleum and have passed into the temperature range where dry gas may be formed. However, because of the inconsistencies between the level of thermal maturation indicated by the vitrinite-reflectance (R_o) values and the other geochemical maturation parameters, the paleotemperatures are believed to have been lower than those required for peak gas generation. The threshold for intense oil generation as defined by Hunt (1979) is placed at 10,500 ft (3,202 m) and is based on the significant increase in the concentration of the C_4 to C_7 gasoline-range hydrocarbons (fig. 52). Peak oil generation appears to have occurred between 13,000 and 15,000 ft (3,965 to 4,575 m). The change in the slope of the R_o profile below 6,500 ft (1,981 m) may have been influenced by oxidized vitrinite or recycled organic matter, which would yield an anomalously high paleotemperature history for the strata down to at least 15,630 ft (4,764 m). Below this depth, the degree of influence that Cambrian metamorphism may have had on the strata is unknown. Similarly, there is no clear evidence for a massive Jurassic thermal event associated with plate breakup in the COST No. G-1 well.

KEROGEN TYPES AND THERMAL MATURATION FOR THE COST NO. G-2 WELL

The data on the relative kerogen types and abundance in the COST No. G-2 well are inconsistent (fig. 54). The analyses reported by Core Laboratories, Inc., show a relatively large percentage of inertinite and exinite along with a comparatively small contribution of amorphous-algal kerogen. The relative percentages of kerogen types and abundances determined by GeoChem Laboratories, Inc., show a significant amount of marine, amorphous-herbaceous organic matter (fig. 54). Whether this inconsistency in the kerogen characterization is due to sample contamination, analytical procedure, or inhomogenous sample suites is not known. Smith (1980) has suggested that the Core Laboratories procedure may have inadvertently regarded the amorphous, sapropelic type of organic matter as a mud contaminant and that the GeoChem Laboratories, Inc., estimates of amorphous kerogen may have been slightly high.

The stable carbon isotope ratios for the Tertiary and Cretaceous kerogen and solvent-soluble fractions (paraffin-naphthenes, aromatics, total extractable hydrocarbons) range from −24 to −28 permil. With the exception of one sample interval (16,200 ft; 4,938 m), the stable-carbon-isotope ratios range from −22 to −29 permil for organic matter from the Upper Jurassic (5,960 to 11,800 ft; 1,817 to 3,597 m) and Middle Jurassic strata (11,800 to 18,000 ft; 3,597 to 4,586 m). The Middle Jurassic rocks below 18,000 ft (5,486 m) have $\delta^{13}C$ values that range from −24 to −28 permil (fig. 54). The $\delta^{13}C$ composition of a number of Cretaceous and Jurassic kerogens were reported to range from −22 to −28 permil

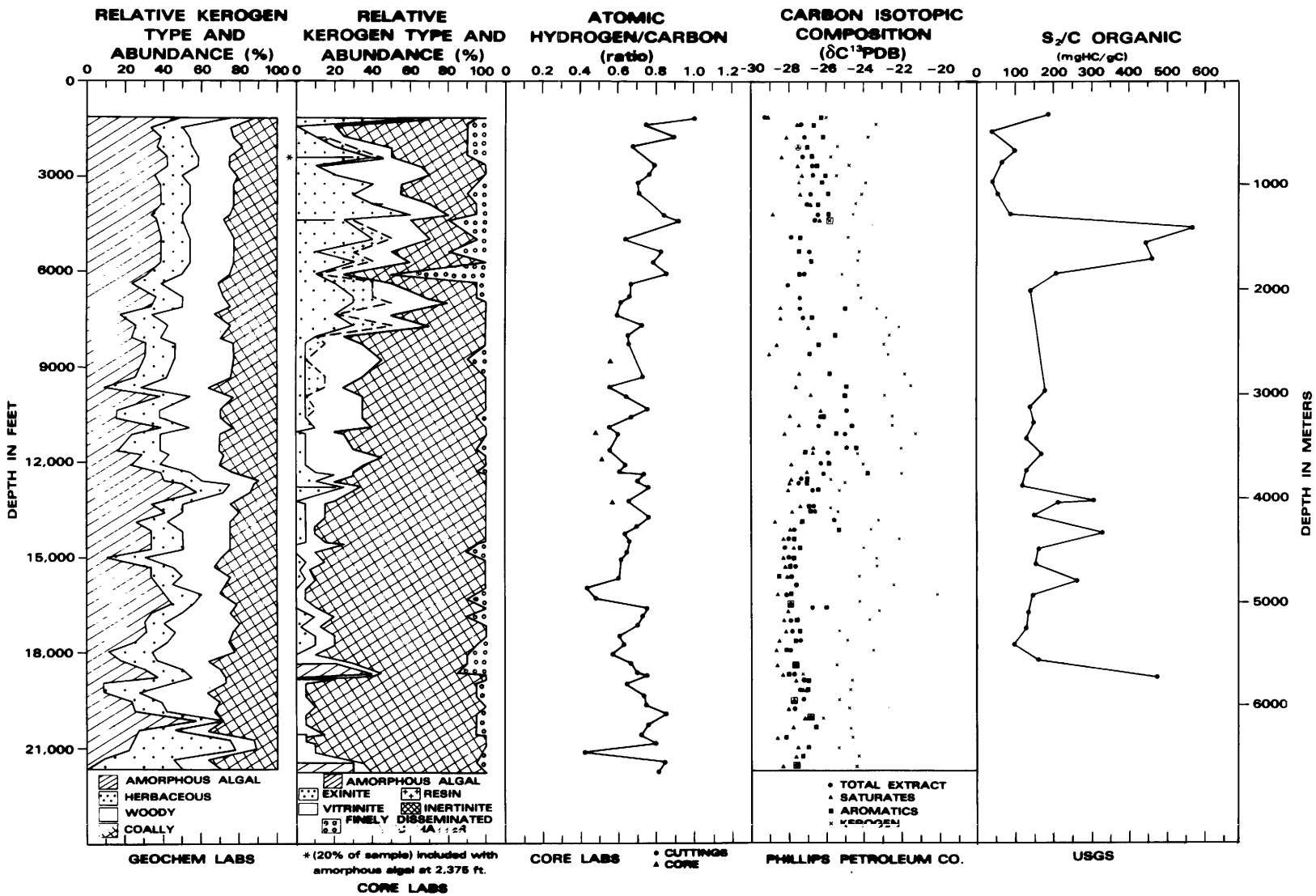

FIGURE 54.—Summary profiles of indicators of types of organic matter present in the COST No. G-2 well as a function of depth of burial.

(Degens, 1969). Such an isotopic spread is believed to be characteristic of organic matter derived from predominantly open-marine sources and is consistent with the stable carbon isotope ratios in almost all of the Cretaceous and Jurassic kerogens in the COST No. G-2 well.

There is a difference of 4 permil between the $\delta^{13}C$ values of saturated paraffins-naphthenes, aromatic hydrocarbons, and total extractable hydrocarbons, and those of the kerogens from the COST No. G-2 well (fig. 54). This spread of values suggests that a genetic relationship probably does not exist between the extractable bitumens and the kerogens. However, it is possible that thermal-maturation processes can induce carbon isotopic fractionation and exchange during catagenesis and metagenesis (Galimov, 1973; Tissot and Welte, 1978) and that the $\delta^{13}C$ balance in kerogen is generated at an early stage of diagenesis when all the humic acid enters the kerogen structure (Galimov, 1980).

The kerogen types and abundances reported by Core Laboratories, Inc., show major amounts of woody to coaly (type III) kerogen and a very small amount of the amorphous algal (type I) variety in the COST No. G-2 well (fig. 54). In contrast, the kerogen types and abundances as determined by GeoChem Laboratories, Inc., show that the amorphous and herbaceous (type I and II) varieties compose 40 to 50 percent of the solid organic matter present in the Cretaceous and Jurassic strata (fig. 54). The stable carbon isotope ratios reported in this study were determined on the kerogen and bitumen extracts prepared by GeoChem Laboratories, Inc. (fig. 54), but other stable carbon isotope ratios reported by Phillips Petroleum Co. are consistent with the type and abundance of kerogens reported by GeoChem Laboratories, Inc. If, however, the woody and coaly-humic (type III) kerogens were the most abundant species in the GeoChem Laboratories, Inc., samples, then the $\delta^{13}C$ ratios determined on the bitumen extracts and kerogen isolates should have been isotopically lighter, trending toward the -30 to -31 permil range characteristic of more terrigenous kerogen.

For that part of the Lower Cretaceous section between 4,510 and 6,000 ft (1,375 and 1,829 m), the thermal pyrolysis hydrogen index (S_2/Org. C) averages 491 mg HC/g Org. C and suggests the presence of a more hydrogen-rich type of kerogen that is suitable for the generation of liquid petroleum hydrocarbons (fig. 54; table 6). For the underlying Upper and Middle Jurassic rocks below 6,000 ft (1,829 m), the more hydrogen-poor, gas-prone kerogens have thermal-pyrolysis hydrogen indices (S_2/Org. C) that average 161 and 193 mg HC/g Org. C, respectively (fig. 54). Hunt (1979) has shown that the hydrogen to carbon ratios for the inertinite type of kerogen fall within the 0.3 to 0.45 range, whereas the woody type of humic kerogen has hydrogen to carbon ratios from 0.3 to 1.0. The hydrogen to carbon ratios for these Cretaceous and Jurassic sediments are in the 0.5 to 0.8 range and are more consistent with a woody humic type rather than a coaly (inertinite) type of kerogen (fig. 54).

Below about 9,600 ft (2,926 m) the Upper and Middle Jurassic strata of the COST No. G-2 well are predominantly calcareous shales, limestones, dolomites, and anhydrites. The carbonate and evaporite strata are believed to have been deposited in shallow-water, restricted marine environments, and contain only small amounts of terrestrially derived (type III) kerogens (fig. 54). The terrestrial (type III) kerogens present in these carbonate strata are believed to be largely recycled. Highly carbonized organic matter such as inertinite is fairly resistant to weathering and may be transported without significant further loss of hydrogen to new depositional basins and mixed with young, thermally immature organic matter (Tissot and Welte, 1978). If the organic matter that has been identified as inertinite or coal in the COST No. G-2 well is truly as abundant as indicated by Core Laboratories, Inc., then the potential for generation of gas is very poor (fig. 54). On the other hand, if the woody-humic type III kerogens are more abundant, as the hydrogen to carbon ratios seem to suggest, then the potential for gas generation may be significant, depending upon the abundance of primary solid organic matter and the time and intensity of thermal maturation.

The possibility of mud additive contamination or coaly cavings cannot be discounted as a cause of the inconsistent kerogen-type determinations. Moreover, the probability of two laboratories receiving totally and consistently dissimilar sample suites seems rather remote. Therefore, the reported differences in the kerogen types and their relative abundances may be related to the analytical techniques and methods employed in

the preparation and identification of the kerogen types.

The TAI, vitrinite reflectance (R_o), CPI, and temperature of maximum pyrolysis yield (T_{S_2}) maturation parameters for the G-2 well samples are shown in figure 55. During the thermal maturation process (as the burial depth and temperature increase), the breaking of carbon-carbon bonds occurs more and more frequently, and, depending upon the predominant type of organic matter, varying proportions of light (C_1 to C_4) hydrocarbons and gasoline range (C_4 to C_7) hydrocarbons are produced (Tissot and Welte, 1978). The profiles of the concentrations of the C_1 to C_4 and C_5 to C_7 hydrocarbons, the percent gas wetness, and the $n\text{-}C_4/n\text{-}C_7$ molecular ratio are shown in figure 56. Although the $n\text{-}C_4/n\text{-}C_7$ ratio is less than unity in several isolated intervals of the COST No. G-2 well, the effect of diesel fuel on the thermal maturation characteristics of the C_{15+} liquid hydrocarbons below 12,000 ft (3,660 m) is believed to be minimal. The total concentration of C_1 to C_7 hydrocarbons in the Cretaceous and Jurassic strata is low, usually less than 1500 ppm, which may be related to the poor source-rock quality.

The two sets of TAI data are inconsistent in their description of the levels of thermal maturity for similar burial depths (fig. 55). Because the TAI profile established by Core Laboratories, Inc., includes samples down to a burial depth of only 12,000 ft (3,658 m), their data do not permit the development of a complete, comparative thermal maturation interpretation of the COST No. G-2 well and will not be discussed further. The TAI values reported by GeoChem Laboratories, Inc., include samples from the entire well and are discussed below. The level of thermal maturation indicated by Core Laboratories, Inc., vitrinite reflectance (R_o) measurements is inconsistent with and abnormally high when compared with the level of thermal maturation indicated by the liquid C_{15+} hydrocarbon CPI ratios and the thermal pyrolysis yield (T_{S_2}) values, and by the TAI values reported by GeoChem Laboratories, Inc.

Below 3,500 ft (1,067 m) the vitrinite reflectance values appear to be grouped into several families of straight-line relationships, each with a slightly different slope, that may suggest the presence of different past geothermal gradients. Any offset at the breakpoint of the straight-line relationship has been interpreted by Dow (1977) to signify a possible unconformity (fig. 55). The possibility of recycled organic matter as a factor in the unusually high vitrinite reflectance measurements must not be discounted. If the level of thermal maturation were as advanced, for such shallow burial depths, as the vitrinite reflectance values suggest, then the concentrations of C_1 to C_4 light hydrocarbons and C_4 to C_7 gasoline-range hydrocarbons generated would be expected to be much greater. Furthermore, the saturated paraffin-naphthene hydrocarbon molecular distribution and composition would be expected to show a more mature character. Because the TAI values determined by GeoChem Laboratories, Inc., and the CPI values and thermal pyrolysis measurements made by the USGS are in agreement, it is believed that the threshold of intense oil generation begins between 9,000 and 10,000 ft (2,743 and 3,048 m) in the COST No. G-2 well, and peak generation and maturation processes occur between about 14,000 and 18,000 ft (4,267 and 5,486 m). It is important to note that the threshold or transition temperature of intense oil generation tends to be higher or to occur at greater burial depths in carbonates than in shales. This tendency is consistent with the idea that the activation energy for kerogen decomposition in limestones and dolomites would be higher than in clays because of the catalytic effect of the clays (Hunt, 1979). Localized zones of high heat flow may play a significant role in thermal maturation within the Georges Bank basin and the possibility may exist for dry gas generation in the Jurassic of the COST G-2 area below 18,000 ft (5,486 m). However, because of the poor-to-fair quality of the source rocks, the potential for significant resources may be reduced.

SUMMARY AND IMPLICATIONS FOR OIL AND GAS GENERATION

The Tertiary strata of the COST No. G-1 well (1,013 to 1,030 ft; 309 to 314 m) and the COST No. G-2 well (1,100 to 1,310 ft; 355 to 399 m) are characterized by thin layers of unconsolidated, coarse quartz sands and light-yellow to buff calcareous muds and siltstones, respectively. Because of the extremely shallow burial depths, the thermally immature nature of the lignitic to

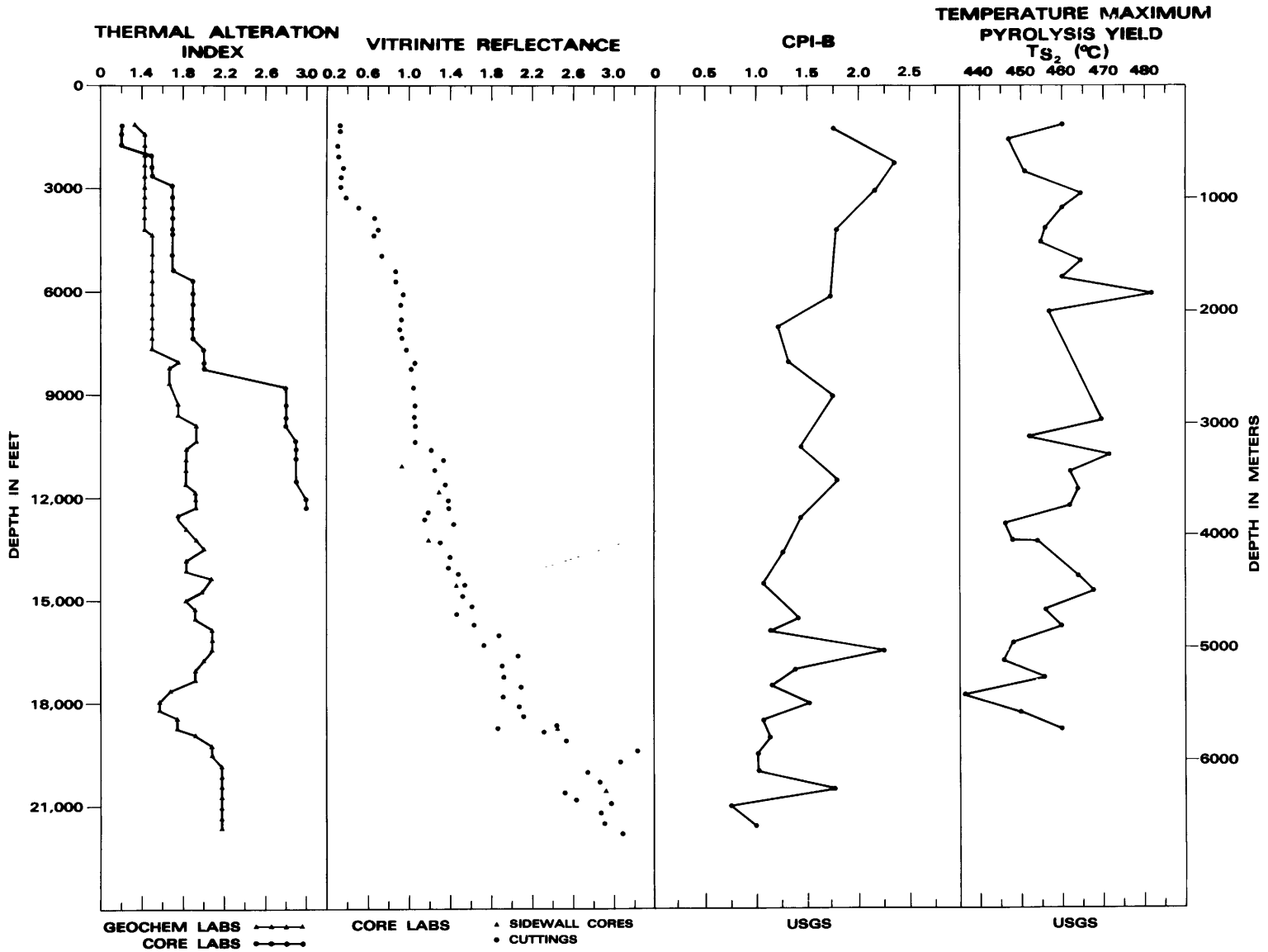

FIGURE 55.—Maturity profiles of organic matter as a function of depth of burial for samples from the COST No. G-2 well.

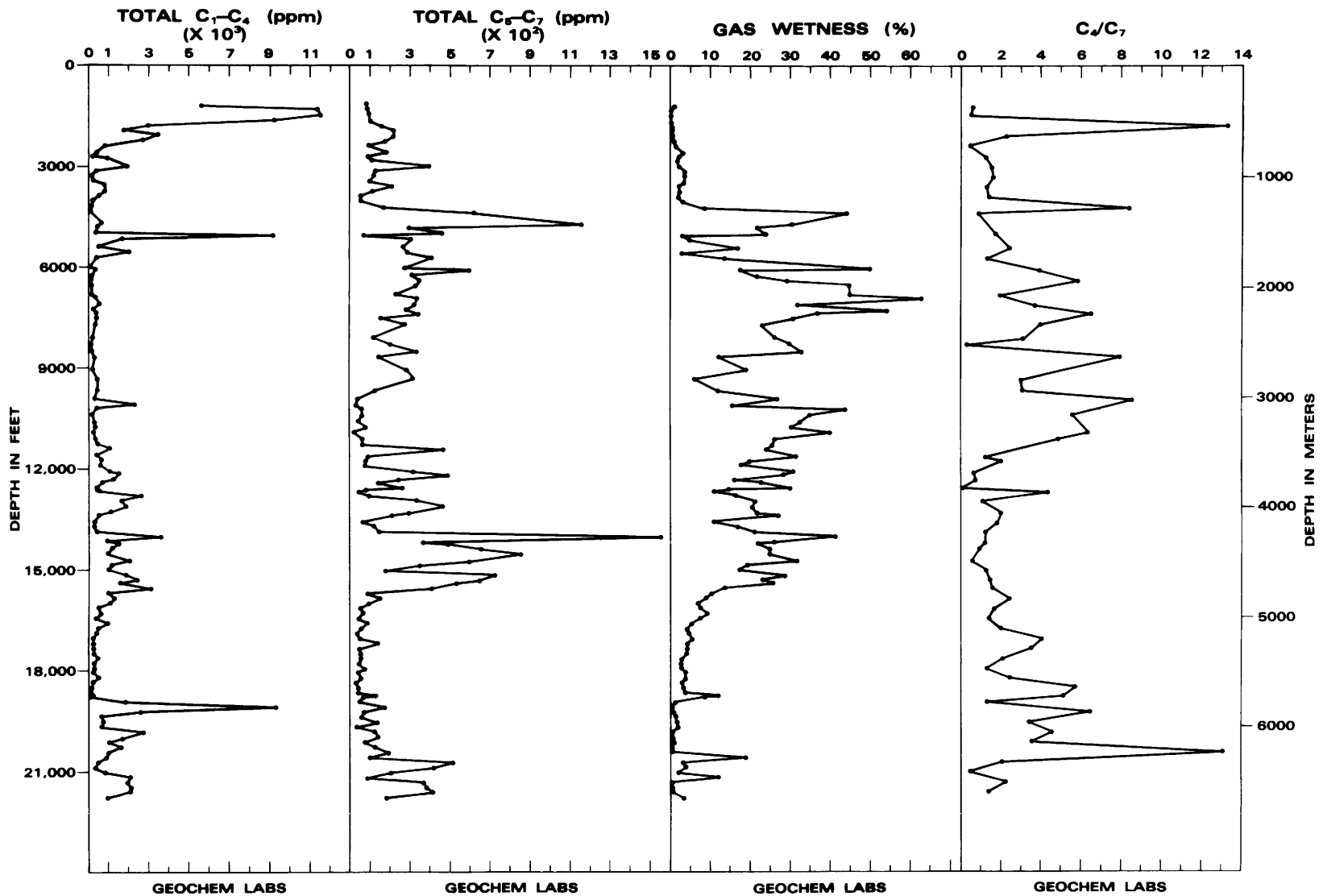

FIGURE 56.—Summary of C_1 to C_7 hydrocarbon analyses of samples from the COST No. G-2 well.

woody kerogens, and the character of the extractable organic matter, the Tertiary is not considered a target for oil or natural gas exploration in the Georges Bank region.

Cretaceous strata were penetrated in the COST No. G-1 well from 1,030 to 5,290 ft (314 to 1,612 m) and in the COST No. G-2 well from 1,310 to 5,960 ft (399 to 1,817 m). Source-rock richness characteristics for the Cretaceous in these two wells are in the poor-to-fair quality range. This interpretation is based on the average total organic carbon values of 0.46 to 0.85 (weight percent), and average total extractable hydrocarbons of 33 and 93 ppm for the G-1 and G-2 wells, respectively. The Cretaceous kerogens have hydrogen to carbon ratios that range from 0.63 to 0.97. Such ratios are comparable with type II and III terrestrially derived, hydrogen-poor, humic, gas-prone kerogens. The molecular distribution and concentration of the C_{15+} saturated paraffin-naphthene hydrocarbons, the low temperature of maximum pyrolysis yield (T_{S_2}), and TAI levels of 1.4 to 1.6 suggest that the Cretaceous extractable organic matter and kerogens have not yet experienced a sufficient time and temperature history to allow the generation of petroleum hydrocarbons and gas.

The vitrinite reflectance values suggest that a much higher degree of thermal maturity may have existed during the Cretaceous of the Georges Bank basin than is suggested by the other light optical, pyrolysis, and geochemical maturation parameters. This inferred higher level of thermal maturation may be the result of prior thermal histories imprinted on recycled organic matter. The indigenous extractable hydrocarbons present in the Cretaceous sediments down to 6,000 ft (1,829 m) in the COST Nos. G-1 and G-2 wells are believed to be thermally immature and have not been produced by petroleum-generating processes.

The potential for mud-additive influence from diesel fuel or other additives such as barite, spersene, bentonite, carboxymethylcellulose, pipe dope, and lignosulfonate (leonardite) cannot be disregarded. The mud-additive effects are not believed to have been pervasive but rather are restricted to certain zones, influencing the character of the indigenous C_{15+} hydrocarbons at specific intervals in the Jurassic below 12,000 ft (3,660 m). The mud-additive effect on the extractable organic matter is believed to be localized and restricted because of the consistently low total organic carbon values and the lack of a uniform mud-additive fingerprint on the hydrocarbon molecular composition and distribution of the entire suite of samples.

The Middle Jurassic strata of the COST No. G-2 well below 13,650 ft (4,161 m) are characterized by abundant shallow-water dolomite, limestone, and anhydrite-evaporite facies. The Jurassic section of the G-1 (5,290 to 15,630 ft; 1,612 to 4,764 m) has a higher percentage of sand and silt, and less carbonate and argillaceous sediment than the G-2. This difference is also reflected in the distribution and type of the solid organic matter in the samples. The Jurassic kerogens in the G-1 are predominantly terrigenous, humic, and gas-prone (type III), with little of the hydrogen-rich, oil-prone (type I) variety. The Jurassic strata of the G-2 (5,960 to 21,874 ft; 1,817 to 6,667 m) contain amorphous and algal (type I) gas-prone and herbaceous (type II) and woody (type III) kerogens. In the COST No. G-1 well, the average total organic carbon values for the Upper, Middle, and Lower Jurassic samples are 0.73, 0.25, and 0.11 weight percent, respectively, and the values for total extractable hydrocarbons in these strata are 38, 36 and 39 ppm, respectively. These source-rock organic-richness values are considered to be very poor to poor. For the Upper and Middle Jurassic shales of the COST No. G-2 well, the average total organic carbon values are 0.62 and 0.23 weight percent, and the average total-extractable-hydrocarbon concentrations are 155 and 170 ppm, respectively. Although the source-rock organic-richness characteristics of the G-2 Jurassic strata appear to be better than those of the Jurassic in the G-1, such values only indicate a poor-to-fair oil and gas source rock potential.

The possibility exists that oxidized vitrinite or recycled organic matter in the Jurassic of the COST Nos. G-1 and G-2 wells may have influenced the vitrinite reflectance values by imparting abnormally high thermal-maturity levels acquired from earlier thermal histories. Because of the consistent agreement between the temperature of maximum pyrolysis yield (T_{S_2}), the thermal alteration index, and the molecular distribution and concentration of the C_{15+} hydrocarbons, the peak of liquid hydrocarbon generation is placed at burial depths of about 13,000 to 15,000 ft (3,962 to 4,572 m) in the COST G-1. The

depth of peak petroleum generation is believed to occur in the COST G-2 between 14,000 and 18,000 ft (4,267 and 5,486 m).

In the COST No. G-1 well, the thermal-chemical maturation processes may be influenced by the presence of localized metamorphism. How representative the thermal maturity data from the COST Nos. G-1 and G-2 wells may be for a regional view of the Georges Bank basin is open to question, because the basin appears to be characterized by a complex thermal and burial history, and the effects of possible overburden loss in the Tertiary and Cretaceous have not yet been evaluated. Localized zones of abnormally high heat flow may have existed along with patches of organic-rich Jurassic evaporite-reefal carbonate rocks. Such factors are believed to be critical in controlling the maturation processes and occurrence of possible deep Jurassic gas. Because of the predominance of the hydrogen-poor kerogens, the potential for generation may exist at greater depths in the vicinity of the COST No. G-2 well. However, because of the poor to fair source-rock quality, the commercial attractiveness may be significantly diminished.

Thermal History of the Georges Bank Basin

Michael A. Arthur

A study of the thermal history of the Atlantic continental margin basins is necessary for an evaluation of the possibility of generating hydrocarbons from potential source rocks. The depths at which petroleum and thermogenic gas may have been generated can be estimated from present-day thermal gradients taken from well temperature logs (Tissot and others, 1974), but this approach is more useful for near-surface, younger sedimentary horizons (100–120 m.y. old), which probably have not been affected by burial temperatures higher than those existing today. However, the older, more deeply buried strata, particularly those deposited within 50–70 m.y. after the initiation of rifting along the Atlantic continental margin, may have been initially subjected to higher temperatures and may have generated hydrocarbons early in their evolution. The thermal gradient probably decreases both through time and with depth in sedimentary basins along rifted passive margins (Royden and others, 1980). Also, older strata such as those in thinner sedimentary sequences on the continental rise may have been heated sufficiently to produce significant amounts of petroleum or gas early in the history of sedimentation without deep burial. Therefore it is important to know the thermal history of a sedimentary basin as well as its modern thermal gradient, because generation and preservation of petroleum hydrocarbons is a function of both time and temperature (Waples, 1980).

The purpose of this paper is to discuss aspects of the present-day thermal gradient and the thermal history of the Georges Bank basin based on data from the COST Nos. G-1 and G-2 wells. Aspects of basin subsidence, sedimentation, and continental margin evolution are discussed with regard to the indications of thermal maturity in sedimentary organic matter and possible hydrocarbon generation in the Georges Bank basin. The discussion of thermal history is based largely on recent models of the thermal evolution of passive margins (Steckler and Watts, 1978; Royden and others, 1980; Angevine and Turcotte, 1981) and is intended only to place some limits on estimates of the petroleum potential of the landward part of the Georges Bank basin.

PRESENT-DAY THERMAL GRADIENT

Figure 57 illustrates the downhole temperature profiles for the COST Nos. G-1 and G-2 wells based on Schlumberger temperature logs (Scholle and others, 1980). The geothermal gradients calculated by applying linear regression analysis to these data (Jackson and Heise, 1980; Heise and Jackson, 1980) are 1.26° F per 100 ft (23.0° C/km) for the G-1 well and 1.34° F per 100 ft. (24.4C/km) for the G-2 well. Jackson and Heise (1980) and Heise and Jackson (1980) have "corrected" the temperature log data at several depths to remove the effects of drilling (normalized to a 25-hr post-drilling period) and determined revised gradients of 1.17° F per 100 ft (21.3° C/km) and 1.46° F per 100 ft (26.6° C/km) for the G-1 and G-2 wells respectively. Corrected bottom-hole or near-bottom-hole temperatures were 247° F (119° C) at 16,400 ft (5,000 m) in the G-1 and 360° F (182° C) at 21,790 ft (6,640 m) in the G-2 well.

The present-day temperature gradients from the Georges Bank COST wells are compared to those of other Atlantic margin COST wells and several other localities in table 7. The gradient at the G-2 well is the highest measured along the Atlantic margin, while that at the G-1 well is close to the average for wells on other parts of the margin. However, it is likely that absolute temperatures and thermal gradients in the lower part of G-1 were once higher because of higher heat flow associated with the extensional thinning of the crust during the rifting in latest

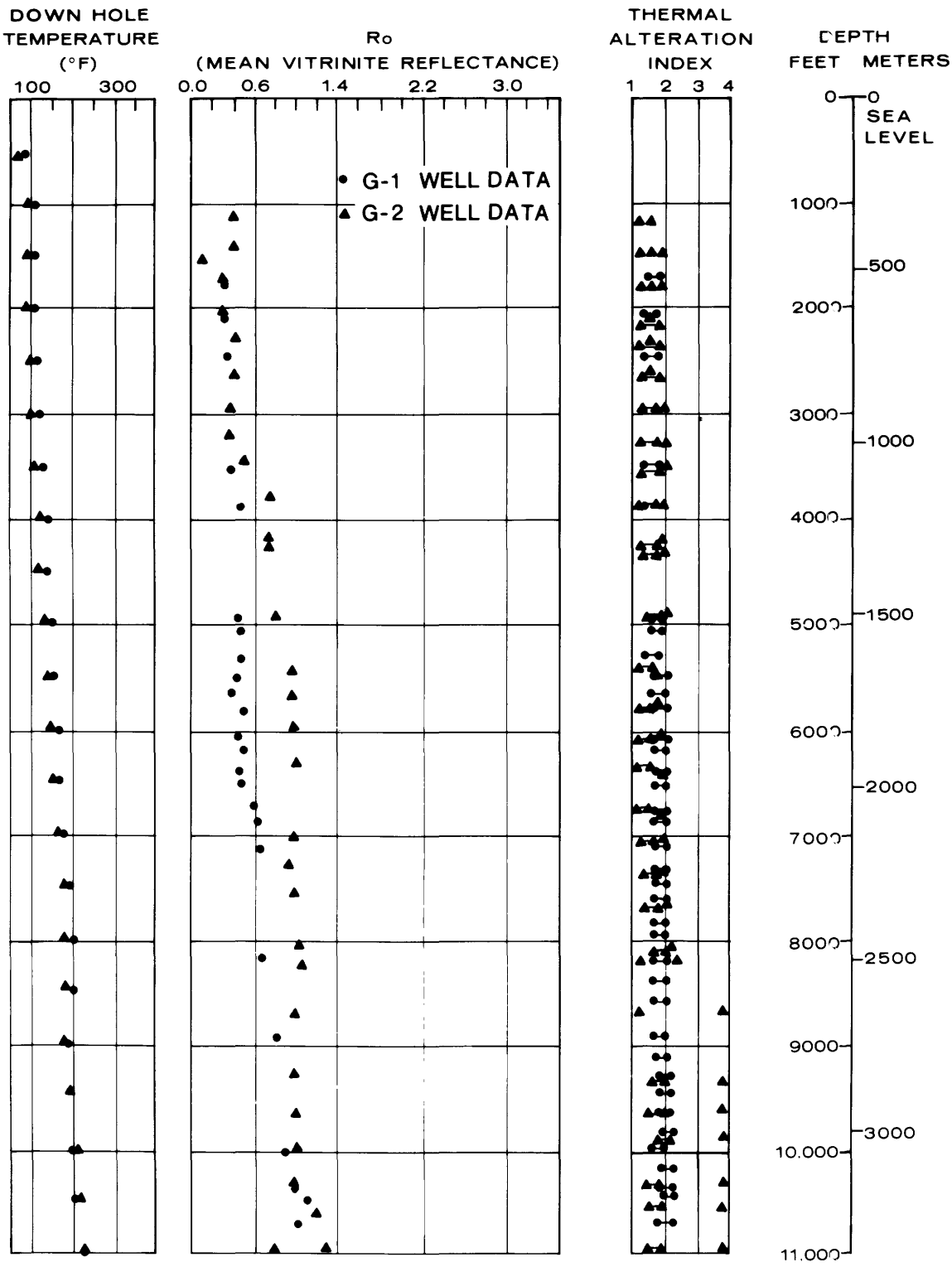

FIGURE 57.—Downhole temperature profiles from temperature logs (Scholle, Krivoy, and Hennessy, 1980; Scholle, Schwab, and Krivoy, 1980), mean vitrinite reflectance values (Superior Oil Co. and Core Laboratories, Inc.), and thermal alteration indices (TAI; GeoChem Laboratories, Inc.) for the COST Nos. G-1 and G-2 wells.

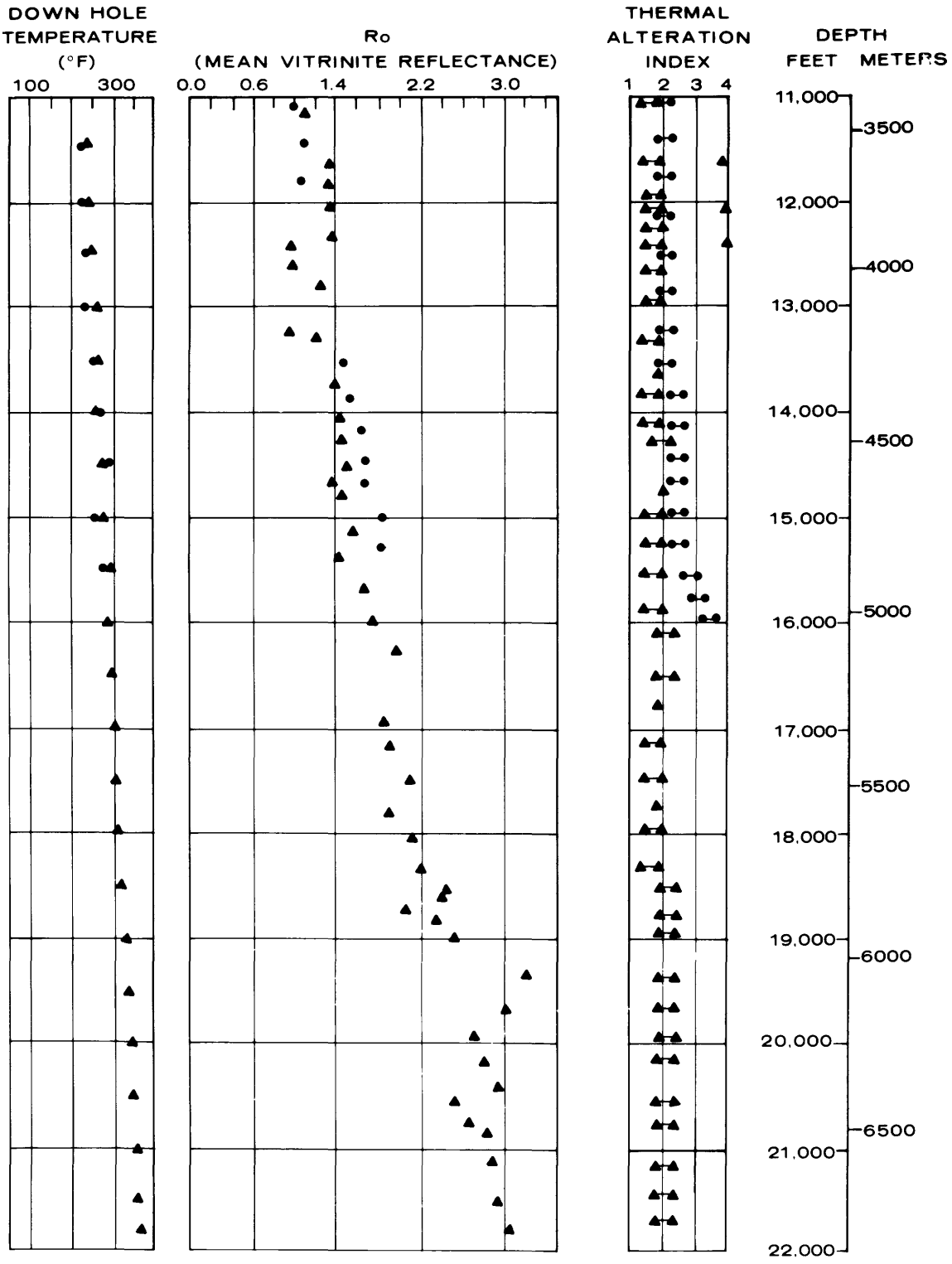

FIGURE 57.—Downhole temperature profiles from temperature logs (Scholle, Krivoy, and Hennessy, 1980; Scholle, Schwab, and Krivoy, 1980), mean vitrinite reflectance values (Superior Oil Co. and Core Laboratories, Inc.), and thermal alteration indices (TAI; GeoChem Laboratories, Inc.) for the COST Nos. G-1 and G-2 wells.—Continued

TABLE 7.—*Geothermal gradients on passive continental margins*

[Data from Jackson and Heise (1980) and Robbins and Rhodehamel (1976)]

Area	Well	Gradient °F/100 ft	Gradient °C/km
Georges Bank	G-1	1.2	22
Do	G-2	1.5	27
Baltimore Canyon	B-2	1.3	24
Do	B-3	1.2	22
Southeast Georgia embayment	GE-1	.9	16
Scotian shelf	[1]	1.2	22
Texas Gulf Coast	[1]	1.6	29
North Sea basin	[1]	1.7	32

[1]Average from several wells.

Triassic-Early Jurassic time. The present-day gradients suggest that there has been no significant hydrocarbon generation above 8,000 ft (2,440 m) in the G-1 well and above 6,700 ft (2,040 m) in the G-2 well, based on the generalizations offered by Pusey (1973) for the "oil window" (150°-300° F; 66°-149° C). Dry gas may be expected below about 18,000 ft (5,490 m) in the G-2 well and below about 16,000 ft (4,870 m) in the vicinity of the G-1 well. Generation of hydrocarbons is a function of time as well as temperature (Lopatin, 1976), and the organic geochemical and thermal maturation data (Miller and others, this volume) generally agree with the estimates given above.

SUBSIDENCE AND THERMAL HISTORY

The subsidence history of the Cost Nos. G-1 and G-2 wells was examined using the method of Steckler and Watts (1978). In this method the sedimentary section recovered in the well is "backstripped" in order to examine the sequential subsidence history of a given part of the continental margin. Sediments of each defined time interval are restored to their former thickness by correcting for compaction, and the amount of subsidence induced by sediment loading is calculated incrementally using the Airy isostatic model and assuming local loading of the crust. The depth to basement after removal of the effects of local sediment (and water) loading are obtained by using the following equation:

$$Y = S^* \frac{(\rho m - \rho s)}{(\rho m - \rho w)} + W_d - \Delta SL \frac{\rho m}{(\rho m - \rho w)}$$

where

Y =depth to basement with no loading ("tectonic component of subsidence")

S^*=interval sediment thickness corrected for compaction

ρm=density of the upper mantle (assumed 3.3 g/cm^3)

ρs=initial density of a given sediment package (calculated)

ρw=density of seawater (assumed 1.03 g/cm^3)

W_d=average water depth during a given time interval

ΔSL=eustatic sea level change (relative to today).

The value of S^* was calculated for a given thickness of sediment by determining the change in porosity during compaction. The lithology of much of the COST Nos. G-1 and G-2 wells is variable, so the assumption of constant grain density does not hold and the single porosity reduction curve with compaction used by Steckler and Watts (1978) and Watts and Steckler (1979) in "backstripping" the COST No. B-2 well is not applicable. Therefore, in this study the sedimentary sequence was subdivided into time intervals using the biostratigraphic age assignments of Poag (this volume). These age assignments may be in error, particularly for the Jurassic part of the sequence in which fossils were sparse. The ratios of sand and shale to carbonate and to evaporite sediments was calculated for each sediment interval using lithologic descriptions (Arthur, this volume; Scholle, Krivoy, and Hennessy, 1980; Scholle, Schwab, and Krivoy, 1980). Clastic sediments were assigned an initial porosity of 52 percent, carbonate sediments a porosity of 30 percent, and evaporites a porosity of 10 percent. The precision of this method is inherently low in such generalized calculations.

Estimates of water depth at the time of deposition are based on those of Poag (this volume), and the sea level curve derived by Watts and Steckler (1979) was used to make the eustatic correction. The data and calculations for the COST No. G-2 well are shown in table 8, and this subsidence history is illustrated in figure 58.

Assuming that the amount of "tectonic" subsidence is related to the amount of crustal thinning during initial rifting, Royden and others (1980)

TABLE 8.—*Data used and results of calculations of basin subsidence at the COST No. G-2 well*

[Depth figures are feet below Kelly Bushing (1 ft=0.3048 m). —, not applicable; (?), uncertain]

Interval	Age to top horizon (m.y.)	Depth to top horizon (feet)	Interval thickness (feet)	Cumulative thickness (feet)	Average porosity (percent)	Lithology[1] (percent)	Average density (g/cm³)	Corrected thickness S^* (feet)
Water	—	—	272	21,920	—	—	—	—
Holocene and Pleistocene	0	351	749	21,648	52	95-5-0	2.00	749
Pliocene and Miocene	1.8	1,100	150	20,820	45	95-5-0	2.10	158
Eocene	38	1,250	74	20,670	45	95-5-0	2.10	78
Lower Santonian	80	1,324	376	20,596	42	95-5-0	2.15	409
Coniacian	83	1,700	420	20,220	40	95-5-0	2.10	466
Lower Turonian	90	2,120	150	19,800	37	90-10-0	2.10	169
Upper and middle Cenomanian	92	2,270	60	19,650	37	90-10-0	2.10	68
Aptian	107	2,330	480	19,590	35	90-10-0	2.10	551
Barremian	115	2,810	1,110	19,110	33	90-10-0	2.15	1,296
Hauterivian	120	3,920	590	18,000	30	82-18-0	2.25	696
Valanginian	126	4,510	930	17,410	25	85-15-0	2.35	1,150
Berriasian	131	5,440	480	16,480	25	58-42-0	2.55	565
Tithonian	135	5,920	780	16,000	20	58-42-0	2.65	958
Upper Kimmeridgian	137	6,700	960	15,220	20	70-30-0	2.45	1,204
Lower Kimmeridgian	140	7,660	1,000	14,260	25	80-20-0	2.45	1,226
Oxfordian(?)	142	8,660	1,440	13,260	20	60-40-0	2.50	1,774
Callovian(?)	150	10,100	2,000	11,820	5	42-53-5	2.65	2.665
Bathonian(?)	156	12,100	2,000	9,820	5	20-75-5	2.65	2.568
Bajocian(?) and Aalenian(?)	164	14,100	900	7,820	7	5-62-33	2.95	1.058
Toarcian(?) and Upper Pliensbachian(?)	174	15,000	1,900	6,920	2	12-64-24	2.85	2.391
Lower Pliensbachian(?) and Sinemurian(?)	180	16,900	1,100	5,020	2	8-80-12	2.85	1,401
Hettangian(?) and Rhaetian(?)	189	18,000	3,870	3,920	1	17-50-33	2.85	4.882
Rhaetian(?)	192	21,870	>50	50	4	0-0-100	3.00	50

Interval	Corrected density ρs (g/cm³)	Corrected Cumulative thickness (feet)	Non-load subsidence (feet)	Estimated water depth (feet)	Total non-load subsidence (feet)	Sea level correction (feet)	Corrected subsidence (feet)	Cumulative subsidence (feet)
Water	—	—	—	—	—	—	—	—
Holocene and Pleistocene	2.0	21,970	479	272	751	185	566	13,871
Pliocene and Miocene	1.99	21,171	92	200	292	185	107	13,305
Eocene	1.99	21,027	45	200	345	351	−6	13,198
Lower Santonian	1.98	21,022	240	600	840	596	244	13,204
Coniacian	1.89	20,771	292	600	892	596	292	12,960
Lower Turonian	1.86	20,261	108	200	308	432	−124	12,668
Upper and middle Cenomanian	1.85	20,105	44	300	344	400	−66	12,792
Aptian	1.83	20,136	359	50	409	80	329	12,858
Barremian	1.84	19,818	841	50	891	60	831	12,529
Hauterivian	1.91	18,647	421	50	471	81	390	11,698
Valanginian	1.90	18,158	715	50	765	120	645	11,308
Berriasian	2.17	17,110	285	300	585	135	450	10.663
Tithonian	2.16	16,718	487	60	547	135	412	10,213
Upper Kimmeridgian	1.95	15,976	722	50	772	135	637	9.801
Lower Kimmeridgian	2.00	14,993	709	50	759	135	624	9.164
Oxfordian(?)	2.03	14,086	1,003	50	1,053	(?)	1,053	8.540
Callovian(?)	1.99	12,792	1,553	50	1,603	(?)	1,603	7,487
Bathonian(?)	2.06	10,529	1,418	0	1,418	(?)	1,418	5.889
Bajocian(?) and Aalenian(?)	2.51	8,212	377	0	377	(?)	377	4.466
Toarcian(?) and Upper Pliensbachian(?)	2.26	7,584	1,112	10	1,122	(?)	1,122	4.089
Lower Pliensbachian(?) and Sinemurian(?)	2.24	5,500	664	10	674	(?)	674	2,967
Hettangian(?) and Rhaetian(?)	2.26	4,932	2,271	10	2,281	(?)	2,281	2.293
Rhaetian(?)	2.80	50	12	0	12	(?)	12	12

[1]Relative abundance of clastic, carbonate, and evaporite sediments, respectively.

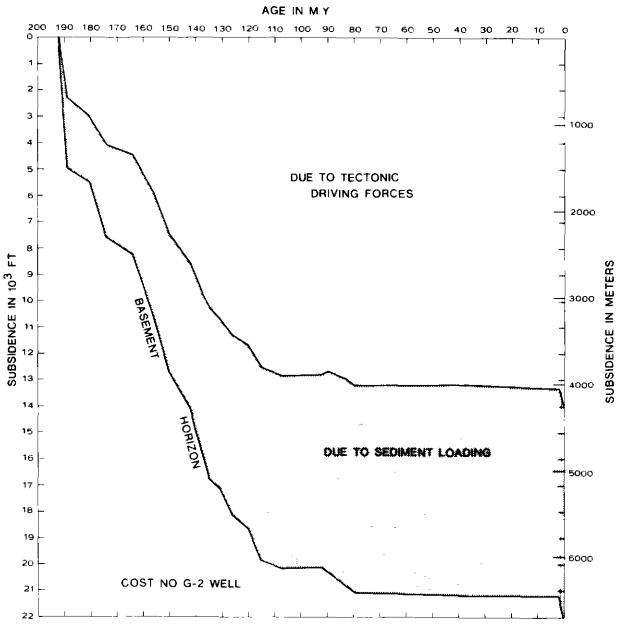

FIGURE 58.—Subsidence history of the basement (194 m.y. B.P.) and sedimentation at the COST G-2 well. Stippled area shows subsidence due to sediment loading assuming local loading and Airy isostasy. The clear portion is that part of the subsidence due to cooling after crustal thinning or dike intrusion following rifting. See text and table 8 for details of reconstruction.

and Angevine and Turcotte (1981) have demonstrated that the history of heat flow in continental margins can be modeled. The heat flow models allow reconstruction of the general thermal history of sedimentary horizons of different ages, assuming decay of the initial heat flux without addition of heat from other sources, an average thermal conductivity for the basin sediment sequence, and continuous thermal equilibrium within the sequence. These are all reasonable assumptions for the Georges Bank basin.

Royden and others (1980) have constructed thermal models for crust of various thicknesses. They defined a factor, γ, which equals 0 for normal continental crust and 1 for oceanic crust. The crust at the COST No. G-2 well was thinned to a γ value of 0.6 on the basis of the calculated amount of "tectonic" subsidence (Sawyer and others, in press), while the crust at the COST No. G-1 well was thinned to a γ value of 0.4. Sawyer and others (in press) arrived at these values using modeling techniques more sophisticated than those used in this study. The total tectonic subsidence derived here (fig. 58) is about 1,640 to 1,969 ft (500–600 m) greater than in the Sawyer and others model.

Figure 59 shows the model of Royden and others (1980) for the evolution of geotherms in a basin in which the initial thinning occurred at about 200 m.y. B.P. and had a γ value of 0.6 (the COST No. G-2 estimate). Estimates of the burial history of several sedimentary horizons are also illustrated. From these data, time-temperature profiles can be constructed (Waples, 1980). These are shown in table 9.

TIME-TEMPERATURE INDICES AND HYDROCARBON MATURATION

On the basis of temperatures of maximum pyrolysis, thermal alteration indices, and the concentrations of C_{15+} hydrocarbons, Miller and others (this volume) have inferred that peak thermal maturation of hydrocarbons occurs between 13,000 and 16,000 ft (3,960 and 4,570 m) in the COST No. G-1 well and between 14,000 and 18,000 ft (4,270 and 5,490 m) in the COST No. G-2 well. Miller and others (this volume) place the "threshold of intense oil generation" at about 9,000 to 10,000 ft (2,750 to 3,050 m) in the COST Nos. G-1 and G-2 wells. The estimated "oil window" occurs between about 8,000 and 16,000 ft (2,440 and 4,570 m) in the G-1 well and between 6,700 and 17,000 ft (2,040 and 5,180 m) in the G-2 well. There is a general agreement between the very general estimates of the "oil window" and organic geochemical indicators of thermal maturity of organic matter.

Vitrinite reflectance values, commonly used indicators of thermal maturity, are shown in figures 60, 61, and 62, (analysis by Superior Oil Company for the COST No. G-1 well and by Core Laboratories, Inc., for the COST No. G-2 well). Thermal alteration indices (TAI, figs. 57 and 60) were determined by GeoChem Laboratories, Inc. A vitrinite reflectance (R_o) value of 0.6 is believed to represent the onset of thermal maturation and hydrocarbon generation (Dow, 1977; Hunt, 1979). This value occurs at an anomalously shallow depth of about 3,800 ft (1,160 m) in the G-2 well in Cretaceous sediments and at about 7,000 ft (2,130 m) in the G-1 well in Upper Jurassic sedimentary rocks. The "oil floor" (R_o = 1.35) should occur at about 13,500 ft (4,120 m) in the G-1 well and 11,500 ft (3,510 m) in the G-2 well. However, Miller and others (this volume) have discussed the other indications of organic

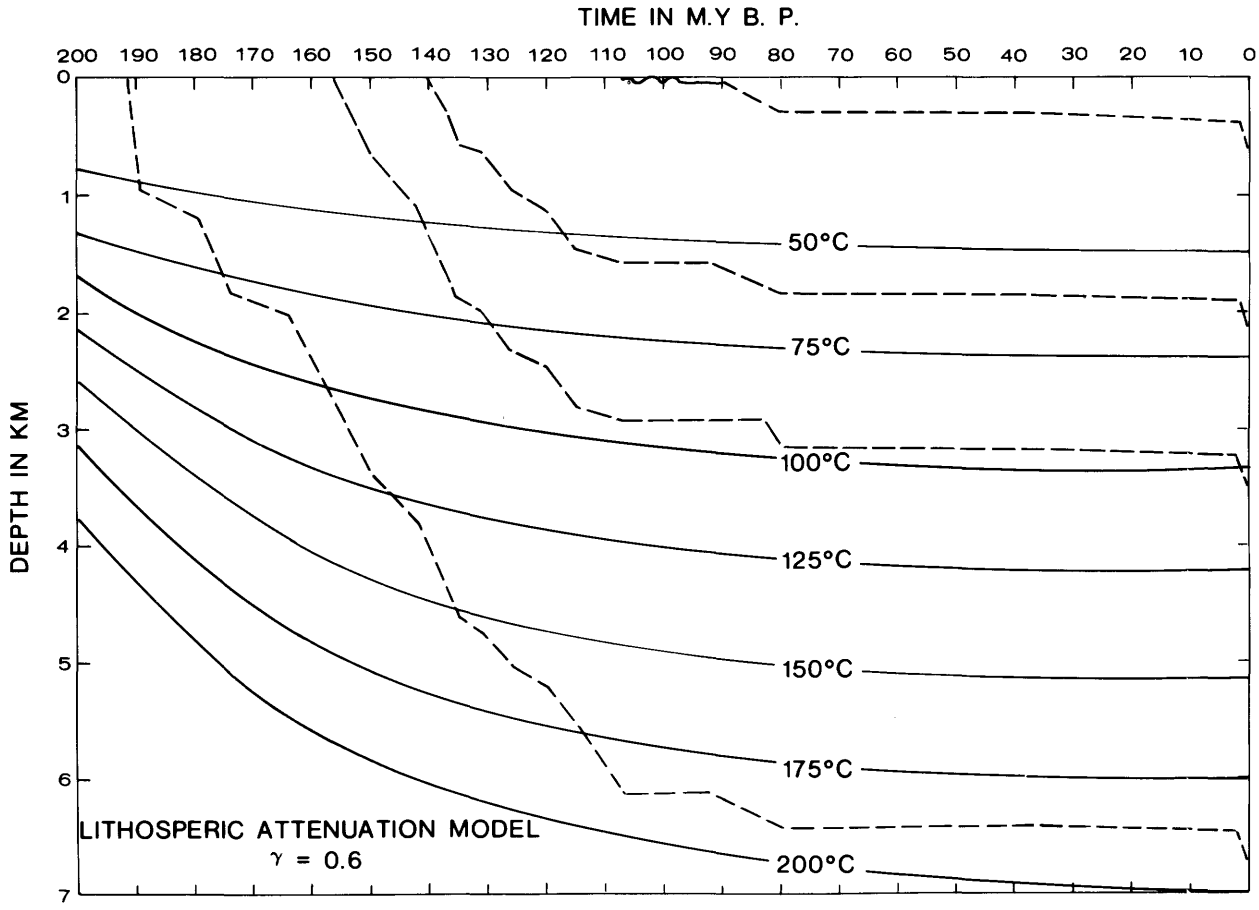

FIGURE 59.—Thermal model based on the amount of crustal thinning (γ=0.6) at the COST No. G-2 well (after Royden and others, 1980). The burial histories of sediments approximately 191, 156, 140, and 107 m.y. old (dashed lines) are shown relative to the time-temperature field. These traces were used to calculate the time-temperature indices in table 9.

maturation, which conflict with the vitrinite reflectance data in the COST No. G-2 well. Figure 60 suggests that vitrinite reflectance values are generally too high when compared with TAI in the same samples.

It is possible that the anomalous reflectance values are from reworked or highly oxidized vitrinite derived from a previous sedimentary cycle, or that there is some nonsystematic error in the reflectance determinations. The first possibility is geologically reasonable, but the COST Nos. G-1 and G-2 wells do not exhibit the same pattern of reflectance values with depth, as would be expected if the sediment at both wells was derived from the same source. The reflectance values increase normally and systematically downhole in the G-1 well (figs. 61, 62), and R_o values of equivalent strata in the G-2 well are considerably higher, which suggests errors in the measurements for the G-2 well or bias towards the higher rank vitrinite in each sample.

Figure 62 is a semilog plot of vitrinite reflectance and downhole temperature. The G-1 data plot on a straight line segment with relatively little scatter, suggesting that the values are reasonable and that they increase in a predictable fashion with increasing temperature. The G-2 data define several line segments having different slopes. The values from about 12,750 ft (3,890 m) to the bottom of the hole define a line having about the same slope as the G-1 data. This pattern suggests that the G-2 data from the Jurassic and older section may be accurate. In fact, they reflect a somewhat lower reflectance value for a given temperature than do the G-1 data. The problem occurs in the reflectance values from 914 to 12,750 ft (278 to 3,890 m) in the G-2 well. These data suggest an anomalous

TABLE 9.—*Time-temperature indices for representative horizons in the COST No. G-2 well*

[TTI, time-temperature index; r^n, assumed increase in rate of maturation relative to the 100 °—110 °C interval, as described in Waples (1980)]

Temp. interval (°C)	r^n	Δ Time (m.y.)	Interval TTI	Total TTI	m.y. B.P.	Equivalent R_o
191-m.y.-old sediment (now at 20,000 ft (6,096 m))						
20–30	2^{-8}	1.0	.004	.004	190	<0.3
30–40	2^{-7}	0.5	.004	.008	189.5	<.3
40–50	2^{-6}	0.5	.008	.016	189	<.3
50–60	2^{-5}	10	.32	.33	179	<.3
60–70	2^{-4}	4	.26	.59	175	<.3
70–80	2^{-3}	2	.25	.84	173	<.4
80–90	2^{-2}	14	3.5	4.34	159	.5
90–100	2^{-1}	4	2.0	6.34	155	.55
100–110	1	3.5	3.5	9.84	151.5	[1]0.6
110–120	2	4	8	17.8	147.5	[1] .65
120–130	2^2	9	36	53.8	138.5	[1] .9
130–140	2^3	4	32	85.8	134.5	[1]1.05
140–150	2^4	2.5	40	125.8	132	[1]1.2
150–160	2^5	8.5	272	397.8	123.5	1.7
160–170	2^6	11	704	1,108.8	112.5	2.1
170–180	2^7	6	768	1,869.8	106.5	3.8
180–190	2^8	110	28,160	30,029.8	—	4.2
156-m.y.-old sediment (now at 12,100 ft (3,688 m))						
20–30	2^{-8}	6	.024	.024	150	<0.3
30–40	2^{-7}	3	.024	.048	147	<.3
40–50	2^{-6}	3.5	.056	.114	143.5	<.3
50–60	2^{-5}	3.5	.112	.226	140	<.3
60–70	2^{-4}	6	.384	.610	134	<.3
70–80	2^{-3}	9	1.13	1.73	125	.45
80–90	2^{-2}	7	1.75	3.48	—	.5
90–100	2^{-1}	118	59	62.48	118	[2] .95
140-m.y.-old sediment (now at 7,680 ft (2,340 m))						
20–30	2^{-8}	9	.036	.036	131	<0.3
30–40	2^{-7}	6	.048	.084	125	<.3
40–50	2^{-6}	4	.064	.148	121	<.3
50–60	2^{-5}	32	1.02	1.17	89	.4
60–70	2^{-4}	89	5.70	6.87	—	[3] .55

[1]In empirical oil-generation window between 11,480 and 15,580 ft (3,500 and 4,750 m) burial depth (only 50 m.y. after deposition).
[2]In oil-generation window at approximately 95 m.y. B.P. at burial depth of 9,500 ft (2,900 m).
[3]Immature.

thermal event that affected only the Upper Jurassic through Upper Cretaceous section of the COST No. G-2 well. Although such a thermal event would not be impossible, it is unlikely that the heating would have increased vitrinite rank without altering TAI values or other indicators of thermal maturity. Therefore the anomalously high average R_o values probably do not reflect such an event.

Despite the problem with the vitrinite reflectance values in the G-2 well, the estimates of thermal maturity by Miller and others (this volume) are in general agreement with the thermal model approach. Different estimates are obtained from models of the thermal history of the sediments. The thermal model constructed in figure 59 was used to calculate time-temperature indices (TTI shown in table 9; method outlined by Waples, 1980) for the following horizons at the COST No. G-2 site: 191 m.y. (20,000 ft; 6,100 m present depth); 156 m.y. (12,000 ft; 3,690 m present depth); 140 m.y. (7,680 ft; 2,340 m present depth); and 107 m.y. (2,330 ft; 710 m present depth). The burial history of each of these sedimentary layers is shown superimposed on the theoretical depth distribution of temperature through time in the Georges Bank basin. The calculation of TTI for each horizon gives a general indication of the thermal maturity of each horizon, based on the data of Waples (1980).

The organic matter in the strata near the base of the G-2 well is overly mature on the basis of the calculated TTI; that is, below the "oil window" but still within the dry gas stability field. The TTI history indicates that these strata reached the oil window within 50 m.y. after their

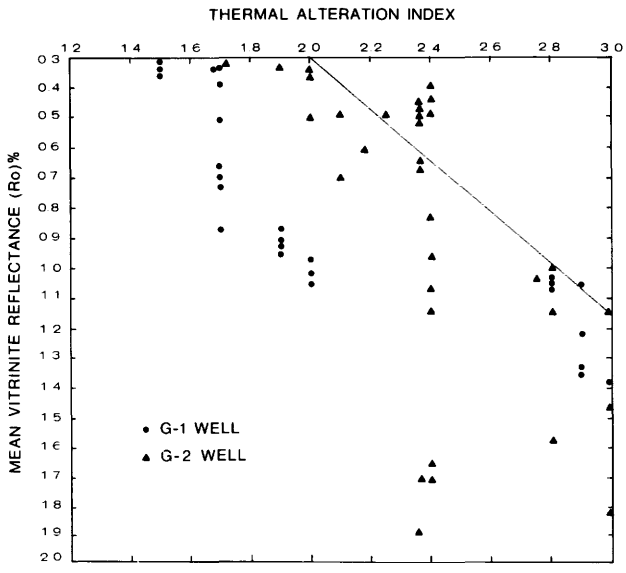

FIGURE 60.—Mean vitrinite reflectance values versus thermal alteration indices (TAI) for samples from COST wells G-1 and G-2. Line indicates optimum relationship between the two values.

deposition (at a burial depth of about 11,500 ft (3,500 m)). The TTI values also indicate that these strata remained within the "oil window" for only 15 m.y. TTI estimates suggest that those units presently buried deeper than 18,000 ft (5,490 m) are overly mature.

The onset of thermal maturation of the organic matter in the sediments deposited about 156 m.y. B.P. is estimated to have occurred about 95 m.y. B.P. at a depth of about 9,514 ft (2,900 m). The stratum is still within the zone of hydrocarbon generation based on calculated TTI values.

The organic matter laid down at 140 m.y. B.P. is still immature on the basis of TTI values. Sediments near the G-2 well above about 8,500 ft (2,600 m) have TTI values that apparently indicate thermal immaturity, which is consistent with the organic geochemical data.

The models suggest that the thermal history of the area surrounding the COST No. G-1 well was similar to that at the G-2 well except for somewhat lower temperatures at given depths in G-1. Therefore the maturation horizons should be lower in the G-1 well, which is in agreement with the present-day difference in thermal gradient at the two wells, but not with the organic maturation indicators.

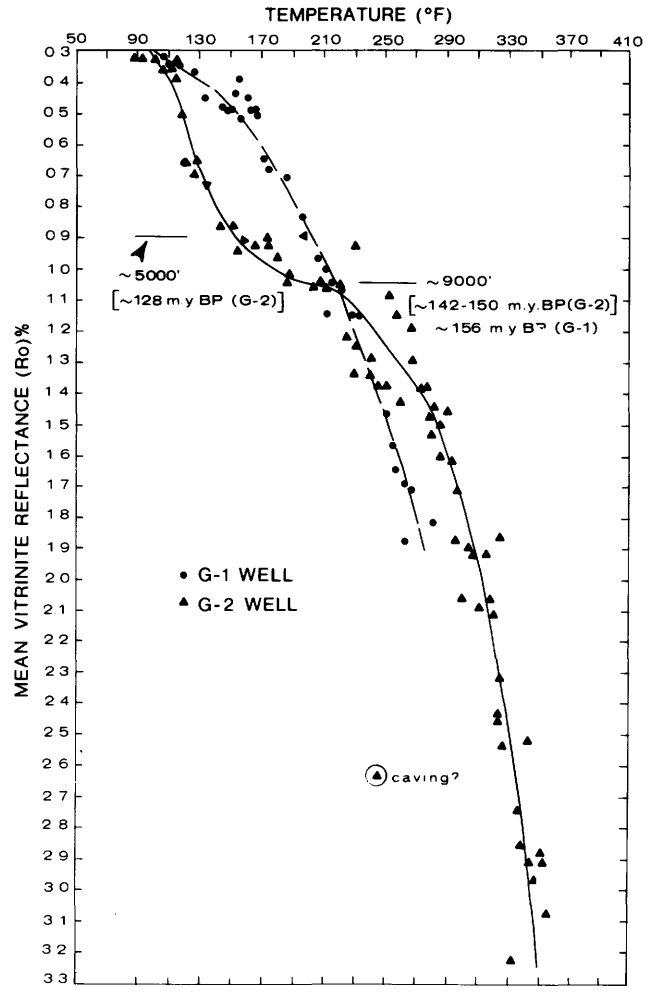

FIGURE 61.—Mean vitrinite reflectance (R_o) versus present in situ temperature (linear plot) for samples from COST wells Nos. G-1 and G-2. Note differences between the two wells.

CONCLUSIONS

There is conflicting evidence of the degree of thermal maturation of organic matter in the COST Nos. G-1 and G-2 wells. The estimates of Miller and others (this volume) are that peak thermal maturation occurs between 13,000 and 15,000 ft (3,960 to 4,570 m) in the COST No. G-1 well and at 14,000 to 18,000 ft (4,270 to 5,490 m) in the COST No. G-2 well, with the "threshold of intense oil generation" occurring in both wells at about 9,000 to 10,000 ft (2,750 to 3,050 m). These estimates are based mainly on the concentration of C_{15+} hydrocarbons, the temperatures of maximum pyrolysis, and thermal alteration index (TAI) values. The modern thermal gradient at the two wells, the vitrinite reflectance values, and

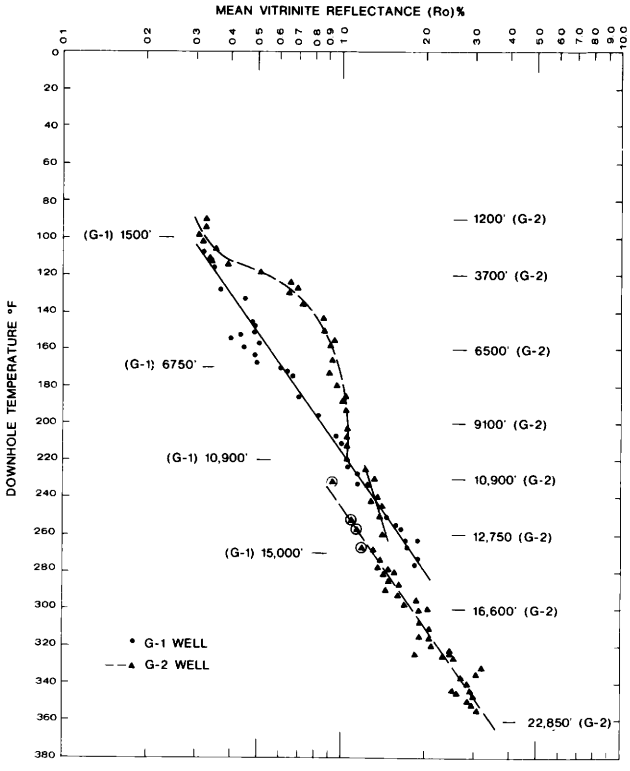

FIGURE 62.—Semilog plot of mean vitrinite reflectance (R_o) versus present in situ temperature for samples from COST wells Nos. G-1 and G-2.

thermal models and calculated time-temperature indices (TTI) suggest that the onset of thermal maturation should occur at slightly shallower depths in the two wells; a depth of 8,500 ft (2,590 m) in the G-2 well seems reasonable for the beginning of thermal maturity. TAI values below this depth are around 2 and the carbon preference index (CPI) is about 1.5 and decreases downhole. These values are taken as an indication of the onset of thermal maturity.

Previous estimates of the depth of the beginning of maturation in other Atlantic area COST wells are about 9,000 ft (2,750 m) in the GE-1 well, 11,300 ft (3,450 m) in the B-2 well, and 14,300 ft (4,350 m) in the B-3 well. The COST No. G-2 well does have the highest present-day geothermal gradient of these wells; however, thermal maturation is affected by the richness and type of organic matter in the sediment. Therefore the prospects for significant generation and accumulation of oil and gas from in situ sources in the Georges Bank basin near the COST No. G-1 or G-2 well are not good, regardless of the thermal history of the basin. (See Miller and others, this volume.)

Geophysical Studies of the COST Nos. G-1 and G-2 Wells

David J. Taylor and R. C. Anderson

Digital well log data from the COST Nos. G-1 and G-2 wells were used to compute subsurface velocities and synthetic seismograms. The interval-traveltime log from each well was integrated over each respective depth range, producing a relationship between depth and two-way traveltime for a seismic wave propagating through the subsurface. This relationship was used to convert the suite of well logs recorded as a function of linear depth to linear functions of time. The interval-traveltime log also provided other velocity information relevant to seismic reflection processing and interpretation. Synthetic seismograms were also computed using the velocity and density logs from the wells. The synthetic seismograms were bandpass filtered to match the seismic field data for correlation, and then spliced into the seismic line at the appropriate location.

VELOCITY INFORMATION

The average velocity function, shown in figure 63 for the COST No. G-1 well and figure 64 for the COST No. G-2 well, can be used to compute the depth of a seismic reflection given its one-way time position. Average velocities are also used in the migration processing of seismic data in areas of geologic structure. The root-mean-square velocity shown on the same plots can be used for computing normal-moveout times, an important step to perform prior to the stacking process of multifold seismic reflection data. These velocities are only applicable in areas where the subsurface layers are relatively flat.

The curve that relates depth to two-way traveltime below the sea floor is shown in figure 65 for both wells. Because the wells are fairly close to each other, the curves nearly overlap throughout the extent of the logs. This crossplot can be used directly to determine the depth of a reflector given its two-way time position on the seismic line.

SEISMIC DATA

Two multichannel seismic reflection lines were recorded for the USGS in 1977 by Digicon, Inc. of

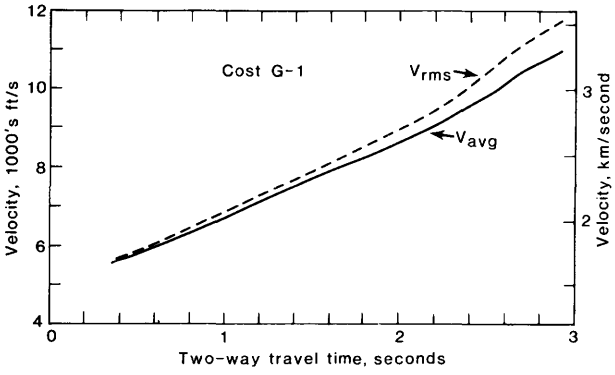

FIGURE 63.—Average velocity (V_{avg}) and root-mean-square velocity (V_{rms}) as a function of two-way traveltime from sea-level datum for the COST No. G-1 well.

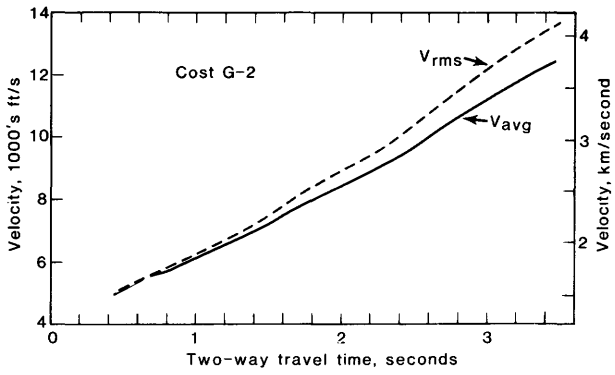

FIGURE 64.—Average velocity (V_{avg}) and root-mean-square velocity (V_{rms}) as a function of two-way traveltime from sea-level datum for the COST No. G-2 well.

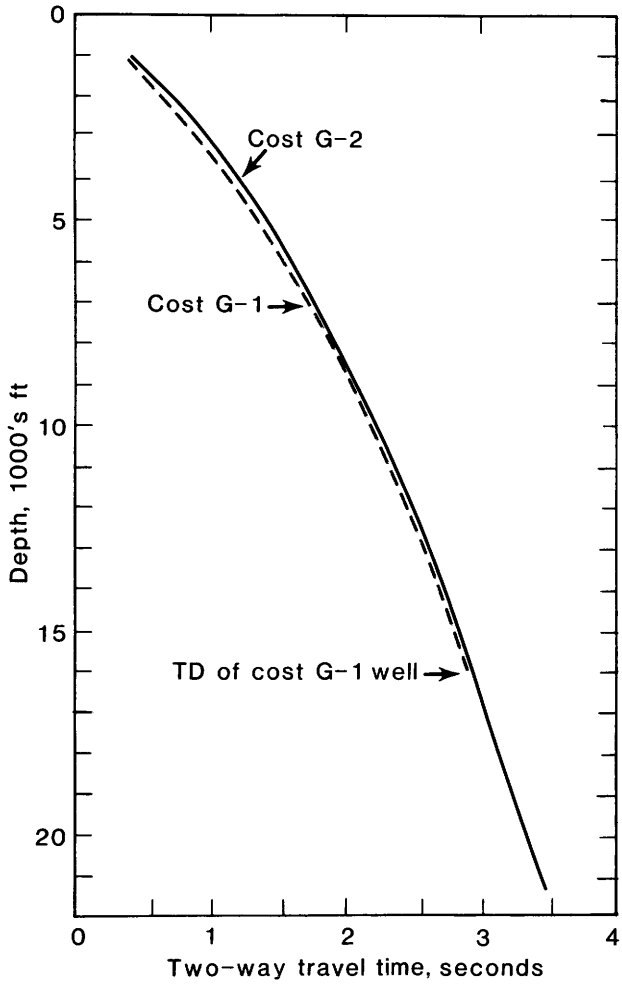

FIGURE 65.—Two-way traveltime below sea-level datum as a function of depth for the COST No. G-1 and COST No. G-2 wells.

Houston, Tex., to tie the COST Nos. G-1 and G-2 wells into the regional network of USGS multichannel seismic reflection lines on the Atlantic Outer Continental Shelf (AOCS). The orientations of these seismic lines with respect to regional USGS seismic reflection lines and the Cost Nos. G-1 and G-2 well locations are shown in figure 66. Line 77-1 crosses the COST No. G-1 well at shotpoint 95, and line 77-2 crosses the COST No. G-2 well at shotpoint 96. Both lines were recorded for 36-fold common-depth-point (CDP) multiplicity with a record length of 7 seconds two-way time. Shotpoint 350 on line 77-1 intersects USGS line 12 at shotpoint 10,800. Shotpoint 205 on line 77-2 intersects USGS line 1 at shotpoint 1,200.

Both seismic lines 77-1 and 77-2 were recorded on a 48-channel streamer at a 4-millisecond sampling interval. The data processing of each line consisted of the following procedures. After demultiplexing and applying exponential gain to the field tapes, velocity analyses were performed on both seismic lines at 1-mi (1.6-km) intervals for normal-moveout correction and stacking. To attenuate multiple reflections and reverberations, two deconvolution filters were applied to the stacked data. After deconvolution a set of bandpass filters of 10 to 35 Hz from 0 to 1.6 seconds, and 5 to 25 Hz from 1.6 to 4.0 seconds were applied to remove extraneous noise left on the data. A final gain process (AGC) based on 1-second sliding windows was applied to balance the amplitudes on the section.

SYNTHETIC SEISMOGRAMS

Using the digitized interval-traveltime and density logs from the two COST wells, zero-offset synthetic seismograms were computer generated and correlated to the multichannel reflection seismic lines described in the previous section. A reflection coefficient series was first generated by converting the log data from depth to time, and computing the change of acoustic impedance (product of density and velocity) across each time layer. These reflection coefficients were then filtered with a bandpass filter whose passband was chosen to match that of seismic reflection lines 77-1 and 77-2.

The generation and utilization of synthetic seismograms is well described by Sengbush and others (1961) and Peterson and others (1955). The shortcomings of the methods used in constructing accurate synthetic seismograms are that plane waves are assumed, the source wavelet is usually not known, interbed multiples are not properly modeled, absorption and attenuation are not computed, and the effects of noise are not added. The effects of these problems are not corrected and degrade the comparison of synthetic seismograms to field data, although correlations are still worth making.

The seismic lines were deliberately recorded close to the two COST wells to allow a reliable correlation of well data with seismic data. Based on the results in figures 67 and 68, there are certain areas of the log where the correlations to the

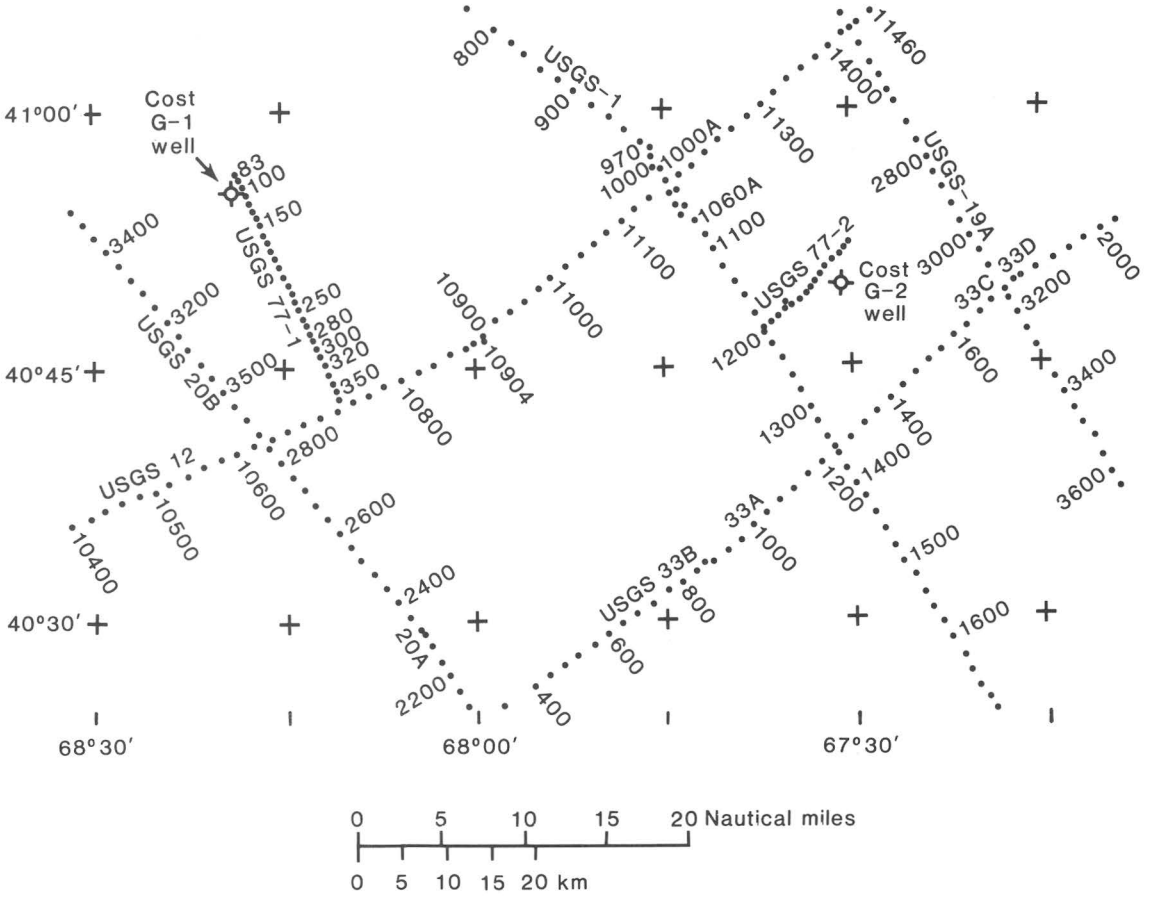

FIGURE 66.—Locations of seismic lines 77-1 and 77-2 with respect to the COST wells and other regional USGS seismic reflection lines.

seismic data are very good, while at other locations there are reflection amplitudes on the synthetic seismogram that are not as prevalent on the seismic data. We suspect that the seismic data provide the more accurate description of the subsurface geology, and it is the well log data that is in error, mainly because of the inaccurate measurement of the true formation velocities by the interval-traveltime log. The log data were not edited prior to the generation of the synthetic seismograms, although the data were smoothed to reduce noise.

Selected data-versus-depth curves from both wells were converted to two-way traveltime and plotted with the synthetic seismograms for G-1 (fig. 69) and for G-2 (fig. 70). These curves include caliper, gamma ray, conductivity, neutron porosity, and interval velocity derived from the interval-traveltime curve. Age boundaries and a condensed description of lithology are also included in these figures. The figures show the correlation of lithology and porosity with seismic reflection expression, and demonstrate (under ideal conditions) the "detectability" of particular geologic horizons. Obtaining a reasonably good correlation of the synthetic seismogram data to the seismic reflection field data is desirable, so that major geologic boundaries can accurately be defined and carried away from the well to other regional seismic lines.

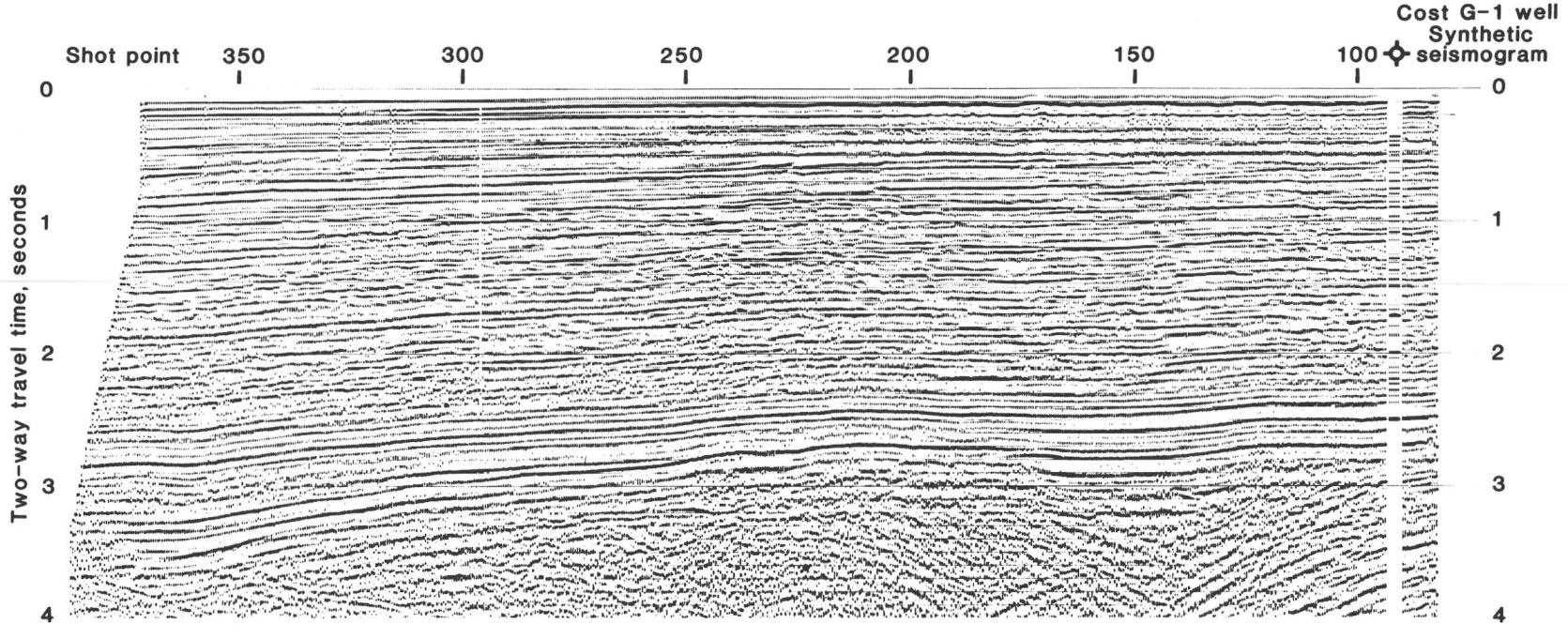

FIGURE 67.—Seismic reflection line 77-1 with the spectrally matched synthetic seismogram from the COST No. G-1 well spliced into the line.

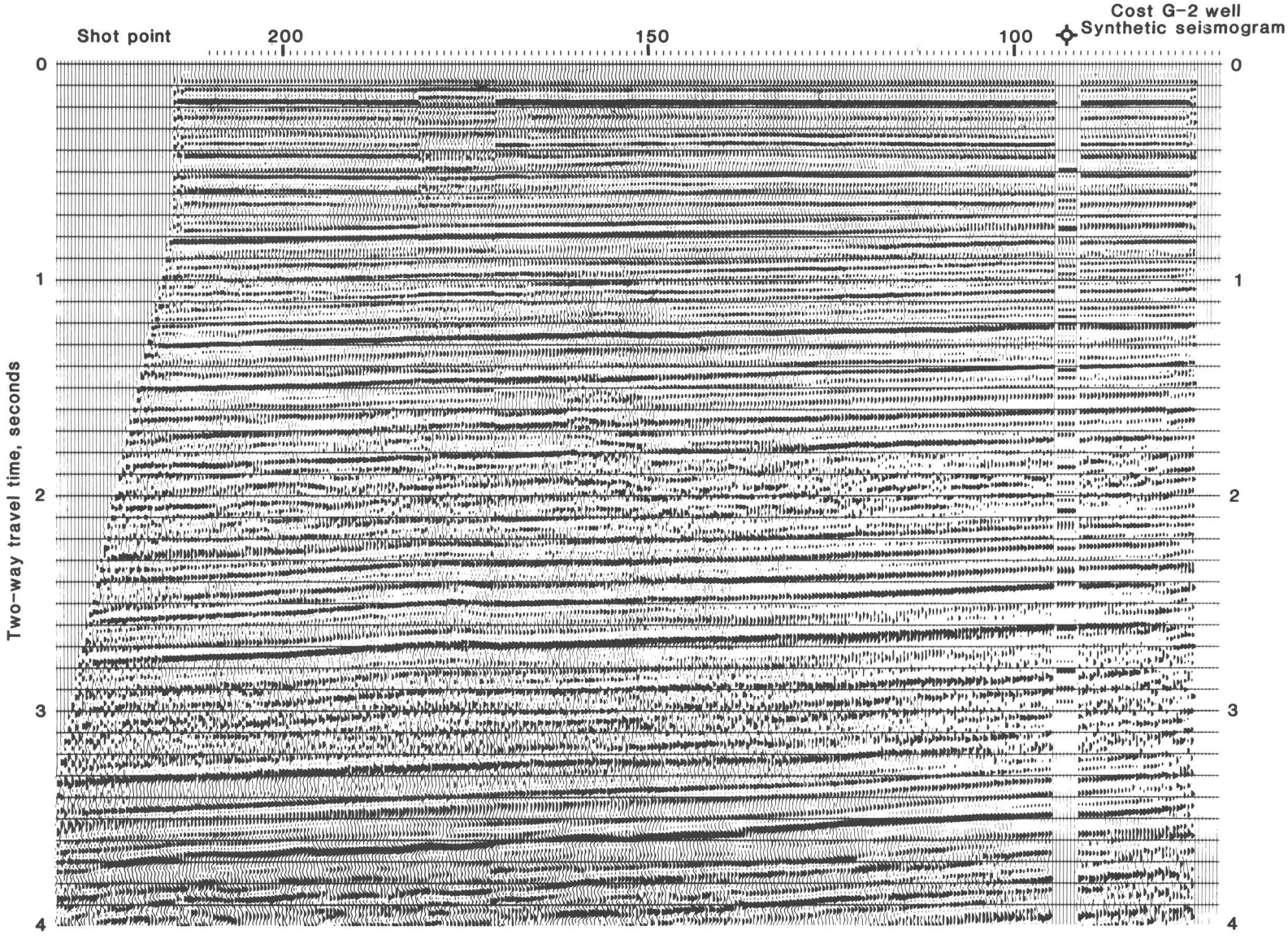

FIGURE 68.—Seismic reflection line 77-2 with the spectrally matched synthetic seismogram from the COST No. G-2 well spliced into the line.

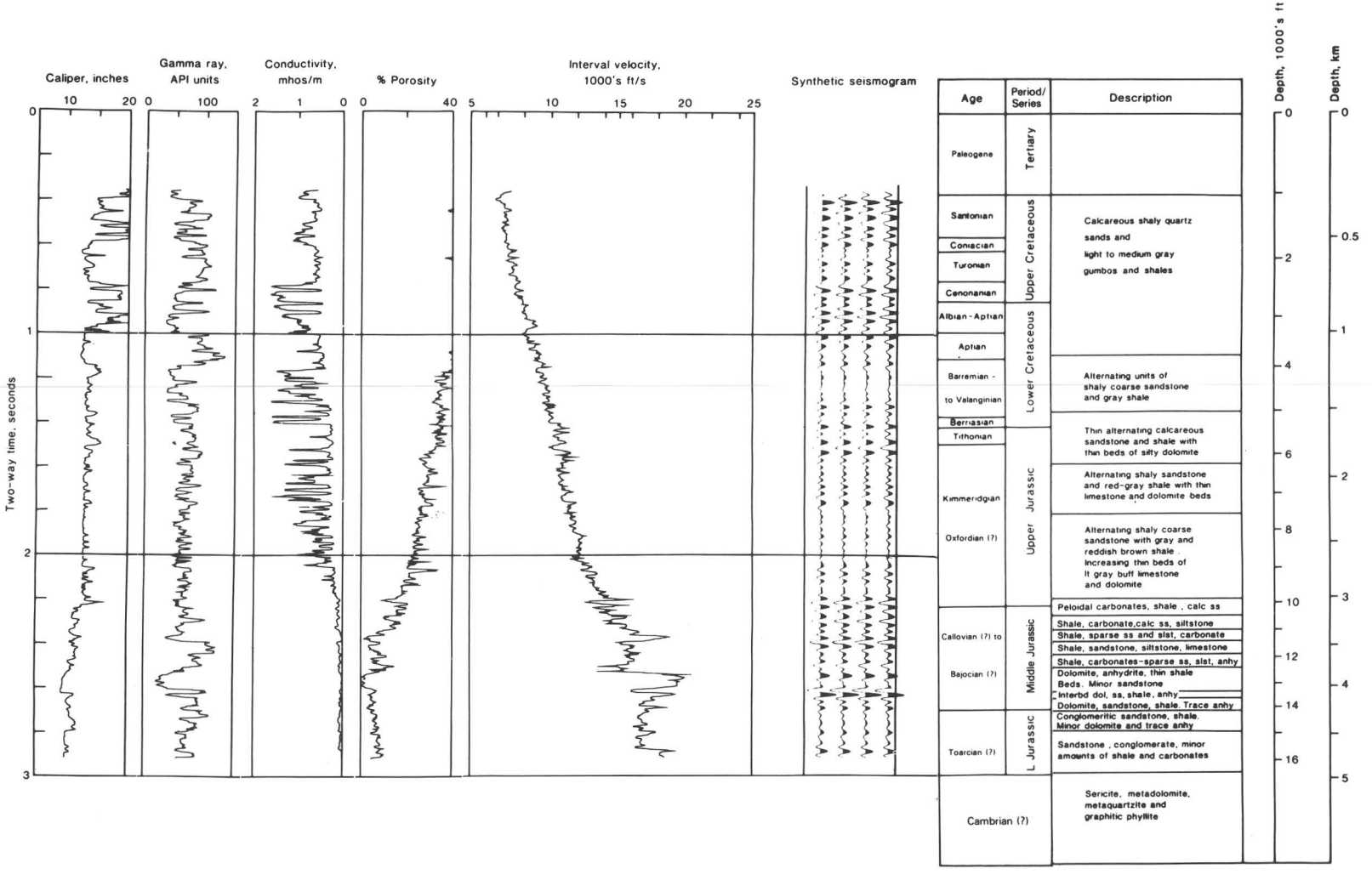

FIGURE 69.—Selected log curves and the synthetic seismogram from the COST No. G-1 well plotted as a linear function of time. Age boundaries and lithologic descriptions from Amato and Simonis (1980).

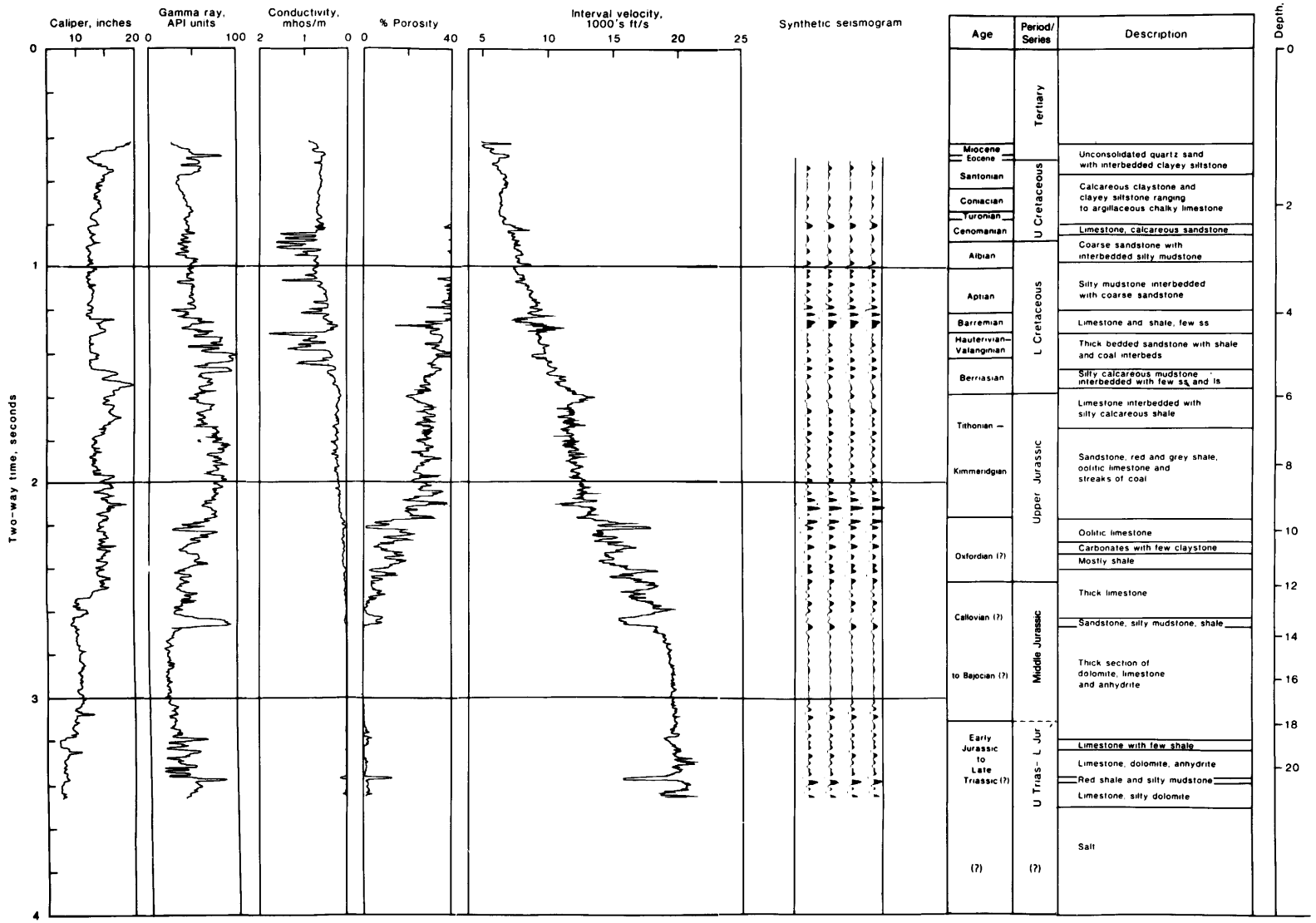

FIGURE 70.—Selected log curves and the synthetic seismogram from the COST No. G-2 well plotted as a linear function of time. Age boundaries and lithologic descriptions from Amato and Simonis (1980).

Basement Structure, Sedimentation, and Tectonic History of the Georges Bank Basin

Kim D. Klitgord, John S. Schlee, and Karl Hinz

INTRODUCTION

The sediment-filled basins beneath Georges Bank formed as the continental margin subsided during and following the rifting of Africa from North America. We shall develop a tectonic history for this region by examining the crustal foundation beneath these basins and by outlining the stages in sedimentary buildup. The analysis of magnetic and gravity data integrated with seismic reflection profiles provides clues as to the nature of basement rocks, their depth of burial, composition, and tectonic setting. The interpretation of seismic reflection profiles and the correlation of seismic stratigraphic units with lithostratigraphic units at the COST Nos. G-1 and G-2 wells gives a history of basin filling over the past 200 m.y., including major trends in rock types and their thicknesses, relative ages of interregional unconformities, and the relationship of the basin sedimentation to the construction of the adjacent continental slope and rise.

Before the G-1 and G-2 wells were drilled, most of the information concerning the subsurface of Georges Bank was derived from a combination of geophysical data and the extrapolation of stratigraphy from the Shell Mohawk well on the Scotian shelf. (See, for instance, Ballard and Uchupi, 1972; Mattick and others, 1974; Schlee and others, 1976, 1979; Klitgord and Behrendt, 1979; Austin and others, 1980.) In this report, magnetic and gravity data are used in conjunction with multichannel seismic reflection data (fig. 71) to outline the basement structures, to interpolate seismic basement features between seismic lines, and to provide depth estimates for basement in regions of limited acoustic penetration.

The seismic stratigraphy for the Georges Bank shelf, slope, and rise was determined from correlation with the lithostratigraphy at the Shell Mohawk well (Schlee and others, 1976), at the COST Nos. G-1 and G-2 wells (Amato and Bebout, 1980; Amato and Simonis, 1980; Poag, this volume), at the Nantucket well (Folger and others, 1978), and at Deep Sea Drilling Project (DSDP) sites (Klitgord and Grow, 1980). Additional information concerning the shallow stratigraphy was provided by the 1976 Atlantic Margin Coring Project (AMCOR) (Hathaway and others, 1976, 1979) and other multichannel seismic data (Austin and others, 1980). The correlation of deep-sea and shelf seismic stratigraphy is tenuous, because a buried shelf edge of Lower Cretaceous and older carbonate rocks (Schlee and others, 1979) obscures the acoustic record of the transition across the shelf and slope.

Interval velocities determined from the USGS multichannel seismic data have been used to correlate the seismic stratigraphy on the seismic lines with the lithostratigraphy in the various drill holes (Schlee and others, 1976; Ditty, 1980; Waetjan, 1980; Poag, this volume). This same velocity information has also been used to produce depth sections (fig. 72), isopach maps, and structure contour maps (fig. 3 in Schlee and Klitgord, this volume). The interval velocities were determined from the multichannel profile velocity scans using the method of Taner and Koehler (1969).

BASEMENT STRUCTURE

MAGNETIC ANOMALY DATA

Magnetic surveys of the Georges Bank region were conducted in 1965-1968 by Project MAGNET (U.S. Naval Oceanographic Office, 1966; Taylor and others, 1968; Kane and others,

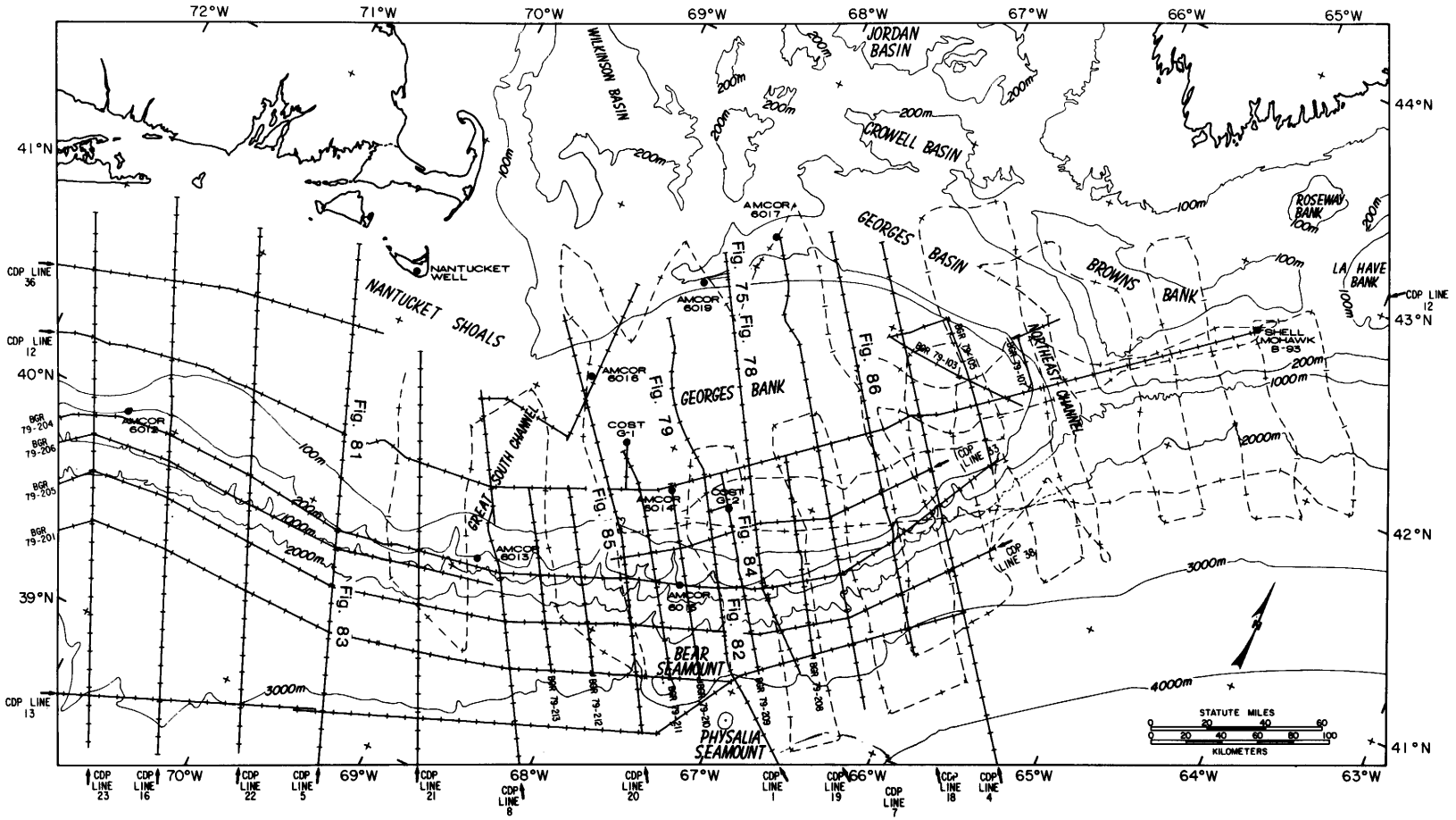

FIGURE 71.—Multichannel seismic reflection profiles in the Georges Bank region. U.S. Geological Survey common depth point (CDP) profiles (24- or 48-channel stacks) and Bundesanstalt für Geowissenschaften und Rohstoffe (BGR) profiles (48-channel stacks) are shown as solid lines with crossticks at 10-km intervals. Woods Hole Oceanographic Institution (WHOI) CDP profiles (6-channel stacks) are indicated by dashed lines. Bathymetric contours, in meters, are from Uchupi (1966). Continental Offshore Stratigraphic Test (COST) drill sites and Atlantic Margin Coring Program (AMCOR) drill sites are shown by circles.

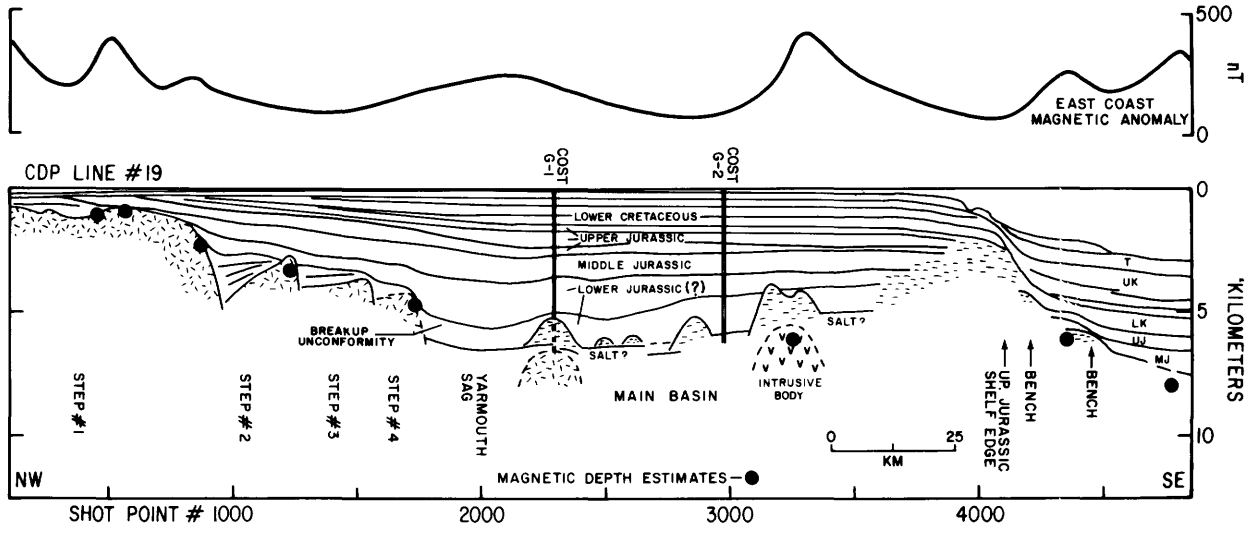

FIGURE 72.—Typical cross section and magnetic anomaly profile for the Georges Bank basin based on CDP line 19. The dashed basement beneath the breakup unconformity is inferred from adjacent seismic profiles and magnetic data. The locations of the COST Nos. G-1 and G-2 wells are projected onto the cross section. Ages of seismic stratigraphic units are from Poag (this volume). Solid dots show locations of depth-to-magnetic-basement estimates from Klitgord and Behrendt (1979).

1972) and again in 1975 by LKB Resources, Inc., for the USGS (Klitgord and Behrendt, 1977, 1979). The magnetic anomaly contour map (fig. 73) is a composite of these two surveys plus some data published by the Geological Survey of Canada (Haworth and MacIntyre, 1975). A 50-nanotesla (1 nT=1 gamma) contour interval was used for the entire map (2 nT and 10-nT contours are also available for the LKB/USGS survey; Behrendt and Klitgord, 1979). Flight lines for the LKB/USGS survey have a spacing of 2.5 km (1.5 mi) at an elevation of 300 m (984 ft) over eastern Georges Bank and 3.2 km (2.0 mi) at an elevation of 450 m (1,475 ft) over western Georges Bank. The Project MAGNET survey (U.S. Naval Oceanographic Office, 1966) was flown at an elevation of 750 m (2,461 ft), and flight line spacing was about 8 km (5 mi). For a more complete discussion of these two surveys, see Taylor and others (1968) and Klitgord and Behrendt (1979).

Basement structures were mapped using inferred magnetic source depths to interpolate seismic basement structures between seismic lines. Depth-to-magnetic basement estimates were determined for the entire LKB/USGS survey (fig. 74) (Klitgord and Behrendt, 1979). A comparison between these depth-to-magnetic basement estimates and a seismic depth section (fig. 72) demonstrates the close correlation between magnetic and seismic basement. Also, low magnetic anomalies correlate well with shallow grabens (fig. 75); narrow magnetic highs border the edges of the grabens and may be caused by intrusive igneous features along the edges of the grabens.

GRAVITY ANOMALY DATA

The gravity anomaly map (fig. 76) is a composite of several maps (Kane and others, 1972; Haworth and MacIntyre, 1975; Grow and others, 1976; 1979) that were based on marine profiles and measurements from a few bottom stations. Free-air gravity anomalies with a 10-mGal contour interval were used offshore south of lat 42° N. and simple Bouguer gravity anomalies with a 10-mGal contour interval were used onshore and offshore north of lat 42° N. The most prominent gravity feature in this area is the large peak and trough at the shelf break. This anomaly is produced by the horizontal density contrast between sediment and water in the vicinity of the shelf break and slope (Worzel and Shurbet, 1955). The calculation of Bouguer anomalies or isostatic anomalies (Talwani and Eldholm, 1973; Rabinowitz, 1974; Rabinowitz and LaBrecque, 1977; Grow and others, 1979) removes most of this edge-effect anomaly. An example of this can be seen in the Bouguer anomaly contours north of lat 42° N. and in the isostatic anomaly calculated along CDP line 5 (fig. 77).

Gravity anomalies over the shelf reflect the same general basement structure indicated by the magnetic and seismic data. The northeast-trending gravity highs over Martha's Vineyard and Nantucket, and between Step #1 and Step #2 (lat 42° N., long 68° W.), are located above basement highs. The northeast-trending gravity low around lat 41° N., long 69° W., coincides with the deepest part of the Georges Bank basin (Schlee and others, 1976) and extends to the northeast over the broad basement sag just north of the Yarmouth arch. The gravity field over the main basin seaward of the Yarmouth arch is dominated by the edge-effect anomaly at the shelf break.

SEISMIC BASEMENT

Seismic reflection profiles across the Georges Bank region (fig. 71) show great variability in depth and character of seismic (acoustic) basement. Except in the vicinity of the carbonate buildup associated with the ancient shelf edges (Schlee and others, 1976, 1979) there is a general seaward deepening of seismic basement. We use the term crystalline basement to refer to the surface that is the bottom of the sedimentary fill and the top of metamorphic or igneous rocks. Seismic basement is the surface of maximum interpretable acoustic penetration, and the depth to that surface can vary between seismic lines, depending upon data quality. We have attempted to interpret those regions where seismic basement does not coincide with crystalline basement.

The deep structure for Georges Bank can be divided into four characteristic zones: (1) a low-relief zone of Paleozoic or older metamorphic and igneous rocks that is present on the shallow stable platforms; (2) a block-faulted zone of Paleozoic or older metamorphic or igneous rocks that deepens seawards in distinct steps; (3) a zone of very thick sediments with prograding carbonate deposits at its seaward edge; and (4) a zone of oceanic basement that was generated by sea-floor spreading. Crystalline basement and seismic basement usually coincide in zone 1 (continental crust) and zone 4 (oceanic crust). The seismic basement in zone 1 is characterized by a very strong reflector associated with short-wavelength undulating relief in some areas, sets of diffraction patterns in other areas, and negligible relief in still other areas. The seismic basement in zone 4 is characterized by closely space hyperbolic echoes and generally low relief.

The most complex area of basin development is in zones 2 and 3, where seismic basement rarely coincides with crystalline basement. On many of the seismic profiles the breakup unconformity (Falvey, 1974) coincides with seismic basement, and the nature of crystalline basement somewhere beneath it can be inferred only from the character and shape of this unconformity surface. Across the block-faulted zone 3, a number of half-grabens that form subbasins lie beneath the breakup unconformity. Sediments within these grabens appear as zones of seaward- or landward-dipping reflectors truncated by the breakup unconformity (fig. 78). The unconformity deepens abruptly over the downthrown side of the graben (shotpoint 900, fig. 78) and then levels off until encountering the next graben (shotpoint 1220, fig. 78). The diffraction pattern and rough seismic basement on the upthrown side of the half-graben (shotpoint 1200, fig. 78) may indicate crystalline basement; on some profiles, this rough basement can be traced beneath the dipping reflectors. On profiles where the breakup unconformity coincides with seismic basement (fig. 79), these same narrow zones of steep dips (separated by more gently dipping segments) give the seismic basement a steplike appearance. We infer that crystalline basement, as illustrated in figure 78, is probably a series of half-grabens beneath these steps. Seaward of this block-faulted zone, seismic basement is usually an interval of chaotic reflectors, either directly beneath or at the breakup unconformity. The recovery of halite at the bottom of the COST No. G-2 well (Amato and Simonis, 1980), from the stratigraphic unit that we would place directly below the breakup unconformity suggests that salt forms seismic basement. The patches of chaotic reflectors directly below the unconformity have been interpreted by Poag (this volume) as carbonate mounds. Seaward of the COST No. G-2 well, seismic basement becomes shallower because of a prograding carbonate buildup near the Jurassic and Lower Cretaceous shelf edge. We cannot identify crystalline basement in this region.

DISCUSSION

The basement structure map for the Georges Bank region (fig. 73) combines magnetic basement (fig. 74) and seismic basement information.

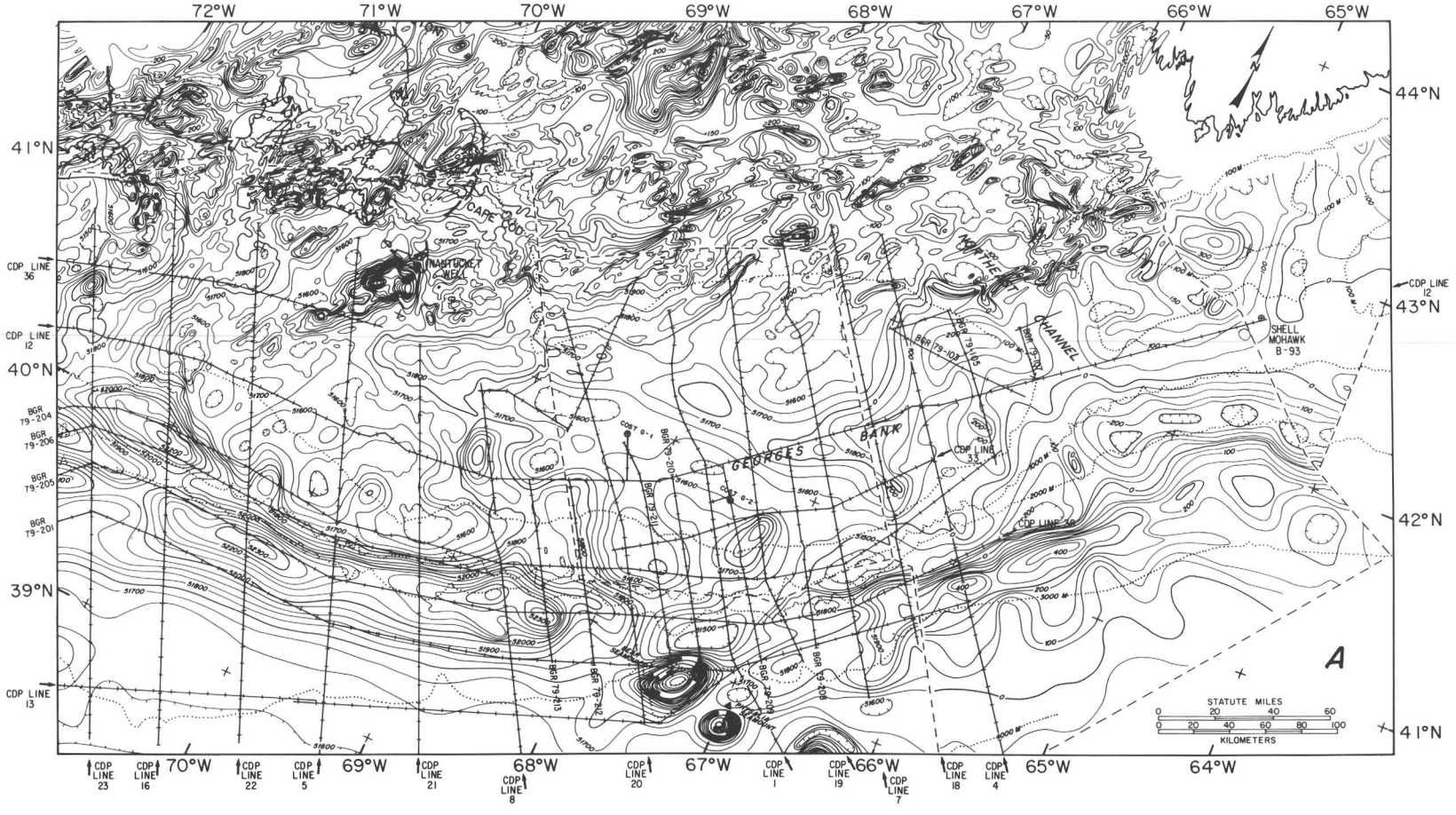
72°W
71°W
70°W
69°W
68°W
67°W
66°W
65°W
44°N
43°N
42°N
41°N
40°N
39°N
CAPE COD
NANTUCKET WELL
GEORGES BANK
NORTHEAST CHANNEL
SHELL MOHAWK B-93
CDP LINE 36
CDP LINE 12
CDP LINE 33
CDP LINE 13
CDP LINE 23
CDP LINE 16
CDP LINE 22
CDP LINE 5
CDP LINE 21
CDP LINE 8
CDP LINE 20
CDP LINE 1
CDP LINE 19
CDP LINE 7
CDP LINE 18
CDP LINE 4
BGR 79-204
BGR 79-206
BGR 79-205
BGR 79-201
BGR 79-103
BGR 79-105
BGR 79-209
BGR 79-211
BGR 79-213
BGR 79-212
BGR 79-208
COST G-1
COST G-2
A
STATUTE MILES
KILOMETERS

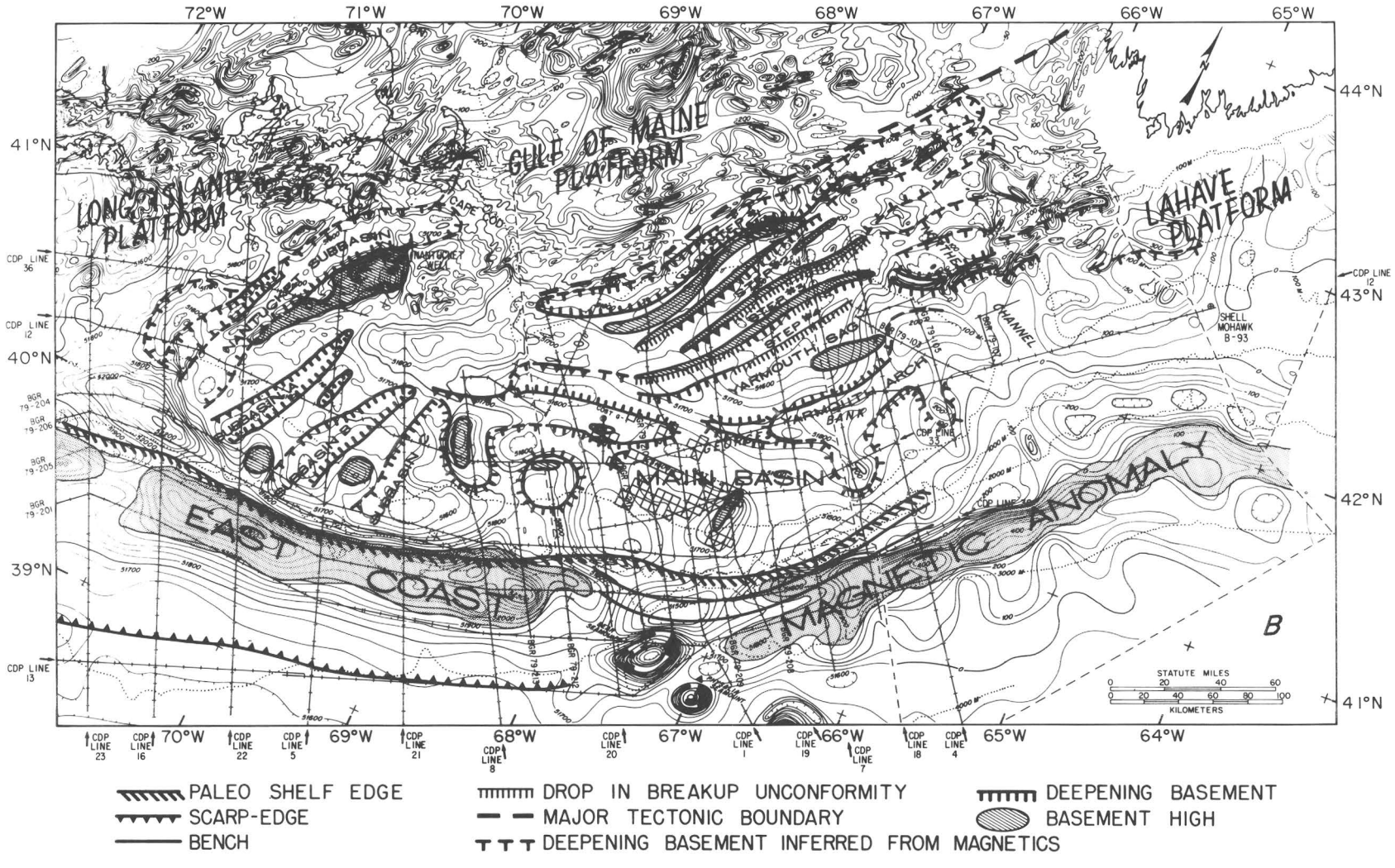

FIGURE 73.—Magnetic anomaly maps of the Georges Bank area, composited from the maps of Klitgord and Behrendt (1977) and Haworth and MacIntyre (1975). Contour interval 50 nT; Universal Transverse Mercator projection. *A*, USGS and BGR multichannel seismic line locations superimposed. *B*, Tectonic structure (Schlee and Klitgord, this volume, fig. 4) superimposed.

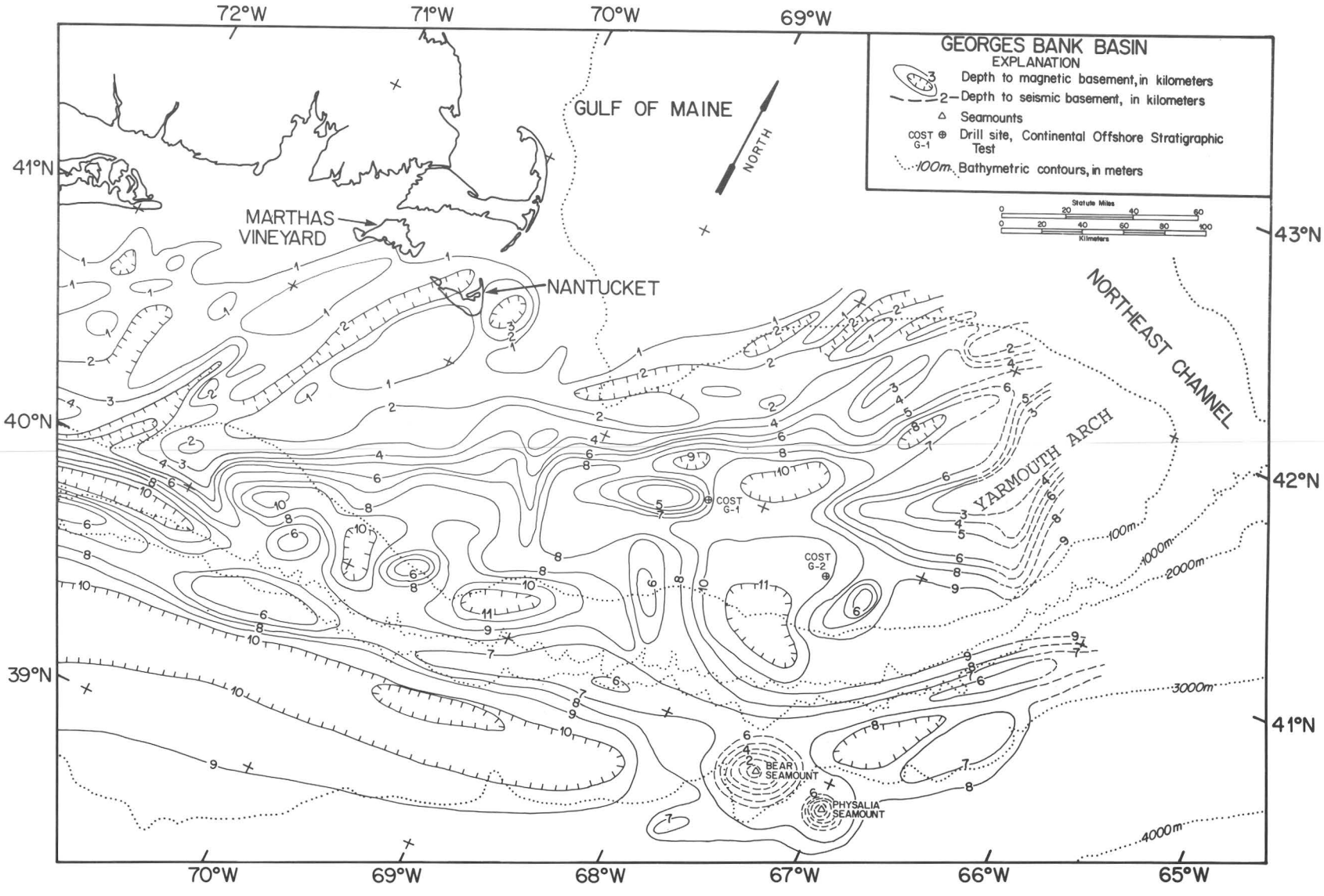

FIGURE 74.—Depth to magnetic basement in the Georges Bank area. Contour interval 1 km (0.62 mi); Universal Transverse Mercator projection. Depths were determined using magnetic depth estimates to interpolate between CDP lines 1, 4, 5, 7, 8, 12, and 13. From Klitgord and Behrendt (1979, fig. 7*C*).

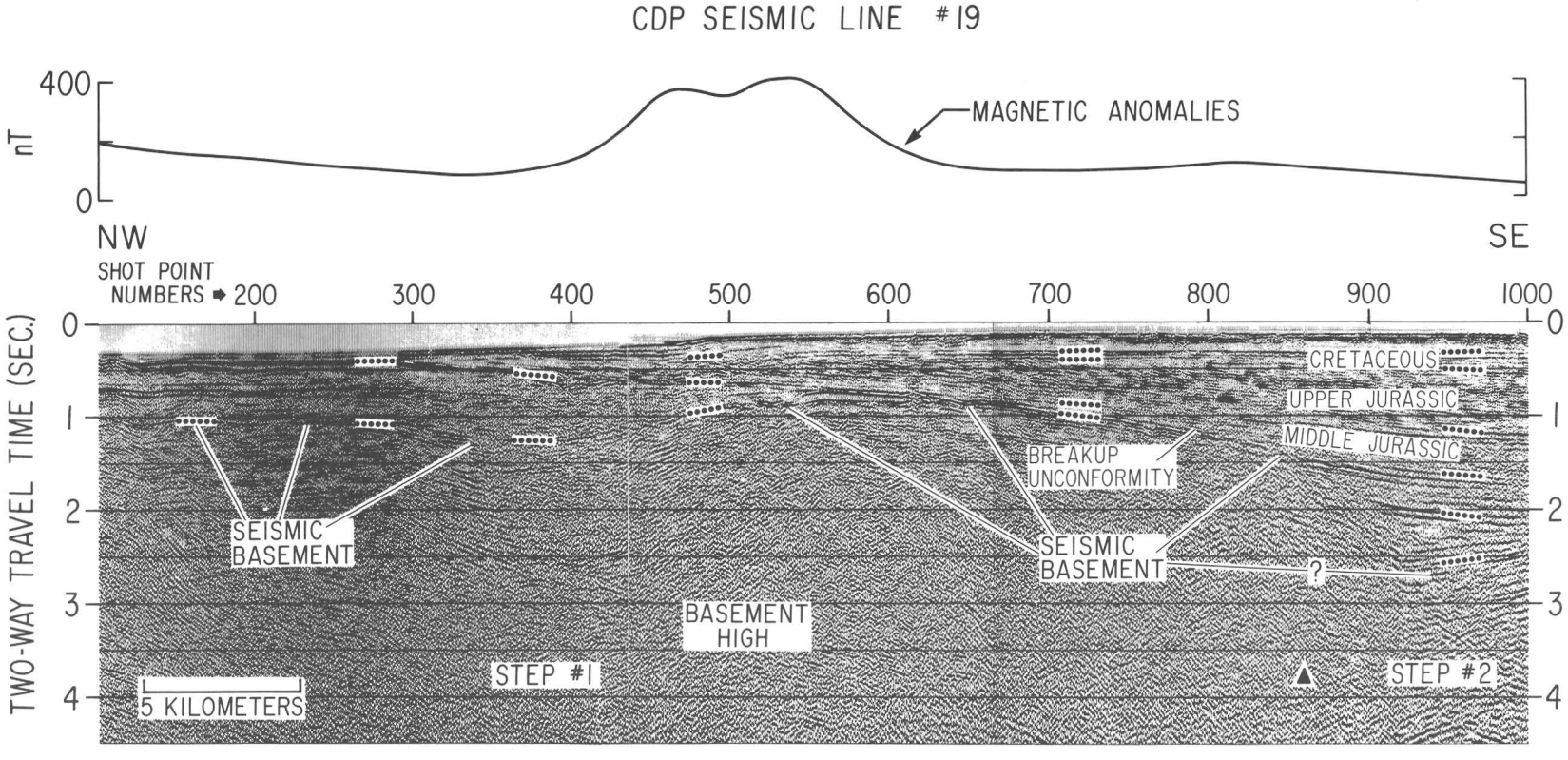

FIGURE 75.—Magnetic anomaly and seismic reflection profiles for a portion of CDP line 19 across Step #1. Note the correspondence between the magnetic high and the basement high, and between the magnetic low and the basement trough. See figure 71 for location.

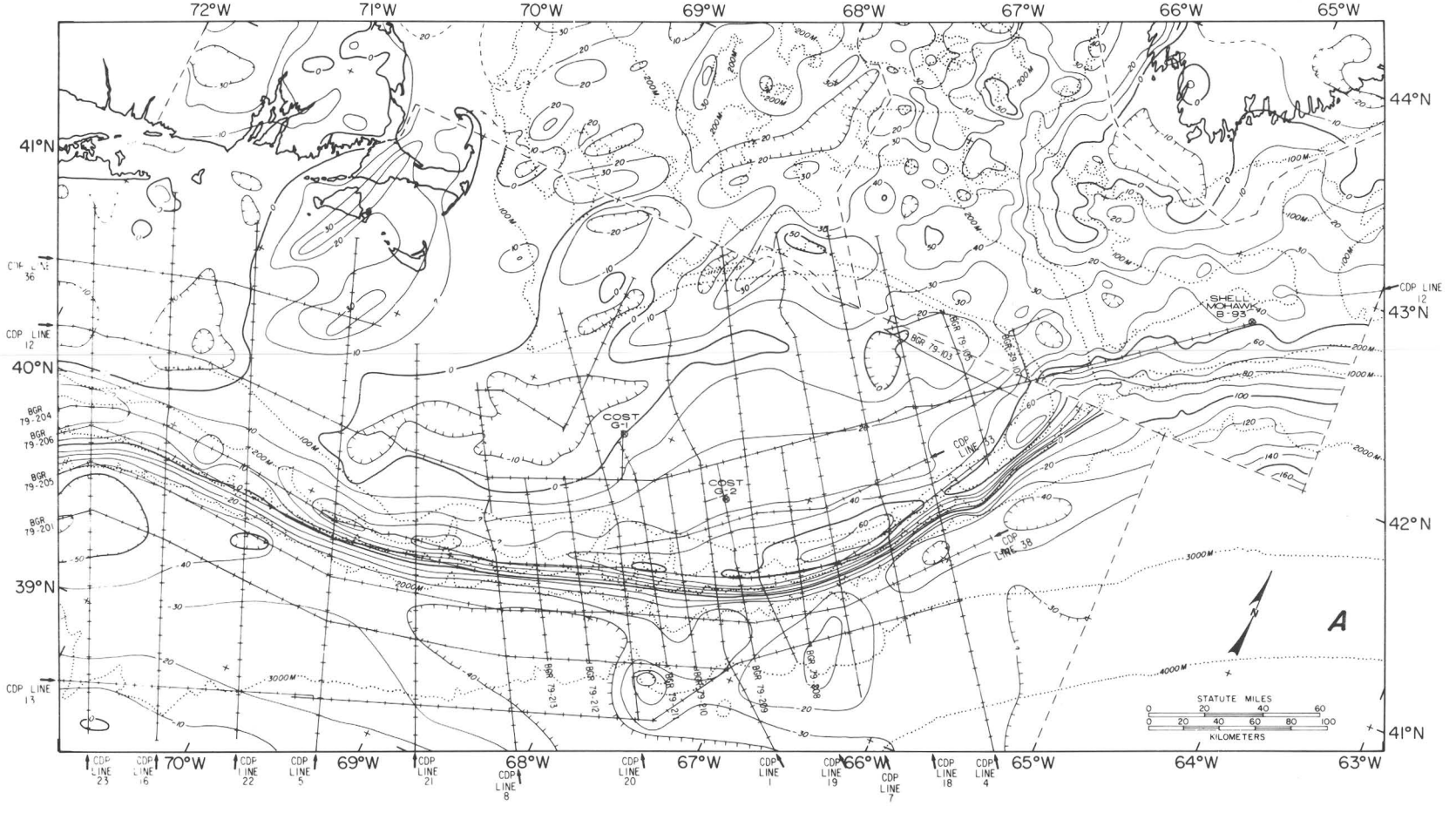
72°W
71°W
70°W
69°W
68°W
67°W
66°W
65°W
44°N
43°N
42°N
41°N
40°N
39°N
CDP LINE 12
CDP LINE 13
CDP LINE 38
CDP LINE 53
SHELL MOHAWK B-93
COST G-1
COST G-2
BGR 79-103
BGR 79-204
BGR 79-206
BGR 79-205
BGR 79-201
BGR 79-213
BGR 79-212
BGR 79-210
BGR 79-209
BGR 79-208
100M
200M
1000M
2000M
3000M
4000M
A
STATUTE MILES
0 20 40 60
KILOMETERS
0 20 40 60 80 100
CDP LINE 23
CDP LINE 16
CDP LINE 22
CDP LINE 5
CDP LINE 21
CDP LINE 8
CDP LINE 20
CDP LINE 1
CDP LINE 19
CDP LINE 7
CDP LINE 18
CDP LINE 4
63°W

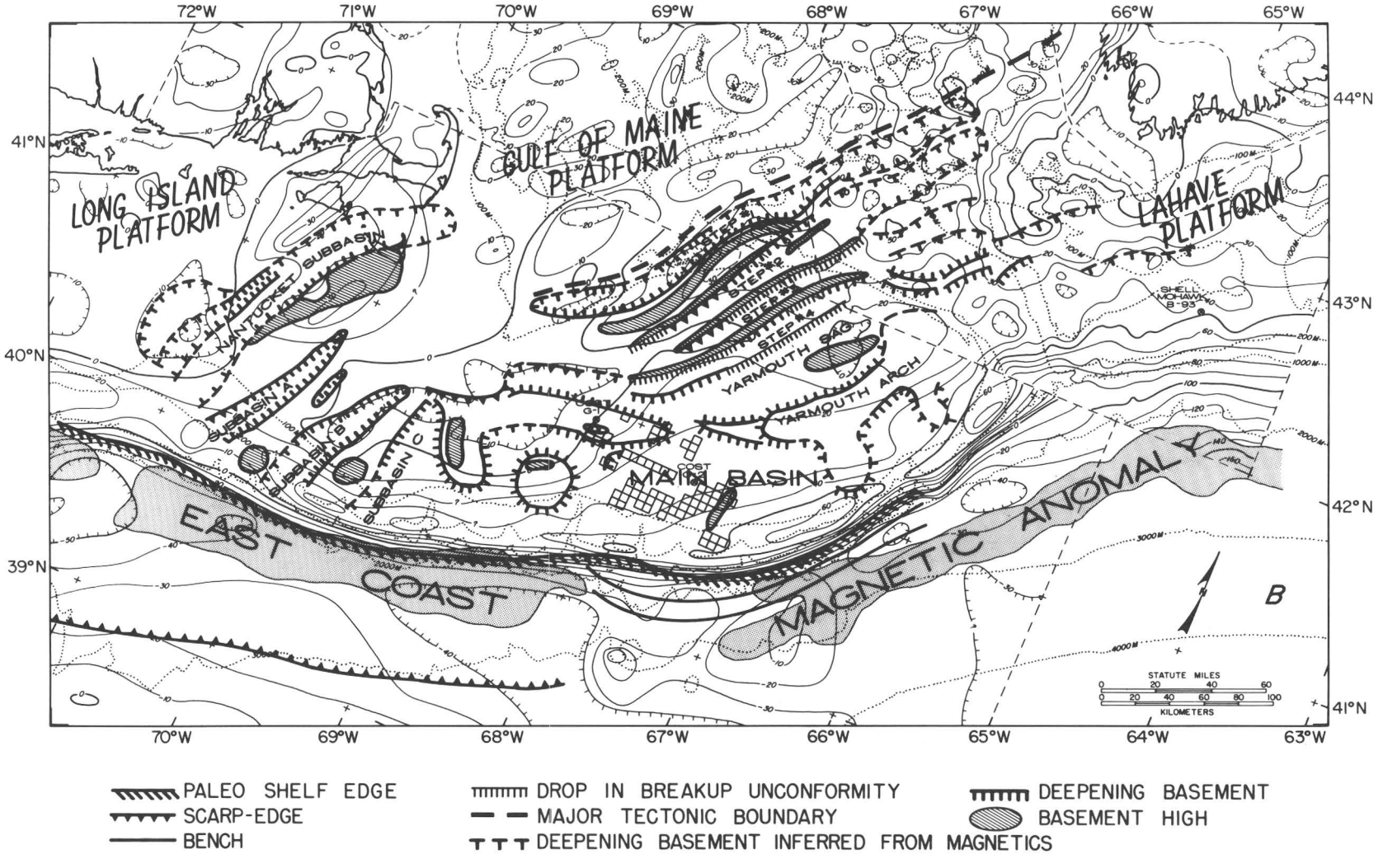

FIGURE 76.—Gravity anomaly maps of the Georges Bank area, composited from the free-air gravity anomaly map of Grow and others (1976) and the Bouguer gravity anomaly maps of Kane and others (1972) and Haworth and MacIntyre (1975). Contour interval 10 mGal; Universal Transverse Mercator projection. *A*, USGS and BGR multichannel seismic line locations superimposed. *B*, Tectonic structure (Schlee and Klitgord, this volume, fig. 4) superimposed.

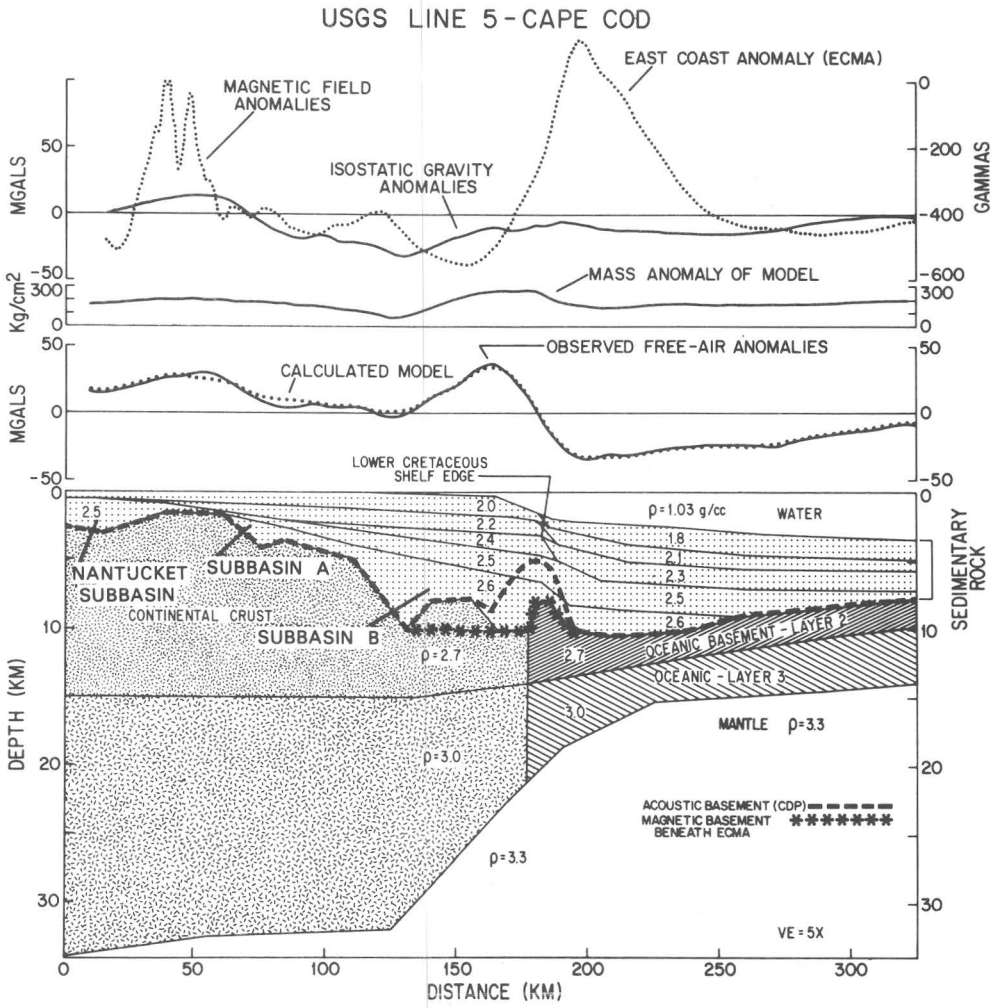

FIGURE 77.—Two-dimensional gravity model for CDP line 5. Sediment thickness and densities are inferred from the multichannel velocities. Magnetic basement from Klitgord and Behrendt (1979) was used for the base of the sediments in the vicinity of the East Coast magnetic anomaly, where seismic basement is the top of the Jurassic shelf-edge bank. The upper and lower crust were assumed to have densities of 2.7 and 3.0 g/cm³ respectively, although no refraction data are available. The relative shape of the crust-mantle boundary was modified to fit the gravity data, but the absolute depth-to-Moho could be in error by several kilometers. This line typifies the narrow zone of progressively deepening small subbasins between stable platforms of continental crust (just to the left of the profile) and oceanic crust (to the right of the 200-km mark) and demonstrates a rapid crustal thinning over a distance of only 100 km (62 mi). From Grow, Bowin, and Hutchinson (1979, fig. 5).

Shallow, stable platforms lie northeast, north, and northwest of Georges Bank, where seismic basement is less than 2 km (6,600 ft) deep. The block-faulted zone seaward of the platforms is divided into two segments, one southeast of the Long Island platform and the other southeast of the Gulf of Maine platform. These two segments are separated by a set of east-west structures near lat 41° N. Seismic basement depths at the top edges of the grabens and basins range from less than 2 km (6,600 ft) to more than 6 km (19,700 ft); several thousand meters of sediments fill isolated basins beneath the breakup unconformity. Seaward of the block-faulted zone, the main basin lies beneath the outer Georges Bank and contains more than 6.5 km (21,500 ft) of sediments. The Jurassic-Lower Cretaceous shelf edge forms the seaward border of both the main basin and the small subbasins to the west. Oceanic basement can be traced landward to within 50 km

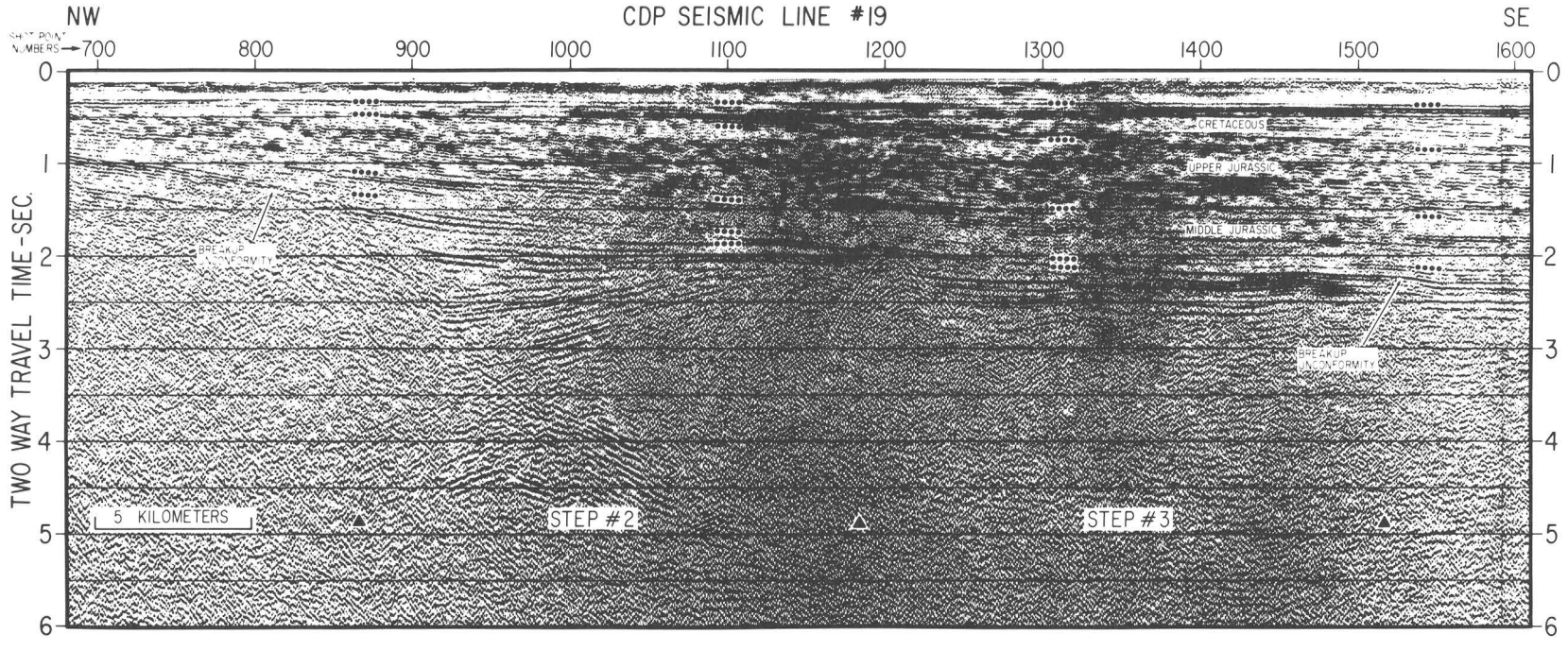

FIGURE 78.—A portion of CDP line 19 showing the landward-dipping reflectors beneath the breakup unconformity for the half-grabens that form Steps #2 and #3. The basement hinge for Step #2 is at shotpoint 1200; the hinge for Step #3 is at shotpoint 1500. Drops in the breakup unconformity area indicated by triangles. See figure 71 for location.

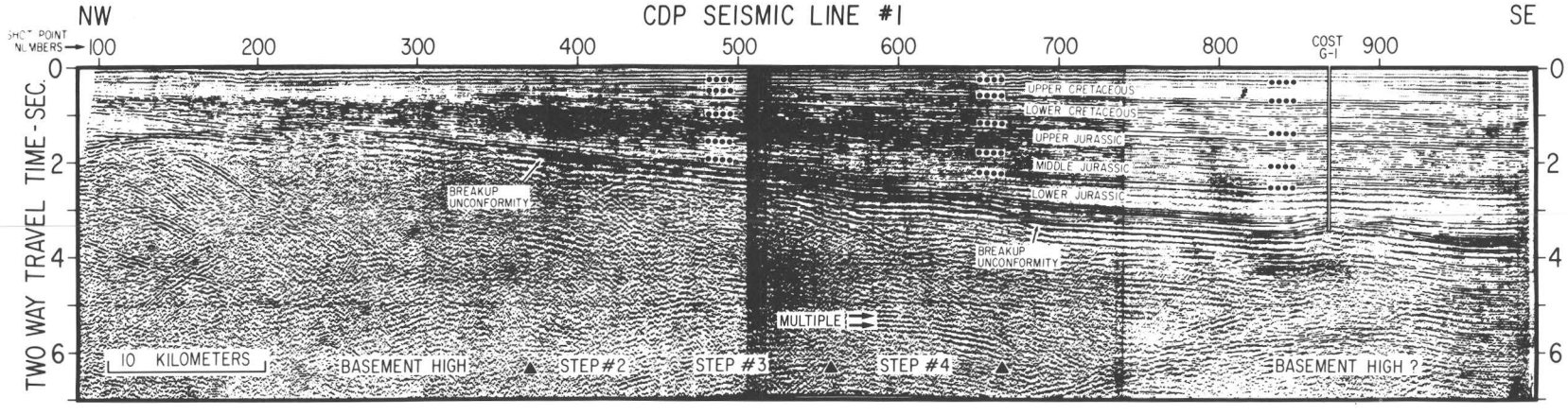

FIGURE 79.—A portion of CDP line 1 over the buried steps. See figure 71 for location. Notice the drops in the breakup unconformity (triangles) to the left of Steps #2, between Steps #3 and #4, and to the right of Step #4. Steps #2 and #3 have merged on this line. The small basement high that the COST No. G-1 well penetrated is seen as a small rise in the breakup unconformity. The deep reflectors at 6 sec to the right of Step #4 may be real (Schlee and others, 1976), indicating a thick sequence of prerift and synrift sediment in this region. Also, these deep reflectors possibly are pegleg multiples off landward-dipping synrift sediments obscured by the acoustic reflectors associated with the breakup unconformity (3 to 4 sec depth) but similar to those shown in figure 78.

(31 mi) of the axis of the East Coast magnetic anomaly (ECMA) on most of the seismic profiles and to within 20 km (12.4 mi) of it on some lines. The depths of these structures are shown in the series of cross sections in figure 80.

The block-faulted zone southeast of the Gulf of Maine platform deepens in a series of steps into a broad sag (the Yarmouth sag) before abutting against the Yarmouth arch. There may be a small subbasin beneath the breakup unconformity at

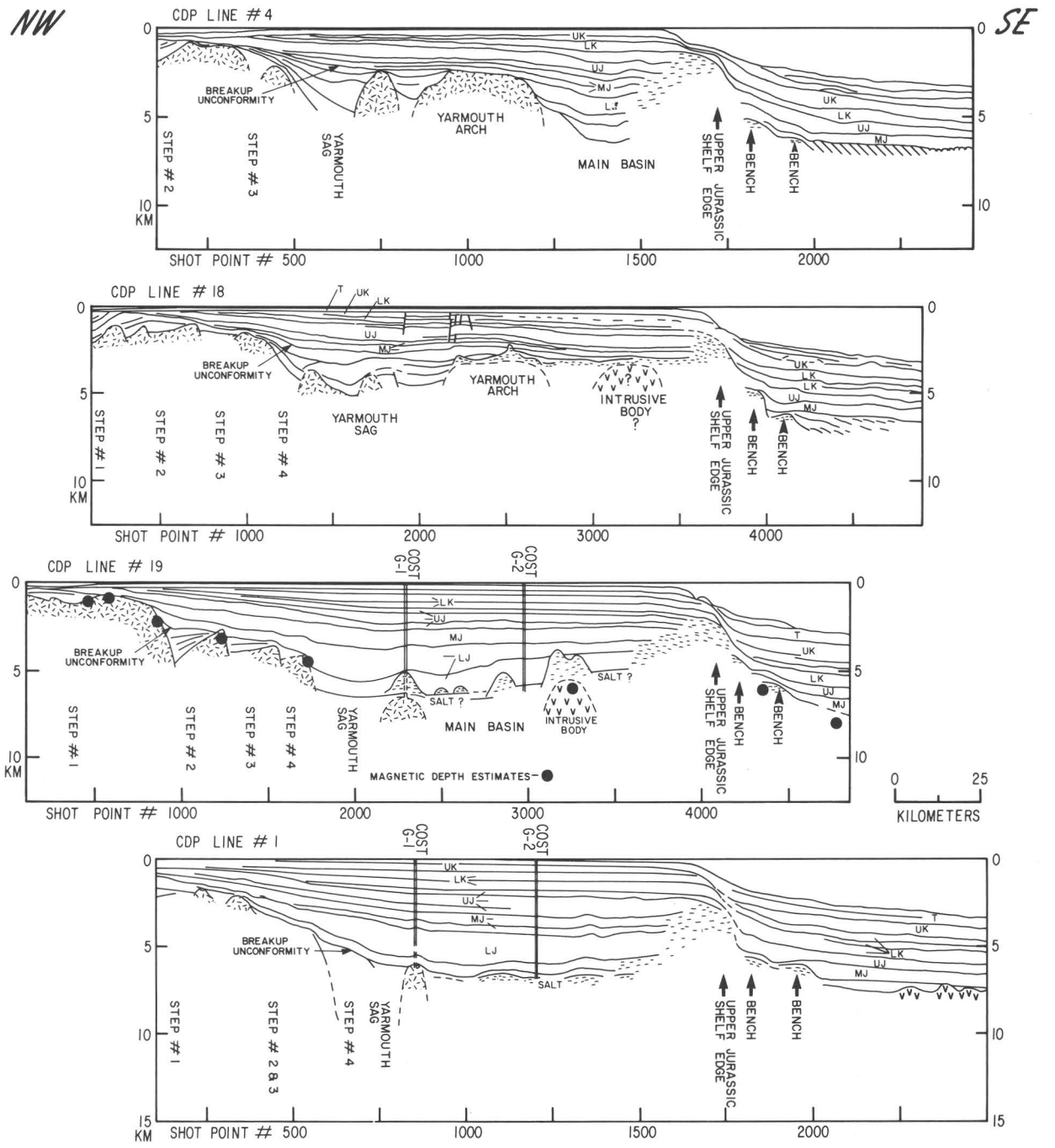

FIGURE 80.—Interpretive cross sections of the Georges Bank basin seaward of the Gulf of Maine platform along CDP lines 4, 18, 19, and 1. See figure 71 for locations. UK, Upper Cretaceous; LK, Lower Cretaceous; UJ, Upper Jurassic; MJ, Middle Jurassic; LJ, Lower Jurassic(?).

each of these steps but these subbasins can be seen on only some of the seismic profiles. Step #1 is a linear trough that is well defined on most multichannel seismic profiles (fig. 75; basin at 0000h on line 17–19, fig. 5 of Austin and others, 1980) and even on some single-channel profiles (such as fig. 3B of Ballard and Uchupi, 1972, and fig. 4 of Oldale and others, 1974). Step #1 lies at the hinge zone between the Gulf of Maine platform (which contains a number of the other Triassic grabens; Ballard and Uchupi, 1972) and the deepening basement to seaward. Steps #1 and #2 are separated by a broad basement high (fig. 75) that is associated with a large positive magnetic anomaly and a high gravity anomaly. These two potential field highs suggest that a mafic intrusive body separates the two basins. Step #2 is a half-graben that is well defined on common-depth-point (CDP) line 4 (Grow and Schlee, 1976) and line 19 (fig. 78). On CDP lines 1, 7, and 18, the breakup unconformity dips steeply along the landward edge of the step. This graben can also be seen on some single-channel seismic profiles (such as fig. 3C of Ballard and Uchupi, 1972). Step #3 also clearly appears as a half-graben on line 19 (fig. 78), but the other seismic lines show only a small basement high on each side of the step. Between Step #3 and the Yarmouth arch, the broad Yarmouth sag (including Step #4) overlies a major gravity low. The Yarmouth sag deepens to the southwest and includes a small basement high on CDP line 4 (Grow and Schlee, 1976) and line 18 (fig. 78). The basin becomes very deep where it is crossed by CDP lines 7, 19 and 1. Only the steeply dipping sides of the Yarmouth sag can be seen on lines 7 and 19 but suggestions of a deep crystalline basement can be seen on CDP line 1 (shotpoints 550 to 850, fig. 79). On line 1 the drop in the breakup unconformity is visible at both edges of Step #4, but the drop is negligible on lines 18 and 7. We consider the Yarmouth arch the seaward end of this block-faulted zone. The arch deepens to the southwest until on line 19 (shot point 2250, fig. 80) it is only a small basement high with a possible carbonate mound on top (Poag, this volume). The small basement high on CDP line 1 (shotpoint 880, fig. 79) is interpreted, using the magnetic data, to be a continuation of the small east-west basement high encountered on CDP lines 8 and 20, which was drilled into at the COST No. G-1 well (fig. 73). It may be connected to the Yarmouth arch. The small east-west basin just north of this high is either a continuation of the Yarmouth sag or a separate subbasin.

The basement of the block-faulted zone to the southeast of the Long Island platform does not deepen in a steplike fashion, but it does contain four small, elongate subbasins (fig. 73). The depth to the tops of these subbasins increases gradually to the southeast, as shown in figure 81. All of these basins deepen to the south, where their seaward margins are obscured by the carbonate buildup near the Jurassic-Lower Cretaceous shelf edge. The Nantucket subbasin is well defined on CDP lines 5 (Grow and Schlee, 1976) and 36, and the northwestern part of the basin can be seen on line 22. The rest of the outline of the subbasin was determined from the magnetic data (fig. 74) and the gravity data. Nowhere do the margins of the Nantucket subbasin exceed 4 km (13,000 ft). There is a seismic basement high (fig. 81) associated with a large magnetic high and gravity high between the Nantucket subbasin and subbasin A. We interpret this basement high to be the upper surface of a mafic body similar to that noted previously between Steps #1 and #2. Subbasin A (fig. 81) gradually deepens to the south, but its margins do not exceed 5 km (16,400 ft) depth; it appears as a half-graben on CDP line 22. Subbasin B also appears on CDP line 5 (fig. 81) where it is deeper and broader than Subbasin A. The deepest of this western set of subbasins, Subbasin C, broadens to the east and may merge with the main basin (fig. 73). Subbasin C is bounded on the west by a small basement high that may represent an intrusive igneous feature; to the northeast is a larger basement high. As with the other three subbasins, the seaward edge of Subbasin C is obscured by the carbonate buildup near the Jurassic-Lower Cretaceous shelf edge.

The main basin of the Georges Bank lies between the Yarmouth arch and the ECMA. The region of greatest sediment accumulation (Schlee and Klitgord, this volume, fig. 3) encompasses this main basin and the Yarmouth sag. The COST No. G-2 well was drilled into the main basin and encountered salt at a depth of about 21,300 ft (6.5 km) (Amato and Simonis, 1980). This salt unit forms seismic basement beneath most of the main basin, but there are deeper reflectors beneath the salt layer towards the edges of the main basin. There may be an additional 3 to 4 km (9,800 to 13,100 ft) of Mesozoic sediments

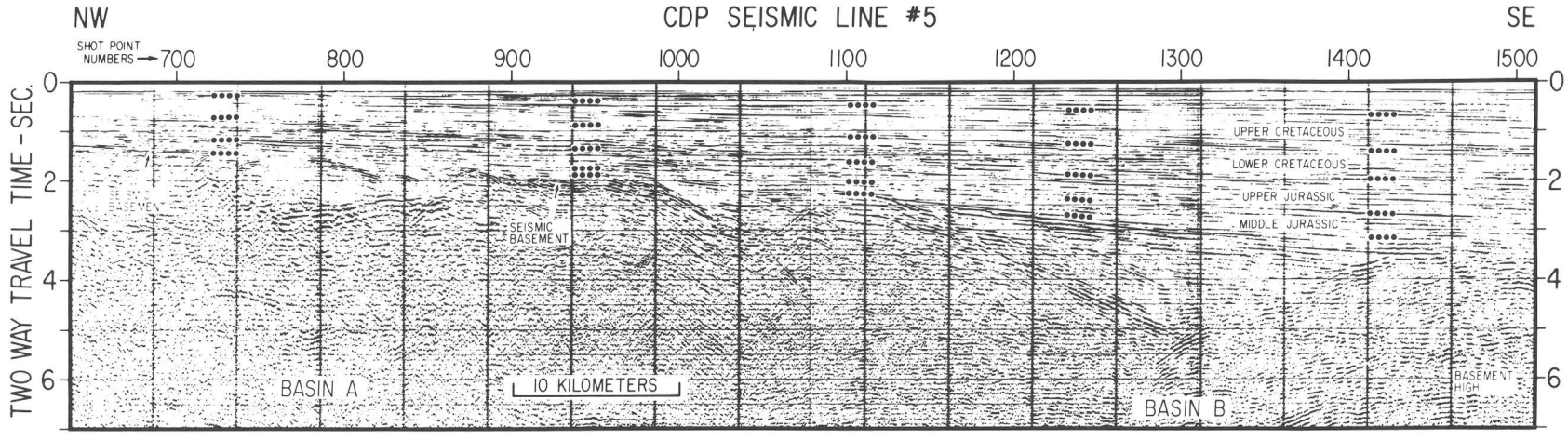

FIGURE 81.—A portion of CDP line 5 across the prerift or synrift basins. See figure 71 for location. Note the changes in slope in the breakup unconformity and the basins beneath the unconformity.

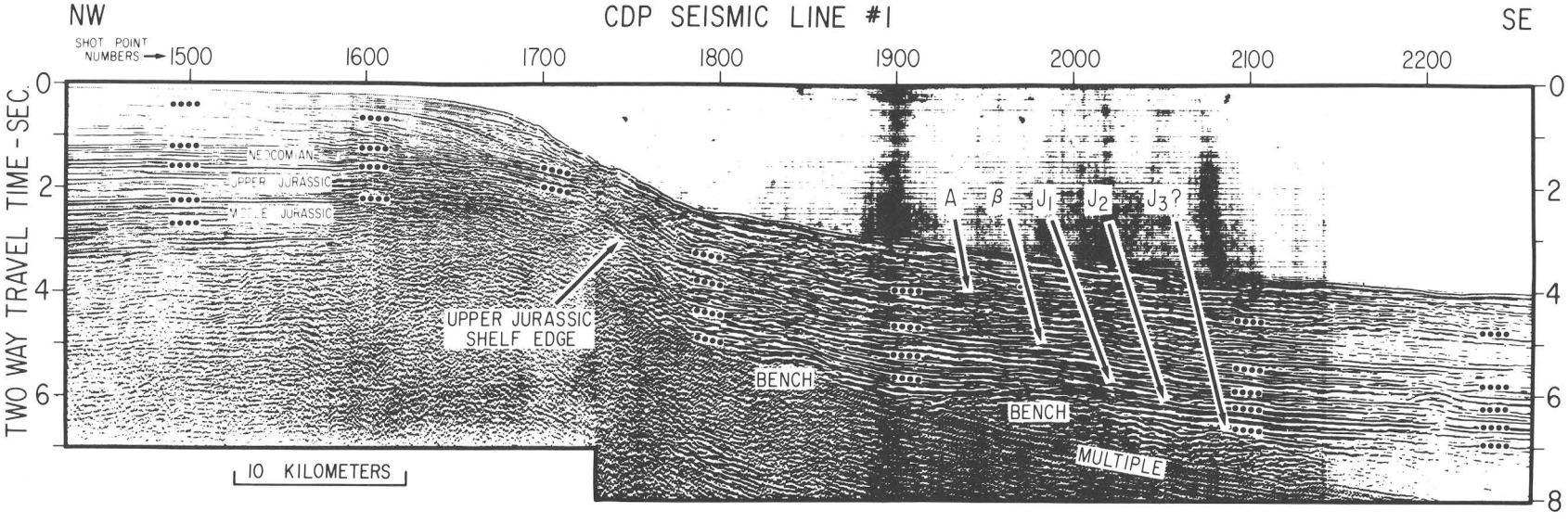

FIGURE 82.—Portion of CDP line 1 across the Jurassic shelf edge. See figure 71 for location. The identification of the deep sea Jurassic units are from Klitgord and Grow (1980). The age identification of the shelf seismic units are from Poag (this volume). Note how the deep reflectors J_3, J_2, and J_1, onlap the buried benches and the Upper Jurassic shelf edge, respectively.

beneath this seismic basement. A buried igneous body is located just east of the COST No. G-2 well in the main basin and it may protrude more than 3,300 ft (1 km) above the salt layer (line 19, shotpoint 3300, fig. 80). The seaward edge of the main basin is formed by a series of three benches (figs. 72, 80, and 82) that form descending steps seaward. The most landward bench is the same Upper Jurassic-Lower Cretaceous shelf edge that has been identified along the entire margin (Schlee and others, 1979). The two most seaward benches may be the erosional relics of Middle and Lower Jurassic shelf edges or elevated blocks of crystalline basement. The seismic reflectors J_1, J_2, and J_3, which onlap these three benches, have been identified as the tops of Upper, Middle, and Lower(?) Jurassic units respectively (Klitgord and Grow, 1980). The seismic basement just landward of the Upper Jurassic shelf edge is the top of the prograding carbonate buildup. The magnetic basement (fig. 74) reflects the deep main basin, the Yarmouth sag, the small high between them, and the buried intrusive feature in the main basin. The shallow ridge in the magnetic basement beneath the landward edge of the ECMA coincides with the most seaward bench. Although the estimated depth of magnetic basement is slightly shallower than the depth of seismic basement, the error associated with such estimates (Klitgord and Behrendt, 1979) would permit the two basement depths to be about the same.

The crystalline basement seaward of the ECMA is primarily igneous rock that forms the top of oceanic crust. Seismic basement to within 50 km (31 mi) of the ECMA is marked by hyperbolic echoes, a signature typical of oceanic basement (Grow, Mattick, and Schlee, 1979; Klitgord and Grow, 1980). Seismic basement and crystalline basement coincide to the east of a basement scarp 50 km (31 mi) east of the ECMA (fig. 73*B*). The acoustic horizon J_3 terminates at this scarp and forms seismic basement on most of the multichannel seismic profiles southwest of the New England Seamounts. The irregular, hyperbolic echo type seismic basement beneath the J_3 reflector can be traced landward of this scarp on CDP lines 5 (fig. 83) and 22 to within 20 km (12.4 mi) of the ECMA. This suggests that oceanic basement (and the underlying oceanic crust) may continue landward to the ECMA (Grow, Mattick, and Schlee, 1979). Crustal velocity information for the area off the New Jersey coast within 50 km (31 mi) of the ECMA indicates that crustal structure is similar to that normally found for oceanic crust (Sheridan and others, 1979). In the vicinity of the New England Seamounts, the seismic basement has a shingled character (fig. 5 of Schlee and others, 1976) that can be traced landward to the axis of the ECMA. This acoustic characteristic of shingle-like reflections is common for a carbonate buildup, but it also could result from volcanic debris from the New England Seamounts or an overlapping of sedimentary and volcanic layers near a spreading center.

The New England Seamount chain intersects the margin of the Georges Bank at the southwestern edge of the main basin and the three benches described above. This point of intersection, where Bear Seamount lies within the gap in the ECMA, coincides with the zone of east-west structures that separates the block-faulted zone seaward of the Long Island platform from the block-faulted zone seaward of the Gulf of Maine platform. The most likely igneous intrusive features landward of Bear Seamount are the body within the main basin, one feature between subbasins A and B, and one feature between subbasins B and C. The seismic data from the two highs between subbasin C and the main basin suggest that these are more likely structural basement highs.

BASIN FILL

The 6,350 km (3,943 mi) of multichannel CDP seismic reflection profiles collected for the USGS over the Georges Bank area (fig. 71) have allowed a clear look at deeper basement structures and the mapping of key reflectors within the sedimentary section. Analysis of the sedimentary sequences interpreted from these profiles indicates the existence of rift and postrift basin fill above an extensively block-faulted basement. The geometry of the several subbasins (fig. 3, Schlee and Klitgord, this volume) determined from the reflection profiles is similar to the pattern obtained using the depth-to-basement estimates inferred from the magnetic data (fig. 74).

Two profiles (figs. 84 and 85) demonstrate the arrangement and character of reflectors in the Georges Bank basin. Bundesanstalt für Geowissenschaften und Rohstoffe (BGR) line 209 (fig. 84) crosses the site of the COST No. G-2 well, and the 60-km (37-mi) section of line 20 shown in

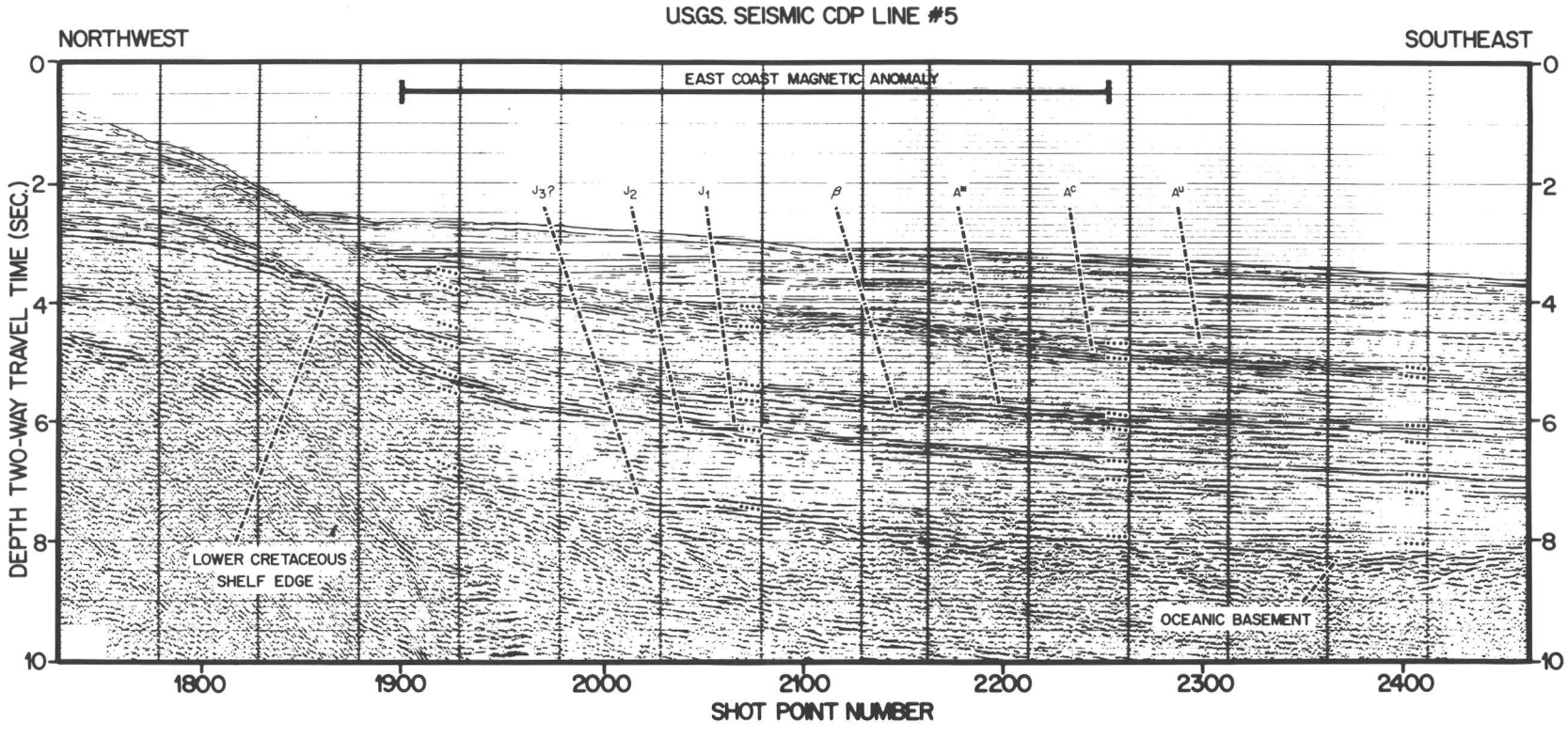

FIGURE 83.—Portion of CDP line 5 across the Jurassic shelf edge. See figure 71 for location. Note the deep reflector J_3 that onlaps basement near shotpoint 2300 and the lack of the benches seen on CDP line 1 (fig. 82).

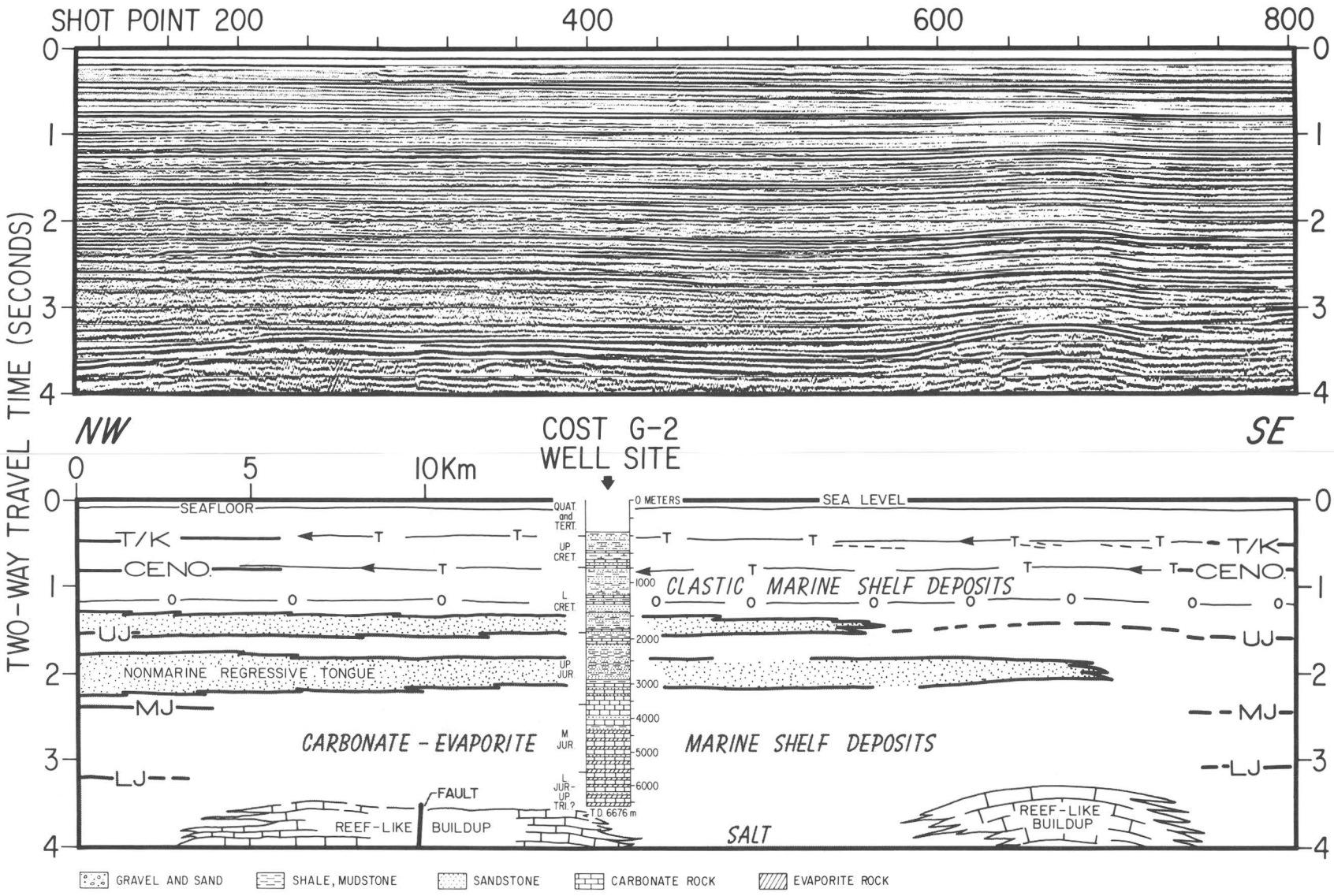

FIGURE 84.—A part of BGR line 209 across central Georges Bank basin. The actual time-scaled profile is shown and an interpretation of the stratigraphy is given below it. Also superimposed on the interpretation section is the lithology of the COST No. G-2 well at the approximate position where the profile crossed the drill site. T/K, Tertiary/Cretaceous boundary; CENO., Cenomanian; UJ, near the top of the Upper Jurassic section; MJ, within the Middle Jurassic section; LJ, near the base of the Lower Jurassic(?) section. T marks a thin transgressive unit. O marks the correlation with the "O marker"—a zone of limestone within the Missisauga Formation beneath the Scotian margin (Jansa and

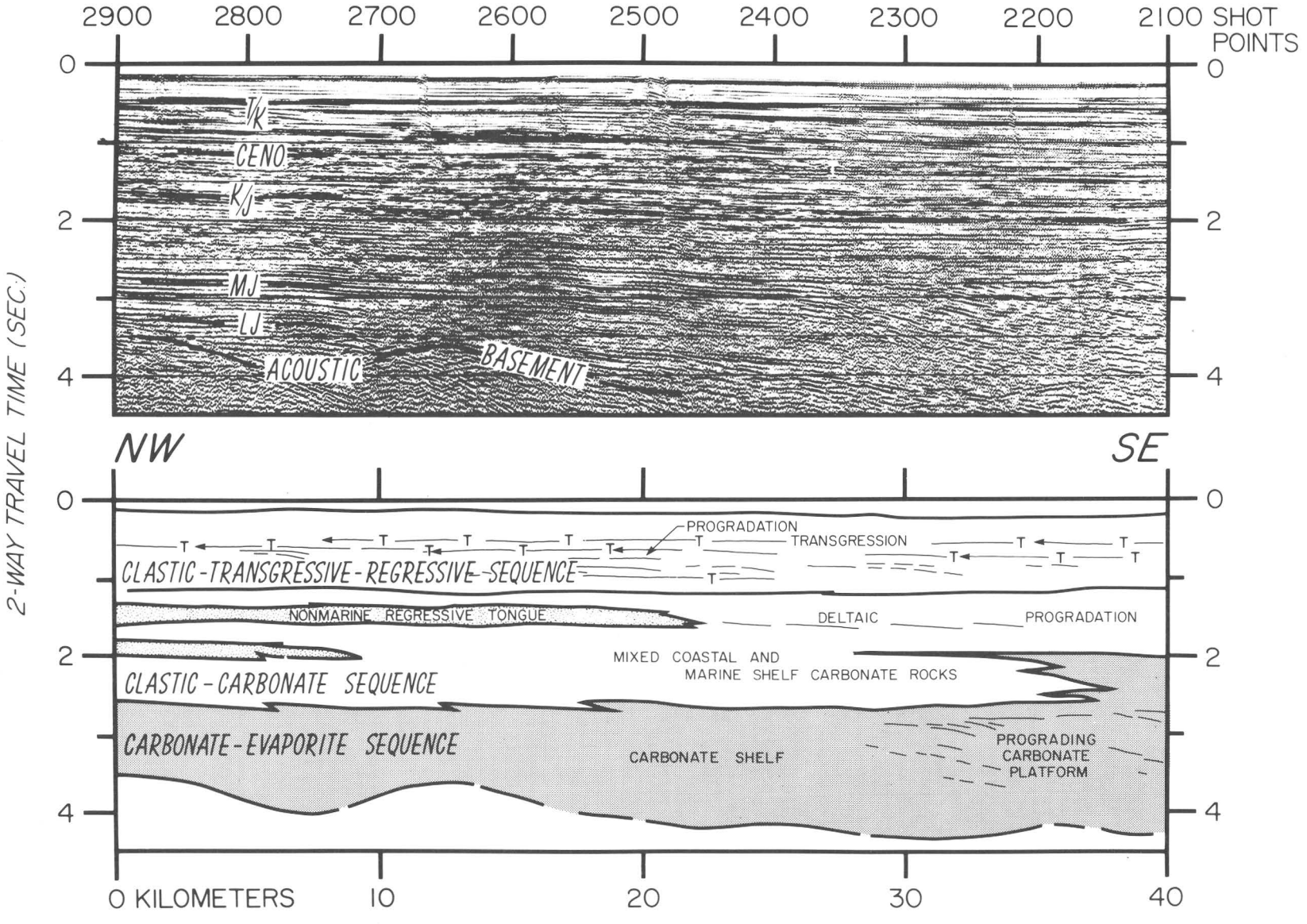

FIGURE 85.—A part of line 20 across the west-central part of Georges Bank basin. Below, the interpretation of the profile gives main stratigraphic sequences thought to compose the sedimentary section, and inferred environments of deposition. T/K, Tertiary/Cretaceous boundary; K/J Cretaceous/Jurassic boundary; CENO., Cenomanian; MJ, within the Middle Jurassic section; LJ, near the base of the Lower Jurassic(?) section. T marks a thin transgression unit. See figure 71 for location.

figure 85 spans the west-central part of the basin. Beneath the subhorizontal, parallel arrangement of reflectors above an irregular seismic basement is a second set of reflectors tilted at a low angle. It is important to distinquish between the horizontal reflectors and those with a low-angle tilt, because they represent the two main kinds of deposits in the basin: synrift and postrift sedimentary rocks. The boundary between these two reflectors is interpreted to be Falvey's (1974) breakup unconformity, which resulted from the change in tectonism from block-faulting to broad crustal extension as the thinned crustal foundations of the basin sank during the separation of Africa from North America. The key unconformity is best developed in the area where platforms and basins meet. Within the central part of the main basin, the deposits are comformable.

RIFT DEPOSITS

The acoustic character of the sediments beneath the breakup unconformity can be seen most clearly beneath the landward half of Georges Bank. As shown by part of line 18 (fig. 86) across the eastern side of the bank (fig. 2, Schlee and Klitgord, this volume), seismic basement appears at slightly less than 2-1/2 seconds two-way traveltime around shotpoint 1360, drops to slightly more than 3 seconds in the central part of the profile, and then rises again to 2-1/2 seconds around shotpoints 1800–1900 (fig. 86). Reflectors dip gently to the northwest (left) beneath a probable unconformity (arrow, fig. 86) within a graben 15 km (9.3 mi) across. These reflectors are inferred to be part of a rift sequence that formed prior to the main phase of basin subsidence (parallel reflectors above the unconformity).

The character of reflectors within the rift sequence changes across the main basin. On line 18, more or less continuous reflectors that show strong acoustic reflectivity are interpreted to be marine shelf deposits of interbedded carbonate and evaporite rocks. On two other profiles (figs. 84 and 85), inferred rift deposits display similar reflector characteristics. Yet on the northwestward continuation of profiles 18 and 20, equivalent reflectors become discontinuous, and their amplitude is variable; both charactistics are indicative of a nonmarine clastic sedimentary sequence, similar to the section drilled in the lowest part of the COST No. G–1 well. For line 20 bordering the Long Island platform, the reflectors below horizon LJ (correlated with the breakup unconformity) are areally restricted by irregular highs in seismic basement (fig. 85). Seismic reflectors are moderately continuous to discontinuous and show a wide range of seismic amplitude and a splayed arrangement. The sequence is interpreted to consist of interbedded marine (carbonate-evaporite rock) and nonmarine

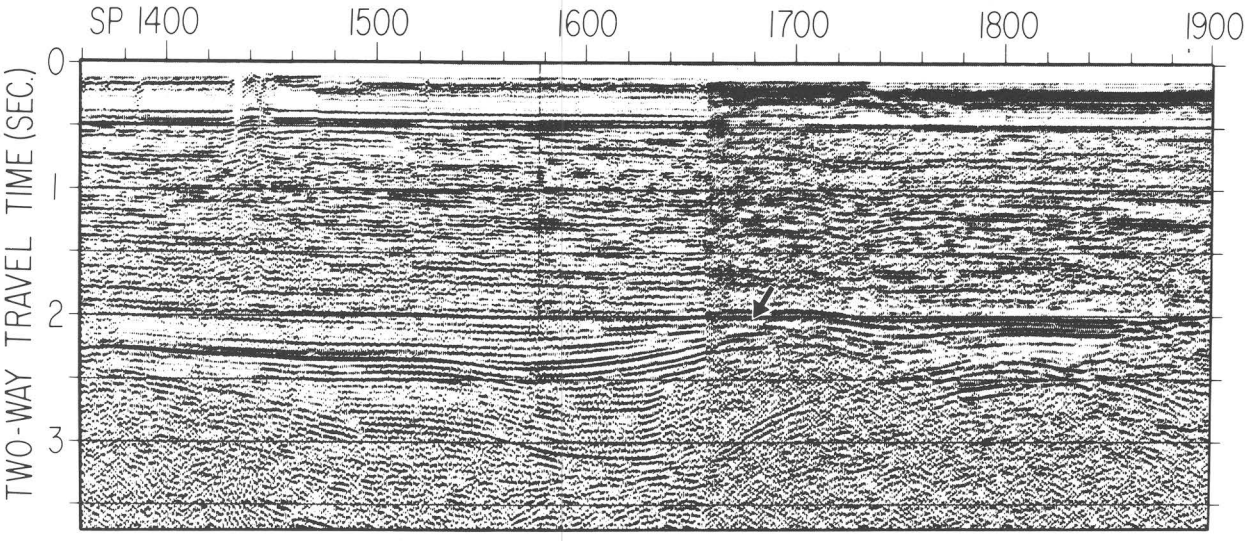

FIGURE 86.—A part of seismic line 18 between shotpoints 1360 and 1900. Notice conspicuous unconformity (arrow) forming the upper boundary of inferred rift deposits within a graben. See figure 71 for location.

clastic rocks that filled a rift prior to continental separation. Basement rocks are not obvious on BGR line 209 (fig. 84), probably because they are masked by the thick beds of limestones and anhydrite encountered in the lower part of the COST No. G-2 hole. BGR line 209 crosses the site of the COST No. G-2 well, where the deepest rock drilled was halite, which is of unknown age but probably correlates with the Argo Formation (Early Jurassic? to Late Triassic?) on the Scotian margin (Given, 1977; Barss and others, 1979; Poag, this volume). Reflectors associated with horizon LJ (Lower Jurassic?) are bowed-up areas of inferred carbonate accretion (possible reef). The largest of these, at shotpoint 680 (fig. 84), is 8 km (5 mi) across and appears to have been built over a basement high which can be seen on crossline 33. Between these bowed-up areas reflectors are horizontal and are thought to represent marine shelf deposits that accumulated over the central southern part of the basin.

EARLY POSTRIFT DEPOSITS

Above the breakup unconformity, the character of seismic reflectors varies within the basins. On the western flank of the LaHave platform, there are a few moderately continuous reflectors and many discontinuous ones of low to high seismic amplitude. This pattern of reflectors indicates a mixed marine and nonmarine sequence similar to the interbedded sandstone, shale, and limestone sampled in the COST No. G-1 well.

On BGR line 209, reflectors are parallel and weakly to strongly continuous. The zone of low continuity parallel reflectors between horizons MJ and LJ (Middle Jurassic and Lower Jurassic? on fig. 84) is interbedded limestone and anhydrite and a few beds of sandstone and siltstone. Reflector continuity and amplitude within this interval (MJ-LJ) increases to the southeast, indicating density contrasts between groups of strata that are not evident on BGR line 209 near the site of the COST No. G-2 well. The upper part of the early postrift section (to horizon UJ) shows the interfingering of probable alluvial and sublittoral coastal deposits and carbonate shelf deposits. A zone of weakly continuous, low-amplitude reflectors extends to the southeast (to the right on fig. 84) before changing acoustic character. In the COST No. G-2 well, rocks equivalent to this interval are gray sandstone, shale, limestone, and a few thin streaks of coal (Scholle, Schwab, and Krivoy, 1980; Simonis, 1980), thought to have been deposited in water depths of less than 30 m (100 ft) (Bielak and Simonis, 1980; Scholle, Schwab, and Krivoy, 1980).

Line 20 (fig. 85) displays some of the same changes in reflector characteristics noted in BGR line 209. The profile between horizons LJ and MJ is marked by strong high-amplitude, continuous reflectors. They continue to the southeast (to the right on fig. 85) where individual reflectors in foreset arrangement climb to the right, indicating that the margin in this area prograded seaward during the Jurassic. Between horizons MJ and UJ (Middle Jurassic and Upper Jurassic) there are less continuous and variable-amplitude reflectors which become even more prevalent to the northwest. As on BGR line 209, these zones of discontinuous variable-amplitude reflectors extend as tongues from the northwest. The moderate- to low-continuity reflectors are interpreted to be sequences of nonmarine sandstones and shale that change laterally to mixed littoral and inner-shelf sediments. One of these tongues above horizon UJ projects well into the basin (shotpoint 2400, fig. 85) and is in an interval in which a few reflectors appear to be moderately continuous; these zones of continuous reflectors are interpreted to be marine shelf deposits laid down during transgressive phases of margin sedimentation (T-T symbol, fig. 85). Seaward (to the right) of this uppermost tongue (shotpoint 2400), reflectors are faint and dip seaward at a low angle, an arrangement that probably indicates a deltaic progradation of the shelf in this area during the Early Cretaceous. The pattern of outbuilding is similar to that described by Jansa and Wade (1975b) for the Early Cretaceous Mississauga Formation on the northern Scotian margin, although sediments there are thicker.

LATE POSTRIFT DEPOSITS

Cretaceous and younger sedimentary rocks make up the third broad group of distinctive reflectors beneath Georges Bank (figs. 84 and 85). They occupy the upper 1.2 seconds (two-way traveltime) of the seismic records and are characterized by thin zones of fairly continuous reflectors of moderate amplitude, usually one or two wavelets thick, separated by thicker intervals of weakly continuous reflectors. Toward the outer

part of the shelf are faint reflectors arranged in broad foresets. The difference in acoustic character between this group of reflectors and the underlying group is the absence of the tonguelike, discontinuous reflectors of variable amplitude.

In the COST No. G-2 well, this youngest group of reflectors is produced by a section of interbedded claystone, siltstone, sandstone, and a few thin beds of limestone of Barremian, Aptian, Cenomanian, and Coniacian Ages (Simonis, 1980; Scholle, Schwab, and Krivoy, 1980; Poag, this volume). Some of the limestone beds can be correlated with the persistent thin zone of reflectors described on BGR line 209; one group of strong reflectors marked by the symbol 0-0-0 on figure 84, is thought to correlate with the O marker delineated in wells on the Scotian margin. The O marker off eastern Canada is a zone of thin Barremian limestone beds approximately 1.6 ft (0.5 m) thick within the Missisauga Formation (McIver 1972; fig. 4 of Given 1977).

Rocks from the COST Nos. G-1 and G-2 wells suggest a change in environment from shoreline conditions in the Early Cretaceous to shoreline-marine shelf conditions in the middle Cretaceous. Middle to outer shelf conditions existed at the COST No. G-2 well during the Late Cretaceous and early Tertiary (Bielak and Simonis, 1980; Scholle, Krivoy, and Hennessy, 1980; Scholle, Schwab, and Krivoy, 1980; Lachance and others, 1980; Poag, this volume). There are hiatuses in the COST Nos. G-1 and G-2 wells (see Poag, this volume) between the Barremian and Hauterivian, the Aptian and Cenomanian, the Cenomanian and Turonian, the Turonian and Coniacian, and the Santonian and Tertiary. Some of the unconformities in the Cretaceous seem to be associated with marine transgressions inferred from thin zones of continuous reflectors in the Barremian-Hauterivian (fig. 84; 0-0-0) and the Cenomanian. There are hiatuses in other areas of the Atlantic Continental Shelf. At the COST No. B-3 well in

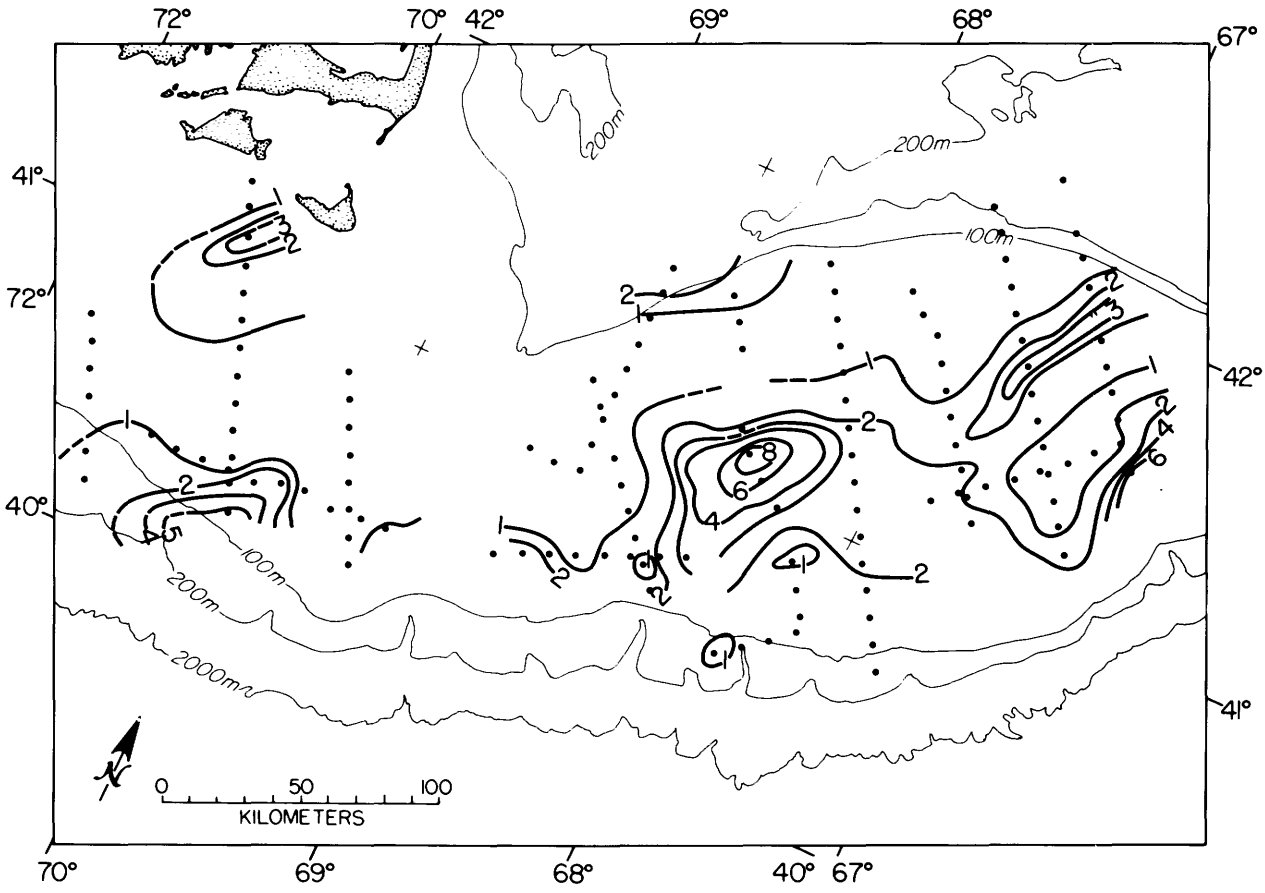

FIGURE 87.—Isopach map of synrift deposits in the Georges Bank basin. Contours are in kilometers, and dots indicate data points obtained from spot calculations along the grid of seismic-reflection profiles.

the Baltimore Canyon trough, unconformities were detected between rocks of the Hauterivian and Barremian, the late Cenomanian and Turonian, the early Turonian and Coniacian, the Late Cretaceous and Eocene, and the late Eocene and late Oligocene (Poag, 1980b). In the Scotian margin wells, Ascoli (1976) lists major hiatuses in rocks of Berriasian, Aptian-early Albian, Cenomanian-Turonian, and Maestrichtian-late Eocene age. These intervals of widespread erosion during the Barremian, Cenomanian, and Late Cretaceous-early Tertiary indicate numerous short-term changes in sea level on the Atlantic margin and support the generalized coastal onlap-offlap curve of Vail and others (1977). The occurrence of marine shelf conditions in Late Cretaceous-early Tertiary time that resulted in similar seismic characteristics on widely spaced profiles is further evidence of a widespread marine transgression (Pitman, 1978; Vail and others, 1977) that affected continental margins bordering most of the world's oceans.

BASIN GEOMETRY OF SEDIMENTARY FILL

As noted by Schlee and Klitgord (this volume) the Georges Bank basin is a collection of smaller subbasins (fig. 73). Interpretations from a grid of multichannel seismic reflection profiles suggest that the area has been built in rift phase and postrift phase (figs. 87 and 88).

Sediments of the rift phase are thick, irregularly distributed, and areally restricted to several elongate subbasins bordering the platforms. The subbasins have a northeast trend and contain 1 to 3 km (3,300 to 9,800 ft) of probable earliest Jurassic and older red beds, limestones, and evaporites. The thickest rift deposits are under the south-central part of the bank in the Yarmouth sag and in the main basin, where as much

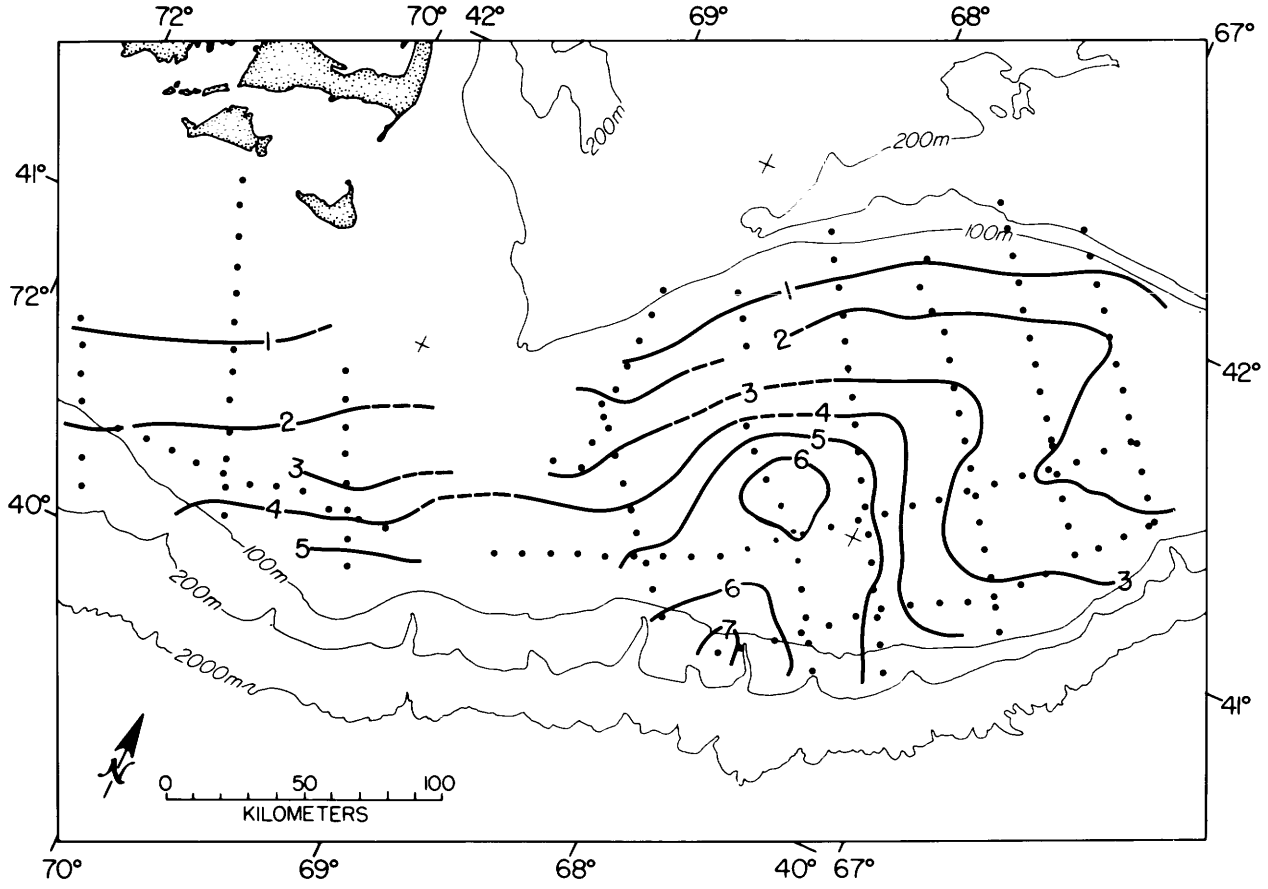

FIGURE 88.—Isopach map of postrift sedimentary section (Jurassic and Cretaceous only) for the Georges Bank basin. Contours are in kilometers, and dots indicate data points obtained from spot calculations along the grid of seismic-reflection profiles.

as 6 to 8 km (20,000 to 26,000 ft) of sediment appears to be present (fig. 87). During the postrift phase of basin history the pattern of subsidence changed from narrow rifts to a broad subsiding area that encompassed the earlier formed rifts and had a sedimentary blanket as much as 6 to 7 km (20,000 to 23,000 ft) thick (fig. 88). Large amounts of both rift and postrift sediments accumulated in the south-central part of the Georges Bank marking this area as the main basin. Much less sediment (1 to 2 km; 3,300 to 6,600 ft) accumulated on the landward periphery of the set of subbasins, even above earlier formed rifts where 2 to 3 km (6,600 to 9,900 ft) of sediment was deposited earlier. A comparison of the two isopach maps (figs. 87 and 88) indicates that subsidence was rapid and localized at the beginning of basin formation, but slowed and covered a larger area in the late Mesozoic.

The postrift basin geometry was controlled by the formation of a continental shelf, slope, and rise as the new Atlantic ocean basin was created to the east. The buildup of a carbonate bank-reef complex near the shelf break trapped a thick accumulation of sediments on the shelf during the Jurassic and Early Cretaceous (Schlee and others, 1979). This shelf edge formed the seaward edge of the series of coalescing Atlantic marginal basins and its position has varied through time (Grow, Mattick, and Schlee, 1979; Schlee and others, 1979). During the Cretaceous, the overall rate of sediment accumulation decreased on the shelf, and there may have been a slight landward retreat of the shelf edge (Schlee and others, 1976, 1979; Uchupi and others, 1977). In the Cenozoic, the major realm of sedimentation was offshore (Tucholke and Mountain, 1979) and only a thin veneer accumulated on the shelf (Schlee and others, 1976; Austin and others, 1980).

The location of the shelf edge during the Jurassic is not clearly defined but the seismic and magnetic evidence suggest a small seaward progradation on the western side of Georges Bank (Mattick and others, 1981), and a landward retreat on the eastern side. As already mentioned, the arrangement of reflectors on line 20 suggests a seaward-prograding carbonate sequence (fig. 85) similar to that seen in the Baltimore Canyon trough (Grow, 1980). On the profiles east of line 20, the retreat or cutting-back of the shelf during the Jurassic is suggested by the buried benches that form ascending steps landward (fig. 82). Our estimates of the location of the Early Jurassic shelf edge (east of line 20) put it consistently beneath the landward edge of the ECMA (fig. 73), suggesting that a common structural control for the shelf edge and the ECMA developed during the earliest stages of the margin development.

TECTONIC HISTORY

The tectonism associated with the rifting and continued separation of Africa from North America provided the dominant control for basin development and the sedimentary wedge construction. The rate of crustal subsidence on different parts of the margin was probably strongly influenced by the early tectonic history (Steckler and Watts, 1978; McKenzie, 1978; Royden and others, 1980). The distribution of the numerous subbasins and the accumulation history of the sedimentary fill provide the basic data to determine subsidence rates, from which can be inferred thermal history (Royden and others, 1980) and tectonic history.

PALEOGEOGRAPHIC RECONSTRUCTION

Prior to Early Jurassic time (fig. 89*A*), northwest Africa was adjacent to the Georges Bank region (Bullard and others, 1965; LePichon and others, 1977; Klitgord and Schouten, 1980). The locus of rifting during the Late Triassic and Early Jurassic suggests that the region now occupied by Georges Bank lay in a shear zone between the Triassic grabens in New Jersey and Connecticut and those in Northwest Africa and the Iberian Peninsula (Van Houten, 1977; Manspeizer and others, 1978). As a result, numerous grabens formed in the Georges Bank region in the latest Triassic or earliest Jurassic (Ballard and Uchupi, 1972). During the earliest stages of rifting and continental drift, crustal blocks formed by offsets just south of Georges Bank and just southeast of the southern tip of Nova Scotia along the breakup edge (fig. 89*B*) probably restricted water circulation. As the continents continued to drift apart, these ocean basins merged to form the early Atlantic Ocean basin. The restricted water circulation in the Middle and Early Jurassic led to salt deposition. Thick salt accumulations to the north of the offset off the southern tip of Nova Scotia may account for the pervasive diapirism north of Georges Bank.

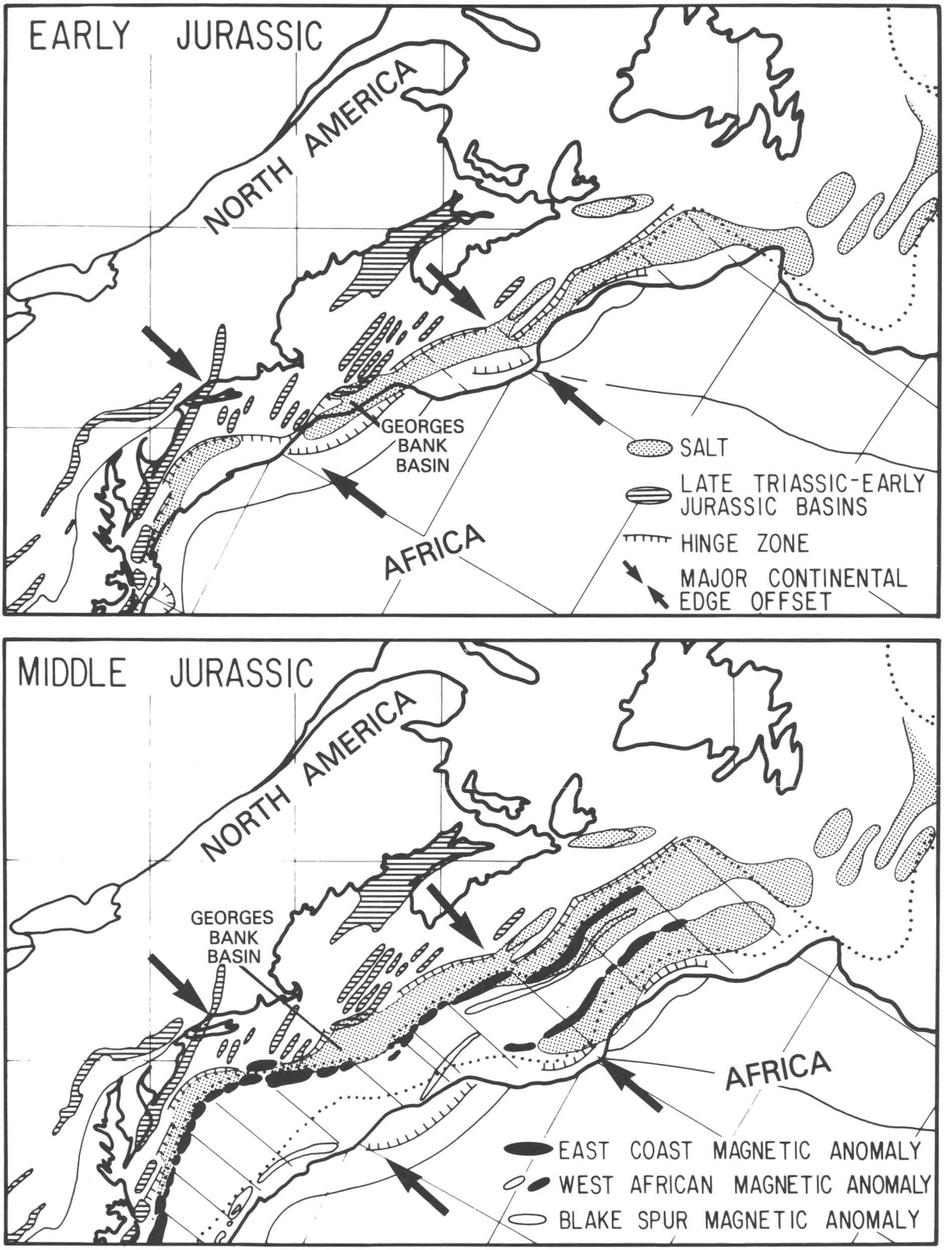

FIGURE 89.—Reconstructions of the Atlantic Ocean during the Early and Middle Jurassic. Note the possible barriers to water circulation during the early period of ocean opening just to the northeast and just to the southwest of the Georges Bank basin. The locations of Lower Jurassic(?) and Upper Triassic(?) salt deposits are indicated. From Klitgord and Schouten (1980).

TECTONIC STAGES

The development of the Georges Bank basin began with the rifting of Paleozoic or older crust during the Late Triassic as at least three or four graben-like, northeast-oriented subbasins formed along the edge of the Long Island–Gulf of Mexico platform. Their trend was parallel to the landward edges of the Carolina trough, the Baltimore Canyon trough, and the Scotian basin. Prerift and synrift sediments filled these subbasins, which were tilted by later tectonic activity on the borders of the structures. As the two continents began to separate, the intrusion of igneous rock probably altered and broadened what now forms the main basin seaward of the Yarmouth arch (fig. 73). The restricted oceanic circulation at this time (late rifting stage to early drifting stage) would have resulted in evaporite deposition over much of the region.

At the end of the Early Jurassic, a new ocean basin was beginning to form. The sediment fill which had been previously trapped within the subsiding marginal subbasins, eventually spilled over into the ocean basin forming a continental shelf, slope, and rise. A less restricted basin circulation at this time probably facilitated the building of a broad carbonate platform and is marked in the stratigraphic data by the breakup unconformity. As crust cooled, subsidence was greatest near the earlier igneous intrusions and slower near the edges of the old platforms, resulting in increased subsidence to the southeast away from the Long Island platform and the Gulf of Maine, and to the southwest away from the LaHave platform. This pattern of Early and Middle Jurassic differential subsidence can be seen in the undulating pattern of the breakup unconformity above the synrift sediments. The breakup unconformity dips gently seaward over large distances but drops rapidly within a number of narrow zones, giving it a stair step appearance.

During the Middle and Late Jurassic, the infilling of sediments continued on a rapidly subsiding shelf while a thin wedge of sediments accumulated on the slope and rise. The position of the shelf edge changed during this time as sea level fluctuated (Vail and others, 1977). Numerous subbasins coalesced into a broader basin beneath the south-central Georges Bank; its extension to the northeast was divided by the Yarmouth arch into a shallower landward limb (the Yarmouth sag) and a deeper seaward limb (the Scotian basin). By the Cretaceous, shelf sediment accumulation had slowed and the accumulation pattern was more uniform over the whole shelf, no longer reflecting the deeper basement structures.

The Cenozoic tectonic history of Georges Bank has most likely been one of local and regional response to forces such as sea level fluctuation, sediment loading, and ice sheet loading and rebound. The subsidence from crustal cooling was negligible by then (Steckler and Watts, 1978), and only a thin veneer of sediments accumulated on the shelf. The shallowest of the rift subbasins identified from seismic data, Step #1, lies along the northern edge of the bank and may have controlled its location. The shelf break was cut back as a result of erosion associated with the continuing sea level fluctuations. Evidence for Cenozoic tectonic activity, aside from slumping near the shelf break, is minimal, although Uchupi and others (in press) have found evidence of possible faulting near the northeast channel.

TECTONIC SETTINGS OF THE COST NOS. G–1 AND G–2 WELLS

The COST Nos. G–1 and G–2 wells are only about 65 km (40.4 mi) apart but the basement beneath them may be significantly different. The COST No. G–1 well was drilled on a small basement high adjacent to the Yarmouth sag, which we have inferred to be part of a Triassic or older graben system. This area remained well landward of the shelf edge throughout its history. The COST No. G–2 well lies seaward of this small basement high, and basement beneath the well may have been intruded by Lower Jurassic igneous rocks associated with continental breakup. Both wells were drilled in what probably was part of the early rift basin system, which included sites of salt accumulation. In contrast to the G–1 well, the G–2 well is located in a region that was close enough to the shelf edge throughout its history to record significant facies changes associated with shelf margin migrations.

Conclusions

1. The COST No. G-1 well drilled through 16,071 ft (4,898 m) of sedimentary rocks in the Georges Bank of the North Atlantic Outer Continental Shelf. Seismic correlation with other cored sites on the continental shelf suggests the presence of Tertiary strata above 1,030 ft (314 m), which are disconformable over Cretaceous (santonian) rocks. Foraminifers, calcareous nannofossils, and palynomorphs indicate that the rocks are Cretaceous from 1,030 to 5,400 ft (314 to 1,646 m) and Late Jurassic in age from 5,400 to 10,100 ft (1,646 to 3,079 m). A K/Ar date of 550 m.y. for a phyllite from 16,050 ft (4,892 m) indicates the well bottomed in Cambrian strata.
2. No rocks were recovered from the COST No. G-1 well above 1,030 ft (314 m), but Eocene calcareous nannofossils and foraminifers in the uppermost samples suggest the presence of an Eocene limestone that appears on reflection profiles and in conventional cores. Down to 9,900 ft (3,018 m) the strata are coarse-grained unconsolidated sands and loosely cemented sandstones with beds of gray shale, lignite, and coal. From 9,900 to 12,400 ft (3,780 to 3,018 m) the strata are predominantly gray shale, sandstone, limestone, and dolomite. There are predominantly red shales, sandstones, and conglomerates below 12,400 ft (3,780 m) down to 15,600 ft (4,755 m). Below this are black graphitic slate, phyllite, schist, metadolomite, and metaquartzite.
3. The COST No. G-2 well (drilled 42 mi (68 km) east of COST No. G-1) penetrated 21,874 ft (6,668 m) of sedimentary rocks. Conventional cores and seismic correlation indicated that above 1,300 ft (396 m) are Tertiary strata, which lie unconformably over Cretaceous (Santonian) rocks. The microfossils indicate that Cretaceous strata extend from 1,300 ft (396 m) to 5,920 ft (1,804 m) and that Late Jurassic age strata occur from 5,920 to 10,100 ft (1,804 to 3,079 m). Below this depth, the rocks contain few microfossils and are tentatively dated as Middle and Early Jurassic. The well bottomed in rocks tentatively assigned a Late Triassic age.
4. No rocks younger than Santonian (Cretaceous) were recovered at the G-2 site, but rich foraminiferal assemblages from the uppermost sample suggest the presence of Eocene and younger limestones down to 1,300 ft (396 m). From 1,300 to 4,000 ft (396 to 1,219 m) are unconsolidated sands, sandstones, and calcareous shales. From 4,000 to 13,500 ft (1,219 to 4,115 m) are limestones with interbedded sandstones, and from 13,500 to 21,830 ft (4,115 to 6,654 m) are alternating beds of limestone, anhydrite, and dolomite. The bottom 40 ft (12 m) of section contains salt and anhydrite.
5. The oldest sedimentary rocks at the COST Nos. G-1 and G-2 sites are post-rift Jurassic (possibly Late Triassic) evaporitic and terrigenous deposits. Through the Jurassic and Cretaceous the depositional environment varied between near-shore subaerial to sublittoral and inner to outer shelf conditions. Through the Cretaceous the water was deeper over the G-2 site than over the G-1 site, but shelf conditions prevailed at both until the Paleogene, when slope conditions are inferred.
6. Above 10,000 ft (3,048 m) in the COST No. G-1 well, porosities range from 15 to 33 percent and average 26 percent; below this depth the average porosity is 16 percent. In the COST No. G-2 well above 10,000 ft (3,048 m), porosities range from 15 to 39 percent and average 24 percent; below this depth the average value is 12 percent. The permeabilities are highly variable in both wells: in G-1 0.1 to 8,600 mD above 9,000 ft (2,733 m) and 0.1 to 16 mD below; in G-2 0.1 to 7,100 mD above 10,000 ft (3,048 m) and 0.1 to 0.2 mD below.

7. The present-day geothermal gradients are 1.26° F/100 ft (22.3° C/km) for the COST No. G-1 well and 1.34° F/100 ft (24.4° C/km) for the COST No. G-2 well. The temperature gradient at the COST No. G-2 well is the highest yet measured on the Atlantic margin.
8. Measurements of vitrinite reflectance, color alteration of visible organic matter, and various organic geochemical properties indicate that the Tertiary and Cretaceous strata of both wells appear to have poor petroleum source-rock potential because the organic matter is thermally immature and the total organic carbon contents are less that 1 percent. The Jurassic rocks may have poor-to-fair potential for gas generation. The Jurassic hydrocarbons are thermally mature, but the average organic carbon contents are also less that 1 percent, and the organic matter is largely of terrestrial origin.

REFERENCES CITED

Allemann, F., Catalano, R., Fares, F., and Remane, J., 1971, Standard calpionellid zonation (Upper Tithonian-Valanginian) of the western Mediterranean province: Proceedings of the Second International Conference on Planktonic Microfossils, Rome, 1970, v. 2, p. 1337-1340.

Amato, R. V., and Bebout, J. W., eds., 1980, Geologic and operational summary, COST No. G-1 well, Georges Bank area, North Atlantic OCS: U.S. Geological Survey Open-File Report 80-268, 112 p.

Amato, R. V., and Simonis, E. K., eds., 1980, Geologic and operational summary, COST No. G-2 well, Georges Bank area, North Atlantic OCS: U.S. Geological Survey Open-File Report 80-269, 116 p.

Angevine, C. L., and Turcotte, D. L., 1981, Thermal subsidence and compaction in sedimentary basins—Application to Baltimore Canyon trough: American Association of Petroleum Geologists Bulletin, v. 65, p. 219-225.

Ascoli, P., 1976, Foraminiferal and ostracod biostratigraphy of the Mesozoic-Cenozoic, Scotian shelf, Atlantic Canada, *in* Schafer, C. T., and Pelletier, B. R., eds., First International Symposium on Benthonic Foraminifera of Continental Margins: Maritime Sediments Special Publication 1, pt. B, p. 653-677.

Austin, J. A., Uchupi, E., Schaughnessy, D. R., III, and Ballard, R. D., 1980, Geology of New England passive margin: American Association of Petroleum Geologists Bulletin, v. 64, no. 4., p. 501-526.

Baker, D. R., 1972, Organic geochemistry and geologic interpretations, *in* Billings, G. K., Garrels, R. M., and Lewis, J. E., Paper on low-temperature geochemistry: Journal of Geological Education, v. 20, p. 221-224.

Baker, D. R., and Claypool, G. E., 1970, Effects of incipient metamorphism on organic matter in mudrock: American Association of Petroleum Geologists Bulletin, v. 54, no. 3, p. 456-467.

Ballard, R. D., 1975, Triassic rift structure in Gulf of Maine: American Association of Petroleum Geologists Bulletin, v. 59, no. 7, p. 1041-1072.

Ballard, R. D., and Uchupi, Elazar, 1972, Carboniferous and Triassic rifting—A preliminary outline of the tectonic history of the Gulf of Maine: Geological Society America Bulletin, v. 83, no. 8, p. 2285-2302.

Barss, M. S., Bujak, J. P., and Williams, G. L., 1979, Palynological zonation and correlation of sixty-seven wells, eastern Canada: Canada Geological Survey Paper 78-24, 118 p.

Bartenstein, Helmut, 1974, *Lenticulina (Lenticulina) nodosa* (Reuss 1863) and its subspecies—Worldwide index foraminifera in the Lower Cretaceous: Eclogae Geologicae Helvetiae, v. 67, p. 539-562.

Bartenstein, Helmut, Bettenstaedt, Franz, and Kovatcheva, Todorka, 1971, Foraminiferen des bulgarischen Barrême, ein Beitrag zur weltweiden Unterkreide-Stratigraphie: Neues Jahrbuch für Geologie und Paläontologie, v. 139, no. 2, p. 125-162.

Bebout, J. W., 1980, Biostratigraphy, *in* Amato, R. V., and Simonis, E. K., eds., Geologic and operational summary, COST No. G-2 well, Georges Bank Area, North Atlantic OCS: U.S. Geological Survey Open-File Report 80-269, p. 20-32.

Behrendt, J. C., and Klitgord, K. D., 1979, High resolution aeromagnetic anomaly map of the U.S. Atlantic continental margin: U.S. Geological Survey Geophysical Investigations Map GP-931, scale 1:1,000,000.

Benson, W. E., and others, 1976, Deep-Sea drilling in the North Atlantic: Geotimes, v. 21, no. 2, p. 23-26.

Berggren, W. A., and Van Couvering, J. A., 1974, The late Neogene—Biostratigraphy, geochronology, and paleoclimatology of the last 15 million years in marine and continental sequences: Palaeogeography, Palaeoclimatology, Palaeoecology, v. 16, p. 1-216.

Bielak, L. E., and Simonis, E. K., 1980, Paleoenvironmental analysis, *in* Amato, R. V., and Simonis, E. K., eds., Geologic and operational summary, COST No. G-2 well, Georges Bank area, North Atlantic OCS: U.S. Geological Survey Open-File Report 80-269, p. 29-32.

Blow, W. H., 1969, Late middle Eocene to Recent planktonic foraminiferal biostratigraphy, *in* Proceedings of the First International Conference on Planktonic Microfossils, Geneva, 1967: Leiden, Netherlands, E. J. Brill, v. 1, p. 199-421.

Bostick, N. H., Cashman, S. M., McCulloh, T. H., and Waddell, C. T., 1978, Gradients of vitrinite reflectance and present temperature in the Los Angeles and Ventura basins, California, *in* Oltz, D. F., ed., A symposium in geochemistry—Low temperature metamorphism of kerogen and clay minerals: Los Angeles, Society of Economic Paleontologists and Mineralogists, Pacific Section, p. 65-79.

Bukry, David, 1973, Low-latitude coccolith biostratigraphic zonation, *in* Edgar, N. T., Saunders, J. B., and others, eds., Initial reports of the Deep Sea Drilling Project, v. 15: Washington, D.C., U.S. Government Printing Office, p. 685-703.

Bukry, David, 1975, Coccolith and silicoflagellate stratigraphy, northwestern Pacific Ocean, Deep Sea Drilling Project, Leg 32, *in* Larson, R. L., Moberly, R., and others, eds., Initial Reports of the Deep Sea Drilling Project, v. 32: Washington, D.C., U.S. Government Printing Office, p. 677-701.

Bullard, E. C., Everett, J. E., and Smith, A. G., 1965, Fit of the continents around the Atlantic, *in* Blackett, P. M. S., Bullard, E. C., and Runcorn, S. K., eds., A symposium on continental drift: Royal Society of London, Philosophical Transactions, Series A, v. 258, p. 41-75.

Bush, P. R., 1970, A rapid method for the determination of carbonate carbon, and organic carbon: Chemical Geology, v. 6, p. 52-62.

Claypool, G. E., and Baysinger, J. P., 1978, Thermal analysis/pyrolysis of Cretaceous sapropels, DSDP Leg 44, Hole 391C, Blake-Bahama basin, *in* Benson, W. E., and Sheridan, R. E., eds., Initial reports of the Deep Sea Drilling Project, v. 44: Washington, D.C., U.S. Government Printing Office, p. 635-638.

Claypool, G. E., Love, A. H., and Maughan, E. K., 1978, Organic geochemistry, incipient metamorphism, and oil generation in black shale members of Permian Phosphoria Formation, Western Interior United States: American Association of Petroleum Geologists Bulletin, v. 62, p. 98-120.

Claypool, G. E., Lubeck, C. M., Baysinger, J. P., and Ging, T. G., 1977, Organic geochemistry, *in* Scholle, P. A., ed., Geological studies on the COST No. B-2 well, U.S. Mid-Atlantic Outer Continental Shelf area: U.S. Geological Survey Circular 750, p. 46-59.

Claypool, G. E., and Reed, P. R., 1976, Thermal-analysis technique for source-rock evalation—Quantitative estimate of organic richness and effects of lithologic variation: American Association of Petroleum Geologists Bulletin, v. 60, p. 608-612.

Degens, E. T., 1969, Biogeochemistry of stable carbon isotopes, chap. 12 *of* Eglinton, G., and Murphy, M. T., eds., Organic geochemistry, methods and results: Heidelberg, Springer Verlag, p. 304-329.

Ditty, P. S., 1980, Seismic velocity and correlations, *in* Amato, R. V., and Bebout, J. W., eds., Geologic and operational summary, COST No. G-1 well, Georges Bank area, North Atlantic OCS: U.S. Geological Survey Open-File Report 80-268, p. 59-67.

Dow, W. G., 1977, Kerogen studies and geological interpretations: Journal of Geochemical Exploration, v. 7, p. 79-99.

Eliuk, L. S., 1978, The Abenaki Formation, Nova Scotia shelf, Canada—A depositional and diagenetic model for a Mesozoic carbonate platform: Bulletin Canadian Petroleum Geology, v. 26, no. 4, p. 424-514.

Espitalie, J., Madec, M., and Tissot, B., 1977, Source rock characterization method for petroleum exploration: Offshore Technology Conference, 9th, Houston, Tex., May 2-5, 1977, Proceedings, v. 3, p. 439-441.

Falvey, D. A., 1974, The development of continental margins in plate tectonic theory: Australian Petroleum Exploration Association Journal, v. 14, p. 95-106.

Folger, D. W., Hathaway, J. C., Christopher, R. A., Valentine, P. C., and Poag, C. W., 1978, Stratigraphic test well, Nantucket Island, Massachusetts: U.S. Geological Survey Circular 773, 28 p.

Galimov, E. M., 1973, Izotopy ugleroda v neftegazovoy geologii: Moscow, Izdatel'stvo Nedra, 384 p. English translation, 1975, Carbon isotopes in oil-gas geology, 395 p., available from U.S. Department of Commerce, National Technical Information Service, Springfield, VA 22161, as rept. no. NASA TT F-682.

_____1980, C^{13}/C^{12} in kerogen, chap. 9 *of* Durand, Bernard, ed., Kerogen, insoluble organic matter from sedimentary rocks: Paris, Techi, p. 271-300.

Gibson, T. G., Hazel, J. E., and Mello, J. F., 1968, Fossiliferous rocks from submarine canyons off northeastern United States: U.S. Geological Survey Professional Paper 600-D, p. D222-D230.

Given, M. M., 1977, Mesozoic and early Cenozoic geology of offshore Nova Scotia: Bulletin of Canadian Petroleum Geology, v. 25, p. 63-91.

Gradstein, F. M., Williams, G. L., Jenkins, W. A. M., and Ascoli, P., 1975, Mesozoic and Cenzoic stratigraphy of the Atlantic continental margin, eastern Canada, *in* Yorath, C. J., Parker, E. R., and Glass, D. J., eds., Canada's continental margins and offshore petroleum exploration: Canadian Society of Petroleum Geologists, Memoir 4, p. 103-131.

Grow, J. A., 1980, Deep structure and evolution of the Baltimore Canyon Trough in the vicinity of the COST No. B-3 well, *in* Scholle, P. A., ed., Geological studies of the COST No. B-3 well, United States Mid-Atlantic Continental Slope: U.S. Geological Survey Circular 833, p. 117-126.

Grow, J. A., Bowin, C. O., and Hutchinson, D. R., 1979, The gravity field of the U.S. Atlantic continental margin: Tectonophysics, v. 59, p. 2752.

Grow, J. A., Bowin, C. O., Hutchinson, D. R., and Kent, K. M., 1976, Preliminary free-air gravity anomaly map along the Atlantic continental margin between Virginia and Georges Bank: U.S. Geological Survey Miscellaneous Field Studies Map MF-795, Scale 1:1,200,000.

Grow, J. A., Mattick, R. E., and Schlee, J. S., 1979, Multichannel seismic depth sections and interval velocities over Outer Continental Shelf and upper continental slope between Cape Hatteras and Cape Cod, *in* Watkins, J. S., Montadert, Lucien, and Dickerson, P. W., eds., Geological and geophysical investigations of continental margins: American Association of Petroleum Geologists Memoir 29, p. 65-83.

Grow, J. A., and Schlee, J. S., 1976, Interpretation and velocity analysis of U.S. Geological Survey multichannel reflection profiles 4, 5, and 6, Atlantic Continental Margin: U.S. Geological Survey Miscellaneous Field Studies Map MF-808.

Grow, J. A., and Sheridan, R. E., 1981, Deep structure and evolution of the continental margin off the eastern United States, *in* Geology of continental margins: International Geological Congress, 26th, Paris, July 7-17, 1980, Colloque C3 (Oceanologica Acta, no. SP, supp. to v. 4), p. 11-19.

Hardenbol, J., and Berggren, W. A., 1978, A new Paleogene numerical time scale, *in* Cohee, G. V., Glaessner, M. F., and Hedberg, H. D., eds., Contributions to the geologic time scale: American Association of Petroleum Geologists, Studies in Geology no. 6, p. 213-234.

Hathaway, J. C., Poag, C. W., Valentine, P. C., Miller, R. E., Schultz, D. M., Manheim, F. T., Kohout, F. A., Bothner, M. H., and Sangree, D. A., 1979, U.S. Geological Survey core drilling on the Atlantic Shelf: Science, v. 206, no. 4418, p. 515-527.

Hathaway, J. C., Schlee, J. S., Poag, C. W., Valentine, P. C., Weed, E. G. A., Bothner, M. H., Kohout, F. A., Manheim, F. T., Schoen, R., Miller, R. E., and Schultz, D. M., 1976, Preliminary summary of the 1976 Atlantic Margin Coring Project of the U.S. Geological Survey: U.S. Geological Survey Open-File Report 76-844, 217 p.

Haworth, R. T., and MacIntyre, J. B., 1975, The gravity and magnetic field of Atlantic offshore Canada: Canada Geological Survey Paper 75-9 (Canada Hydrographic Service Marine Science Paper no. 16), 22 p.

Heise, B. A., and Jackson, D. S., 1980, Geothermal gradient, *in* Amato, R. V., and Simonis, E. K., eds., Geologic and operational summary, COST No. G-2 well, Georges Bank area, North Atlantic OCS: U.S. Geological Survey Open-File Report 80-269, p. 53-55.

Hollister, C. D., Ewing, J. I., Habib, D., Hathaway, J. C., Laucelot, Y., Luterbacher, H. P., Paulus, F. J., Poag, C. W., Wilcoxon, J. A., and Worstell, P., 1972, Site 107—Upper continental rise: *in* Hollister, C. D., and Ewing, J. I.: Washington, D. C. U.S. Government Printing Office, Initial Reports of the Deep-Sea Drilling Project, v. 11 p. 351-356.

Hunt, J. M., 1967, The origin of petroleum in carbonate rocks, *in* Bissell, H. J., and Fairbridge, R. W., eds., Carbonate rocks: New York, Elsevier, p. 225-251.

_____1974, Hydrocarbon and kerogen studies, *in* van der Borch, C. C., and others, eds., Initial Reports of the Deep Sea Drilling Project, v. 22: Washington, D.C., U.S. Government Printing Office, p. 673-675.

_____1978, Characterization of bitumens and coals: American Association of Petroleum Geologists Bulletin, v. 62, p. 301-303.

_____1979, Petroleum geochemistry and geology: San Francisco, W. H. Freeman and Co., 617 p.

International Biostratigraphers, Inc., 1976, Biostratigraphy of the Ocean Production Company COST G-1 Georges Bank test: Houston, Texas, International Biostratigraphers, Inc., 16 p.

_____1977, Biostratigraphy of the Ocean Production Company COST G-2 Georges Bank test: Houston, Texas, International Biostratigraphers, Inc., 18 p.

Jackson, D. S., and Heise, B. A., 1980, Geothermal gradient, *in* Amato, R. V., and Bebout, J. W., eds., Geologic and operational summary, COST No. G-1 well, Georges Bank area, North Atlantic OCS: U.S. Geological Survey Open-File Report 80-268, p. 79-81.

Jansa, L. F., Enos, Paul, Tucholke, B. E., Gradstein, F. M., and Sheridan, R. E. 1979, Mesozoic-Cenozoic sedimentary formations of the North American Basin; western North Atlantic, *in* Talwani, Manik, Hay, William, and Ryan, W. B. F., eds., Deep drilling results in the Atlantic Ocean—Continental margins and paleoenvironment: Washington, American Geophysical Union, Maurice Ewing Series 3, p. 1-57.

Jansa, L. F., Ramane, J., and Ascoli, P., 1980, Calpionellid and foraminiferal-ostracod biostratigraphy at the Jurassic-Cretaceous boundary, offshore eastern Canada: Rivista Italiana Paleontologia e Stratigrafia, v. 86, p. 67-126.

Jansa, L. F., and Wade, J. A., 1975a, Geology of the continental margin off Nova Scotia and Newfoundland, *in* van der Linden, W. J. M., and Wade, J. A., eds., Offshore geology of eastern Canada, v. 2, Regional geology: Geological Survey of Canada Paper 74-30, p. 51-105.

_____1975b, Paleogeography and sedimentation in the Mesozoic and Cenozoic, southeastern Canada, *in* Yorath, C. J., Parker, E. R., and Glass, D. J., eds., Canada's continental margins and offshore petroleum exploration: Canadian Society of Petroleum Geologists, Memoir 4, p. 79-102.

Judkins, T. W., Simonis, E. K., and Heise, B. A., 1980, Correlation with other wells, *in* Amato, R. V., and Simonis, E. K., eds., Geological and operational summary, COST No. G-2 well, Georges Bank Area, North Atlantic OCS: U.S. Geological Survey Open-File Report 80-269, p. 33-36.

Kane, M. F., Yellin, M. J., Bell, K. G., and Zietz, Isidore, 1972, Gravity and magnetic evidence of lithology and structure in the Gulf of Maine region: U.S. Geological Survey Professional Paper 726-B, 22 p.

Klitgord, K. D., and Behrendt, J. C., 1977, Aeromagnetic anomaly map of the U.S. Atlantic continental margin: U.S. Geological Survey Miscellaneous Field Studies Map MF-913, 2 sheets, scale 1:1,000,000.

_____1979, Basin structure of the U.S. Atlantic continental margin, *in* Watkins, J. S., Montadert, L., and Dickerson, P. W., eds., Geological and geophysical investigations of continental margins: American Association of Petroleum Geologists Memoir 29, p. 85-112.

Klitgord, K. D., and Grow, J. A., 1980, Jurassic seismic stratigraphy and basement structure of western North Atlantic magnetic quiet zone: American Association of Petroleum Geologists Bulletin, v. 64, no. 10, p. 1658-1680.

Klitgord, K. D., and Schouten, Hans, 1980, The U.S. Atlantic continental margin, fracture zones and basement structures: International Geological Congress, 26th, Paris, France, July 7-17, 1980, Resumes/Abstracts, v. 3, p. 1344.

Lachance, D. J., 1980, Lithology, *in* Amato, R. V., and Bebout, J. W., eds., Geologic and operational summary, COST No. G-1 well, Georges Bank area, North Atlantic OCS: U.S. Geological Survey Open-File Report 80-268, p. 16-22.

Lachance, D. J., and Amato, R. V., 1980, Core descriptions and analyses, *in* Amato, R. V., and Bebout, J. W., eds., Geologic and operational summary, COST No. G-1 well, Georges Bank area, North Atlantic OCS: U.S. Geological Survey Open-File Report 80-268, p. 27-38.

Lachance, D. J., Bebout, J. W., and Bielak, L., 1980, Depositional environments, *in* Amato, R. V., and Bebout, J. W., eds., Geological and operational summary, COST No. G-1 well, Georges Bank area, North Atlantic OCS: U.S. Geological Survey Open-File Report 80-268, p. 53-58.

LePichon, Xavier, Sibuet, J. C., and Francheteau, Jean, 1977, The fit of the continents around the North Atlantic Ocean: Tectonophysics, v. 38, p. 169-209.

Lewis, R. S., and Sylvester, R. E., 1977, Shallow sedimentary framework of Georges Bank: American Association of Petroleum Geologists Bulletin, v. 61, p. 808.

Lloyd, A. J., 1962, Polymorphinid, miliolid and rotaliform foraminifera from the type Kimmeridgian: Micropaleontology, v. 8, no. 3, p. 369-383.

Lopatin, N. V., 1976, K opredeleniyu vliyaniya temperatury i geologicheskogo vremini na katageneticheskiye protsessy uglefikatsii i neftegazoobrazovaniya [Determination of the influence exerted by temperature and geologic time upon catagenic processes of coalification and oil and gas formation], *in* Vassoyevich, N. B., and Timofeyev, P. P., eds., Issledovaniya organicheskogo veshchestva sovremennykh i iskopayemykh osadkov: Moscow, Izdatel'stvo Nauka, p. 361-366.

Louis, M. C., and Tissot, B. P., 1967, Influence de la temperature at de la pression sur la formation des hydrocarbures dans les argiles a kerogene: World Petroleum Congress, 7th, Mexico, 1967, Proceedings, v. 2, p. 47-60.

Malinowski, M. J., 1980, Core descriptions and analyses, *in* Amato, R. V., and Simonis, E. K., eds., Geologic and operational summary, COST No. G-2 well, Georges Bank area, North Atlantic OCS: U.S. Geological Survey Open-File Report 80-269, p. 57-76.

Manspeizer, Warren, Puffer, J. H., and Cousminer, H. L., 1978, Separation of Morocco and eastern North America—A Triassic-Liassic stratigraphic record: Geological Society of America Bulletin, v. 89, p. 901-920.

Mattick, R. E., and Bayer, K. C., 1980, Geologic setting and hydrocarbon exploration activity, *in* Scholle, P. A., ed., Geological studies of the COST No. B-3 well, United States Mid-Atlantic continental slope area: U.S. Geological Survey Circular 833, p. 4-12.

Mattick, R. E., Foote, R. Q., Weaver, N. L., and Grim, M. S., 1974, Structural framework of the U.S. Atlantic Outer Continental Shelf north of Cape Hatteras: American Association of Petroleum Geologists Bulletin, v. 58, p. 1179-1190.

Mattick, R. E., Girard, O. W., Jr., Scholle, P. A., and Grow, J. A., 1978, Petroleum potential of U.S. Atlantic slope, rise, and abyssal plain: American Association of Petroleum Geologists Bulletin, v. 62, no. 4, p. 592-608, 8 figs.

Mattick, R. E., Schlee, J. S., and Bayer, K. C., 1981, The geology and hydrocarbon potential of the Georges Bank-Baltimore Canyon area, *in* Kerr, J. W., and Fergusson, A. J., eds., Canadian Atlas of North American Borderlands: Canadian Society of Petroleum Geologists Memoir 7, p. 461-486.

McIver, N. L., 1972, Cenozoic and Mesozoic stratigraphy of the Nova Scotia Shelf: Canadian Journal of Earth Sciences, v. 9, p. 54-70.

McKenzie, Dan, 1978, Some remarks on the development of sedimentary basins: Earth and Planetary Science Letters, v. 40, p. 25-32.

Miller, R. E., Schultz, D. M., Claypool, G. E., Smith, M. A., Lerch, H. E., Ligon, D., Gary, C., and Owings, D. K., 1979, Organic geochemistry, *in* Scholle, P. A., ed., Geological studies of the COST GE-1 well, United States South Atlantic Outer Continental Shelf area: U.S. Geological Survey Circular 800, p. 74-92.

Miller, R. E., Schultz, D. M., Claypool, G. E., Smith, M. A., Lerch, H. E., Ligon, D., Owings, D. K., and Gary, C., 1980, Organic geochemistry, *in* Scholle, P. A., ed., Geological Studies of the COST No. B-3 well, United States Mid-Atlantic Continental Slope area: U.S. Geological Survey Circular 833, p. 85-104.

Oldale, R. N., Hathaway, J. C., Dillon, W. P., Hendricks, J. D., and Robb, J. M., 1974, Geophysical observations on the northern part of the Georges Bank and adjacent basins of the Gulf of Maine: American Association of Petroleum Geologists Bulletin, v. 58, no. 12, p. 2411-2427.

Pessagno, E. A., Jr., 1967, Upper Cretaceous planktonic foraminifera from the western Gulf Coastal Plain: Palaeontographica Americana, v. 5, p. 245-445.

Peterson, R. A., Fillipone, W. R., and Coker, F. B., 1955, The synthesis of seismograms from well log data: Geophysics, v. 20, p. 516-538.

Pitman, W. C., III, 1978, Relationship between eustacy and stratigraphic sequences of passive margins: Geological Society of America Bulletin, v. 89, no. 9, p. 1389-1403.

Poag, C. W., 1978, Stratigraphy of the Atlantic Continental Shelf and Slope of the United States: Annual Review of Earth and Planetary Sciences, v. 6, p. 251-280.

_____1980a, Foraminiferal stratigraphy and paleoecology, *in* Mattick, R. E., and Hennessy, J. L., eds., Structural framework, stratigraphy, and petroleum geology of the area of Oil and Gas Lease Sale No. 49 on the U.S. Atlantic Continental Shelf and Slope: U.S. Geological Survey Circular 812, p. 35-48.

_____1980b, Foraminiferal stratigraphy, paleoenvironments, and depositional cycles in the outer Baltimore Canyon trough, *in* Scholle, P. A., ed., Geological studies of the COST No. B-3 well, United States Mid-Atlantic Continental Slope area: U.S. Geological Survey Circular 833, p. 44-65.

Poag, C. W., and Hall, R. E., 1979, Foraminiferal biostratigraphy, paleoecology, and sediment accumulation rates, *in* Scholle, P. A., ed., Geological studies of the COST GE-1 well, United States South Atlantic Outer Continental Shelf area: U.S. Geological Survey Circular 800, p. 49-63.

Pusey, W. C., III, 1973, The ESP-kerogen method—How to evaluate potential gas and oil source rocks: World Oil, v. 176, no. 5 (April 1), p. 71-75.

Rabinowitz, P. D., 1974, The boundary between oceanic and continental crust in the western North Atlantic, *in* Burk, C. A., and Drake, C. L., eds., The geology of continental margins: New York, Springer-Verlag, p. 67-84.

Rabinowitz, P. D., and LaBreque, J. L., 1977, The isostatic gravity anomaly—Key to the evolution of the ocean-continent boundary at passive continental margins: Earth and Planetary Science Letters, v. 35, p. 145-150.

Robbins, E. I., and Rhodehamel, E. C., 1976, Geothermal gradients help predict petroleum potential of Scotian shelf: Oil and Gas Journal, v. 74, no. 9 (March 1), p. 143-145.

Royden, Leigh, Sclater, J. G., and von Herzen, R. P., 1980, Continental margin subsidence and heat flow—Important parameters in formation of petroleum hydrocarbons: American Association of Petroleum Geologists Bulletin, v. 64, p. 173-187.

Ryan, W. B. F., Cita, M. B., Miller, E. L., Hanselman, D., Nesteroff, W. D., Hecker, B., and Nibblelink, M., 1978, Bedrock geology in New England Submarine Canyons: Oceanologica Acta, v. 1, p. 233-254.

Sawyer, D. S., Swift, A., and Sclater, J. G., and Toksoz, M. N., Extensional model for the subsidence of the northern United States Atlantic continental margin: Geology [in press].

Schlee, J. S., Behrendt, J. C., Grow, J. A., Robb, J. M., Mattick, R. E., Taylor, P. T., and Lawson, B. J., 1976, Regional framework off northeastern United States: American Association of Petroleum Geologists Bulletin, v. 60, no. 6, p. 926-951.

Schlee, J. S., Dillon, W. P., and Grow, J. A., 1979, Structure of the continental slope off the eastern United States, *in* Doyle, L. J., and Pilkey, O. H., eds., Geology of continental slopes: Society Economic Paleontologists and Mineralogists Special Paper 27, p. 95-118.

Schlee, J. S., and Jansa, L. F., 1981, The paleoenvironment and development of the eastern North American continental margin, *in* Geology of continental margins: International Geological Congress, 26th, Paris, July 7-17, 1980, Colloque C3 (Oceanologica Acta, no. SP, supp. to v. 4), p. 71-80.

Scholle, P. A., 1977a, Data summary and petroleum potential, *in* Scholle, P. A., ed., Geological studies on the COST No. B-2 well, U.S. Mid-Atlantic Outer Continental Shelf area: U.S. Geological Survey Circular 750, p. 8-14.

_____ed., 1977b, Geological studies on the COST No. B-2 well, U.S. Mid-Atlantic Outer Continental Shelf area: U.S. Geological Survey Circular 750, 71 p.

_____ed., 1979, Geological studies of the COST GE-1 well, United States South Atlantic Outer Continental Shelf area: U.S. Geological Survey Circular 800, 114 p.

_____1980, Geological studies of the COST No. B-3 well, United States Mid-Atlantic Continental Slope area: U.S. Geological Survey Circular 833, 132 p.

Scholle, P. A., Krivoy, H. L., and Hennessy, J. L., 1980, Summary chart of geological data from the COST No. G-1 well, U.S. North-Atlantic Outer Continental Shelf: U.S. Geological Survey Oil and Gas Investigations Chart OC-104, 1 sheet.

Scholle, P. A., Schwab, K. A., and Krivoy, H. L., 1980, Summary chart of geological data from the COST No. G-2 well, U.S. North Atlantic Continental Shelf: U.S. Geological Survey Oil and Gas Investigations Chart OC-105, 1 sheet.

Sengbush, R. L., Lawrence, P. L., and McDonal, F. J., 1961, Interpretation of synthetic seismograms: Geophysics, v. 26, p. 45-58.

Sheridan, R. E., Grow, J. A., Behrendt, J. C., and Bayer, K. C., 1979, Seismic refraction study of the continental edge off the eastern United States: Tectonophysics, v. 59, 1-26.

Simonis, E. K., 1979, Petroleum potential, *in* Amato, R. V., and Simonis, E. K., eds., Geological and operational summary, COST No. B-3 well, Baltimore Canyon trough area, Mid-Atlantic OCS: U.S. Geological Survey Open-File Report 79-1159, p. 100-105.

_____1980, Lithologic description, *in* Amato, R. V., and Simonis, E. K., eds., Geologic and operational summary, COST No. G-2 well, Georges Bank area, North Atlantic OCS: U.S. Geological Survey Open-File Report 80-269, p. 14-19.

Smith, M. A., 1980, Geochemical analysis, *in* Amato, R. V., and Simonis, E. K., eds., Geologic and operational summary, COST No. G-2 well, Georges Bank area, North Atlantic OCS: U.S. Geological Survey Open-File Report 80-269, p. 77-99.

Smith, M. A., and Shaw, D. R., 1980, Geochemical analysis, *in* Amato, R. V., and Bebout, J. W., eds., Geologic and operational summary, COST No. G-1 well, Georges Bank area, North Atlantic OCS: U.S. Geological Survey Open-File Report 80-268, p. 82-91.

Stahl, W. J., 1978, Source rock-crude oil correlation by isotopic type curve: Geochimica et Cosmochimica Acta, v. 42, p. 1573-1577.

Stainforth, R. M., Lamb, J. L., Luterbacher, Hanspeter, Beard, J. H., and Jeffords, R. M., 1975, Cenozoic planktonic foraminiferal zonation and characteristics of index forms: University of Kansas Paleontological Contributions, art. 62, p. 1-162e; Appendix, p. 163-425.

Steckler, M. S., and Watts, A. B., 1978, Subsidence of the Atlantic-type continental margin of New York: Earth and Planetary Science Letters, v. 41, p. 1-13.

Steinkraus, W. E., 1980, Biostratigraphy, *in* Amato, R. V., and Bebout, J. W., eds., Geologic and operational summary, COST No. G-1 well, Georges Bank area, North Atlantic OCS: U.S. Geological Survey Open-File Report 80-268, p. 39-52.

Swetland, P. J., Patterson, J. M., and Claypool, G. E., 1978, Petroleum source-bed evaluation of Jurassic Twin Creek Limestone, Idaho-Wyoming thrust belt: American Association of Petroleum Geologists Bulletin, v. 62, p. 1075-1080.

Talwani, Manik, and Eldholm, Olav, 1973, Boundary between continental and oceanic crust at the margin of rifted continents: Nature, v. 241, p. 325-330.

Taner, M. T., and Koehler, F., 1969, Velocity spectra digital computer derivation and applications of velocity functions: Geophysics, v. 34, p. 792-812.

Taylor, P. T., Zietz, Isidore, and Dennis, L. S., 1968, Geologic implications of aeromagnetic data for the eastern continental margin of the United States: Geophysics, v. 33, p. 755-780.

Tissot, B., Demaison, G., Masson, P., Delteil, J. R., and Combaz, A., 1980, Paleoenvironment and petroleum potential of Middle Cretaceous black shales in Atlantic basins: American Association of Petroleum Geologists, Bulletin, v. 64, p. 2051-2063.

Tissot, B., Deroo, G., and Herbin, J. P., 1979, Organic matter in Cretaceous sediments of the North Atlantic—Contribution to sedimentology and paleogeography, *in* Talwani, Manik, Hay, William, and Ryan, W. B. F., eds., Deep drilling results in the Atlantic Ocean—Continental margins and paleoenvironments: Washington, American Geophysical Union, Maurice Ewing Series 3, p. 362-374.

Tissot, B., Durand, B., Espitalie, J., and Combaz, A., 1974, Influence of nature and diagenesis of organic matter in formation of petroleum: American Association of Petroleum Geologists Bulletin, v. 58, no. 3, p. 499-506.

Tissot, B. P., and Welte, D. H., 1978, Petroleum formation and occurrence, a new approach to oil and gas exploration: New York, Springer-Verlag, 538 p.

Tucholke, B. E., 1979, Relationships between acoustic stratigraphy and lithostratigraphy in the western North Atlantic basin, *in* Tucholke, B. E., and Vogt, P. R., and others, Initial reports of the Deep Sea Drilling Project: Washington, U.S. Government Printing Office, v. 43, p. 827-846.

Tucholke, B. E., and Mountain, G. S., 1979, Seismic stratigraphy, lithostratigraphy and paleosedimentation patterns in the North American Basin, *in* Talwani, Manik, Hay, William, and Ryan, W. B. F., eds., Deep drilling results in the Atlantic Ocean—Continental margins and paleoenvironment: Washington, American Geophysical Union, Maurice Ewing Series 3, p. 58–86.

Tucholke, B. E., and Vogt, P. R., 1979, Western North Atlantic—Sedimentary evolution and aspects of tectonic history, *in* Tucholke, B. E., Vogt, P. R., and others, 1979, Initial reports of the Deep Sea Drilling Project: Washington, U.S. Government Printing Office, v. 43, p. 791–825.

Uchupi, Elazar, 1966, Structural framework of the Gulf of Maine: Journal of Geophysical Research, v. 71, p. 3013–3028.

Uchupi, Elazar, Austin, J. A., Jr., and Gever, D. H., Pre-Cenozoic faulting in the eastern end of Georges Bank: [in press].

Uchupi, Elazar, Ballard, R. D., and Ellis, J. P., 1977, Continental Slope and upper rise off western Nova Scotia and Georges Bank: American Association of Petroleum Geologists Bulletin, v. 61, p. 1483–1492.

U.S. Naval Oceanographic Office, 1966, Total magnetic intensity aeromagnetic survey 1964–1966—U.S. Atlantic coastal region: Washington, D.C., U.S. Naval Oceanographic Office, 15 sheets, scale 1:500,000.

Vail, P. R, and Mitchum, R. M., Jr., 1979, Global cycles of relative changes of sea level from seismic stratigraphy, *in* Watkins, J. S., Montadert, L., and Dickerson, P. W., Geological and geophysical investigations of continental margins: American Association of Petroleum Geologists Memoir 29, p. 469–472.

Vail, P. R., Mitchum, R. M., Jr., Todd, R. G., Widmier, J. M., Thompson, S., III, Sangree, J. B., Bubb, J. N., and Hatelid, W. G., 1977, Seismic stratigraphy and global changes of sea level, *in* Payton, C. E., ed., Seismic stratigraphy—Applications to hydrocarbon exploration: American Association of Petroleum Geologists Memoir 26, p. 49–212.

Valentine, P. C., 1980, Calcareous nannofossil biostratigraphy, paleonvironments, and post-Jurassic continental margin development, *in* Scholle, P. A., ed., Geological studies of the COST No. B-3 well, United States Mid-Atlantic continental slope area: U.S. Geological Survey Circular 833, p. 67–83.

_____1981, Continental margin stratigraphy along U.S. Geological Survey seismic line 5—Long Island platform and western Georges Bank basin: U.S. Geological Survey Miscellaneous Field Studies Map MF-857.

Valentine, P. C., Uzmann, J. R., and Cooper, R. A., 1980, Geology and biology of Oceanographer submarine canyon: Marine Geology, v. 38, p. 283–312.

van Hinte, J. E., 1976a, A Jurassic time scale: American Association of Petroleum Geologists Bulletin, v. 60, p. 489–497.

_____1976b, A Cretaceous time scale: American Association of Petroleum Geologists Bulletin, v. 60, p. 498–516.

Van Houten, F. B., 1977, Triassic-Liassic deposits of Morocco and eastern North American—Comparison: American Association of Petroleum Geologists Bulletin, v. 61, p. 79–99.

Vassoyevich, N. B., Korchagina, Yu. I., Lopatin, N. V., and Chernyshev, V. V., 1970, Glavanaya faza nefteobrazovaniya [Principal phase of oil formation]: Moskovskogo Universiteta Vestnik, Series 4, Geologii, v. 24, no. 6, p. 3–27; English translation *in* International Geology Review, v. 12, no. 11, p. 1276–1296.

Wade, J. A., 1977, Stratigraphy of Georges Bank basin—Interpretation from seismic correlation to the western Scotian Shelf: Canadian Journal Earth Science, v. 14, no. 10, p. 2274–2283.

Waetjan, H. H., 1980, Seismic velocity and reflection correlation, *in* Amato, R. V., and Simonis, E. K., eds., Geologic and operational summary, COST No. G-2 well, Georges Bank area, North Atlantic OCS: U.S. Geological Survey Open-File Report 80–269, p. 37–44.

Waples, D. W., 1980, Time and temperature in petroleum formation—Application of Lopatin's method to petroleum exploration: American Association of Petroleum Geologists Bulletin, v. 64, p. 916–926.

Watts, A. B., and Steckler, M. S., 1979, Subsidence and eustasy at the continental margin of eastern North America, *in* Talwani, Manik, Hay, William, and Ryan, W. B. F., eds., Deep drilling results in the Atlantic Ocean—Continental margins and paleoenvironment: Washington, American Geophysical Union, Maurice Ewing Series 3, p. 218–234.

Weed, E. G. A., Minard, J. P., Perry, W. J., Jr., Rhodehamel, E. C., and Robbins, E. I., 1974, Generalized pre-Pleistocene geologic map of the northern United States continental margin: U.S. Geological Survey Miscellaneous Geologic Investigations Map I-861, scale 1:1,000,000.

Worzel, J. L., and Shurbet, G. L., 1955, Gravity anomalies at continental margins: National Academy of Sciences, Proceedings, v. 41, p. 458–469.

Yen, T. F., 1972, Terrestrial and extraterrestrial stable organic molecules, *in* Landel, R. F., and Rembuum, A., eds., Chemistry in space: New York, Elsevier, p. 105–153.

☆ U.S. GOVERNMENT PRINTING OFFICE: 1982—576-034/127